Advances in Industrial Control

Springer
London
Berlin
Heidelberg
New York
Barcelona
Hong Kong
Milan
Paris
Santa Clara
Singapore
Tokyo

Other titles published in this Series:

Model Predictive Control in the Process Industry
E.F. Camacho and C. Bordons

H∞ Aerospace Control Design: A VSTOL Flight Application
R.A. Hyde

Neural Network Engineering in Dynamic Control Systems
Edited by Kenneth Hunt, George Irwin and Kevin Warwick

Neuro-Control and its Applications
Sigeru Omatu, Marzuki Khalid and Rubiyah Yusof

Energy Efficient Train Control
P.G. Howlett and P.J. Pudney

Hierarchical Power Systems Control: Its Value in a Changing Industry
Marija D. Ilic and Shell Liu

System Identification and Robust Control
Steen Tøffner-Clausen

Genetic Algorithms for Control and Signal Processing
K.F. Man, K.S. Tang, S. Kwong and W.A. Halang

Advanced Control of Solar Plants
E.F. Camacho, M. Berenguel and F.R. Rubio

Control of Modern Integrated Power Systems
E. Mariani and S.S. Murthy

Advanced Load Dispatch for Power Systems: Principles, Practices and Economies
E. Mariani and S.S. Murthy

Supervision and Control for Industrial Processes
Björn Sohlberg

Modelling and Simulation of Human Behaviour in System Control
Pietro Carlo Cacciabue

Modelling and Identification in Robotics
Krzysztof Kozlowski

Spacecraft Navigation and Guidance
Maxwell Noton

Robust Estimation and Failure Detection
Rami Mangoubi

Adaptive Internal Model Control
Aniruddha Datta

Price-Based Commitment Decisions in the Electricity Market
Eric Allen and Marija Ilić

Jan Tommy Gravdahl and Olav Egeland

Compressor Surge and Rotating Stall

Modeling and Control

With 58 Figures

Springer

Dr. Jan Tommy Gravdahl
Dr. Ing. Olav Egeland
Department of Engineering Cybernetics,
Norwegian University of Science and Technology,
O.S. Bragstadsplass 8, N-7034 Trondheim, Norway

Advances in Industrial Control

Professor Dr -Ing M. Thoma
Westermannweg 7
40419 Hannover
Germany

Professor H. Kimura
Department of Mathematical Engineering and Information Physics
Faculty of Engineering
The University of Tokyo
7-3-1 Hongo
Bunkyo Ku
Tokyo 113
Japan

Professor A.J. Laub
College of Engineering - Dean's Office
University of California
One Shields Avenue
Davis
California 95616-5294
United States of America

Professor J.B. Moore
Department of Systems Engineering
The Australian National University
Research School of Physical Sciences
GPO Box 4
Canberra
ACT 2601
Australia

Dr M.K. Masten
Texas Instruments
2309 Northcrest
Plano
TX 75075
United States of America

Professor Ton Backx
AspenTech Europe B.V.
De Waal 32
NL-5684 PH Best
The Netherlands

To Gøril, Irja, Mina and Birk

Jan Tommy Gravdahl

To Trude, Tom, Randi, Kristin and Haakon

Olav Egeland

SERIES EDITORS' FOREWORD

The series *Advances in Industrial Control* aims to report and encourage technology transfer in control engineering. The rapid development of control technology impacts all areas of the control discipline. New theory, new controllers, actuators, sensors, new industrial processes, computer methods, new applications, new philosophies..., new challenges. Much of this development work resides in industrial reports, feasibility study papers and the reports of advanced collaborative projects. The series offers an opportunity for researchers to present an extended exposition of such new work in all aspects of industrial control for wider and rapid dissemination.

Operating plant as close as possible to constraint boundaries so often brings economic benefits in industrial process control. This is the conundrum at the heart of this monograph by Tommy Gravdahl and Olav Egeland on stall control for compressors. Operation of the compressor closer to the surge line can increase operational efficiency and flexibility

The approach taken by the authors follows the modern control system paradigm: - physical understanding, detailed modelling and simulation studies and finally control studies. The thoroughness of the presentation, bibliography and appendices indicates that the volume has all the hallmarks of being a classic for its subject. Despite the monograph's narrow technical content, the techniques and insights presented should appeal to the wider industrial control community as well as the gas turbine/compressor specialist.

M.J. Grimble and M.A. Johnson
Industrial Control Centre
Glasgow, Scotland, UK

PREFACE

Finally, the first author would like to express his love and deepest gratitude to his family: To his wife Gøril for her love, continued encouragement, support, and many useful suggestions during the work, and to his children Irja, Mina and Birk for their unconditional love.

<div align="right">

Jan Tommy Gravdahl and Olav Egeland

September 1998, Trondheim, Norway

</div>

The monograph makes reference to the following trademarks: MATLAB(R) and SIMULINK(R) are registered trademarks of The Mathworks, Inc.

CONTENTS

LIST OF FIGURES

CHAPTER 1

COMPRESSOR SURGE AND STALL: AN INTRODUCTION

1.1   Introduction

In this monograph, results from an investigation on nonlinear compressor control where active control is used to stabilize the compressor to the left of the surge line are presented. New results within the field of compressor modeling are also included. The work is motivated by the fundamental instability problem of surge and rotating stall which limits the range of operation for compressors at low mass flows.

This instability problem has been extensively studied and industrial solutions based on *surge avoidance* are well established. These solutions are based on keeping the operating point to the right of the compressor surge line using a surge margin. However, there is a potential for

1. Increasing the efficiency of compressors by allowing for operation closer to the surge line than what is the case in current systems, and

2. Increasing the range of mass flows over which the compressor can operate stably.

The increase in efficiency and mass flow range is in particular possible with compressor designs where the design is done with such controllers in mind. This, however, raises the need for control techniques, which stabilize the compressor also to the left of the surge line, as disturbances or set point changes may cause crossing of the surge line. This approach is known as

active surge control. Active surge control is presently an area of very intense research activity, and is also the topic of this text.

In this Chapter, a basic introduction to compressors and compression system instabilities will be given. Further, an overwiev over the current state of compression system modelling and control will be given. This Chapter is organized as follows:

- In Section 1.2, a basic introduction to axial and centrifugal compressors is given.

- Section 1.3 contains an overview of areas of application of compressors, including jet engines, turbochargers and soforth.

- Surge and rotating stall are described in section 1.4.

- In Sections 1.5, 1.6 and 1.7, several dynamic models for compression systems found in the litterature are presented.

- Surge avoidance schemes are discussed in Section 1.8, while several results on acive surge control are presented in Section 1.9

- Finally, in Section 1.10, selection of sensors and actuators for active surge control is studied.

1.2   Compressors

1.2.1   Types of compressors

Ferguson (1963) defines the function of a compressor as:

It is the function of a compressor to raise the pressure of a specified mass flow of gas by a prescribed amount using the minimum power input.

Compressors are used in a wide variety of applications. These includes turbojet engines used in aerospace propulsion, power generation using industrial gas turbines, turbocharging of internal combustion engines, pressurization of gas and fluids in the process industry, transport of fluids in pipelines and so on.

Nisenfeld (1982) divide compressors into four general types: reciprocating, rotary, centrifugal and axial. Some authors use the term radial compressor when refering to a centrifugal compressor. Reciprocating and rotary compressors work by the principle of reducing the volume of the gas, and will not be considered further in this work. Centrifugal and axial compressors, also known as turbocompressors or continuous flow compressors, work by the principle of accelerating the fluid to a high velocity and then converting

this kinetic energy into potential energy by decelerating the gas in diverging channels. In axial compressors the deceleration takes place in the stator blade passages, and in centrifugal compressors it takes place in the diffuser. The increase in potential energy of the fluid is manifested by a pressure rise. This conversion can be explained from the Bernoulli equation:

$$\frac{p_1}{\rho} + \frac{C_1^2}{2} + gz_1 = \frac{p_2}{\rho} + \frac{C_2^2}{2} + gz_2,$$

where p is the pressure, ρ is the density of the fluid, C is the velocity of the fluid and gz the potential energy per unit mass. Subscripts 1 and 2 denotes properties before and after deceleration, respectively. The equation is a special case of the law of conservation of energy developed for flowing fluids. Bernoulli's equation states that the sum of kinetic energy $\frac{C^2}{2}$, potential energy gz and pressure head $\frac{p}{\rho}$ at one set of conditions is equal to their sum at another set of conditions. Hence, decrease in kinetic energy implies an increase in potential energy and pressure.

One obvious difference between the two types of turbocompressors is that, in axial compressors, the flow leaves the compressor in the axial direction, whereas in centrifugal compressors, the flows leaves the compressor in a direction perpendicular to the axis of the rotating shaft. Axial compressors can accept higher mass flow rates than centrifugal compressors for a given frontal area. This is one reason for axial compressors dominance in jet engines, where frontal area is of great importance. Another reason for this is that for gas turbines, or jet engines, specific fuel consumption decreases with increasing pressure ratio. According to (Cohen *et al.* 1996), the axial compressor, using multiple stages, can achieve higher pressure ratio and efficiency than the centrifugal. However, as Cumpsty (1989) states, the efficiency question is not altogether clear.

Here, both types of continuous flow compressor will be studied. According to Ferguson (1963), compressors may be known as fans, blowers, boosters, turbochargers, exhausters or compressors, the distinctions between these types being vague. Broadly speaking, fans are low pressure compressors and blowers are medium-pressure compressors. Boosters, exhausters and turbochargers are named from their application. The literature on compressors in general is vast, and a basic introduction is given by e.g. Ferguson (1963), Cherkassky (1980) or Cohen *et al.* (1996), and more advanced topics are covered by e.g. Greitzer (1985*a*) or Cumpsty (1989).

1.2.2   The axial compressor, principles of operation

A stage of an axial compressor consists of a row of rotor blades and a row of stator blades. A single stage, as shown in Figures 1.1 and 1.2, has often

a too low pressure ratio (1.1:1 to 1.2:1 according to Mattingly (1996)) for most applications. This is due to the limit imposed on the rate of change of the crossectional area in a diffusing flow. Therefore, it is very common to use multistage axial compressors in which case the compressor consists of a series of stages, each having a row of rotor blades and a row of stator blades, where the number of stages depends of the desired pressure ratio. The flow path in an axial compressor has a decreasing cross-sectional area. This decrease is in the direction of flow and is in proportion to the increasing density of the gas. In Figures 1.1 and 1.2, the numbers 1,2 and 3 refers to the same locations in the compressor. Location 1 is the rotor inlet, location 2 is rotor exit or stator inlet, and location 3 is stator exit. In these sketches, no tangential component of the velocity at the rotor inlet has been drawn. If inlet guide vanes are used, the flow is guided into the first stage, and C_1 is given a suitable tangential component.
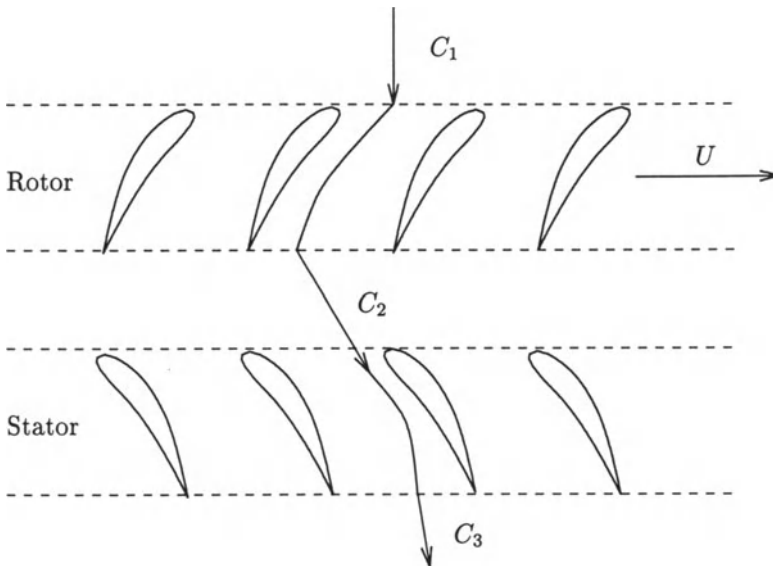
Figure 1.1: *Blade rows (Cylindrical cross section).*

The compressor consists essentially of two assemblies: the rotor (spool with rotor blades) and the stator (casing with stator blades). The gas is accelerated in the rotor blades, and decelerated in the stator blades, thereby converting the kinetic energy gained in the rotor into static pressure. All the power is transferred to the gas in the rotor, the stator merely transforms kinetic energy to an increase in static pressure with the stagnation temperature remaining constant.
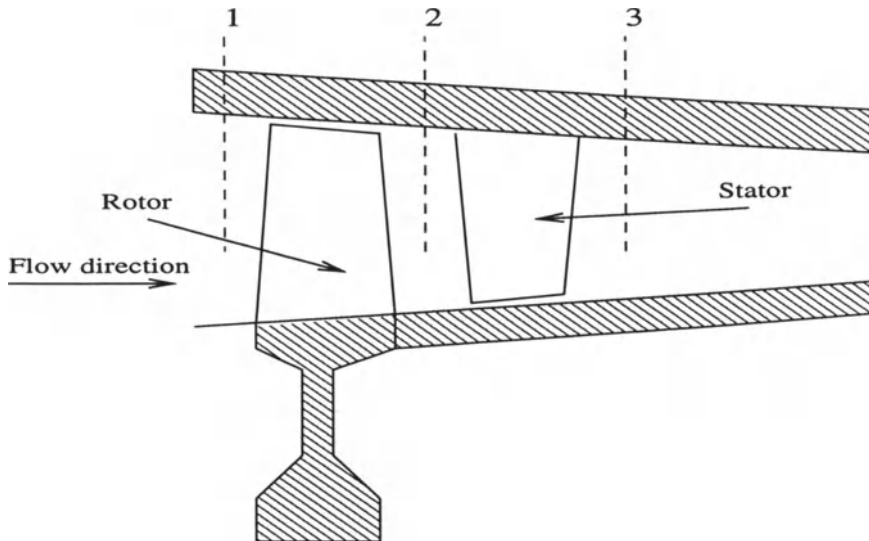
Figure 1.2: *One stage of an axial compressor (Axial cross section).*

The reader is referred to Horlock (1958) and Cohen *et al.* (1996) for comprehensive treatment of axial compressor fundamentals including references.

1.2.3 The centrifugal compressor, principles of operation

The centrifugal compressor consists essentially of a stationary casing containing a rotating impeller which imparts a high velocity to the fluid, and a number of fixed diverging passages in which the air is decelerated with a consequent rise in static pressure. The latter process is one of diffusion, and consequently, the part of the compressor containing the diverging passages is known as the diffuser. Figure 1.3 is a diagrammatic sketch of the impeller and diffuser of a centrifugal compressor. The impeller is mounted on a shaft which is either a direct extension of the drive shaft or a separate shaft supported by bearings and driven through a coupling. The shaft and impeller assembly, called the rotor, are seated in the casing.

The impeller:
The fluid is sucked into the impeller eye and whirled round at high speed by the vanes on the impeller disc. According to Cohen *et al.* (1996), at any point in the flow through the impeller, the centripetal acceleration is obtained by a pressure head, so that the static pressure of the fluid increases from the eye to the tip of the impeller. The remainder of the static pressure rise is obtained in the diffuser, and it is common to design the compressor so that
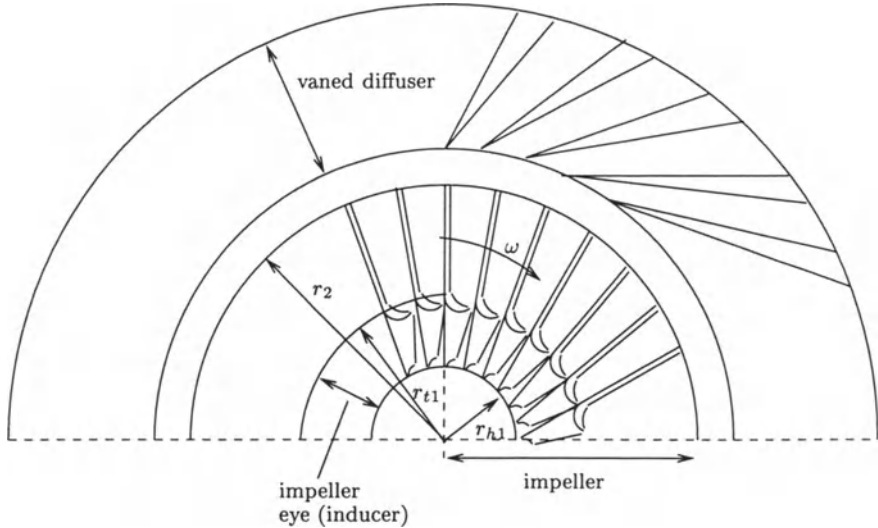
Figure 1.3: *Diagrammatic sketch of a radially vaned centrifugal compressor. Shown here with a vaned diffuser.*

about half the pressure rise occurs in the impeller and half in the diffuser. As no work is done on the fluid in the diffuser, the energy absorbed by the compressor will be determined by the conditions at the inlet and outlet of the impeller. The flow in the impeller is not completely guided by the vanes and hence the effective fluid outlet angle is not equal to the vane outlet angle. To account for this deviation, a factor known as the slip factor is used to correct the energy transfer calculated from simple one-dimensional theory.

The diffuser:
It is more difficult to obtain efficient deceleration of flow than it is to obtain efficient acceleration. If divergence in the diffuser is too rapid, the fluid will tend to break away from the the walls of the diverging passage, reverse its direction and flow back in the direction of the pressure gradient. This may lead to the formation of eddies with consequent transfer of some kinetic energy into internal energy and a reduction of useful pressure rise. On the other hand, a small angle of divergence will lead to a long diffuser and high losses due to friction. In order to carry out the diffusion in as short a length as possible, the air leaving the impeller may be divided into a number of separate diverging passages separated by fixed diffuser vanes, resulting in a vaned diffuser. However, in industrial applications where size may be of secondary importance a vaneless diffuser may have the economic advantage as it is much cheaper to manufacture than the vaned diffuser. A vaneless dif-

fuser is a simple annular channel, and is therefore also known as an annular diffuser, in which the radial velocity component is reduced by area increase and the tangential velocity component by the requirement of constant fluid angular momentum. If the disadvantage of the annular diffuser is its bulk, the advantage is its wide range of operation. A vaned diffuser may have a higher peak efficiency than an annular diffuser, but its mass flow range is considerable less because of early stall of the diffuser vanes. This will be treated in detail in Chapter 5.

The volute
The function of the volute (also known as a scroll or a collector) is simply to
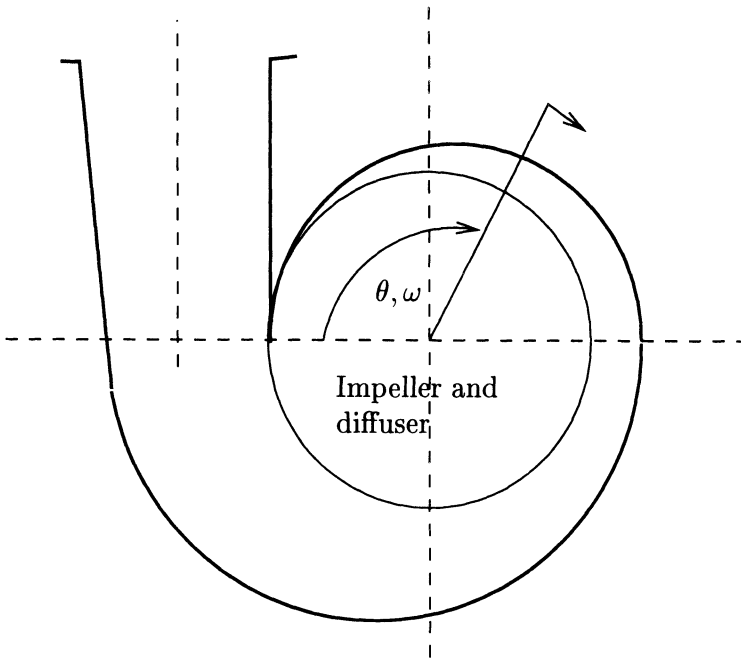
Figure 1.4: *Diagrammatic sketch of centrifugal compressor fitted with a volute.*

collect the diffuser exit flow, and to guide it as efficiently as possible to the compressor outlet, without impeding the effectiveness of the diffuser, (Watson and Janota 1982). Volutes are used for industrial gas turbines, turbochargers and other applications where size is not of great importance. For aircraft jet engines, where volume and frontal area are important, other solutions are used.

1.3 Application of compressors

1.3.1 Gas turbines and jet engines for propulsion and power generation

A gas turbine consists of a compressor, combustion chamber and turbine. The compressor provides a certain pressure rise to the working fluid, which is usually air. In the combustion chamber, fuel is burned in the compressed air and thus raising the temperature. Expansion over the turbine then produces a useful power output in addition to the power needed to drive the compressor. A simple gas turbine is sketched in Figure 1.5. Gas turbines are used in a variety of applications, such as electricity production, aircraft propulsion and marine propulsion.
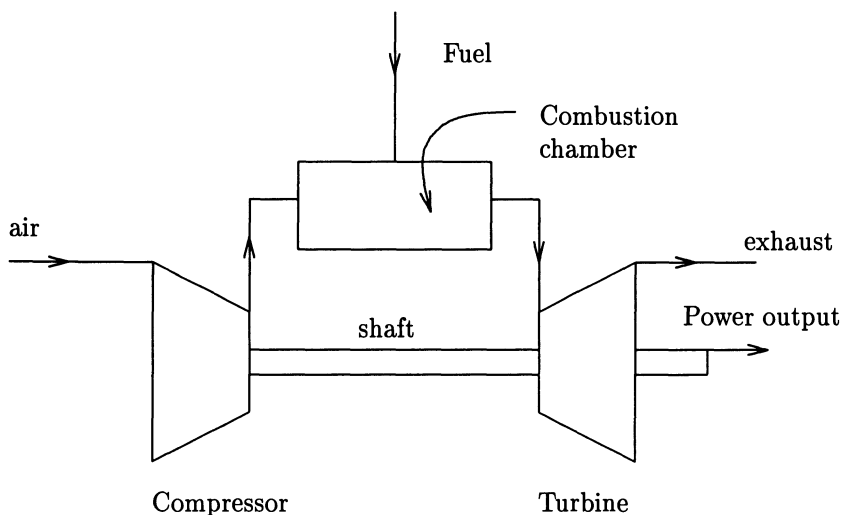
Figure 1.5: *Sketch of simple gas turbine.*

The first gas turbine to deliver positive (excess) power was constructed by the Norwegian Ægidius Elling in 1903, (Johnson and Mowill 1968). According to Johnson (1985), his machine used a six stage centrifugal compressor with variable-geometry diffusers and water injection between stages. The gas turbine produced 8 kW of power. Elling patented his first gas turbine concept in 1884, and several more during the first three decades of the twentieth century. In 1933, Elling wrote: "When, in 1882, I started work on the gas turbine, it was with aeronautics in mind and I firmly believe that aeronautics is still waiting for the gas turbine", (Johnson 1985).

Aircraft propulsion

According to the foreword by Hans von Ohain in Mattingly (1996), several gas turbine concepts intended for aircraft propulsion were patented during the first two decades of the twentieth century, but the aircraft industry was yet not ready for this technology. One problem was finding materials that could withstand the high temperatures of the gas turbine, and another was the too-slow speed capability of the aerovehicles of that time, (Mattingly 1996). Therefore, the first patent of a turbojet engine, which was later developed, produced and used for aircraft propulsion was that of Frank Whittle in 1930. Independent of this, Hans von Ohain patented a jet engine in 1935. The first flight powered by a gas turbine took place on August 27, 1939, when the He-178 aircraft flew using a He.S3B jet engine constructed by von Ohain. On May 15, 1941 the Gloster-Whittle E28/39 took off using Whittles jet engine.[1]

In Mattingly (1996), several types of gas turbine engines or jet engines are distinguished: turbojet, turbofan, turboprop and turboshaft. The essential component of these engines is the gas generator, which consists of a (multi-stage) compressor, combustion chamber and (multistage) turbine, as shown in Figure 1.5. The purpose of the gas generator is to produce high-temperature and high pressure gas. By adding a inlet and nozzle to the gas generator, a turbojet can be constructed, as shown in Figure 1.6 a). The first gas turbines by von Ohain and Whittle were turbojets, and since then there has been an enormous development in construction and development of turbojets, especially for propulsion of military aircraft. The thrust of a turbojet is developed by the acceleration of the exhaust flow through the nozzle. A gas generator that drives a propeller, as sketched in Figure 1.6 b), is known as a turboprop engine. In a turboprop the total thrust is achieved through a combination of the thrust from the propeller and the thrust from the exhaust in the nozzle. Turboprops are used for low-speed aircraft. A turbofan is shown in Figure 1.6 c). Here, the turbine also powers a ducted fan (low pressure ratio compressor) placed in front of the compressor. Part of the airflow is bypassed the gas generator and forms an annular propulsive jet of cooler air surrounding the hot jet. This results in a jet of lower mean velocity and lower thrust specific fuel consumption (fuel mass flow per unit thrust), (Mattingly 1996). The bypass also significantly reduces exhaust noise. The turboshaft, as shown in Figure 1.6 d), is used in helicopters. In this case the turbine drives the main and tail rotors of the helicopter through a complex gear-box and frequently two engines are coupled to a single rotor, (Cohen *et al.* 1996).

---

[1]Whittle (1953) claims that the He-178 flew for only ten minutes and never flew again, and that no other jet aircraft flew before the Gloster-Whittle E28/39. On the other hand, in the foreword of Mattingly (1996), von Ohain claims that in addition to the August 27 1939 flight, the He.S3B flew again on November 1st the same year, and the He-280 flew using two He.S8A engines in late March 1941.

A wide variety of jet engines can be found among the four types described
above. Centrifugal or axial compressors or both may be used, the engine can
have one or several spools and free power turbines and afterburners may be
fitted. There are also variations in how many compressor and turbine stages
the engines may have.
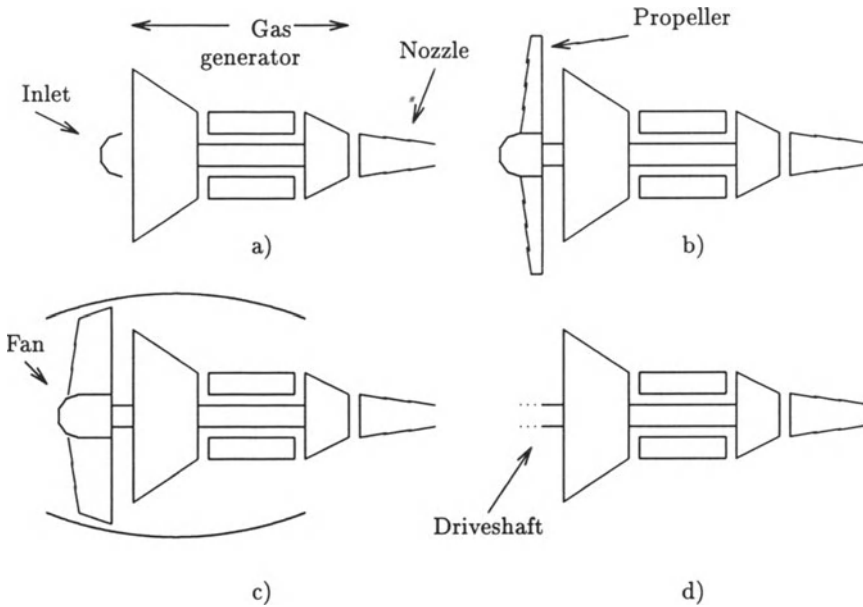
Figure 1.6: *Different types of gas turbine type of engines for aircraft propul-
sion. a) Turbojet, b) Turboprop, c) Turbofan, d) Turboshaft*

Marine propulsion

Gas turbines are used for propulsion of both military and commercial ma-
rine vessels. Usually, the gas turbines employed are aeroderivatives, that is,
modified versions of gas turbines designed for aircraft propulsion. Commer-
cial ships using gas turbines include yachts, fast ferries, fast cargo ships and
recently also cruise liners. A disadvantage of the gas turbine in naval use is
its poor specific fuel consumption at part load. To overcome this, gas tur-
bines are used in combined power plants together with steam turbines, diesel
engines and other gas turbines.

The main advantage for using gas turbine propulsion for high speed craft is
the low weight of a gas turbine compared to a diesel engine. Other advantages
of gas turbine propulsion include the possibility for very low environmental

emissions, the high reliability inherited from the aircraft engines, size, and availability. It is easier to replace a lightweight gas turbine than a large diesel engine.

In other areas of transportation (railroads, trucks, cars, etc) the gas turbine has been considered without making any real impact. The major problem being the part-load fuel consumption, (Cohen *et al.* 1996).

Power generation

Gas turbines are widely used in industrial power plants or to drive other equipment. Both aeroderivatives and heavy-duty gas turbines specifically designed for industrial purposes are used. Power plants that produce electricity using gas turbines were earlier used for peaking and emergency applications. However, today it is more usual to use such powerplants for base-load duty. Gas turbines are also widely used in combined cycle (CC) plants in combination with steam turbines or diesel engines. Another major market for electricity generation is the provision of power for off-shore oil and gas production platforms. Gas turbines also find use in combined heat and power (CHP) plants (also known as cogeneration plants) plants, where a combined production of heat and power takes place. Different types of CC and CHP plants are discussed by Ordys *et al.* (1994).

Numerous papers and textbooks have been written on gas turbines, see e.g. Whittle (1981), Cohen *et al.* (1996) or Mattingly (1996).

1.3.2   Compression in the process industry

Compressors are used for many different purposes in a wide variety of industrial processes. Examples are refrigeration systems for low-temperature distillation, ammonia production, urea production, nitric acid production and oil-gas separation on offshore production platforms, (Balchen and Mummé 1988). Many types of compressors are used in this industry, but among the most important are centrifugal compressors.

1.3.3   Transportation of gases and fluids in pipelines

Compressors are often used to provide the pressure differential needed to move gases through chemical processes and fluids through pipelines. Pipeline compressors operate with high flows and low compression ratios. According to Pichot (1986), a usual compression ratio for this application is $1.1 - 1.3$ for single impeller compressors operating in series, and slightly higher for compressors operating in parallel.

A major difference between liquids and gases is that for most practical purposes most liquids can be assumed to be incompressible. Therefore, the dynamic characteristics of a gas are very different from those of a liquid even though the static characteristics are similar. Pressure buildup can be very fast in a liquid system, and very slow in a gas. The pressure effect in a long, small-diameter pipe is distributed along the pipe, requiring analysis by the means of partial differential equations. For an overview on this subject, see Thorley and Tiley (1987).

Pumps and compressors used for transportation can be driven by electrical motors or gas turbines. For natural gas transmission pipelines, it is usual that the compressors are powered by gas turbines. The reason for this is that the turbines use the fluid being pumped as fuel. According to Cohen *et al.* (1996), a typical pipeline might consume 7-10 per cent of the throughput for compression purposes. A schematic drawing of a pipeline compressor powered by a gas turbine with a free power turbine is shown in Figure 1.7. The gas turbine is fed with fuel from the pipeline.
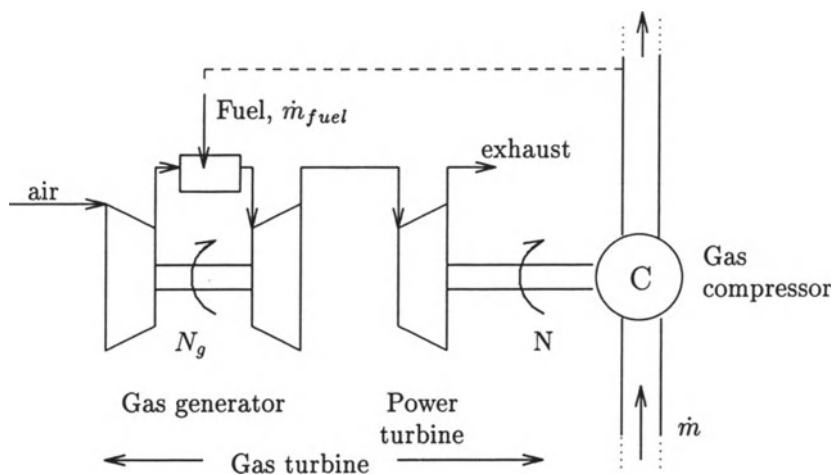
Figure 1.7: *Pipeline compressor powered by gas turbine.*

1.3.4 Supercharging of internal combustion engines

Another area where compressors are used is in supercharging of internal combustion engines. Watson and Janota (1982) defines supercharging as the introduction of air (or air/fuel mixture) into an engine cylinder at a density greater than ambient. The maximum power a given IC engine can deliver is limited by the amount of fuel that can be burned. This again, is limited by

the amount of air that is introduced into the cylinder each cycle. By increasing the density of the air prior to injection into the cylinder, the power of the engine will be increased. Due to the different nature of spark ignition (petrol) engines and compression ignition (diesel) engines, turbocharging was earlier mostly used on diesel engines. This is due to problems with engine knock in petrol engines if the cylinder pressure is too high. However, this problem can be remedied by the use of exhaust waste gates and a number of other techniques. According to Heywood (1988) the term supercharging refers to all methods of increasing the inlet air pressure: Mechanical supercharging, one and two stage turbocharging with or without intercooler, engine driven compressor and turbocharger and turbocomponding.
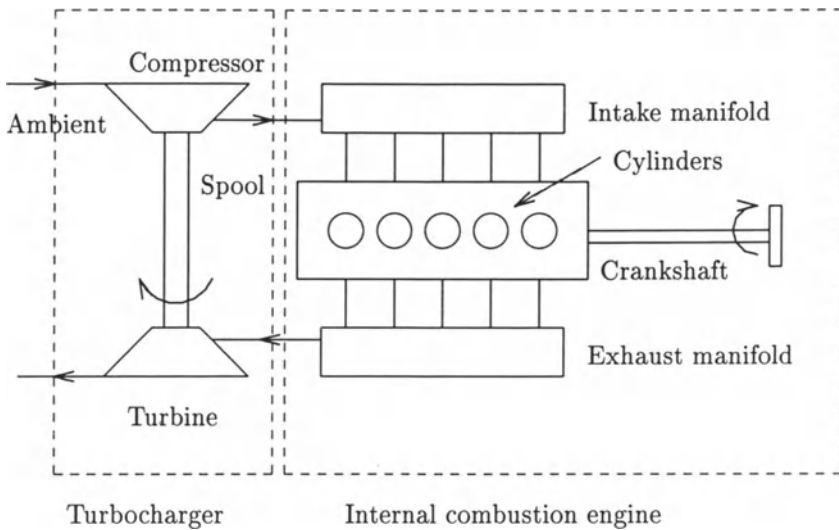
Figure 1.8: *A turbocharged engine with constant pressure turbocharging.*

The most common method of supercharging is turbocharging. The principle is shown in Figure 1.8: The high energy exhaust flow is used to drive a turbine, which in turn powers the compressor which compresses the intake air. The compressor and turbine form a self-contained unit: The turbocharger. Two different approaches can be distinguished, constant pressure turbocharging and pulse turbocharging. In constant pressure turbocharging, a large chamber is connected to the exhaust manifolds of all the engines cylinders. This causes the flow to the turbine to be essentially steady (constant pressure). The pulse method on the other hand, employs no such chamber, and the turbine operates with varying pressure. The idea is to utilize the high kinetic energy of the exhaust leaving the cylinder.

1.4   Stability of Compression Systems

The useful range of operation of turbocompressors, both axial and centrifugal, is limited, by choking at high mass flows when sonic velocity is reached in some component, and at low mass flows by the onset of two instabilities known as surge and rotating stall. Traditionally, surge and rotating stall have been avoided by using control systems that prevent the operating point of the compressions system to enter the unstable regime to the left of the *surge line*, that is the stability boundary. A fundamentally different approach, known as active surge/stall control, is to use feedback to stabilize this unstable regime. This approach will be investigated in this book, and it will allow for both operation in the peak efficiency and pressure rise regions located in the neighborhood of the surge line, as well as an extension of the operating range of the compressor.

Compression systems such as gas turbines can exhibit several types of instabilities: combustion instabilities, aeroelastic instabilities such as flutter, and finally aerodynamic flow instabilities, which this study is restricted to.

As mentioned, two types of aerodynamic flow instabilities can be encountered in compressors: *surge* and *rotating stall*. The instabilities limit the flow range in which the compressor can operate. Surge and rotating stall also restrict the performance (pressure rise) and efficiency of the compressor. According to de Jager (1995) this may lead to heating of the blades and to an increase in the exit temperature of the compressor.

1.4.1   Surge

Surge is an axisymmtrical oscillation of the flow through the compressor, and is characterized by a limit cycle in the compressor characteristic. An example of such a characteristic is shown as the S-shaped curve in Figure 1.9. The characteristic show the pressure rise over the compressor as a function of the mass flow. The dotted segment of the curve indicates that this section usually is an approximation of the physical system, as it is difficult to measure experimentally. Surge oscillations are in most applications unwanted, and can in extreme cases even damage the compressor. As discussed by Erskine and Hensman (1975) and Greitzer (1981), surge can also induce vibrations in other components of the compression system, such as e.g. connected piping. It is common to distinguish between at least two different types of surge: 1) Mild/Classic surge and 2) Deep surge. A combination of surge and rotating stall is known as modified surge. For more information on different types of surge, consult Greitzer (1981) or de Jager (1995). According to Whittle (1953), surge was recognized as a serious problem in designing compressors already in the first jet engine designs.

Surge is essentially a one-dimensional phenomenon with an unsteady, but circumferentially uniform, annulus-averaged mass flow. This holds for fully developed surge, but is not the case during the initial surge transient. According to Cumpsty (1989), one of the most damaging effects of surge in high pressure ratio axial compressors is the very large transverse load placed on the rotor and the casing because of non-axisymmetric surge. This may lead to severe blade rubbing and then a range of further damage. The origin of this non-axisymmetry is that in the initial phase of surge, the reverse flow has to grow from some initiation point and the axial length of the compressor is likely to be considerably less than the circumference. Mild/classic surge is a phenomenon with oscillations in both pressure and flow in the compressor system, while in deep surge, the mass flow oscillations have such a large amplitude, that flow reversal occurs in the compression system. A drawing of a typical deep surge cycle is shown in Figure 1.9. The cycle starts at (1) where the flow becomes unstable. It then jumps to the reversed flow characteristic (2) and follows this branch of the characteristic until approximately zero flow (3), and then jumps to (4) where it follows the characteristic to (1), and the cycle repeats.
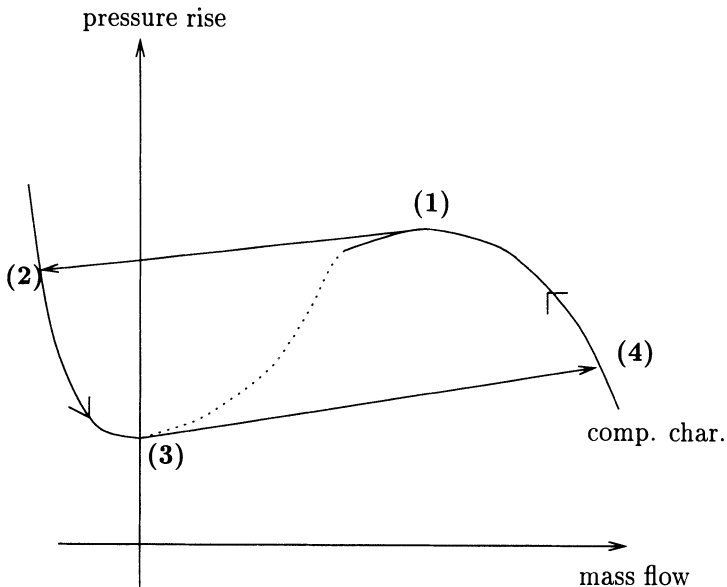
Figure 1.9: *Compressor characteristic with deep surge cycle, de Jager (1995).*

The mechanism behind surge can be explained as follows (Watson and Janota 1982). First, consider a compressor operating between two constant pressure reservoirs. The compressor is equipped with a downstream throttle valve. First the compressor operates at point A on the compressor characteristic of

Figure 1.10. Imagine a sudden disturbance, in the form of partially closing the throttle valve and thereby temporarily reducing the flow (not beyond the maximum of the characteristic). This results in an increase in the delivery pressure from the compressor and a reduction in compressor flow. The increased delivery pressure encourages a larger mass flow through the throttle, reducing compressor delivery pressure and increasing compressor flow. This is therefore self compensating, an inherently stable system.

Now, consider the compressor operating at point B on the compressor characteristic of Figure 1.10. A reduction in mass flow would now result in reduced compressor delivery pressure reducing flow though the throttle, moving the operating point further and further to the left. Eventually, the mass flow reduction would be so great that the pressure upstream of the throttle falls below the compressor delivery pressure (whose minimum is given by the centrifugal pressure rise at zero flow, point C). Mass flow will then increase until the system is drawn back to operating point B, and the whole cycle repeat. This discussion also shows that operating points with positive compressor characteristic slope are unstable and operating points with negative compressor characteristic slope are stable. Surge can occur in both axial and
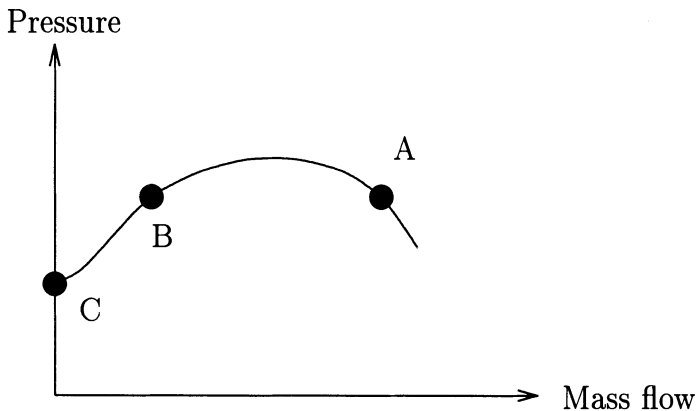
Figure 1.10: *Compressor characteristic.*

centrifugal compressors, and as pointed out above, positive compressor characteristic slope is a necessary condition for surge to occur. For centrifugal compressors, the components are strongly coupled and it is the combined effect of the various components of the compressor that determine the system instability. The system instability is influenced by the matching of the components such as the impeller, diffuser and volute.

Dean (1974) studied a basic compression system with centrifugal compressor,

plenum and throttle. For this case the flow is stable if

$$\frac{\partial PR}{\partial m} \leq 0, \qquad (1.1)$$

where PR is is the overall compressor total-to-static pressure ratio and m is the mass flow rate. The pressure ratio is the product of the pressure ratios of the n individual components such that

$$PR = \prod_{i=1}^{n} PR_i, \qquad (1.2)$$

where PR_1 could be the pressure ratio of the impeller and so on. Now, the stability criterion (1.1) can be written

$$\frac{\partial PR}{\partial m} = PR \sum_{i=1}^{n} \frac{1}{PR_i} \frac{\partial PR_i}{\partial m} \triangleq PR \sum_{i=1}^{n} SP_i \leq 0. \qquad (1.3)$$

Components for which SP_i is positive are destabilizing and those for which it is negative are stabilizing (Cumpsty 1989). There is much variation in the literature on determining which component is the most important contributor to instability. Elder and Gill (1985) found that the semi-vaneless space between the impeller and the diffuser has the most negative SP, whereas in Fink *et al.* (1992) found that it was the vaneless diffuser while Dean (1974) the vaned diffuser. Wo and Bons (1994) carried out a detailed component-by-component stability analysis of a centrifugal pump and found the most destabilizing component to be the vaneless pipe diffuser. Similar results were found by Hunziker and Gyarmathy (1994) who found that the diffuser channels play an inherently destabilizing role while the impeller and the diffuser inlet are typically stabilizing.

The frequency of surge oscillations are typically much less (more than an order of magnitude) than those associated with rotating stall. Experiments done by e.g. Hansen *et al.* (1981) or Pinsley *et al.* (1991) show that the surge frequency is of the same magnitude as the Helmholtz frequency of the system. According to Willems (1996), the surge frequency during deep surge (surge with flow reversal) is normally well below the Helmholtz frequency since it is set by the plenum filling and emptying time. The surge frequency decreases with increasing rotational speed and increasing positive compressor characteristic slope.

1.4.2   Rotating Stall

Rotating stall can occur in both axial and centrifugal compressors. Although rotating stall is known to occur in centrifugal compressors, see e.g. Emmons *et al.* (1955), there exists little theory on the subject, and according to

de Jager (1995) its importance is still a matter of debate. Here, only rotating stall in axial compressors will be considered, and when it is referred to rotating stall it is to be understood that an axial compressor is considered.

Rotating stall is an instability where the circumferential flow pattern is disturbed. This is manifested through one or more *stall cells* of reduced, or stalled, flow that propagate around the compressor annulus at a fraction of the rotor speed. Following Greitzer (1980), the stall cell propagation speed may be 20-70% of the rotor speed. Cumpsty and Greitzer (1982) derived a model for stall cell speed, showing that stall cell speed increases with increasing number of compressor stages. Rotating stall leads to a reduction of the pressure rise of the compressor, and in the compressor map this corresponds to the compressor operating on the so called in-stall characteristic, see Figure 1.12.
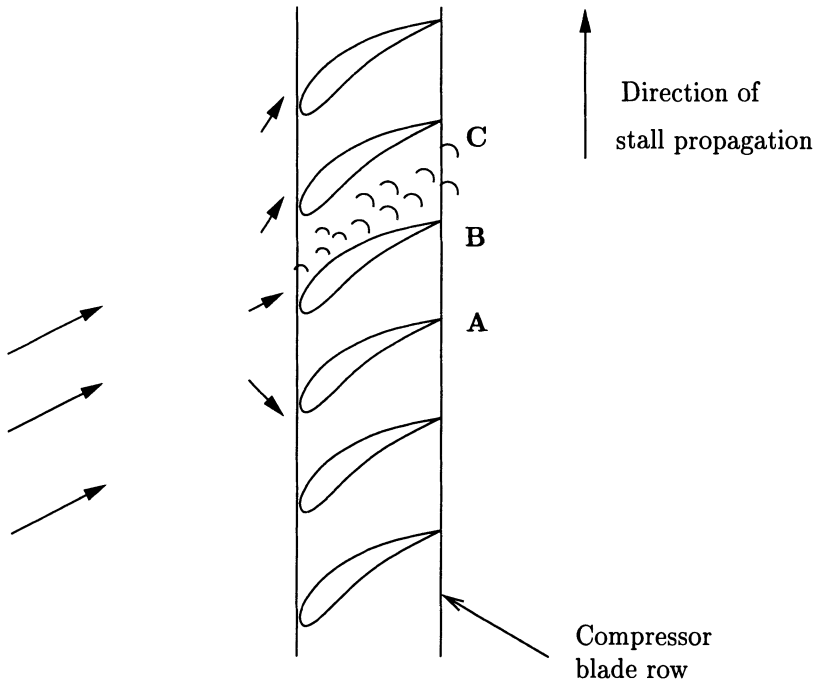
Figure 1.11: *Physical mechanism for inception of rotating stall, Emmons et.al. (1955).*

The basic explanation of the rotating stall mechanism was given by Emmons *et al.* (1955) and can be summarized as follows. Consider a row of axial compressor blades operating at a high angle of attack, as shown in Figure 1.11. Suppose that there is a non-uniformity in the inlet flow such that a locally higher angle of attack is produced on blade B which is enough to stall it. The

flow now separates from the suction surface of the blade, producing a flow blockage between B and C. This blockage causes a diversion of the inlet flow away from B towards A and C, resulting in a increased angle of attack on C, causing it to stall. Thus the stall cell propagate along the blade row.

It is common to distinguish between at least two types of rotating stall, full-span and part-span. In full-span stall, the complete height of the annulus is stalled, while in part-span rotating stall a restricted region of the blade passage is stalled. Full-span stall is most likely to occur in high hub/tip ratio axial compressors, and according to Giannissis et al. (1989) part-span stall is more relevant to high-speed multistage compressors. There can be various degrees of rotating stall depending of the size of the area of the compressor annulus being blocked. In addition to the problem related to reduced pressure rise due to rotating stall, there is also the problem of vibrations in the blades as stall cells rotate at a fraction of rotor speed. Thus, the blades passes in and out of regions of stalled flow which can, according to Horlock (1958), Greitzer (1981) and Pinsley et al. (1991), induce vibrations in the blades. Moreover, if a natural frequency of vibration of the blades coincides with the frequency at which the stall cell pass a blade, the result is resonance and possible mechanical failure due to fatigue.

Another consequence of rotating stall is the hysteresis occurring when trying to clear the stall by using the throttle. This phenomenon is depicted in Figure 1.12, and might be described in the following manner: Initially the compressor is operating stably (1), then a disturbance drives the equilibrium over the surge line resulting in rotating stall, and a operating point on the low pressure in-stall[2] characteristic (2). By opening the throttle to clear the stall, a higher throttle opening than initially (3) is required, before the operating point is back on the stable compressor characteristic (4). There are several degrees of the severity of this hysteresis. This depends on the so called skewness of the compressor characteristic. This is treated in detail by Wang and Krstić (1997a), Sepulchre and Kokotović (1996) and Protz and Paduano (1997).

It should be noted that although rotating stall is not considered important for centrifugal compressors, see e.g. Day (1994) and de Jager (1995), it can nonetheless occur in these machines, (Willems 1996). In fact, the first report of rotating stall was in a centrifugal compressor, (Cheshire 1945). Watson and Janota (1982) states that rotating stall may or may not lead to stage instability, but can introduce aerodynamically induced vibrations resulting in increased noise level. Normally the compressor can operate quite stably, although some of its components may be in a mode of stall. Cumpsty (1989) claims that this tolerance to stalled regions is largely due to that so

---

[2]A technique for extracting the in-stall characteristic for an axial flow compressor is presented by Lorenzo et al. (1986)

pressure
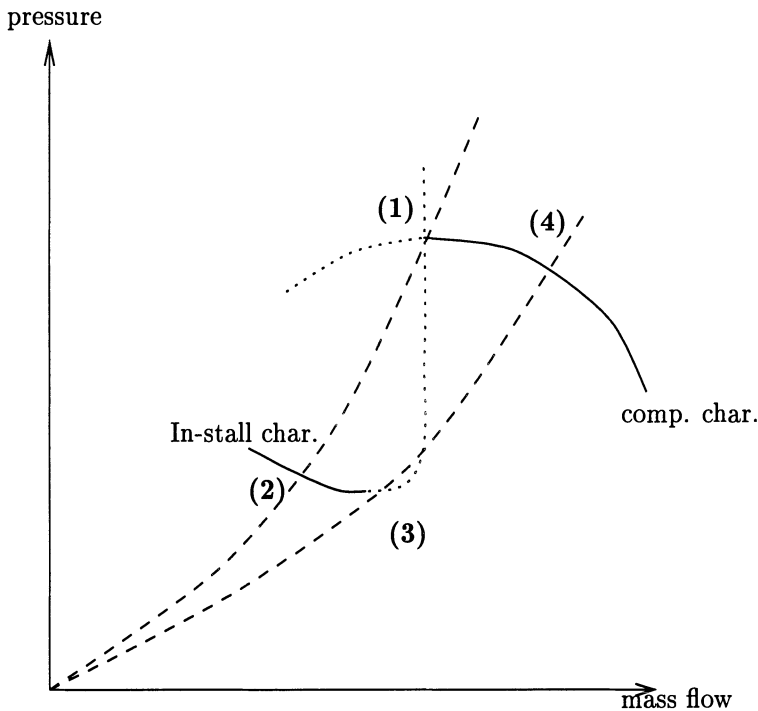
Figure 1.12: *Schematic drawing of hysteresis caused by rotating stall. Solid lines represent stable equilibria and dotted lines represent unstable equilibria. The dashed lines are the throttle lines for the onset and clearing of stall.*

much of the pressure rise is being produced by centrifugal effects which will occur even in the presence of rotating stall cells or other forms of separated flow. However, at some point where the stall becomes severe, it may induce stage instability and surge, (Watson and Janota 1982). This is confirmed experimentally by Fink *et al.* (1992) who found that impeller stall initiated deep surge in a high-speed single-stage centrifugal compressor.

1.4.3   Other instabilities

Several other instabilities can be encountered in compression systems. Examples are combustion instabilities in gas turbines, aeroelastic instabilities such as flutter, mass flow and pressure oscillations (buzz) in supersonic intakes diffusers, self-exited lateral vibrations (rotor whirl), instabilities in two-phase flow systems and so on. A thorough review of such instabilities (in addition to surge and rotating stall) can be found in Greitzer (1980) and Cumpsty (1989). They will, however, not be treated further in this text.

1.5   Previous work on modeling of axial compression systems

1.5.1   Why model compression systems?

One answer to this question is:

> The development of a suitable control system requires a deep understanding of the transient behavior of the gas turbine to be controlled, particularly for new types of engines where no previous experience exists. If a mathematical model or "simulation" describing the engine dynamics is constructed and stored in a suitable computer, it can provide designers of gas turbines with an extremely versatile tool with which to investigate a wide variety of problems.
>
> "Gas Turbine Theory"
> Cohen, Rogers and Saravanamuttoo (1996)

This quote can be extended to include other compression systems than gas turbines, such as turbochargers, pipeline compressors and so on. As surge and rotating stall are possibly hazardous phenomena, it would be fortunate to have mathematical models to use for control design before actually testing control algorithms on full scale compressors. This is of course a cost-issue, it is very much cheaper to crash a simulation program than an actual gas turbine, or to put it in the words of Onions and Foss (1982): "Suitable simulations allow more cost effective and wider insight into the problems, including exploration of the extreme limits of the engine operating range without risk". Experimental investigations are, according to Saravanamutto (1982), essential but very costly and potentially dangerous. The use of mathematical models can give a deep insight into engine transient behavior, and can, if properly used, significantly reduce the need for experimentation.

In the case of aircraft propulsion, it is of major interest to be able to predict unstable operation of the compressor using a mathematical model. This is due to the fact that if the compressor enters rotating stall, it may be necessary to shut down the engine and restart it. This scenario is also known as nonrecoverable stall or stall stagnation and is described by Stetson (1982).

Badmus et al. (1991) classified the available compressor models as either one-dimensional or two-dimensional, corresponding to the assumed dimensionality of the underlying fluid flow. Both classes of models have the capability to accurately predict and model compressor surge. However, only the two-dimensional models are capable of predicting rotating stall per se, as rotating stall is inherently a two dimensional phenomenon. An early contribution to rotating stall analysis was given by Takata and Nagano (1972), and Longley

(1994) presented a review of different approaches to modeling the non-steady fluid dynamics associated with two-dimensional compressor flow fields. One-dimensional models are capable only of predicting and modeling the *state* of rotating stall as a condition of steady, greatly reduced, annulus-averaged compressor mass flow.

1.5.2 The model of Greitzer (1976)

Although dynamic models of basic compression systems (as shown in Figure 1.13) have been available since 1955 as derived in the paper by Emmons *et al.* (1955), a major step forward in this field was made in 1976 when a nonlinear dynamic model for a basic axial compression system was presented by Greitzer (1976*a*). In this context, a *basic compression system* consists of a (axial or centrifugal) compressor with ducting working between a large constant pressure reservoir (ambient) and a plenum volume containing compressible gas. The plenum volume discharges through a throttle valve into another large reservoir. This basic compression system can be regarded a very simple model of a gas turbine, where the plenum plays the role of the combustion chambers and the throttle resembles the turbine. A major draw-
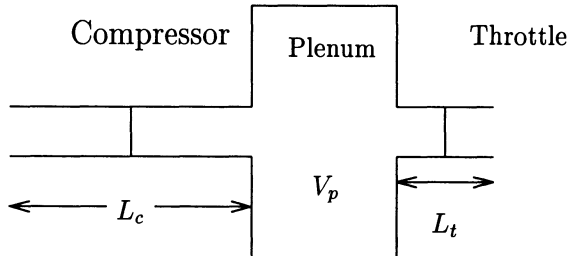
Figure 1.13: *Basic compression system*

back of earlier models such as the one by Emmons *et al.* (1955) was that they were *linearized*, and therefore fundamentally unable to describe the large amplitude pulsations encountered during a surge cycle due to their restriction to small perturbations from an equilibrium. Before the results of Greitzer (1976*a*), it was known that surge tend to occur for high speeds and large plenum volumes, and rotating stall for lower speeds and smaller volumes, but no systematic rules had been developed for determining which instability the compressor would enter. This was finally answered by Greitzer (1976*a*) by introduction of the celebrated Greitzer's B-parameter

$$B = \frac{U}{2\omega_H L_c} = \frac{U}{2a}\sqrt{\frac{V_p}{A_c L_c}}, \qquad (1.4)$$

where U is the mean rotor velocity, ω_H is the Helmholtz resonator frequency, L_c is the effective compressor and duct length, V_p is the plenum volume and A_c is the flow-through area.

By modeling the compressor and throttle as actuator discs, assuming low Mach numbers and low pressure ratios compared to ambient, Greitzer proposed the model:

$$\frac{d\Phi}{d\xi} = B(\Psi_c(\Phi) - \Psi) \tag{1.5}$$

$$\frac{d\Phi_T}{d\xi} = \frac{B}{G}(\Psi - \Psi_T(\Phi_T)) \tag{1.6}$$

$$\frac{d\Psi}{d\xi} = \frac{1}{B}(\Phi - \Phi_T(\Psi)) \tag{1.7}$$

$$\frac{d\Psi_c}{d\xi} = \frac{1}{\tilde{\tau}}(\Psi_{c,ss} - \Psi_c), \tag{1.8}$$

where all variables have been nondimensionalized and Φ is the compressor mass flow, Ψ_c is the compressor pressure rise, Ψ is the pressure difference across the duct, Φ_T is the throttle mass flow, $G = \frac{L_T A_c}{L_c A_T}$ is a constant, Ψ_T is the throttle pressure drop, ξ is time, $\tilde{\tau}$ is the compressor time constant and $\Psi_{c,ss}$ is the (nonlinear) steady-state compressor pressure rise characteristic. Mass flows have been normalized using $\rho U A_c$, pressure differences using $\frac{1}{2}\rho U^2$ and time using $\frac{1}{\omega_H}$. Equations (1.5)-(1.8) constitute, respectively, the momentum balance for the compressor ducting, the momentum balance for the throttle ducting, the mass balance for the plenum, and the relaxation equation describing the compressor response to departure from steady state. By assuming small inertial forces in the throttle duct (G is small) and considering the compressor pressure rise to be quasi-steady ($\tilde{\tau}$ is small), a simplified model can be found found:

$$\frac{d\Phi}{d\xi} = B(\Psi_c(\Phi) - \Psi) \tag{1.9}$$

$$\frac{d\Psi}{d\xi} = \frac{1}{B}(\Phi - \Phi_T(\Psi))$$

The nonlinear dynamic model (1.9) has been used by numerous authors for surge control design. The main contribution of Greitzer (1976a) is the finding of the B-parameter and showing that $B > B_{crit}$ leads to surge and $B < B_{crit}$ leads to rotating stall. These findings were also verified experimentally using a three stage axial compressor in the companion paper Greitzer (1976b).

The Greitzer model is also studied in Oliva and Nett (1991), where essentially arbitrary compressor and throttle characteristics were considered. As a consequence of this more general approach, an explicit characterization of the way in which the nonlinear dynamical behavior exhibited by the model depends on the compressor and throttle characteristics was obtained.

Stability analysis of the Greitzer model

The stability of the basic compression system can be studied by analyzing the nonlinear surge model (1.9). When linearizing (1.9), the following model is found

$$
\begin{pmatrix} \dot{\Phi} \\ \dot{\Psi} \end{pmatrix} = \underbrace{\begin{pmatrix} Ba_c & -B \\ \frac{1}{B} & -\frac{1}{Ba_T} \end{pmatrix}}_{A} \begin{pmatrix} \Phi \\ \Psi \end{pmatrix}, \tag{1.10}
$$

where a_c and a_T are the slopes of the compressor characteristic and the throttle pressure drop characteristic, respectively. Such a linear surge model was also studied by Stenning (1980). The eigenvalues of the matrix A of equation (1.10) are found by solving the characteristic equation

$$
\lambda^2 + \left(\frac{1}{Ba_T} - Ba_c \right) \lambda + \left(1 - \frac{a_c}{a_T} \right) = 0, \tag{1.11}
$$

with respect to λ, which gives

$$
\lambda = \frac{ -\left(\frac{1}{Ba_T} - Ba_c \right) \pm \sqrt{ \left(\frac{1}{Ba_T} - Ba_c \right)^2 - 4 \left(1 - \frac{a_c}{a_T} \right) } }{2}. \tag{1.12}
$$

The expression for the eigenvalues reveals that the stability boundary is set by a relation between the slope of the compressor characteristic, the slope of the load line, and the Greitzer B-parameter. By examining (1.11), it is seen that the system is unstable if either of the two bracketed expressions are negative. If $\left(1 - \frac{a_c}{a_T} \right) < 0$, that is the slope of the compressor characteristic is steeper than the slope of the throttle line, the system is *statically unstable*. This is illustrated in Figure 1.14 (point A). If $\left(\frac{1}{Ba_T} - Ba_c \right) < 0$ the system is *dynamically unstable* (point B in Figure 1.14). The point of dynamic instability is usually located just to the left of the peak of the compressor characteristic. As can be seen, the condition for dynamic instability is dependent on B, so for given compressor and throttle characteristics, changing the value of B can considerably alter the damping and hence the system dynamic response. If the dimension-full version of the Greitzer model is used, the following characteristic equation is found, Greitzer (1985b):

$$
\lambda^2 + \left(\frac{a^2 L_c}{V_p A_c} \frac{1}{a_{T,dim}} - a_c \right) \frac{A_c}{L_c} \lambda + \omega_H^2 \left(1 - \frac{a_{c,dim}}{a_{T,dim}} \right) = 0, \tag{1.13}
$$

where ω_H^2 is the Helmholtz frequency. From (1.13) it can be concluded that the Helmholtz frequency is equal to the resonance frequency of the compressor-plenum subsystem at the top of the compressor characteristic, Willems (1996).

The use of the terms *dynamic stability* and *static stability* is common in the compressor literature. Static stability implies that the states of the system continually increase, that is the equilibrium of the linear model (1.10) is either a saddle or an unstable node. Dynamic instability implies that the states oscillates with continually increasing amplitude, that is the equilibrium is an unstable focus. This is studied in more detail in Appendix A.

As a rule, stall and surge occur at the local maximum of the compressor characteristic or at a point of the compressor characteristic with a certain positive slope. The surge point will be located some small distance to the left of the peak. This is an approximation of the condition for dynamic instability. According to Cumpsty (1989), the peak of the compressor characteristic provides a convenient working approximation for the surge point. The same conclusion is drawn by Stenning (1980), where it is also pointed out that rotating stall occurs at the peak of the compressor characteristic.
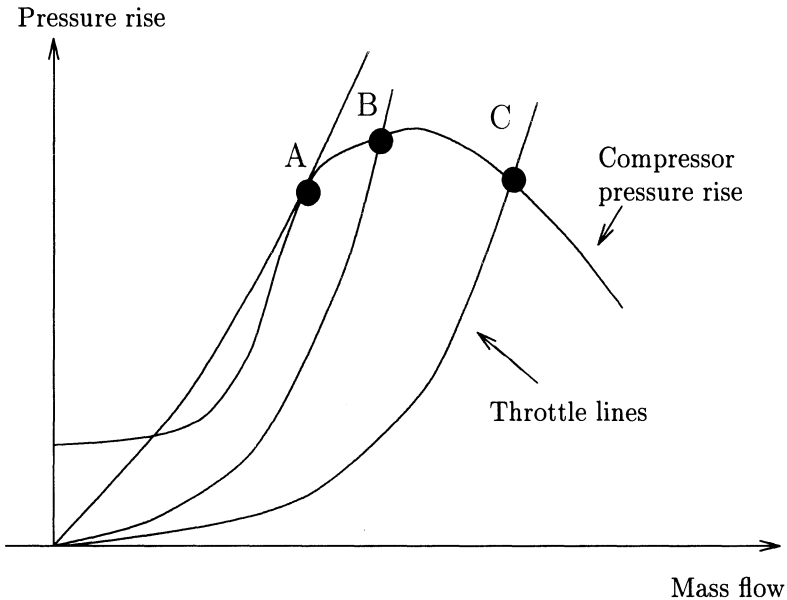
Figure 1.14: *Statically unstable (A), dynamically unstable (B), and Stable (C) operating points.*

In the case of turbochargers for internal combustion engines, the pressure downstream of the compressor is fluctuating due to the periodic suction strokes of the pistons. As a result, even though the mean mass flow rate might lie to the right of the surge line calculated when considering steady conditions downstream of the compressor, the minimum mass flow rate (at the peak of the pulse) may cause surge to develop. Watson and Janota (1982) conclude that fluctuating pressure downstream of the compressor can cause

the surge line to shift towards larger mass flow rates.

Another approach frequently used to investigate stability of compression systems is bifurcation analysis, which will be presented at the end of Section 1.5.3.

1.5.3   The model of Moore and Greitzer (1986)

While the model of Greitzer (1976a) is capable of simulating surge oscillations, rotating stall is manifested as a pressure drop. Motivated by the problems of nonrecoverable stall in gas turbines and the results of Moore (1984c), Moore and Greitzer (1986) proposed a model for multi-stage axial compressors describing the post-stall behavior of a compression system, where rotating stall (that is, disturbed flow coefficient) is included as a state. The model is capable of describing post-stall transients, that is transients subsequent to onset of compression system instabilities, associated with both surge and rotating stall.

Following Willems (1996), the Moore-Greitzer model is derived as follows. Using a stage-by-stage approach, the fluid dynamics in the inlet and exit compressor duct, inlet and exit guide vanes and each compressor stage, i.e. one stator-rotor combination, are combined in the local momentum balance. Furthermore, the annulus-averaged momentum balance and the mass balance of the plenum are applied to describe the dynamic behavior of the compression system. By normalizing pressures with ρU^2, time with U/R and mass flows with $\rho U A_c$, a set of three coupled nonlinear differential equations, one partial and two ordinary, are found:

$$\frac{d\Psi}{d\xi} = \frac{1}{4B^2 l_c}\left(\Phi(\xi) - \Phi_T(\Psi)\right) \tag{1.14}$$

$$\frac{d\Phi}{d\xi} = \frac{1}{l_c}\left(\frac{1}{2\pi}\int_0^{2\pi}\Psi_c(\Phi - \frac{\partial^2 Y}{\partial\theta^2})d\theta - \Psi(\xi)\right)$$

$$\frac{\partial Y}{\partial\xi} = \frac{1}{m}\left(\Psi_c(\Phi - \frac{\partial^2 Y}{\partial\theta^2}) + \frac{1}{2a}(2\frac{\partial^3 Y}{\partial\xi\partial\theta^2} + \frac{\partial^3 Y}{\partial\theta^3}) - \Psi(\xi) - l_c\frac{d\Phi}{d\xi}\right),$$

where ξ is nondimensional time, θ is the circumferential coordinate and $Y(\xi,\theta)$ is a disturbance velocity potential that represents the nonaxisymmetric flow disturbances, the stall cell. By using a Galerkin approximation assuming a single-term harmonic wave approximation for the disturbance velocity potential and a third order polynomial compressor characteristic

$$\Psi_c(\Phi) = \Psi_{c0} + H\left(1 + \frac{3}{2}\left(\frac{\Phi}{W} - 1\right) - \frac{1}{2}\left(\frac{\Phi}{W} - 1\right)^3\right), \tag{1.15}$$

the Moore-Greitzer model is found as:

$$\dot{\Psi} = \frac{W/H}{4B^2}\left(\frac{\Phi}{W} - \frac{1}{W}\Phi_T(\Psi)\right)\frac{H}{l_c} \tag{1.16}$$

$$\dot{\Phi} = \frac{H}{l_c}\left(-\frac{\Psi - \psi_{c0}}{H} - \frac{1}{2}\left(\frac{\Phi}{W} - 1\right)^3 + 1 + \frac{3}{2}\left(\frac{\Phi}{W} - 1\right)\left(1 - \frac{J}{2}\right)\right)$$

$$\dot{J} = J\left(1 - \left(\frac{\Phi}{W} - 1\right)^2 - \frac{J}{4}\right)\varrho,$$

where $J = A^2$ and A (the rotating stall amplitude) is the time varying amplitude of the harmonic wave approximation

$$Y = WA(\xi)\sin(\theta - r(\xi)) \tag{1.17}$$

for the disturbance velocity potential. The rest of the notation is explained in Section 2.2.1. A more detailed study of the Moore-Greitzer model is undertaken in Chapter 4, where the model is extended to include time varying spool speed.

Although the Moore-Greitzer model is very simple compared to the rather complex phenomena it models, it has been successfully compared to experimentally results, see Greitzer and Moore (1986). In particular it was confirmed that small values of B tend to give rotating stall and large values of B tend to give surge. In the case of pure surge, that is $J \equiv 0$, the Moore-Greitzer model (1.16) is reduced to the Greitzer model (1.9), but with different coefficients due to the two different ways of nondimensionalizing time.

Some simple simulations of the model are shown in Figure 1.15. The simulations were carried out using MATLAB and SIMULINK. Numerical values of parameters were taken from Greitzer and Moore (1986). An unstable equilibrium is studied by chosing a throttle opening such that the equilibrium of the system is to the right of the surge line. The three leftmost plots show the mass flow coefficient, pressure coefficient and squared rotating stall amplitude for the unstable equilibrium and a B parameter set to $B = 1$. The compressor undergoes deep surge oscillations. In the three rightmost plots, the only change is that the B-parameter has been reduced to $B = 0.4$, which results in the compressor going into rotating stall instead. It can bee seen that rotating stall leads to severely lower mass flow and pressure rise.

An extension to the Moore-Greitzer model is presented by Moore (1986), who derives a model that predicts how rotating stall or surge develop under the influence of harmonic inlet distortion. The distortion is modeled as

$$\phi_\infty = \Phi(\xi) - \epsilon\sin\theta, \tag{1.18}$$
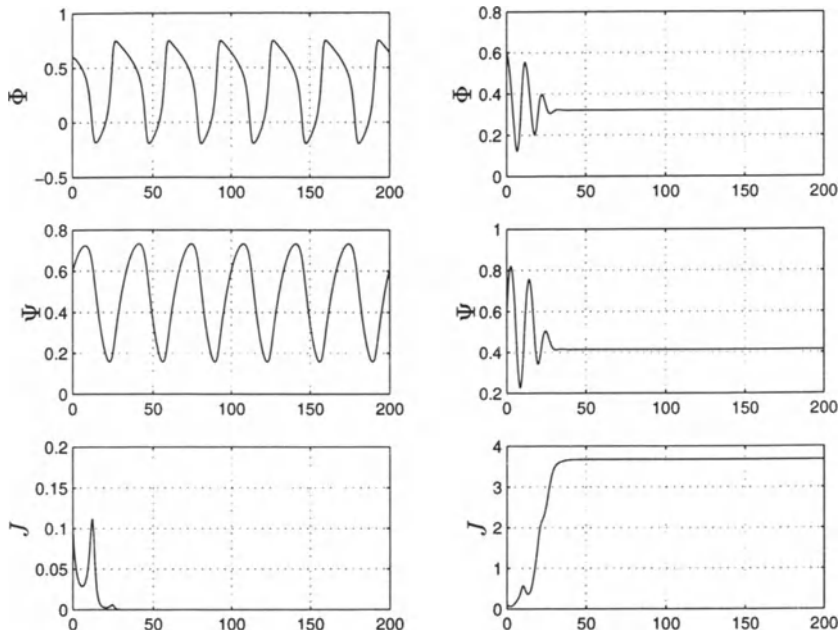
Figure 1.15: *Simulations of the Moore-Greitzer model. All states are plotted versus nondimensional time ξ. The curves to the left are with $B = 1$, and surge oscillations are seen. The curves to the right are with $B = 0.4$, and rotating stall is the result.*

where ϕ_∞ is the local axial flow coefficient evaluated far upstream and ϵ is the amplitude of the velocity distortion. Moore (1986) carries out the complete derivation of a modified Moore-Greitzer model and studies the effect of the distortion. It is concluded that large distortion favor the development of rotating stall. Extensions to Moore-Greitzer by including viscous, dissipative forces in the unsteady performance of the blade row are presented in Adomatis and Abed (1993) and Wang *et al.* (1994). Extensions concerning the inclusion of higher order harmonics in the Galerkin approximation are presented in Adomatis and Abed (1993), Mansoux *et al.* (1994), Gu *et al.* (1997a), Humbert and Krener (1997) and Leonessa *et al.* (1997a).

The Moore-Greitzer model with other types of compressor characteristics than the third order polynomial has also been studied. Harris and Spang (1991) extend the Moore-Greitzer model to include two families of compressor characteristics: odd-polynomial and even-polynomial. From their investigations, Harris and Spang (1991) conclude that compressors that can operate stably over a narrow (wide) range of flows are likely to incur small (large) flow distortion when stall occurs. Wang and Krstić (1997a) introduce the term left-skew and right-skew compressor characteristics, where the slope of

the compressor characteristic is steeper on one side of the maximum that the other. It is shown that if the characteristic is much steeper to the left (that is the characteristic is right skew) of the peak, the compression system undergo a much deeper hysteresis when trying to clear rotating stall with the throttle. Wang and Krstić (1997a) use a single parameter to vary the skewness of a modified version of the third order polynomial compressor characteristic.

Stability Analysis of the Moore-Greitzer model

As mentioned at the end of Section 1.5.2, bifurcation theory is a tool widely used to analyze the stability of compression systems. Following Mees (1983), the word "bifurcate" means "split into two", and in mathematics a bifurcation is a forking in a certain type of graph. A forking in a bifurcation graph for a dynamic systems corresponds to a *qualitative* change in the system being described. For a simple dynamic system like

$$\dot{x} = \mu - x^2, \tag{1.19}$$

μ can be treated as a bifurcation parameter and the equilibria of the system can be plotted versus the bifurcation parameter in a so called bifurcation digram. When $\mu < 0$ there are no equilibria, but at $\mu = 0$ the qualitative behavior of the system changes, and for $\mu > 0$ there exists two possible equilibria, one stable and one unstable.

In the case of the Moore-Greitzer model, several different bifurcation phenomena occur. If the compression system equilibrium is located at the peak of the compressor characteristic and the throttle is closed just beyond the surge point, two qualitatively different situations can occur. Depending on the magnitude of the B-parameter, a so-called Hopf-bifurcation resulting in limit oscillations (surge) or a stationary bifurcation resulting in rotating stall might occur. The stationary bifurcation may be *subcritical* or *supercritical*. The subcritical bifurcation produces a jump to the stable part of the in-stall characteristic and also hysteresis, while the supercritical bifurcation implies soft transition into rotating stall with no hysteresis. This can be exploited in control design and will be further discussed in Section 1.9.3.

The use of this technique in the field of compressor stability analysis was pioneered by McCaughan (1989) and McCaughan (1990), where the three-state Moore-Greitzer model was studied. McCaughan (1989) found that B is a bifurcation parameter for the model, and by varying B the model can exhibit both surge and rotating stall in accordance with the results of Greitzer and Moore (1986). Abed *et al.* (1990) and Abed *et al.* (1993) used bifurcation theory to examine the boundary between surge and rotating stall using the simpler model of Greitzer (1976a). Bifurcation theory has also found use in the field of stall and surge controller design. Liaw and Abed (1992) and Liaw and Abed (1996) used this method to derive a simple controller for rotating

stall in the Moore-Greitzer model. The main idea is to design a controller that changes the bifurcation properties of the system. This method has since been used in a number of publications.

1.5.4   Other models

In this section a number of other models for compression systems will be presented.

Davis and O'Brien (1987) present a one-dimensional compression system model for multistage axial compressors. Included in the system is a portion of the compressor inlet ducting and a plenum (combustor) volume. The compressor and ducting system are modeled by an overall control volume which in turn is divided into a set of elemental control volumes. Acting on the overall control volume is an axial-force distribution, FX, attributable to the effects of the compressor blading and walls of the system. The rate of heat added to the fluid and shaft work done on the fluid are represented by distributions Q and SW, respectively. Then, the principles of conservation of mass, momentum and energy are applied to the elemental control volume. Quasi-steady pressure and temperature characteristics provide pressure and temperature performance for each stage as a function of flow. Davis and O'Brien (1987) state that for dynamic events such as surge and rotating stall, steady characteristics are not necessarily correct. To provide dynamic characteristics, a first-order time lag on the stage forces has been added in the rotating stall region:

$$\tau \frac{dFX}{dt} + FX = FX_{ss}, \tag{1.20}$$

where τ is a time constant and FX_{ss} is the steady state force. The resulting model is validated with experimental results for a three-stage, low-speed compressor and a nine-stage, high-pressure compressor. Different experiments with both high and low values of Greitzer's B-parameter were conducted. The models were found to correctly model both deep and classical surge oscillations and the low mass flow and pressure rise associated with rotating stall. Davis and O'Brien (1987) also study the effect of fuel pulses on post stall behavior, and find that if the compressor is running at high speed, fuel pulses may initiate surge.

Badmus *et al.* (1991) propose a one-dimensional lumped model for generic compression systems. The derivation parallels that of Greitzer (1976*a*), but with a few significant differences. The model is dimension-full and the throttle is modeled as an orifice, so that the pressure drop over the throttle is

$$F(\dot{m}_T, A_T, P_0, T_0) = \text{sgn}(P_p - P_0)\frac{\dot{m}^2}{A_T^2}\left(\frac{RT_0}{2P_0}\right), \tag{1.21}$$

where $\dot{m}_T$ is the throttle mass flow, A_T is the orifice area, P_0, T_0 are the conditions at throttle outlet, R is the gas constant and P_p is the plenum pressure.

In Badmus *et al.* (1995*a*), a compressible viscous flow model is proposed. The model is quasi one-dimensional, and as such is capable only of predicting surge; rotating stall is modeled as reduced annulus averaged mass flow. The quasi one-dimensional assumption implies that all flow properties are essentially constant in any plane normal to the axial direction. The compression system under study consists of inlet, single-stage compressor, compressor discharge bleed, compressor duct, abrupt area change, plenum volume, plenum bleed, nozzle duct and nozzle. Badmus *et al.* (1995*a*) propose that each of these components can be modeled by the principles of conservation of mass, energy and momentum and the governing equations for a calorically perfect single species gas. Of the above mentioned components, the dynamics of the compressor discharge bleed, abrupt area change, plenum bleed and nozzle are residualized, that is they are described by algebraic equations. That leaves five components, which can be described by fifteen ODEs. However, the model is simplified further by eliminating the inlet and nozzle duct, leaving a model consisting of nine ODEs. The discretized form of the dimensionless ODEs for the k'th element of each component is, (Willems 1996):

$$\epsilon \frac{d}{dt} \begin{pmatrix} M_{k-1} \\ p_k \\ s_k \end{pmatrix} = \Xi(M,\gamma) \begin{pmatrix} M_k - M_{k-1} \\ p_k - p_{k-1} \\ s_k - s_{k-1} \end{pmatrix} + \Sigma(M,\gamma) \begin{pmatrix} Q \\ f_s \\ f_w \end{pmatrix}$$
$$+ 2\Gamma(M,\gamma)(A_k - A_{k-1}) + \epsilon \begin{pmatrix} 0 \\ -1 \\ \frac{\gamma-1}{\gamma} \end{pmatrix} \frac{dA_k}{dt}, \quad (1.22)$$

where

$$\epsilon = L_k e^{-\frac{1}{2}(s_{k-1} + \frac{\gamma-1}{\gamma} p_{k-1})} \quad (1.23)$$

and γ is the ratio of specific heats. The state variable of the dimensionless equations are the flow Mach number M, dimensionless total pressure p and dimensionless specific entropy s. The forcing terms are dimensionless volumetric heat transfer rate Q, dimensionless specific inviscid and viscous forces f_s, dimensionless specific wall friction force f_w and dimensionless area A. From (1.22) it is seen that the ϵ-parameter determines the relative time scales of the flow dynamics: when ϵ is very small the flow dynamics respond quasi-steadily and the forcing term $\frac{dA_k}{dt}$ has little effect. The subscripts k and $k-1$ denotes the entrance and exit of the k'th element of the compression system component. By using experimental data to identify model parameters and maps, Badmus *et al.* (1995*a*) use (1.22) as building blocks to model the compression system component by component.

Badmus *et al.* (1995*a*) compare the response of their model with experimental data from a compressor rig with excellent results. This agreement is

attributed mainly to the use of effective lengths within the model. Effective length account for the helical path of the flow as it travels through components where rotation is present. For example, the effective length of the compressor is

$$L_{c,e} = L_s + L_{r,e} = L_s + L_r\sqrt{1 + \frac{N^2}{M^2}r_{tip}^2 e^{-A_2}}, \qquad (1.24)$$

where L_s is the axial length of the stator, L_r is the axial length of the rotor and N is rotational speed.

Ishii and Kashiwabara (1996) derive a two-dimensional model for compressible flow in multistage axial compressors. As opposed to the classical Moore-Greitzer model, where compressibility is confined to the plenum, Ishii and Kashiwabara (1996) allow compressibility to be distributed throughout the compressor. Ishii and Kashiwabara (1996) argue that models with compressibility effects only in the plenum are suitable only for compressors with one or a small number of stages and not for multistage compressors. The flow field is modeled using compressible versions of the conservation laws and the equations of motion, leading to a set of nonlinear partial differential equations with all the states (axial and circumferential velocity, pressure, temperature and density) being functions of time, axial coordinate, and angle coordinate. Simulations of the model (using a finite difference method and a Galerkin procedure) are compared to experimental results on a three-stage compressor with excellent results.

As one of the reasons for compression system modeling is the design of surge/stall control algorithms, several authors have derived models with this in mind. The key issue here is that actuators and sensors are accurately modeled and included in the model. Feulner et al. (1996) derive a control oriented two-dimensional compressible flow model for rotating stall in high-speed multistage axial compressors, by using the linearized basic conservation laws of mass, momentum and energy. In high-speed compressors, compressibility effects are important, and must be included in the model. This leads to a distributed mathematical model, described by partial differential equations. The model is augmented to include upstream and downstream geometry, boundary conditions and actuator motion, and then converted to the form of a transfer function.

An alternative model for control of rotating stall in high-speed compressors is presented in Paduano et al. (1994), where two-dimensional compressible flow is studied. Rotating stall was described as a traveling wave, and spatial Fourier analysis was used. Both Paduano et al. (1994) and Feulner et al. (1996) consider one-dimensional actuators. Protz and Paduano (1997) describe how to include two-dimensional actuators in Moore-Greitzer type models.

1.6   Previous work on modeling of centrifugal compression systems

1.6.1   Greitzer-type models for centrifugal compressors

The work of Hansen et.al. (1981)

Although the compression system model of Greitzer (1976a) was originally derived for axial compression systems, Hansen *et al.* (1981) showed that it is also applicable to centrifugal compressors. Hansen *et al.* (1981) find reasonable agreement between experimental results and simulation results of the four-state Greitzer model (1.5)-(1.8) for deep surge in a small single-stage centrifugal turbocharger compressor. The compressor was fitted with a vaned radial diffuser (see Section 1.2.3). The experiments were carried out for two compressor speeds, and the dimensionless compressor characteristic was found to coincide for these speeds. The characteristic was represented by a parabola for negative flow and two different third order polynomials for stable and unstable forward flow.

In order to fit the experimental data to the response of the model Hansen *et al.* (1981) use a smaller value for the compressor flow relaxation time $\tilde{\tau}$. More specifically, $\tilde{\tau}$ is defined as

$$\tilde{\tau} = \frac{\pi R N}{L_c B}, \tag{1.25}$$

where N is the time lag in rotor revolutions, and Hansen *et al.* (1981) use $N = 0.5$ as opposed to the value $N = 2$ used by (Greitzer 1976a). The simulations reasonably fit the experimental results, but there are systematic discrepancies appearing particularly near and after flow reversal. Hansen *et al.* (1981) claims that this may be explained by compressibility effects. In support of this claim, it is said that the terms in the momentum balance that were ignored due to the incompressibility assumption may amount to as much as 25 percent of the terms retained. Further, the fact that the time periods where the ignored terms are significant are short, may explain why the model is still useful. In the discussion of Hansen *et al.* (1981), it is said that compressibility effects, instead of variations in N, also may account for the discrepancies between model and experiments at flow reversal.

The model of Macdougal and Elder (1983)

A model much similar to (1.9) is derived by Macdougal and Elder (1983). The main difference is that Macdougal and Elder (1983) model both the plenum

process and the compressor pressure rise to be polytropic. This results in a
model on the form

$$\frac{dm}{dt} = \frac{An}{L}(\Psi_c - p) \tag{1.26}$$

$$\frac{dp}{dt} = \frac{ZRT_1}{(1-n)V_p}(m - m_T),$$

where n is the polytropic index and Z is the compressibility factor. Note
that the model is not dimensionless, as opposed to the approach of Greitzer
(1976a). The model (1.26) is capable of simulating mild surge oscillations
which corresponds well to experimental results. As the backflow character-
istic for the compressor is not taken into account, deep surge cycles are not
studied.

The work of Fink et.al. (1992)

Fink *et al.* (1992) extend the Greitzer model (1.9) to include centrifugal
compressors with varying rotor speed. The effect of speed variation upon
surge dynamics had been speculated upon by Toyama *et al.* (1977) and Dean
and Young (1977), but no quantitative results emerged before the results of
Fink *et al.* (1992).

The compressor under study is a centrifugal turbocharger compressor with
a high speed radially vaned impeller with vaneless diffuser surrounded by a
volute. It is shown that non-constant speed is important in capturing the
system dynamics. In addition to the assumptions done by Greitzer (1976a),
Fink *et al.* (1992) assume that the gas angular momentum in the compressor
passages is negligible compared to the impeller and spool angular momentum.
Moreover, the ratio of plenum and inlet temperatures is not assumed to be
negligible. By applying conservation of momentum in the compressor duct,
conservation of mass in the plenum and conservation of angular momentum
for the compressor spool, the following model is found after using the same
nondimensionalization as in Greitzer (1976a):

$$\frac{d\Phi}{d\xi} = B(\Psi_c - \Psi) - FB\Phi\Gamma \tag{1.27}$$

$$\frac{d\Psi}{d\xi} = \frac{1}{B}\frac{\tau_p}{\tau_{p0}}(\Phi - \Phi_T) - 2FB\Psi\Gamma \tag{1.28}$$

$$\frac{dB}{d\xi} = FB^2\Gamma \tag{1.29}$$

$$\frac{d\Psi_c}{d\xi} = \frac{1}{\tau}(\Psi_{c,ss} - \Psi_c). \tag{1.30}$$

Equation (1.29), a differential equation for the B-parameter is found by ap-

plying conservation of angular momentum according to

$$I\frac{d\omega}{dt} = T_d - T_c,$$
(1.31)

where I is the spool moment of inertia, ω is the rotational speed and T_d and T_c are the drive and compressor torques, respectively. After nondimensionalizing the torques with $\rho A_c R U^2$ to find Γ, and defining

$$F = \frac{2\rho}{L_c A_c R^2}I,$$
(1.32)

equation (1.29) follows. In equation (1.30), the time constant τ is defined as

$$\tau = \left|\frac{L_m}{\bar{C}}\right| = \frac{L_m}{L_c}\frac{1}{2B|\Phi|},$$
(1.33)

where L_m is the meridional through-flow length of the impeller and vaneless diffuser and $\bar{C}$ is the meridional average flow velocity. The time constant τ is on the order of the compressor through-flow time, and the numerical value used by Fink *et al.* (1992) is $\tau = 0.12$ which corresponds to 2.2 rotor revolutions. This corresponds to the value used by Greitzer (1976a). Physically, the time lag has the effect of flattening the instantaneous compressor characteristic relative to the quasi-steady curve; this leads to a slower growing instability. The model (1.27)-(1.30) can be reduced to Greitzer's model by assuming constant speed ($\Gamma = 0$), setting $\frac{\tau_p}{\tau_{p0}} = 1$ and removing equation (1.30).

Simulations of the model is compared with experimental results, and Fink *et al.* (1992) concludes that the inclusion of the speed variations together with the timelag improves agreement with experiment dramatically. The speed variation is shown to cause a precursor period of mild surge before deep surge, and surge oscillations are shown to cause spool speed oscillations whose amplitude depend on the spool moment of inertia I.

1.6.2   Other models

By combining the basic conservation laws of mass, momentum and energy and the component-by-component analysis described at the end of Section 1.4.1, Elder and Gill (1985) derive a dynamic model capable of simulating surge in a centrifugal compressor. Application of the conservation laws for the inducer, tip, vaneless space, semi-vaneless space, diffuser channel, duct and nozzle results in a model which closely resembles experimental results. Each component is described by its mass flow versus pressure rise characteristic, and it is possible to identify the stalling elements that are responsible for the overall compressor instability.

In the papers Botros *et al.* (1991) and Botros (1994), a model for a pipeline compressor station as depicted in Figure 1.7 is derived. The flow in the pipeline is modeled using the general continuity, momentum and energy equations for one-dimensional unsteady compressible fluid flow in a pipe. This results in a distributed model for the pipeline on the form

$$\frac{\partial z}{\partial t} + \frac{\partial F}{\partial x} + H = 0, \tag{1.34}$$

where $z = (\rho \ m \ p)^{\mathrm{T}}$ is the state vector and F and H are nonlinear functions of z. The spool dynamics of the dual shaft gas turbine/power turbine configuration can be written

$$
\begin{aligned}
I_g N_g \frac{dN_g}{dt} &= \eta_t(N, N_g) Q_{LHV} m_{fuel} - W_t(N, N_g) \\
IN \frac{dN}{dt} &= \eta_m(N, N_g) - \frac{H_p(Q_a, N)\dot{m}}{\eta_p(Q_a, N)},
\end{aligned} \tag{1.35}
$$

where I, I_g, N, N_g are the inertias and speeds of the two shafts, Q_{LHV} is the lower heating value of the fuel, η_t, η_p, and η_m are the thermal, polytropic and mechanical efficiencies, $W_t(N, N_g)$ is the power turbine power and H_p is the polytropic head characteristic of the compressor. As in Macdougal and Elder (1983) the compressor is assumed polytropic:

$$H_p(Q_a, N) = \frac{ZRT_1}{(n-1)/n} \left(\left(\frac{p_2}{p_1} \right)^{\frac{n-1}{n}} - 1 \right). \tag{1.36}$$

However, (1.36) is valid only to the right of the surge point. In order to model (deep) surge cycles, the complete steady characteristic beyond the surge point and into the negative flow is required. This part of the characteristic is approximated with a third order polynomial as done by Greitzer (1976a). The compressor response to transients is further modeled as the first order model

$$\frac{dH}{dt} = \frac{1}{\tau}(H_{ss} - H), \tag{1.37}$$

where H_{ss} is the combination of (1.36) and the cubic of Greitzer (1976a). In Botros *et al.* (1991), the transients of the model is compared to field measurements with good agreement between simulations and measurements.

1.7   Jet engine and gas turbine models

In addition to the compressor models described above, a number of dynamic models of jet engines and gas turbines, which also models surge/stall phenomena, have been published. The number of publications in this field is

vast, and the models presented below must be considered as examples from this literature only. An overview of modeling techniques up till 1982 is given by Saravanamutto (1982). According to this source, the earliest attempts to quantify dynamic jet engine behavior dates back to 1952.
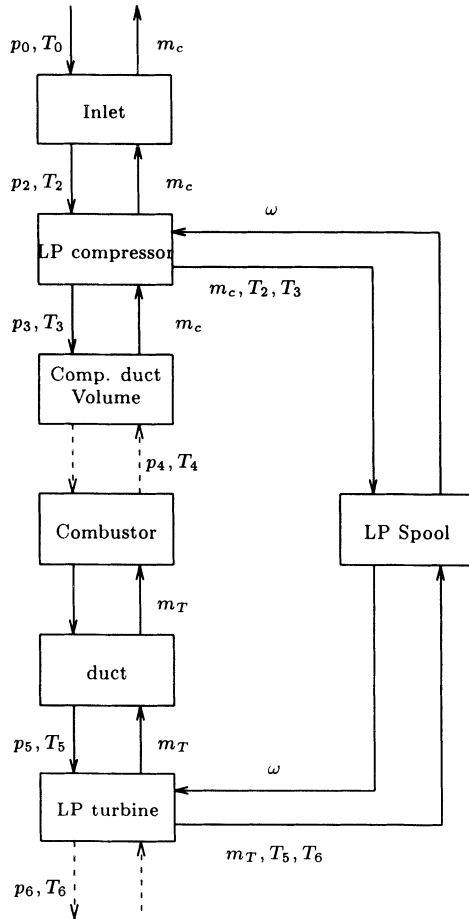
Figure 1.16: *Information flow for jet engine model*

The models of Onions and Foss (1982)

Onions and Foss (1982) present a gas turbine model named "The lumped continuity model". The gas turbine is modeled by breaking it into a series of discrete components such as low and high pressure compressors, combustion chamber, turbines and so on. Then, inter-component volumes and thermodynamic analysis is applied. This method was originally developed by Sara-

vanamuttoo and Fawke (1970), and has been used since for a number of jet
engine models. An information flow diagram of an example model is shown in
Figure 1.16, where some of the components of an engine are included. More
spools, compressors, nozzles and so on can easily be included.

The major assumption is that the performance of each component can be
described by the steady state characteristics and that differential equations
can be introduced to describe the transient behavior between the components.
For volumes with no heat release, the mass balance

$$\frac{dp}{dt} = \frac{K\kappa RT}{V}(\dot{m}_{in} - \dot{m}_{out}) \tag{1.38}$$

is used, and for volumes with heat release, the energy balance must also be
taken into account. In this model the rate of change of the engine shaft(s)
is modeled using the torque balance. If the engine under consideration is
a turbofan, Onions and Foss (1982) provides dynamic equations to describe
the transient behavior of the bypass flow. In order to make the model capa-
ble of simulating surge, Onions and Foss (1982) recognize that momentum
equations in the form

$$\frac{d\dot{m}}{dt} = \frac{KA}{L}(p_{in} - p_{out}) + \frac{F_{net}}{L}, \tag{1.39}$$

where F_{net} are drag forces, are needed. Notice that (1.38) and (1.39) cor-
respond to the Greitzer model. A number of simplifications to the model is
then undertaken. However, the resulting model is not capable of simulating
surge, but the surge line is calculated by means of calculating the eigenvalues
of the linearized model.

Sugiyama *et al.* (1989) use a similar approach as Onions and Foss (1982), and
their nonlinear model is capable of simulating surge oscillations in a turbojet
engine.

The model of Eveker and Nett (1991)

Motivated by the fact that no low order full-engine models with the capability
of demonstrating rotating stall had been published, Eveker and Nett (1991)
developed a model for a single spool centrifugal compressor turbojet engine.
The model has the capability to accurately predict compressor surge. As
opposed to the Moore-Greitzer compressor model, the model of Eveker and
Nett (1991) does not include rotating stall as a state, but the presence of
stall is manifested as a condition of steady, greatly reduced annulus-averaged
compressor mass flow.

Eveker and Nett (1991) use the same modeling approach as Saravanamuttoo
and Fawke (1970), and divides the engine into components. The inlet, com-
pressor, combustor, turbine and nozzle are modeled with algebraic equations.

Dynamic equations are provided for the momentum conservation in the compressor duct, the mass balance and energy conservation in the plenum and the power balance for the spool.

The same modeling technique is used by Qi *et al.* (1992*a*) and Qi *et al.* (1992*b*) to derive thrust controllers for a single spool gas turbine engine.

The model of Nishihara (1993)

A somewhat different approach to surge modeling in gas turbines is taken by Nishihara (1993) who considers a turbo shaft engine with a free power turbine. This helicopter motor has a seven-stage axial compressor closely coupled to a single-stage centrifugal compressor. A multi-element model of a aircraft gas turbine with both axial and centrifugal compressor stages using a Greitzer model for each element is proposed. Nishihara (1993) reports of good agreement between theory and experiment.

Instead of applying fundamental conservation equations as described above, gas turbines can be modeled utilizing real steady state engine performance data as in Biss and Grimble (1994) and Biss *et al.* (1994). Very simple models results if it is further assumed that the gas turbine always is operated close to rated speed as in Rowen (1983). Although these modeling methods may produce simple and accurate models for design conditions, they are unsuitable for surge/stall studies, due to the fact that these instabilities occur at off-design conditions.

1.8 Previous work on surge/stall avoidance

1.8.1 Background and motivation

Surge and rotating stall are highly unwanted phenomena. The number of unwanted effects are several: the introduction of thermal and mechanical loads, oscillations, lowered pressure rise and efficiency. Mazzawy (1980) found that the forces involved may be great enough to cause structural damage. Rotating stall, or more specifically, unrecoverable stall, in gas turbines require engine re-start, and may have catastrophic consequences in e.g. jet engines for aircraft propulsion, or in the words of Mattingly (1996): *"Steady operation above the (surge) line is impossible, and entering the region even momentarily is dangerous to the gas turbine engine"*.

Therefore, the useful range of operation of turbocompressors is limited, by choking at high mass flows when sonic velocity is reached in some component, and at low mass flows by the onset of surge and rotating stall. In conclusion, although it is dangerous to operate the compressor near the surge line, it is

desirable to do so due to the high performance and efficiency obtained there.
Traditionally, this problem has been handled by using control systems that
prevent the operating point of the compression system to enter the unstable
regime to the left of the surge line, that is the stability boundary. This
approach is known as surge/stall avoidance, or surge avoidance in short.
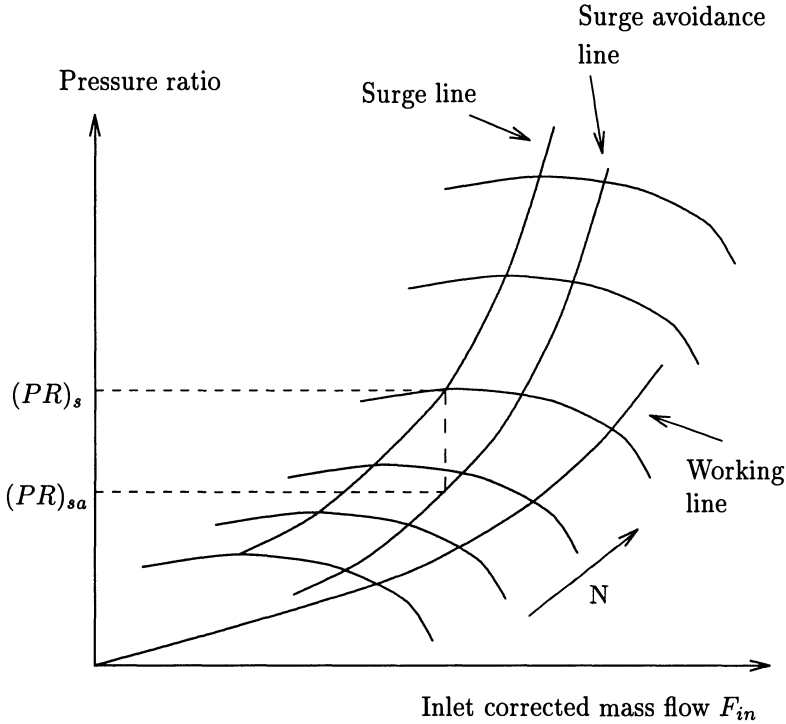
Figure 1.17: *Surge margin*

By using surge avoidance, the compressor is prevented from operating in a
region near and beyond the surge line. This is achieved by e.g. recirculation
of the flow or blowing off flow through a bleed valve. As the compressor
characteristic and thus the surge line may be poorly known, it will often be
necessary to have a fairly conservative *surge margin* between the surge line
and the *surge avoidance line*. The compressor is then not allowed to operate
between these two lines in the compressor map, see Figure 1.17. Accounting
for possible compressor uncertainties and disturbances also affects the size
of the surge margin. As the peak pressure rise and peak efficiency of the
compressor are located close to the surge line, the surge avoidance scheme
limits the performance of the machine. In addition to this, the surge margin
limits the transient performance of the compressor as acceleration of the
machine tends to drive the state of the system towards the surge line. There

are many different ways of defining the surge margin SM, one simple method is

$$SM_1 = \frac{PR_s - PS_{sa}}{PS_{sa}}.$$ (1.40)

where PS_{sa} is the pressure ratio on the surge avoidance line of the compressor for a given speed, and PS_s is the pressure ratio on the surge line for the same mass flow, as shown in Figure 1.17. According to Cumpsty (1989), in a multistage axial compressor in a turbojet it is normal to insist on a 25% surge margin, and Botros and Henderson (1994) quotes 10% as typical in centrifugal pipeline compressors. Following Cumpsty (1989), an altogether more logical definition of the surge margin considers the change in *outlet* corrected mass flow. For a definition of corrected mass flow, see Appendix C. The surge margin is then defined as

$$SM_2 = \frac{F_{out,sa} - F_{out,s}}{F_{out,sa}},$$ (1.41)

and the significance of using the outlet corrected flow is that it gives a measure of the throttle change needed to take the compressor into surge/stall. As most compressor maps are usually quoted in terms of *inlet* corrected mass flow, an alternative definition to (1.41) which retains the physical significance of the outlet corrected flow, but uses the more easily measured inlet corrected flow is

$$SM_3 = 1 - \left(\frac{(p_{0,out}/p_{0,in})_{sa}}{(p_{0,out}/p_{0,in})_s} \cdot \frac{F_{in,s}}{F_{in,sa}} \right).$$ (1.42)

According to Staroselsky and Ladin (1979), there are three common forms of the surge avoidance line. The optimal position of the line is parallel to the surge line as in Figure 1.17. Setting the avoidance line with a slope less than that of the surge line can lead to excess actuation at high pressures, and surge at low pressures during startup and stopping. The third method is to simply select a minimum safe flow, and set a vertical avoidance line, but this can lead to excess actuation at low pressures and surge at high pressures.

A surge avoidance scheme will operate on the following principle: If the working point of the compressor tend to cross the surge avoidance line, that is if the "distance" between the throttle line and the surge line approaches the surge margin SM, some actuation device is activated and the working point is forced to stay to the right of the surge line. Clearly, such a scheme will not allow maximum performance and efficiency to be reached. Nevertheless, this approach is used in most commercial gas turbines and other compressor installations.

An alternative to surge avoidance is *surge detection and avoidance*. Using this strategy, the drawbacks of the surge margin can be avoided by the activation of the controller if the onset of instabilities is detected. Botros and Henderson (1994) lists a number of patented techniques designed to detect the onset

of surge in centrifugal compressors, but the general results of this study applies to axial machines as well. The most successful techniques are based on monitoring various variations in flow, pressure, temperature, speed or other parameters at the compressor inlet or exit, along with their time derivatives or frequency of oscillation. These measurements are compared to threshold values defining the incipient surge and are fed to the surge controller. Botros and Henderson (1994) concludes that the main disadvantages of this strategy are the necessity of large control forces and very fast-acting control systems in order to prevent the incipient surge to grow into a full blown surge cycle. Also, this technique is highly dependent on the compressor at hand, as different compressors exhibit different behaviors during incipient surge. Therefore, surge detection and avoidance has not found wide acceptance.

1.8.2   Industrial solutions to surge avoidance

In, gas turbines, both for power generation and for propulsion, it is common to use bleed valves as surge avoidance actuators. Usually, the compressed high energy bleed flow is not entirely wasted as it can be used for e.g. cabin heat. Other techniques used for surge avoidance in gas turbines are the use of multispool compressors and variable stators. Casing treatment is also a frequently used technique to improve the surge margin in axial compressors, (Takata and Tsukuda 1977).

In centrifugal compression systems in the process industry, recycle valves where some of the compressed fluid is fed back to the compressor intake are commonly used for surge avoidance. Botros and Henderson (1994) group industrial surge avoidance schemes for centrifugal compressors into four categories (all schemes use recycle valve actuation):

- **Conventional anti-surge control** which include methods based on measurements of compressor inlet flow and differential pressure across the compressor. This technique is also called "Flow/ΔP_c". The signal from the flow element, which is usually a differential pressure (ΔP_0) is shown to be proportional to the differential pressure across the compressor. A linear relation is used to describe the surge avoidance line

$$\Delta P_0 = k_1 \Delta P_c + k_2, \qquad (1.43)$$

  where k_1 and k_2 are constants. This method is treated in detail in Nisenfeld (1982) and Balchen and Mummé (1988), and Botros and Henderson (1994) lists many variations of this concept.

- **Flow/rotational speed (Q/N) technique** which use the fan law to nondimensionalize the volumetric flow Q using rotational speed N and the head H across the compressor using N^2. The surge avoidance

line is thus reduced to a control point where $(Q/N)_c$ is constant. If $(Q/N)_{measured} < (Q/N)_c$, the recycle valve is opened.

- **Microprocessor and PLC based controller**. If the relation between ΔP_c and ΔP_0 is far from linear, a direct comparison between the compressor operating point on the compressor characteristic in relation to the surge avoidance line ought to be made. According to Botros and Henderson (1994), this can be accomplished by calculating both the actual flow and the head across the compressor. This requires other measurements such as temperature, inlet pressure and so on, and also use of the compressor characteristic. Computers-based controllers are well suited for this. Most newly designed surge avoidance schemes are of this class.

- **Control without flow measurement**. Because the flow signal is often noisy, inaccurate, and in some cases nonlinear and non-repeatable and also introduce a pressure drop, it is advantageous to avoid flow measurement in the surge avoidance scheme. This can be accomplished by using a $(H/N^2)_c$ ratio instead of $(Q/N)_c$ as in the Q/N-technique. This is possible provided the compressor characteristic is steep enough.

1.9 Active Control of Surge and Rotating Stall

1.9.1 Background and motivation

Active surge/stall control is an approach fundamentally different to surge avoidance. In active surge/stall control, feedback is used to stabilize the unstable regime of the compressor map. It is believed, according to Botros and Henderson (1994) and de Jager (1995), that surge avoidance is a mature field, and that only incremental improvements on existing technology will emerge in the future. Based on this, and the fact that there are several drawbacks, as discussed in the previous Section, connected to the use of surge avoidance, the rest of this text will be concerned with *active surge control*.

The approach of active surge/stall control aims at overcoming the drawbacks of surge avoidance, by stabilizing some part of the unstable area in the compressor map using feedback. This will allow for both operation in the peak efficiency and pressure rise regions located in the neighborhood of the surge line, as well as an extension of the operating range of the compressor. A compressor with active control has effectively a shifted surge line, so also the surge avoidance line can be shifted, thereby enabling the machine to operate in a region where, without active surge control, reliable operation was not possible, (de Jager 1995). The approach was first introduced in the control literature by Epstein *et al.* (1989), and in the last decade, the literature on

feedback stabilization of compression systems has become extensive. This is partly due to the introduction, and success, of the Moore-Greitzer model.

In the literature on developments in the field of jet engines for aircraft propulsion, active stall/surge control is often said to become an important part of future engines. For details see e.g. Epstein (1986), Covert (1995), Ruffles (1996) or DeLaat *et al.* (1996). The term "smart engines" is often used when refering to these engines, see Greitzer (1998). Brown *et al.* (1997) reports of successful in-flight experiments on a F-15 aircraft with active stall control on one engine. Experimental results on laboratory engines are reported by Paduano *et al.* (1993), Ffowcs Williams *et al.* (1993), Haynes *et al.* (1994) and Behnken and Murray (1997).

During the last decade, an increasing number of papers have been published on the topic of active surge/stall control. The interest seems to have been considerable larger for the study of axial compressors than of centrifugals. This is mainly due to the fact that aircraft engines to a large degree use axial compressors, and the gas turbine industry is one of the main sponsors for this type of research.

A review of some methods of active surge/stall control will now be presented. First, methods for surge control in centrifugal and axial compressors will be discussed, and then active controllers for both surge and rotating stall in axial compressors are discussed.

1.9.2   Control of surge in centrifugal and axial compressors

The results of Ffowcs Williams and Huang (1989)

One of the first published results on active surge control was the paper by Ffowcs Williams and Huang (1989), where active stabilization of surge in a centrifugal compression system was studied. Ffowcs Williams and Huang (1989) model their system with the Greitzer model (1.5) with a few modifications: The momentum balance in the compressor duct is augmented with an experimentally determined term $\mu(\Phi - \overline{\Phi})$, where $\overline{\Phi}$ is the average value of Φ, describing the flow resistance in the duct. Also, no lag is assumed in the compressor response. The actuator used is a movable wall in the plenum. The wall surface is part of a mass-spring system responding to the unsteady pressure fluctuation in the plenum and an externally induced force. The displacement ξ_d of the surface is assumed to be proportional to the driving force, and the control force is generated by a feedback system which processes the signal from a plenum pressure sensor. Including the modeling modifications

and the actuator, the nondimensional closed loop system is given by

$$\frac{d\Phi}{d\xi} = B(\Psi_c(\Phi) - \Psi - \mu(\Phi - \overline{\Phi})) \tag{1.44}$$

$$\frac{d\Phi_T}{d\xi} = \frac{B}{G}(\Psi - \Psi_T(\Phi_T))$$

$$\frac{d\Psi}{d\xi} = \frac{1}{B}(\Phi - \Phi_T(\Psi)) - (\eta + Z_{\xi_d})\frac{d\Psi}{d\xi},$$

where the η-term results from the pressure-induced motion of the wall, and

$$Z_{\xi_d} = (\rho a^2 A_{wall}/VK)C, \tag{1.45}$$

where K is the spring stiffness and $C = |C|e^{j\beta}$ is the complex-valued gain of the P-controller. The employed compressor characteristic $\Psi_c(\Phi)$ is the result of empirical curve-fitting to experimental data.

By linearizing (1.44), conditions on the controller gain C are found for the closed loop system to be stable. In experiments on a turbocharger compression system, the movable wall is implemented as a loudspeaker, and Ffowcs Williams and Huang (1989) report of excellent agreement between theory, simulations and experiment. The surge controller was able to stabilize the system both before and after surge had occured. Similar experiments were conducted on a gas turbine engine with centrifugal compressor in Ffowcs Williams and Graham (1990).

Similar results on surge control is also presented in Epstein *et al.* (1989), where control is achieved by the use of complex valued proportional feedback from plenum pressure perturbations to both a movable plenum wall and the throttle.

Gysling *et al.* (1991) also propose to use a movable plenum wall to stabilize surge. Their approach differs from the one of Ffowcs Williams and Huang (1989) in the sense that the wall is a passive element and no energy is fed into the compressor system. By the use of *structural feedback*, the dynamic properties of the systems are modified so that the compression system becomes inherently stable, without external input. By including the dynamics of the movable wall in the Greitzer model and linearizing, conditions on the damping of the wall mass-spring-damper system are found. Gysling *et al.* (1991) conduct experiments with a centrifugal compression system fitted with a movable plenum wall and found the mass flow at which surge occured was lowered with 25%.

The results of Pinsley et.al (1991)

Pinsley *et al.* (1991) study centrifugal compressor surge control using the model (1.9) and the throttle valve as actuator. Similar to Ffowcs Williams

and Huang (1989), the model is linearized, and conditions on the complex-valued gain of the throttle P-controller are found. Again, a plenum pressure sensor was used. Pinsley *et al.* (1991) propose the following control law for the throttle valve area:

$$\delta \hat{A}_T = Z \delta \Psi \hat{A}_T, \qquad (1.46)$$

where δ denotes perturbation quantities, Z is the complex-valued controller gain and $\hat{A}_T$ is the nondimensional throttle valve area. In experiments, a 25% reduction in surge point mass flow was achieved over a range of speeds and pressure ratios.

The results of Ffowcs Williams et.al (1993)

Ffowcs Williams *et al.* (1993) aim at stabilizing both rotating stall and surge in a gas turbine with a centrifugal compressor. An air injector is used as actuator. The air is injected to a point at the outer edge of the impeller eye, parallel to the impeller axis. Based on the two distinct types of instabilities, surge and rotating stall, possibly occuring at the same time, Ffowcs Williams *et al.* (1993) propose two distinct controllers, controller A and controller B.

Controller A is required to eliminate nonaxisymmetric disturbances to the compressor flow. By writing the nonaxisymmetric axial velocity through the compressor as its Fourier series and using the method of Moore (1984*b*) to calculate the pressure rise from ambient to plenum, Ffowcs Williams *et al.* (1993) show that the controller

$$p_u = k(V_a - V), \qquad (1.47)$$

where V_a is the axial flow velocity, V the mean axial flow velocity and k is the controller gain, reduce the energy of the nonaxisymmetric flow at rate

$$R_1 = k \int_0^{2\pi} (V_1 - V)^2 d\theta. \qquad (1.48)$$

Simulations confirm this result, but Ffowcs Williams *et al.* (1993) do not propose an actual control system to be implemented.

Controller B is designed to stabilize surge cycles. Ffowcs Williams *et al.* (1993) use a model similar to (1.9), and introduce the control u into the plenum mass balance such that

$$\frac{dp}{dt} = b(V - V_{throttle}) + u. \qquad (1.49)$$

The controller u is chosen as

$$\begin{aligned} u &= k_2(p - p_E) + k_3 w \\ \frac{dw}{dt} &= k_1 w + (p - p_E), \end{aligned} \qquad (1.50)$$

and the parameters k_i of the controller are chosen by positioning the eigenvalues of the linearized closed loop system in the left half plane. This strategy is confirmed experimentally, with a decreased corrected mass flow at the surge point of 2.6% which corresponds to an increase in delivered power before surge with more than 10%.

The results of Simon and Valavani (1991)

In Simon and Valavani (1991) and Simon (1993), active surge control is done by using a close coupled valve as an actuator. The main idea behind this approach is to use the pressure drop over the valve downstream of the compressor to shape the compressor characteristic at equilibrium. That is, the valve is used to render the slope of the *combined* characteristic of compressor and valve negative, and thereby stabilizing the equilibrium. The Greitzer model (1.9), augmented with bounded time-varying disturbances in mass flow and pressure rise, is used in the analysis. By doing a change of coordinates to $(\hat{\phi}, \hat{\psi})$ such that the equilibrium is shifted to the origin, and using the Lyapunov function (termed the incremental energy of the system):

$$V = \frac{1}{2}\left(\frac{1}{B}\hat{\phi}^2 + B\hat{\psi}^2\right),\qquad(1.51)$$

the following control law is derived:

$$u = \hat{\Psi}_v(\hat{\phi}) = \begin{cases} \min(0, \underline{\hat{\Psi}}_c(\phi)) & , \quad -\hat{\phi}_2 < \hat{\phi} < -\hat{\phi}_1 \\ f(\hat{\phi}) & , \quad -\hat{\phi}_1 < \hat{\phi} < \hat{\phi}_1 \\ \max(0, \overline{\hat{\Psi}}_c(\phi)) & , \quad \hat{\phi}_1 < \hat{\phi} < \hat{\phi}_2, \end{cases} \qquad(1.52)$$

where $f(\hat{\phi})$ is any continuous differentiable function connecting the points $(\hat{\phi}, \Psi_v(-\hat{\phi}_1))$, $(0,0)$ and $(\hat{\phi}, \Psi_v(\hat{\phi}_1))$, and $\underline{\hat{\Psi}}_c(\phi)$ and $\overline{\hat{\Psi}}_c(\phi)$ are the lower and upper bounds on the compressor characteristic, respectively, when taking the disturbances into account. The control law relies on measuring the compressor mass flow, and the resulting controller $u = \hat{\Psi}_v(\hat{\phi})$ prescribes the required pressure drop to be taken over the close coupled valve both to stabilize the equilibrium and to dominate the disturbance. In contrast to previous analyses which used linearized models, Simon and Valavani (1991) are probably the first to use a nonlinear model throughout the design of an anti-surge controller. Moreover, Lyapunovs method is used to derive an asymptotically stabilizing control law.

The work of Nakagawa et.al. (1994)

Nakagawa *et al.* (1994) presents results from an experimental investigation of centrifugal compressor surge control using valves on the suction side of

the compressor to vary the compressor inlet pressure. The valve opening was commanded using a proportional feedback from a pressure sensor located either upstream or downstream of the compressor. The experiments show that surge can be suppressed by using suction side valves.

The work of Willems and de Jager (1998)

Willems and de Jager (1998a) investigate the use of one-sided bleed/recycle control of a laboratory-scale gas turbine installation. The installation consists of a low-speed, single stage, centrifugal compressor driven by an axial turbine, and is described in detail in Meuleman et al. (1998). The model (1.9) is considered, and a bleed valve that that is nominally closed is used as the control. The valve can only be operated to one side (opening the valve) and not to the other side (closing the valve). Willems and de Jager (1998a) show that the compressor mass flow range can be extended significantly with zero or very low bleed flow.

The work of Badmus et.al (1996)

Badmus et al. (1996) study the control of surge in *axial* compression systems by using is a modified version of (1.9), the Greitzer model. As in Badmus et al. (1995a), effective compressor duct length is used. The length used in the model is calculated as

$$l_{total} = l_c l_{ce}, \text{ where } l_{ce} = \sqrt{1 + \frac{\varepsilon^2}{\phi^2}}, \tag{1.53}$$

where l_c is the nondimensional duct length, ϕ is the annulus averaged flow coefficient, and ε is a constant that is tuned to enhance improved transient match between model predictions and experimental data. Badmus et al. (1996) propose to stabilize surge by using a nonlinear Luenberger-type output observer and a nonlinear input-output feedback linearizing controller. The observer is designed by augmenting the right hand side of the dynamic model with a term proportional to the observation error, and it enables an approximate reconstruction of the system states from a single output measurement. Badmus et al. (1996) proceed to design a feedback linearizing controller that achieves a linearization of the dynamics between the measured output (the dynamic pressure at compressor inlet), and the system input variable (the throttle area parameter). The poles of the closed loop linear system are placed by a PD-controller. Stabilization of surge using this scheme is demonstrated by experiments.

Cargill and Freeman (1991) stress the fact that most investigations on active control of surge, both theoretical and experimental, have considered *low speed*

machines, and that control schemes based on this assumption are unlikely to be effective on high speed compressors where compressibility effects introduce additional physical phenomena. In an axial compression system of sufficient length, speed and pressure ratio, surge can begin with a high-amplitude blast wave propagating along the compressor. This wave is initiated by a region of stalled flow at the rear of the compressor. Cargill and Freeman (1991) derive a model for high speed surge, similar in structure to Greitzer's model, and show that in this case the important parameter governing the dynamics is not the B-parameter, but BN, where N is the number of stages. Further, as B is proportional to speed, in high speed systems BN is necessarily large, and it is shown that in this case the expected increase in flow range due to active control is small.

Cargill and Freeman (1991) also show that large BN implies that the surge cycle consist of fast and slow elements, and that the fast elements take place on a time scale equivalent to the time it takes to stall or unstall a blade. Cargill and Freeman (1991) conclude that in the case of high speed compressors, a more promising approach than active control of surge is the suppression of disturbances that would otherwise develop into surge rotating stall.

1.9.3   Control of surge and rotating stall in axial compressors

There has been an increasing frequency of publication within this field over the last couple of years. The results presented below are supposed to be representative. However, new results are presented on every major control conference and this trend seems to continue. Previous overviews of the research in this field has been presented in de Jager (1995), Gu *et al.* (1996), Willems (1996) and Willems and de Jager (1998*b*).

Control of rotating stall using upstream vanes

The first result on active control of rotating stall in axial compressors was presented by Epstein *et al.* (1989). This is a theoretical result, and no attempt are made to discuss the topic of actual implementation in an engine. However, Epstein *et al.* (1989) name several actuators that might be used to implement their algorithm: unsteady jets or wiggling stators far upstream, wiggling inlet guide vanes and downstream pressure perturbation using loudspeakers or pulsing the combustor. In the control scheme derived, control is exercised through an upstream set of vanes that are operated to create a vortical disturbance field. The control action creates an axial velocity disturbance $\delta C_x'$, such that the total disturbance at compressor inlet is

$$\delta C_x = \delta C_{x1} + \delta C_x', \tag{1.54}$$

where δC_{x1} is the disturbance in the inlet flow velocity. Epstein *et al.* (1989) propose to use proportional feedback from the perturbation in the compressor flow coefficient, such that the control law is given as

$$u = \delta\phi' = \frac{\delta C_x'}{U} = Z\delta\phi, \qquad (1.55)$$

where $\delta\phi'$ is the disturbance created by the action of the control vanes, and

$$Z = |Z|e^{i\beta} \qquad (1.56)$$

is the complex valued controller gain. Epstein *et al.* (1989) continue to investigate the influence of the control law parameter Z on the closed loop performance of the compressor. Negative real values of Z, that is $\beta = \pi$, stabilizes rotating stall, but allows surge cycles on the positive sloped part of the compressor characteristic. General complex values of Z allow for the instability point on the peak of the characteristic to be shifted towards lower mass flows. The reduction in stall mass flow can be increased by a proper choice of the phase shift β compared to simple proportional control. It is also noted that wrong choice of β can lead to instability.

The ideas of Epstein *et al.* (1989) were realized by Paduano *et al.* (1993) who used an array of twelve upstream high speed control vanes in a single stage axial compressor to damp out low-amplitude circumferentially traveling waves that may grow into rotating stall. The waves are decomposed into separate spatial Fourier components, and each harmonic is to be controlled individually. The control was implemented using a circumferential array of hot wires to sense propagating waves of axial velocity upstream of the compressor. The stagger angle of each control vane is used as the control, and the control laws employed are on the form

$$(\delta\gamma_{IGV})_n = Z_n C_n, \qquad (1.57)$$

where $\delta\gamma_{IGV}$ is the change in stagger angle, C_n is the spatial Fourier coefficient of mode n, and $Z_n = |Z_n|e^{i\beta_n}$ is the complex controller gain for mode n. Control of the first mode give a decrease of 11 percent of the stalling mass flow, while control of the first three harmonics reduce the stalling mass flow by 23 percent.

The work of Paduano *et al.* (1993) is extended to the multi stage case by Haynes *et al.* (1994) who study a three-stage axial compressor. The same array of twelve upstream vanes is used for stabilization of rotating stall. By controlling the two first modes of rotating stall, an eight percent increase in operating flow range was obtained.

Control of rotating stall using throttle/bleed valves

The use of throttle or bleed valves is considered equivalent in the following, as all authors consider bleed valves downstream of the plenum. Thus, the

bleed flow will enter the equations of the Moore-Greitzer model in the same way as the throttle flow.

By using the throttle valve as a rotating stall actuator it is possible to stabilize the peak of the compressor characteristic, in the sense that the hysteresis loop associated with rotating stall is eliminated. This is achieved by stabilizing the unstable part, plotted as a dotted line in Figure 1.12, of the compressors in-stall characteristic. That is, by controlling rotating stall using the throttle valve as actuator, the operating range of the compressor is not extended, but the hysteresis loop is eliminated.

Bifurcation methods
In Liaw and Abed (1992) and Liaw and Abed (1996) a control law for stabilization of rotating stall in the Moore-Greitzer model using bifurcation analysis is designed. Construction of control laws using bifurcation theory is studied in Abed and Fu (1986) for Hopf-bifurcations and in Abed and Fu (1987) for stationary bifurcations. Gu *et al.* (1997*b*) study output feedback stabilization using bifurcation theory. The bifurcations of the Moore-Greitzer model have previously been studied by McCaughan (1989), and Liaw and Abed (1992) generalize this analysis by considering a general characteristic instead of a third order polynomial compressor characteristic. The throttle is used for actuation, and a control law u is designed for the throttle opening, such that

$$F(\gamma, \psi) = \gamma_T \sqrt{\psi} = (\gamma_0 + u)\sqrt{\psi}. \qquad (1.58)$$

The uncontrolled system will have a subcritical pitchfork bifurcation at the equilibrium which will cause hysteresis. By linearizing the Moore-Greitzer model (1.16), using the rotating stall amplitude A as a state instead of its square, it is shown that the control law (the Liaw-Abed controller)

$$u = kA^2 = kJ \qquad (1.59)$$

renders the stationary bifurcation at the equilibrium to be a supercritical pithfork bifurcation. The reason for the quadratic feedback is that when linearizing the Moore-Greitzer model, it comes clear that the unstable eigenvalue associated with rotating stall is not affected by linear control. Thus, if the throttle is used for actuation, linear control fails. On the other hand, it is shown by Liaw and Abed (1992), that a controller involving higher order terms than kA^2 is unnecessary as this is the only term affecting system stability. According to Liaw and Abed (1996), this introduces a new stable equilibrium near the nominal equilibrium after the nominal equilibrium itself has lost stability, thus eliminating the undesirable jump and hysteresis behavior of the uncontrolled system.

Badmus *et al.* (1995*b*) show that since the Liaw-Abed controller does not use rotating stall phase information, the bandwidth requirements of this controller are relatively low. Simulations show that the stall inception point

can be stabilized even in the face of constraints on the actuator bandwidth and magnitude. The reduced actuation requirements were a consequence of the fact that the goal of this study was not to extend the stable operating range of the compressor, but rather to address persistent disturbances that would otherwise throttle the compressor into rotating stall. The approach is experimentally validated in Badmus *et al.* (1995*c*).

Wang *et al.* (1994) also use the Liaw-Abed controller for control of rotating stall, but also investigate what happens if higher order Moore-Greitzer models are studied. By using a Moore-Greitzer model with N modes of rotating stall, Wang *et al.* (1994) show that the feedback from the squared amplitude of the first harmonic, as in (1.59), is sufficient to eliminate the hysteresis even if higher harmonics of rotating stall are present. Adomatis and Abed (1993) also study rotating stall control in higher order Galerkin approximations of the Moore-Greitzer model, and show that a term describing viscous momentum transportation has to be included in the model in order to prevent all stall modes to have the same amplitude. As in Wang *et al.* (1994), the Liaw-Abed controller is shown to render the stationary bifurcation supercritical also in this case.

Motivated by the fact that the Liaw-Abed controller is dependent on measuring the amplitude of rotating stall, Gu *et al.* (1997*a*) study the problem of rotating stall control with less demanding sensing requirements. Although rotating stall amplitude can be measured, this relies on two-dimensional sensing. This is at present achieved by measuring the local flow coefficient using hot wires, Paduano *et al.* (1993), which are very delicate devices and not very suitable for e.g. gas turbine implementation, (Gu *et al.* 1997*a*).

Gu *et al.* (1997*a*) propose to use the pressure coefficient Ψ for feedback, a measurement that only requires one-dimensional sensing. By using bifurcation theory, it is then shown that the throttle control law

$$u = \frac{K}{\sqrt{\Psi}}, \tag{1.60}$$

where K is a constant, stabilize the unstable part of the in-stall characteristic and thereby eliminate the hysteresis. The in-stall equilibria are shown to be (locally) asymptotically stable. In addition to achieving the same goals as Liaw and Abed (1992), the controller (1.60) shows promise for surge control, a task, according to Gu *et al.* (1997*a*), the Liaw-Abed controller is not well suited for.

Similar results are found by Sparks and Gu (1997), who also use bifurcation theory to study stabilization of a equilibrium distinct from the stall point at the peak of the characteristic. Four different bleed valve controllers are considered:

$$u = K(\Phi - \Phi_0)^2 \tag{1.61}$$

$$u = \frac{K}{\sqrt{\Psi}}(\Phi - \Phi_0)^2 \tag{1.62}$$

$$u = K(\Psi - \Psi_0)^2 \tag{1.63}$$

$$u = \frac{K}{\sqrt{\Psi}}(\Psi - \Psi_0)^2, \tag{1.64}$$

where (Φ_0, Ψ_0) are the equilibrium values. It is shown that the controllers (1.61) and (1.62) stabilize the unstable part of the in-stall characteristics, make the bifurcation supercritical, and eliminate the hysteresis. This is not in contradiction with the results of Liaw and Abed (1992) where it was concluded that only feedback of the square of the rotating stall amplitude affects the bifurcation, because Sparks and Gu (1997) use error states from the equilibrium (Φ_0, Ψ_0), while Liaw and Abed (1992) use error states from the critical point. In addition to the less demanding measurements, the controllers (1.61) and (1.62) may also be effective in controlling surge and coupled stall and surge.

A somewhat different approach to bifurcation stabilization of rotating stall using bleed valves is taken by Larsen *et al.* (1997) who propose to eliminate rotating stall by stabilizing a small limit cycle around the peak of the compressor characteristic. By using the tools of singular perturbations, Larsen *et al.* (1997) show that this is achieved by using the so-called dynamic S-controller

$$u = \frac{1}{\tau s + 1}\chi \tag{1.65}$$

$$\chi = \frac{\Gamma_0 + k(\Psi - \Psi_s(\Phi))}{\sqrt{\Psi}} - \overline{\Gamma}, \tag{1.66}$$

where the equilibrium is determined by Γ_0 and $\overline{\Gamma}$, and $\Psi_s(\Phi)$ is defined to be the Ψ along the locus of stabilizable equilibria of the system.

Krstić and Wang (1997) and Wang and Krstić (1997b) study surge and rotating stall control for deep-hysteresis compressors. A model for deep-hysteresis compressors, or compressors with right-skew compressor characteristic, was developed by Wang and Krstić (1997a). Throttle controllers of the form

$$\gamma_T = \frac{\Gamma + \overline{\beta}^2(c_\Psi \Psi - c_\Phi \Phi + c_R R - d_\Phi \dot{\Phi})}{\sqrt{\Psi}}, \tag{1.67}$$

are considered, and actuator dynamics of the form (1.65) are also taken into account. Krstić and Wang (1997) concludes that for right-skew compressors with actuator dynamics, the controller (1.67) with feedback from Φ, Ψ and R change the bifurcation at the peak from subcritical to supercritical. It is also shown that as actuator bandwidth decreases, the sensing requirements become more demanding. Wang and Krstić (1997b) also show that $\dot{\Phi}$-feedback,

demonstrated by Eveker *et al.* (1995) to be effective in suppressing surge in small-hysteresis compressors, can cause surge in deep-hysteresis compressors.

Another aspect of compressor control is taken into account by Wang *et al.* (1998), Wang (1998) and Krstić and Wang (1998), who apply extremum seeking feedback to the Moore-Greitzer model in order to allow the compressor to operate at the peak of an unknown right-skew compressor characteristic and at the same time ensuring that the bifurcation point is supercritical. A bleed valve controller of the form (1.67) is used. However, due to the high bandwidth requirements of a bleed valve designed to stabilize rotating stall, air injection is used instead of bleed valves in experiments. Krstić and Wang (1998) emphasize that the peak seeking scheme can be combined with any of the stabilizing control laws for surge and rotating stall available in the literature, and also for other actuators than the throttle. These results are confirmed on an experimental compressor rig by Wang *et al.* (1998) and Wang (1998).

All of the above controllers were derived using a one mode Galerkin approximation of the Moore-Greitzer model. Hendrickson and Sparks (1997) discuss the suitability of some of these control laws for higher order approximations. It is found that the improvement of the local and global behavior of the system using these control laws is severely tempered when additional modes in the approximation are considered. These findings motivate alternative control designs to eliminate the hysteresis associated with rotating stall.

Backstepping methods

There has been an number of papers published on stabilization of surge and rotating stall in axial compression systems using throttle control and the backstepping methodology of Krstić *et al.* (1995a). The first of these was Krstić and Kokotović (1995) where control of both surge and rotating stall for the Moore-Greitzer model is undertaken. In the case of pure surge, the following control law for the throttle parameter is found

$$\gamma_T(\Phi, \Psi) = \frac{2 - (\beta^2 k_1 - 1)(\Phi - 1) + \beta^2 k_2(\Psi - \Psi_{c0} - 2))}{\sqrt{\Psi}}, \qquad (1.68)$$

where

$$\beta = \frac{2BH}{W}, \qquad (1.69)$$

and B is Greitzer's B-parameter, Ψ_{c0}, H and W are the parameters of the third order polynomial compressor characteristic and k_1, k_2 are controller parameters. The control law (1.68) was found by using two steps of backstepping and a non-quadratic Lyapunov function, where cancelations of useful nonlinearities were avoided. This control law renders the equilibrium globally asymptotically stable. When using the same approach on the full Moore-Greitzer model, that is rotating stall is taken into account, a similar controller is found. However, the rotating stall controller requires feedback

from the rotating stall amplitude. This non-desirable sensing requirement is alleviated in Krstić *et al.* (1995*b*), where the throttle controller

$$\gamma_T(\Phi, \Psi) = \frac{\Gamma + \overline{\beta}^2 k(\Psi - c_0 \Phi)}{\sqrt{\Psi}},\qquad(1.70)$$

is shown to globally asymptotically stabilize the unstable equilibria on the in-stall characteristic, and thereby eliminating the hysteresis associated with rotating stall. This control law is found by using a two-step backstepping procedure on the full Moore-Greitzer model. In (1.70), $\overline{\beta}$ is a known upper bound on β defined in (1.69), and k and c_0 are controller parameters. The set point parameter Γ depends on the controller gains and the equilibrium value, and is also a bifurcation parameter for the system. The bifurcation properties of the Moore-Greitzer model under control (1.70) is studied in Krstić *et al.* (1998), where it is found that the bifurcation at the peak of the compressor characteristic is changed from subcritical to supercrital, which is also the case for the Liaw-Abed controller (1.59). However, since Krstić *et al.* (1998) use Lyapunov tools, the controller (1.70) achieves , as opposed to the Liaw-Abed controller, not only local, but *global* stability.

Banaszuk and Krener (1997) design throttle controllers for the Moore-Greitzer model with general compressor characteristics. It is shown that every potential axisymmetric equilibrium on the decreasing part of the compressor characteristic, the peak of the characteristic, and every rotating stall equilibrium close to the peak can be globally stabilized by an appropriate choice of the so-called throttle surface and the controller gains. Banaszuk and Krener (1997) stress the use of information about the shape, e.g. slopes and curvatures, of the characteristic instead of using particular parameterizations. As other results on surge/stall controller design are either global for specific characteristic or local for general characteristic, the results of Banaszuk and Krener (1997) fill the gap by providing global results for general characteristics. The throttle surface is the graph of the throttle function

$$\tilde{\Psi}(\Phi, A) = \frac{\Phi - h(\Phi, A)}{c_\Psi}.\qquad(1.71)$$

Construction of the controller is equivalent to choosing the throttle function $\tilde{\Psi}(\Phi, A)$ and the gain c_Ψ. Then, the function $h(\Phi, A)$ can be found from (1.71), and the throttle parameter γ_T can be obtained from

$$\gamma_T = \frac{c_\Psi \Psi + h(\Phi, A)}{\sqrt{\Psi}}.\qquad(1.72)$$

The throttle surface and the gain c_Ψ is found by using a three-step backstepping process. It it named graph backstepping because of its simple graphical interpretation. These results are generalized and presented in detail in Banaszuk and Krener (1998).

Banaszuk *et al.* (1997*b*), Banaszuk *et al.* (1997*a*) and Banaszuk *et al.* (1998) avoid the usual Galerkin approximation, and design throttle controllers for rotating stall and surge in the PDE, or full, Moore-Greitzer model (1.14). Banaszuk *et al.* (1997*b*) derive a controller using the minimum of the stall cell for feedback:

$$\gamma_T = \Phi + \bar{c}_\Psi(\min g, \Phi)(\Psi - \Psi_c(\Gamma) - \bar{c}_\Phi(\min g, \Phi)(\Phi - \Gamma - \bar{c}_g|\min g|))$$
$$(1.73)$$

where $g = -\frac{\partial^2 Y^2}{\partial^2 \theta}$ and Y is defined in (1.14), is found by the use of a three step nonsmooth backstepping procedure using Dini derivatives.

Other methods
Harris and Spang (1991) use a bleed valve to suppress both surge and rotating stall in the Moore-Greitzer model, and thus extend the stable operating regime of the compressor. The control suppresses stall by bleeding air from the plenum in proportion to the squared stall amplitude J and its integral, and it suppresses surge by bleeding in proportion to to the negative rate of change of the mean flow:

$$u = C_1 \int J(\xi)d\xi + C_2 J(\xi) - C_3 \frac{d\Phi}{d\xi}, \qquad (1.74)$$

where the controller gains C_1, C_2 and C_3 are dependent of the physical characteristics of the compressor-plenum system and the throttle setting.

Leonessa *et al.* (1997*a*) derive a multi mode Moore-Greitzer model similar to that of Mansoux *et al.* (1994). By using this model it is shown that the second and higher order harmonics of rotating stall strongly interact with the first harmonic during stall inception. Using Lyapunov stability theory, a nonlinear globally stabilizing throttle control law based on equilibria dependent Lyapunov functions is derived. This control law is compared to a backstepping controller designed for the basic one-mode Moore-Greitzer model. The result is that the multi mode controller stabilizes the system when a two-mode model is used, whereas the backstepping controller drives the system into stall.

Another important aspect of active surge and stall control is the disturbance rejection capabilities and robustness of the proposed controllers. Greitzer and Moore (1986) recognized that research is needed on modeling of disturbances in compression systems. The reason for this being that disturbances may initiate surge or rotating stall. As opposed to most other methods of stall/surge control using the throttle, Haddad *et al.* (1997) take disturbances and uncertainties in the compressor map into account. The Moore-Greitzer model is used, augmented with disturbance signals $w_{1,2}(\xi)$ in the stall amplitude and mass flow equations. The disturbances are assumed to be square integrable, that is $w_{1,2}(\xi) \in \mathcal{L}_2$. A highly nonlinear throttle control law is derived using Lyapunov's method and it is shown that this controller ensures

global asymptotic stability in the case of no disturbances and convergence to a set when the disturbances are present. In a simulation study, the controller is compared to backstepping and bifurcation based controllers. It is demonstrated that the developed disturbance rejection controller is the only one able to reject the disturbances, and that the locally stabilizing bifurcation-based controller actually drives the disturbed system into rotating stall. Haddad *et al.* (1997) also study uncertainties in the compressor characteristic and assume that

$$\Psi_c(\Phi) = \Psi_{c_{nom}} + \Delta\Psi_c(\Phi), \qquad (1.75)$$

where $\Psi_{c_{nom}}$ is the nominal third order polynomial compressor characteristic, and $\Delta\Psi_c(\Phi)$ is an uncertain perturbation of this nominal characteristic. A robust throttle control law is derived using Lyapunov theory, and it is shown to globally stabilize the peak of the nominal compressor characteristic. Via simulations it is demonstrated that the robust controller stabilizes the peak, while backstepping-based and bifurcation-based controllers drive the system into rotating stall. These results are extended to the multi mode case by Leonessa *et al.* (1997*b*).

Control of rotating stall using air injection

By using the throttle valve as an actuator for control of rotating stall and using the bifurcation or backstepping methods of the previous section to design control laws, rotating stall is not suppressed, but the hysteresis associated with it is avoided. Air injection schemes aim at eliminating the stall cells and extending the stable operating range of the compressor.

The first study of air injection as a means of active stall control was presented by Day (1993*a*). This experimental study was conducted on an four stage axial flow compressor fitted with an array of twelve individually controllable injection valves. These valves were positioned near the tips of the first rotor. Two different methods were used to delay the onset of rotating stall. According to the study by Garnier *et al.* (1991), rotating stall in some cases develops from small amplitude disturbances. Day (1993*a*) employs air injection to damp out these disturbances and achieves an improvement in stall margin of four percent. However, several studies such as Day (1993*b*), Lawless *et al.* (1994) or Escuret and Garnier (1996) have shown that stall cells can originate without any detectable precursive build up. In this case Day (1993*a*) used the injection valves to damp out the stall cell *after* it had emerged. This gave an increase in stall margin of about six percent. In the case of surge, it was shown that this instability is preceded by a brief period of rotating stall, and by using the air injection scheme to eliminate the stall, surge is also suppressed.

Khalak and Murray (1994) use a single air injector as an actuator for control of rotating stall, while D'Andrea *et al.* (1995) extend this work and use

three injectors. D'Andrea *et al.* (1995) use pulsed air injection as opposed to the proportional injection studied by Day (1993*a*), as this is regarded a more viable technology for implementation on real gas turbines. D'Andrea *et al.* (1996) explain the stabilizing effect of the pulsed air injection scheme by performing a bifurcation analysis of the Moore-Greitzer model, and model the effect of the air injectors as an unsteady shift in the compressor characteristics.

Behnken and Murray (1997) study the simultaneous stabilization of rotating stall and surge. This is achieved by using a bleed valve for surge and air injection for rotating stall. The controllers are analyzed using the Moore-Greitzer model, and the analysis is based on the surge dynamics acting on a slow time scale relative to the rotating stall dynamics. A bleed valve controller on the form

$$\gamma_T = k_1 \dot{\Phi}, \tag{1.76}$$

where k_1 is a constant is used. The stall control law of Behnken *et al.* (1995) for the air injectors shifts the compressor characteristic such that

$$\Psi_c = \Psi_{c_{nom}} + k_2 J \Psi_{c_u}, \tag{1.77}$$

where $\Psi_{c_{nom}}$ is the usual third order polynomial compressor characteristic, k_2 is a constant and

$$\Psi_{c_u} = c_0 + c_1 \Phi \tag{1.78}$$

is the rotating stall controller. Due to the different time scales of the surge and stall dynamics, the method of singular perturbations is used. The fast (stall) and slow (surge) systems are both shown to be uniformly asymptotically stable and the total system is therefore locally stable. These findings are confirmed experimentally, and a detailed study is found in Behnken (1997). As opposed to the nonaxisymmetric air injection of Behnken *et al.* (1995), Yeung and Murray (1998) use axisymmetric air injection to achieve simultaneous stabilization of stall and surge. Yeung and Murray (1997*a*) use continuous air injection to shift the compressor characteristic and thereby reducing the bandwidth and magnitude requirements of a bleed valve actuator in performing bleed valve control of rotating stall. In van Schalkwyk *et al.* (1997) it is shown that it is possible to increase the stable operating range of an axial compressor operating with large inlet pressure distortion by using a combination of upstream injection and downstream bleeding. Air injectors are also used in Weigl and Paduano (1997) to stabilize stall and increase the operating range of a transonic axial compressor.

Other schemes for rotating stall control

Baillieul *et al.* (1995) use inlet flow disturbances that introduce variations in the shut-off head of the compressor as a means of eliminating the hysteresis

associated with rotating stall. This is an open loop approach, and it is shown by bifurcation analysis that the hysteresis is eliminated.

1.10 Sensor/actuator selection in surge/stall control

1.10.1 Motivation

Among several possible actuators for stabilizing compression systems, the throttle valve or bleed valves have been the most commonly used, at least in the control literature. Other possibilities include variable inlet guide vanes, loudspeaker, tailored structures, recirculation, movable wall, air injection or control valves in various configurations. What actuator to use depends on the application and the compression system at hand, but it is evident that the performance of the closed loop system depends on the right choice of actuator. This is also true for the measurements of the system. Possible choices are mass flow or velocity measurements, total or static pressure measurements at various locations and temperature measurements. Several studies on sensor-actuator selection have been published, some of which will be presented below.

1.10.2 Selection of sensors and actuators for surge control

Simon (1993) and Simon *et al.* (1993) present the first systematic definition of the influence of sensor and actuator selection on increasing the range of stabilized compressor performance. The results show that proper choice of sensor as well as actuator crucially affects the ability to stabilize the compression system. According to Simon *et al.* (1993), theoretically, surge requires only a single sensor and actuator, with many choices available for their type and location. However, as pointed out by van de Wal *et al.* (1997), in practice disturbances and actuator limitations may play a role, and stabilization with a single sensor and actuator may become impossible. Simon *et al.* (1993) study combinations of one of the following sensors:

1. compressor duct mass flow

2. plenum pressure

3. compressor face static pressure

4. compressor face total pressure

with one of the following actuators:

1. injection in the compressor duct

2. close-coupled control valve

3. plenum bleed valve

4. plenum heat addition

5. movable plenum wall.

By using a linearization of the Greitzer model (1.9) and employing feedback control using a *proportional* control law, Simon *et al.* (1993) computed closed loop transfer functions for the various sensor-actuator combinations. By comparing these control schemes it is concluded that there is no best sensor independent of the actuator. The figure of merit used to assess the actuator-sensor pairs was to examine the stability boundaries in a compressor slope versus B-parameter plane. Only the actuators located in the compressor duct, which act upon the compressor duct momentum (close-coupled valve and injector) are capable of stabilization at steep compressor characteristic slopes over the full range of Greitzer's B-parameter. If the combination of mass flow sensing and close coupled valve actuation is used, the compression system may be stabilized over an unlimited range of mass flows, although large values of gain may be required with large slopes or B-parameters. Consequently, this sensor-actuator combination is regarded to be the most promising of the ones evaluated in this study.

Van de Wal et al. (1997) use an Input Output (IO) selection method to select sensors and actuators for the compressor surge control problem. The method is studied in detail in van de Wal (1998). Three candidate actuators: Close-coupled valve, bleed valve and movable plenum wall, and four measurements: Compressor duct mass flow, plenum pressure, total compressor face pressure and static compressor face pressure are proposed. These measurements and actuators are a subset of the ones considered by Simon *et al.* (1993). The IO selection of van de Wal *et al.* (1997) is more rigorous than the one of Simon *et al.* (1993) in the sense that not only single actuator and single sensor solutions are examined. Moreover, as opposed to the proportional controllers of Simon *et al.* (1993), dynamic output feedback is allowed for. The linearization of the Greitzer model (1.9) is also used here, and IO selection is aimed at finding the IO set(s) for which a controller exists that stabilizes the nominal model. This is quantified with a requirement on the $\mathcal{H}_\infty$-norm of the closed loop. In this framework, disturbances, sensor noise and actuator limitations are also taken into account. The proposed actuators and sensors can be combined to 105 different IO sets including the full IO set with all sensors and actuators and 12 IO sets with a single actuator and sensor. Van de Wal et al. (1997)

conclude that among the proposed actuators and sensors, the close-coupled valve and mass flow sensor are the most promising for the considered system, but a movable wall should be added to meet the performance specifications. These findings are presented in more detail in van de Wal and Willems (1996).

It is interesting to note that both studies presented above conclude that actuating the compression system with a close coupled valve with feedback from compressor duct mass flow measurement is the most promising approach of the ones considered. The use of a CCV for surge control will be elaborated upon in Chapter 2.

1.10.3   Selection of sensors and actuators for rotating stall control

Hendricks and Gysling (1994) study sensor-actuator pairings for control of rotating stall in axial compressors. The approach is based on using the sensor to detect the small amplitude traveling waves shown by Garnier *et al.* (1991) to precede rotating stall in some cases. However, Day (1993*b*) among others have shown that this traveling wave is not always present. Hendricks and Gysling (1994) consider the following actuators:

1. circumferential arrays of jets

2. intake ports

3. movable inlet guide vanes

4. downstream valves,

and the following measurements:

1. axial velocity

2. static pressure

3. total pressure.

The jets and intake ports are similar physically, the only difference being their supply pressure. Active control of rotating stall is in this study based on a linear model of its initiation. The model implies that, at the inception of the instability, small amplitude, long wavelength, traveling waves develop in the compressor annulus, grow in amplitude, and eventually develop into rotating stall cells. The study only considers actuators closely coupled to the compressor. This eliminates the time delay associated with the convection of the vortical component of the control disturbance from the actuator to the

compressor, which according to Hendricks and Gysling (1994) was found to
have a destabilizing effect. The controllers used are proportional control laws
with complex gains:

$$u = Zy, \tag{1.79}$$

where $Z = |Z|e^{i\beta}$ is the complex gain and y is the measurement. In addition the actuators are modeled as first-order time-lag systems. Three performance parameters were used in comparing the different control schemes:
the largest positive compressor characteristic slope that the closed loop system can achieve, the phase margin of the controller and the rotation rate
of the controlled perturbation. The comparasion reveals that the most effective method is the use of upstream jets with feedback from axial velocity
measurements.

1.10.4   Actuator requirements

Both Simon *et al.* (1993), Hendricks and Gysling (1994) and van de Wal *et al.*
(1997) recognize actuator constraints such as bandwidth limitations as important problems in chosing sensors and actuators and designing surge/stall-controllers.

In the case of bleed valve actuation of rotating stall, analysis of bleed valve
rate requirements are presented in the series of papers Yeung and Murray
(1997*b*), Wang and Murray (1997), Yeung *et al.* (1998) and Wang and Murray (1998). Yeung *et al.* (1998) use simultaneous air injection and bleed
valve actuation to control rotating stall and show that compressor characteristic actuation via air injection reduces the bleed valve rate and magnitude
requirement for stall control.

CHAPTER 2

CLOSE COUPLED VALVE CONTROL
OF SURGE AND ROTATING STALL
FOR THE MOORE-GREITZER MODEL

2.1 Introduction

2.1.1 Motivation and main idea

In this Chapter, controllers for surge and rotating stall using a CCV are derived. Surge control using a CCV has been studied by several authors. Here, this approach will be used also for rotating stall control. When using the throttle as an actuator for rotating stall control, the *rotating stall-equilibria* to the left of the surge line can be stabilized and the bifurcation is changed from subcritical to supercritical, elliminating the hysteresis. On the other hand, it will be shown here that the use of CCV-control stabilizes a new *axisymmetric* equilibrium to the left of the surge line, at the cost of a certain pressure drop over the valve. This pressure drop is comparable in size to the pressure loss created by operating the compressor in rotating stall.

2.1.2 Previous work

Several possible actuators exists for stabilizing compression systems. Krstić *et al.* (1995*b*), Badmus *et al.* (1996) and others suggest using a variable throttle

valve, Eveker and Nett (1991), Yeung and Murray (1997b) and others use bleed valves. These two actuators have been the most commonly used, at least in the control literature. However, there are many other possibilities: Paduano et al. (1993) use variable inlet guide vanes, a loudspeaker is used by Ffowcs Williams and Huang (1989), tailored structures in Gysling et al. (1991), recirculation is studied by Balchen and Mummé (1988), a movable wall in Epstein et al. (1989) and finally Day (1993a) and Behnken and Murray (1997) employ air injection. However, as mentioned in Section 1.10, Simon et al. (1993) and van de Wal et al. (1997) claimed that the use of a close-coupled valve is among the most promising actuators for active surge control.

The use of a CCV for control of compressor surge was studied by Dussourd et al. (1976), Greitzer (1981), Pinsley et al. (1991), Simon and Valavani (1991), Simon et al. (1993) and Jungowski et al. (1996). Experimental results of compressor surge control using a CCV was reported by Erskine and Hensman (1975) and Dussourd et al. (1977). Simon et al. (1993) compared, using linear theory, this strategy to a number of other possible methods of actuation and sensing. The conclusion was that the most promising method of surge control is to actuate the system with feedback from the mass flow measurement to a CCV or an injector. In line with this conclusion are the recent results of van de Wal and Willems (1996) and van de Wal et al. (1997), where nonlinear controllers were derived based on $\mathcal{H}_\infty$ performance specifications.

Dussourd et al. (1976), Greitzer and Griswold (1976), Dussourd et al. (1977), Greitzer (1977) and Greitzer (1981) conclude that downstream components in compression systems have an impact on the onset of rotating stall. Dussourd et al. (1977) used a CCV to achieve a significant extension of flow range, and it was concluded that the CCV also affected the onset of rotating stall as well as surge. Osborn and Wagner (1970) report of experiments where rotating stall in an axial-flow fan rotor was suppressed, at the cost of a drop in efficiency, by a movable "door" close coupled downstream of the rotor. The door had a similar geometry to that of a axisymmetric nozzle, and the experimental setup simulated a turbofan engine. Greitzer (1977) found that a downstream nozzle shifted the point of onset of rotating stall to lower mass flows, however the effect was strongest for single cell, full span stall. The Moore-Greitzer model, which is going to be used in this Chapter, assumes a high hub to tip ratio compressor, which is likely to exhibit full span stall. Moreover, Greitzer (1977) found that the stabilizing effect of the nozzle falls rapidly with increasing distance between compressor and nozzle, and thereby emphasizing the importance of close coupling between compressor and actuator, a point also made by Hendricks and Gysling (1994). Based on this, the CCV will in this Chapter not only be used to stabilize surge, but also rotating stall.

Simon and Valavani (1991) studied the stability of a compressor with CCV control by using a Lyapunov function termed the incremental energy. The control law developed by Simon and Valavani (1991) requires knowledge of

the compressor characteristic, and additional adjustments to the controller dictated by the Lyapunov analysis is performed in order to avoid a discontinuous controller.

In this Chapter we will use the backstepping methodology of Krstić *et al.* (1995*a*) to derive a control law for a CCV which gives a GAS equilibrium beyond the original surge line. Simon and Valavani (1991) studied the effect on stability of disturbances in pressure rise. This will also be considered here, and in addition we will also consider disturbances in the plenum outflow. In the case of pressure disturbances only, we will derive a controller that only requires knowledge of an upper bound on the slope of the compressor characteristic in order to guarantee stability. Discontinuity is not a problem with this controller. Under mild assumptions on the disturbances, global uniform boundedness and convergence will be proven in the presence of both pressure and mass flow disturbances. Constant disturbances or offsets will also be considered.

Krstić and Kokotović (1995) and Krstić *et al.* (1995*b*) used backstepping to design anti surge and anti stall controllers. The actuator used was a variable throttle. Here, we use the pressure drop across the CCV as the control variable. Pinsley *et al.* (1991) pointed out that in compression systems with large B-parameter, the use of a CCV is expected to be more effective than the use of the throttle in control of surge. In this case the flow through the throttle is less coupled with the flow through the compressor than is the case when the B-parameter is small. Pinsley *et al.* (1991), Krstić and Kokotović (1995) and Krstić *et al.* (1995*b*) use feedback from mass flow and pressure. As will be shown, the application of the backstepping procedure to CCV surge and stall control, in the case of no mass flow disturbances, results in a control law which uses feedback from mass flow only. Although reducing the number of measurements from two to one, measuring mass flow is more challenging than measuring pressure. As opposed to throttle control, CCV control modifies the compressor characteristic. This allows for, at the cost of a pressure loss over the valve, recovery from rotating stall beyond the surge line. Although the pressure rise achieved in the compression system with a steady pressure drop across the CCV is comparable with the pressure rise achieved when the machine is in rotating stall, the CCV approach is to prefer as the possibility for blade vibration and high temperatures is avoided.

2.2 Preliminaries

2.2.1 The Model of Moore and Greitzer

Several dynamic models for the unstable operation of compression systems have been proposed in the last decade, but the model of Moore and Greitzer

(1986) stands out in the sense that rotating stall amplitude is included as a state, and not manifested as a pressure drop which is the case in the other models.
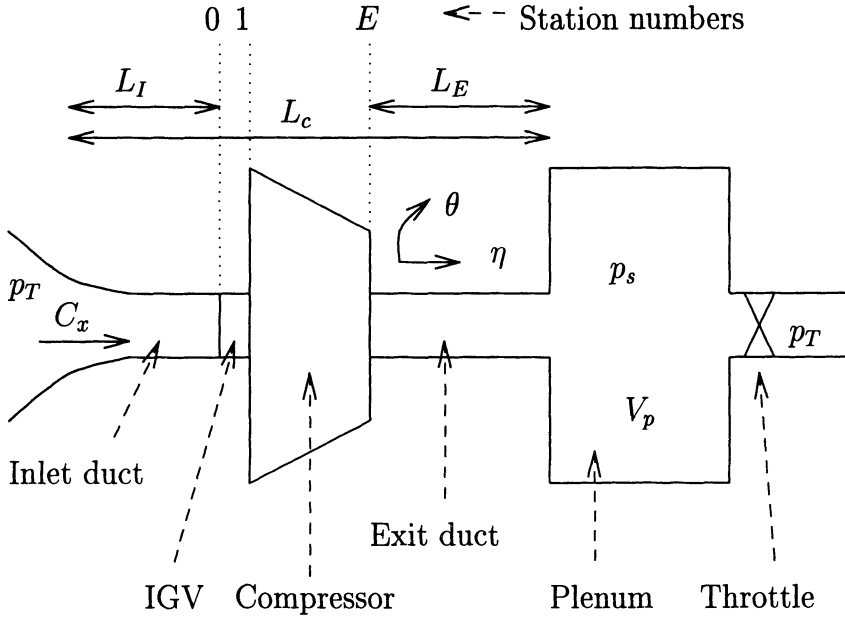
Figure 2.1: *Compression system.*

The low order[1] model of Moore and Greitzer (1986) captures the post stall transients of a low speed axial compressor-plenum-throttle (see Figure 2.1) system. The main assumptions made by Moore and Greitzer (1986) in deriving the model are: incompressible compressor mass flow, compressible flow in the plenum, spatially uniform plenum pressure and short throttle duct. A large hub-to-tip ratio r_{htt} is also assumed, so that a two-dimensional description seems reasonable. Cohen *et al.* (1996) states that

$$r_{htt} > 0.8 \tag{2.1}$$

implies that axial movement of the fluid is dominant and any effect due to radial movement of the fluid is ignored.

The three differential equations of the model result from a Galerkin approximation of the local momentum balance, the annulus-averaged momentum balance and the mass balance of the plenum, as shown in Section 1.5.3. A cubic compressor characteristic is assumed. The model is repeated here for

---

[1]The term "low order" refers to the simplicity of the model, three states, compared to the complex fluid dynamic system it models.

conveinience:

$$\dot{\Psi} = \frac{W/H}{4B^2}\left(\frac{\Phi}{W} - \frac{1}{W}\Phi_T(\Psi)\right)\frac{H}{l_c} \qquad (2.2)$$

$$\dot{\Phi} = \frac{H}{l_c}\left(-\frac{\Psi - \psi_{c0}}{H} - \frac{1}{2}\left(\frac{\Phi}{W} - 1\right)^3 + 1 + \frac{3}{2}\left(\frac{\Phi}{W} - 1\right)\left(1 - \frac{J}{2}\right)\right)$$

$$\dot{j} = J\left(1 - \left(\frac{\Phi}{W} - 1\right)^2 - \frac{J}{4}\right)\varrho$$

where

- Φ is the annulus averaged mass flow coefficient (axial velocity divided by compressor speed), where the annulus average is defined as

$$\frac{1}{2\pi}\int_0^{2\pi}\phi(\xi,\theta)d\theta \triangleq \Phi(\xi),$$

  and $\phi(\xi,\theta)$ is the local mass flow coefficient,

- Ψ is the non dimensional plenum pressure or pressure coefficient (pressure divided by density and the square of compressor speed),

- J is the squared amplitude of rotating stall amplitude

- $\Phi_T(\Psi)$ is the throttle mass flow coefficient and

- l_c is the effective flow-passage nondimensional length of the compressor and ducts defined as

$$l_c \triangleq l_I + \frac{1}{a} + l_E, \qquad (2.3)$$

  where the positive constant a is the reciprocal time-lag parameter of the blade passage.

For a discussion of the employed nondimensionalization, consult Appendix C. The constant $B > 0$ is Greitzer's B-parameter defined by Greitzer (1976a) as

$$B \triangleq \frac{U}{2a_s}\sqrt{\frac{V_p}{A_cL_c}}, \qquad (2.4)$$

where U is the constant compressor tangential speed (in m/s) at mean diameter, a_s is the speed of sound, V_p is the plenum volume, A_c is the flow area and L_c is the length of ducts and compressor. The constant $\varrho > 0$ is defined as

$$\varrho = \frac{3aH}{(1+ma)W}, \qquad (2.5)$$

where m is the compressor-duct flow parameter, H is the semi-height of the compressor characteristic and W is the semi-width of the compressor characteristic. The time variable ξ used throughout this chapter is also nondimensional, and is defined as

$$\xi \triangleq Ut/R \qquad (2.6)$$

where t is the actual time and R is the mean compressor radius. The notation $\dot{\Phi}$ is to be understood as the derivative of Φ with respect to ξ, that is $\dot{\Phi} = \frac{d\Phi}{d\xi}$.

Relaxing the constant speed assumption is important for studying effects of set point changes, acceleration, deceleration, etc. A model taking variable speed into account will be developed in Chapter 4, but will not be considered further here.

In the case of pure surge, that is when $J \equiv 0$, the model reduces to that of Greitzer (1976a):

$$\dot{\Phi} = \frac{1}{l_c}(\Psi_c(\Phi) - \Psi) \qquad (2.7)$$

$$\dot{\Psi} = \frac{1}{4B^2 l_c}(\Phi - \Phi_T(\Psi)).$$

Actually, in Greitzer (1976a), the model was written

$$\dot{\Phi} = B(\Psi_c(\Phi) - \Psi)$$

$$\dot{\Psi} = \frac{1}{B}(\Phi - \Phi_T(\Psi)).$$

The discrepancy in the constants is due to Greitzer (1976a) defining nondimensional time as $\xi = t\omega_H$, where

$$\omega_H = a\sqrt{\frac{A_c}{V_p L_c}} \qquad (2.8)$$

is the Helmholtz frequency. Here, nondimensional time is defined according to (2.6), as was also done by Moore and Greitzer (1986). The model (2.7) was derived for axial compression systems, but it was demonstrated by Hansen *et al.* (1981) that the model also is applicable to centrifugal systems.

The pressure rise of the compressor is a nonlinear function of the mass flow. This function, $\Psi_c(\phi)$, is known as the compressor characteristic. Different expressions for this characteristic have been used, but one that has found widespread acceptance in the control literature is the cubic characteristic of Moore and Greitzer (1986):

$$\Psi_c(\phi) = \psi_{c0} + H\left(1 + \frac{3}{2}\left(\frac{\Phi}{W} - 1\right) - \frac{1}{2}\left(\frac{\Phi}{W} - 1\right)^3\right), \qquad (2.9)$$

where the constant $\psi_{c0} > 0$ is the shut-off value of the compressor characteristic. The cubic characteristic with the parameters ψ_{c0}, W and H is shown in Figure 2.2. Mansoux *et al.* (1994), Sepulchre and Kokotović (1996) and Wang and Krstić (1997*a*) suggest other compressor characteristics for axial compressors, and Hansen *et al.* (1981) presents an alternative polynomial characteristic for centrifugal compressors. However, the cubic seems to capture the general shape of the compressor characteristic of a large class of compressors. The nondimensionalization employed, transforms the usual family of curves in the compressor map, one for each compressor speed, to one single characteristic given by (2.9). Nisenfeld (1982) and Badmus *et al.* (1996) concludes that this is in fact a statement of the Fan law relation. The surge line, which passes through the local maxima of the family of curves is transformed to the local maximum of (2.9). The throttle mass flow $\Phi_T(\Psi)$ is
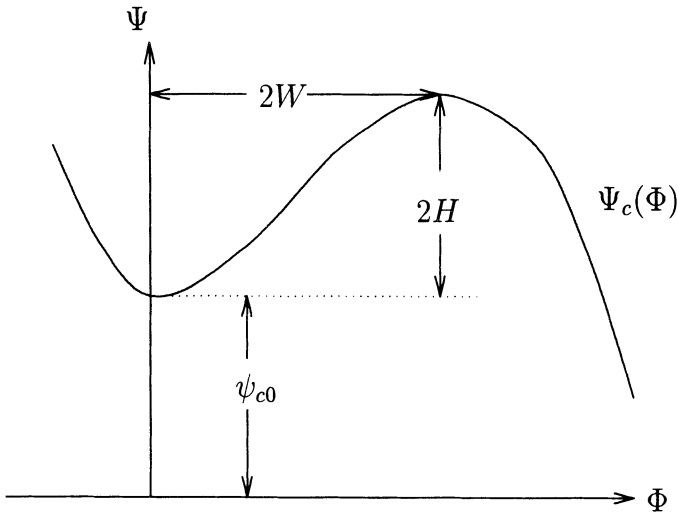
Figure 2.2: *Cubic compressor characteristic of Moore and Greitzer (1986). The constants W and H are known as the semi width and semi height, respectively.*

given by the throttle characteristic

$$\Phi_T(\Psi) = \gamma_T \sqrt{\Psi} \tag{2.10}$$

where γ_T is the throttle gain. The inverse throttle characteristic

$$\Psi_T(\Phi) = \Phi_T^{-1}(\Phi) = \frac{1}{\gamma_T^2}\Phi^2 \tag{2.11}$$

is shown in Figure 2.5.

2.2.2   Close Coupled Valve

A compressor in series with a CCV will be studied in the following. According to Simon and Valavani (1991), with "close-coupled" it is to be understood that the distance between the compressor outlet and the valve is so small that no significant mass storage can take place, see Figure 2.3.
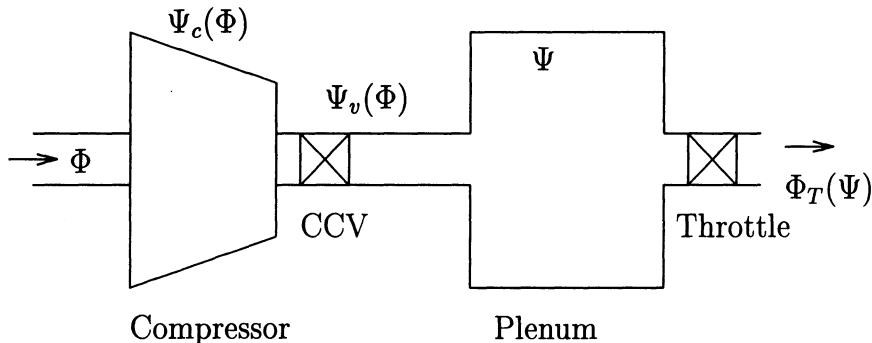
Figure 2.3: *Compression system with CCV*

The assumption of no mass storage between the compressor and the valve allows for the definition of an *equivalent* compressor. This term was introduced by Simon and Valavani (1991). The pressure rise over this equivalent compressor is the sum of the pressure rise over the compressor and the pressure drop over the valve. The pressure drop over the valve will be used as the control. This will allow for manipulation of the equivalent compressor characteristic, given by

$$\Psi_e(\Phi) = \Psi_c(\Phi) - \Psi_v(\Phi), \tag{2.12}$$

where $\Psi_c(\Phi)$ and $\Psi_v(\Phi)$ are the compressor pressure rise and valve pressure drop respectively and Φ is the axial mass flow coefficient. The motivation behind this, is that the slope of the compressor characteristic determines the stability properties of the equilibrium of the system, and this slope can be varied by varying the pressure drop over the CCV. The use of the CCV as an actuator for surge control is also elaborated upon in Section 5.7, where the stabilizing effect of such a valve is discussed in connection with the destabilizing effect of incidence losses.

The CCV has a characteristic given by

$$\Psi_v(\Phi) = \frac{1}{\gamma^2}\Phi^2, \tag{2.13}$$

where $\gamma > 0$ is proportional to the valve opening. We now set out to repeat the modeling and Galerkin approximation of Moore and Greitzer (1986)

with the equivalent characteristic Ψ_e replacing Ψ_c. Equation (5) in Moore and Greitzer (1986), which gives the pressure rise across the compressor, is modified according to

$$\underbrace{\frac{p_E - p_1}{\rho U^2} = N_s F(\phi) - \frac{1}{2a}\left(2\frac{\partial \phi}{\partial \xi} + \frac{\partial \phi}{\partial \theta}\right)}_{\text{Equation (5) in Moore and Greitzer (1986)}} - \Psi_v(\phi) \qquad (2.14)$$

where p_1 and p_E is the static pressure at the entrance and exit of the equivalent compressor, ρ is the constant inlet density, U is the compressor speed at mean diameter, N_s is the number of compressor stages, $F(\phi)$ is the pressure rise coefficient in the blade passage, and θ is the angular coordinate around the wheel. Equation (2.14) now gives the pressure rise over the equivalent compressor.

Using (2.14) as a starting point and following the derivation of Moore and Greitzer (1986), the following model is found[2]:

$$
\begin{aligned}
\dot{\Psi} &= \frac{W/H}{4B^2}\left(\frac{\Phi}{W} - \frac{1}{W}\Phi_T(\Psi)\right)\frac{H}{l_c} \\
\dot{\Phi} &= \frac{H}{l_c}\left(-\frac{\Psi - \psi_{c0}}{H} - \frac{1}{2}\left(\frac{\Phi}{W} - 1\right)^3 + 1 \right. \\
&\qquad\left. + \frac{3}{2}\left(\frac{\Phi}{W} - 1\right)\left(1 - \frac{J}{2}\right) - \frac{1}{\gamma^2}\left(\frac{W^2 J}{2H} + \frac{\Phi^2}{H}\right)\right) \qquad (2.15) \\
\dot{J} &= J\left(1 - \left(\frac{\Phi}{W} - 1\right)^2 - \frac{J}{4} - \frac{1}{\gamma^2}\frac{4W\Phi}{3H}\right)\varrho,
\end{aligned}
$$

which will be used in design of stall/surge controllers in this chapter. In the simpler case of pure surge, J is set to zero, and we are left with the model

$$
\begin{aligned}
\dot{\Psi} &= \frac{1}{4B^2 l_c}(\Phi - \Phi_T(\psi)) \qquad (2.16) \\
\dot{\Phi} &= \frac{1}{l_c}(\underbrace{\Psi_c(\Phi) - \Psi_v(\Phi)}_{\Psi_e(\Phi)} - \Psi)
\end{aligned}
$$

which will used in the study of surge control.

2.2.3 Equilibria

The compressor is in equilibrium when $\dot{\Phi} = \dot{\Psi} = \dot{J} = 0$. If $J(0) = 0$ then $J \equiv 0$ and the equilibrium values ϕ_0 and ψ_0 are given by the intersection

---

[2]The complete derivation is shown in Appendix D.

of $\Psi_e(\Phi)$ and the throttle characteristic. If $J(0) > 0$, and the throttle characteristic crosses Ψ_e to the left of the local maximum, the compressor may[3] enter rotating stall and the equilibrium values ϕ_0 and ψ_0 are given by the intersection of the throttle characteristic and the stall characteristic $\Psi_{es}(\Phi)$ which is found by analyzing the $\dot{J}$-equation of (2.15). It is seen that $\dot{J} = 0$ is satisfied for $J = 0$ or

$$J = J_e = 4 \left(1 - \left(\frac{\Phi}{W} - 1 \right)^2 - \frac{1}{\gamma^2} \frac{4W\Phi}{3H} \right). \tag{2.17}$$

Inserting (2.17) in the $\dot{\Phi}$-equation of (2.15) and setting $\dot{\Phi} = 0$ gives the expression for $\Psi_{es}(\phi)$:

$$\Psi_{es}(\Phi) = \Psi_s(\Phi) + \frac{5}{H}\Psi_v(\Phi) - \frac{8W}{H\gamma^2}\left(1 - \frac{W^2}{3H^2\gamma^2}\right)\Phi, \tag{2.18}$$

where

$$\Psi_s(\Phi) = \psi_{c0} + H\left(1 - \frac{3}{2}\left(\frac{\Phi}{W} - 1\right) + \frac{5}{2}\left(\frac{\Phi}{W} - 1\right)^3\right) \tag{2.19}$$

is the stall characteristic found when the CCV is not present. In Figure 2.4 the various characteristics are shown. As can be seen, the throttle line intersects Ψ_c in a point of positive slope, that is in the unstable area of the compressor map, and the compressor would go into rotating stall or surge. By introducing the CCV, the throttle line crosses the equivalent characteristic Ψ_e in an area of negative slope. This new equilibrium is thus stable.

2.2.4   Change of Variables

The equilibrium of the compression system without the presence of the valve, is at the intersection of the compressor characteristic $\Psi_c(\Phi)$ and the throttle characteristic $\Phi_T(\Psi)$. When introducing the CCV into the system, the equilibrium is shifted to the intersection of the equivalent compressor characteristic $\Psi_e(\Phi)$ and the throttle characteristic $\Phi_T(\Psi)$. The equilibrium values are then related through

$$\psi_0 = \Phi_T^{-1}(\phi_0) = \Psi_e(\phi_0). \tag{2.20}$$

To prepare for the analysis of the system, it is desirable to perform a change of coordinates on the system equations so that the origin becomes the equilibrium under study. The new coordinates are defined as

$$\hat{\psi} = \Psi - \psi_0 \tag{2.21}$$

$$\hat{\phi} = \Phi - \phi_0.$$

---

[3]This depends on the numerical value of B. Greitzer and Moore (1986) showed that small B gives rotating stall, and large B gives surge.
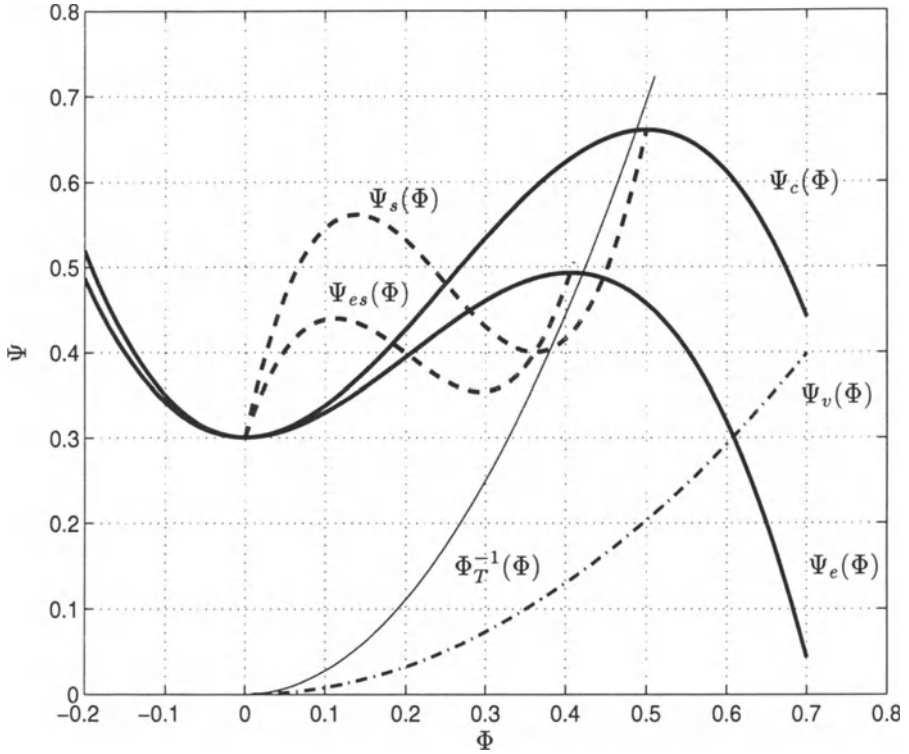
Figure 2.4: *Compressor and throttle characteristics.*

The system characteristics in the new coordinates are defined as

$$
\begin{aligned}
\hat{\Psi}_e(\hat{\phi}) &= \Psi_e(\hat{\phi} + \phi_0) - \Psi_e(\phi_0) \\
&= \Psi_e(\hat{\phi} + \phi_0) - \psi_0 \quad (2.22) \\
\hat{\Psi}'_c(\hat{\phi}) &= \Psi_c(\hat{\phi} + \phi_0) - \psi_0 \quad (2.23) \\
\hat{\Psi}_v(\hat{\phi}) &= \Psi_v(\hat{\phi} + \phi_0) - \psi_0 \quad (2.24) \\
\hat{\Phi}_T(\hat{\psi}) &= \Phi_T(\hat{\psi} + \psi_0) - \phi_0. \quad (2.25)
\end{aligned}
$$

Using (2.9), the transformed compressor characteristic (2.23) can be calculated as

$$
\hat{\Psi}'_c(\hat{\phi}) = \hat{\psi}_{co} - k_3 \hat{\phi}^3 - k_2 \hat{\phi}^2 - k_1 \hat{\phi}, \quad (2.26)
$$

where

$$
\hat{\psi}_{co} = \psi_{co} - \psi_0 - \frac{\phi_0^2 H}{2W^2}\left(\frac{\phi_0}{W} - 3\right), \quad (2.27)
$$

$$k_1 = \frac{3H\phi_0}{2W^2}\left(\frac{\phi_0}{W} - 2\right), \tag{2.28}$$

$$k_2 = \frac{3H}{2W^2}\left(\frac{\phi_0}{W} - 1\right), \tag{2.29}$$

$$k_3 = \frac{H}{2W^3}. \tag{2.30}$$

It can be recognized that $k_3 > 0$, while $k_1 \leq 0$ if the equilibrium is in the unstable region of the compressor map and $k_1 > 0$ otherwise. The sign of k_2 may vary. If $\phi_0 > W$ then $k_2 > 0$, and if $\phi_0 < W$ then $k_2 < 0$.

Using the definition of the equivalent compressor (2.12) and the definition of ψ_0 in (2.20), it can be shown that

$$\psi_0 = \psi_{co} - \frac{\phi_0^2 H}{2W^2}\left(\frac{\phi_0}{W} - 3\right) - \Psi_v(\phi_0). \tag{2.31}$$

Combining (2.31) with (2.27) we get the simple result

$$\hat{\psi}_{co} = \Psi_v(\phi_0), \tag{2.32}$$

which could have been seen directly from Figure 2.5. The Moore-Greitzer model (2.15) can now be written in the new coordinates as

$$\dot{\hat{\psi}} = \frac{1}{4B^2 l_c}\left(\hat{\phi} - \hat{\Phi}_T(\hat{\psi})\right) \tag{2.33}$$

$$\dot{\hat{\phi}} = \frac{1}{l_c}\left(\hat{\Psi}'_c(\hat{\phi}) - \hat{\psi} - \hat{\Psi}_v(\hat{\phi}) - \psi_0 - \frac{3H}{4}J\left(\frac{\Phi}{W} - 1\right) - \frac{W^2 J}{2\gamma^2}\right)$$

$$\dot{J} = \varrho J\left(1 - \left(\frac{\Phi}{W} - 1\right)^2 - \frac{J}{4}\right) - \frac{4W\varrho}{3H\gamma^2}J\Phi,$$

By defining

$$\hat{\Psi}'_c(\hat{\phi}) = \Psi_v(\phi_0) + \hat{\Psi}_c(\hat{\phi}), \tag{2.34}$$

where

$$\hat{\Psi}_c(\hat{\phi}) \triangleq -k_3\hat{\phi}^3 - k_2\hat{\phi}^2 - k_1\hat{\phi}, \tag{2.35}$$

the model (2.33) can be written

$$\dot{\hat{\psi}} = \frac{1}{4B^2 l_c}\left(\hat{\phi} - \hat{\Phi}_T(\hat{\psi})\right) \tag{2.36}$$

$$\dot{\hat{\phi}} = \frac{1}{l_c}\left(\hat{\Psi}_c(\hat{\phi}) - \hat{\psi} - u - \frac{3H}{4}J\left(\frac{\Phi}{W} - 1\right) - \frac{W^2 J}{2\gamma^2}\right)$$

$$\dot{J} = \varrho J\left(1 - \left(\frac{\Phi}{W} - 1\right)^2 - \frac{J}{4}\right) - \frac{4W\varrho}{3H\gamma^2}J\Phi,$$
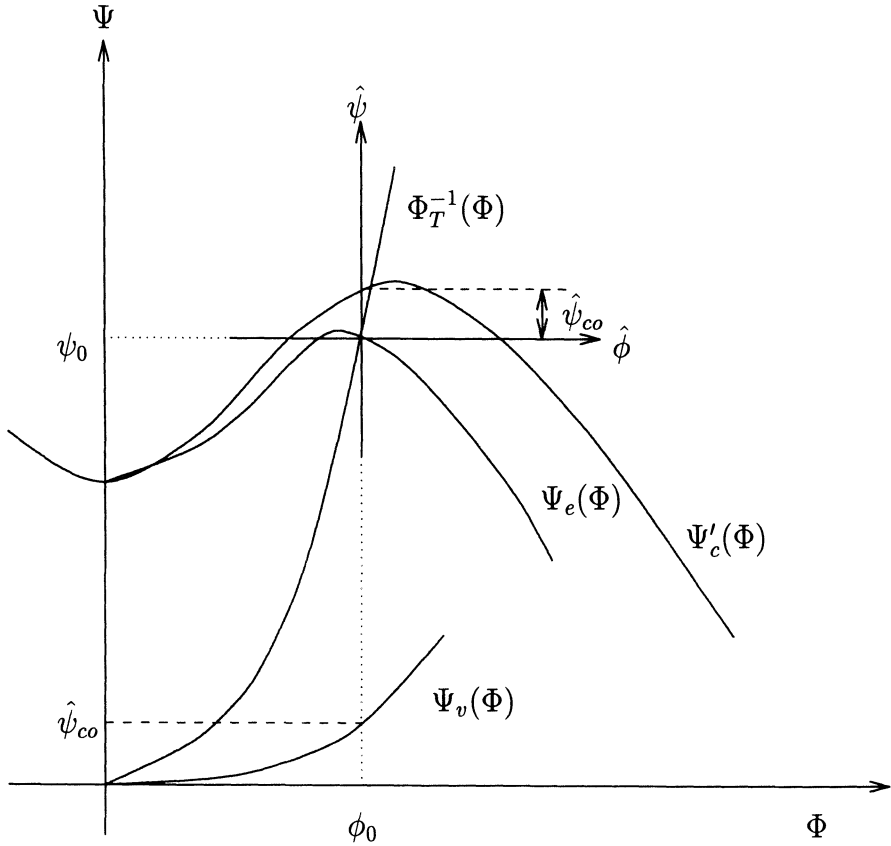
Figure 2.5: *Change of variables, principal drawing*

where the control u has been selected as

$$u = \hat{\Psi}_v(\hat{\phi}) + \psi_0 - \Psi_v(\phi_0) = \Psi_v(\Phi) - \Psi_v(\phi_0). \qquad (2.37)$$

In the case of pure surge, the model (2.36) reduces to

$$\dot{\hat{\psi}} = \frac{1}{4B^2 l_c}(\hat{\phi} - \hat{\Phi}_T(\hat{\psi})) \qquad (2.38)$$

$$\dot{\hat{\phi}} = \frac{1}{l_c}(\hat{\Psi}_c(\hat{\phi}) - u - \hat{\psi})$$

Simon and Valavani (1991) suggested using the pressure drop across the valve as the control variable u. This approach will also be taken here. Our aim will be to design a control law u for the valve such that the compressor can be operated also on the left side of the original surge line without going into

surge or rotating stall. That is, we are going to use feedback to move the surge line towards lower values of Φ, and thus expand the useful range of mass flows over which the compressor can be safely operated.

It is evident that there must exist a pressure drop over the valve when the compressor is operated in a previously unstable area. The price paid for a larger operating range, is some pressure loss at low mass flows. A further discussion of the steady state pressure loss can be found in Simon and Valavani (1991).

2.2.5 Disturbances

As in all types of physical systems, disturbances will occur in the compression system. Greitzer and Moore (1986) stated that this is a topic that need more study, at least in the case of the disturbances initiating stall and surge. Some research have been done in this area. Hynes and Greitzer (1987), DeLaat *et al.* (1996) and others have studied the effect of circumferential inlet flow distortion on the stability properties, and Simon and Valavani (1991), Haddad *et al.* (1997) and others studied mass flow and pressure disturbances. Baghdadi and Lueke (1982) study the effect of inlet temperature distortion and find the effects of this type of distortion to be as significant as those of inlet pressure distortion. From a control theory point of view it is also important to investigate what performance the closed loop system will have when disturbances is taken into account.

As in Simon and Valavani (1991), the effect of a pressure disturbance $\hat{\Psi}_d(\xi)$, and a flow disturbance $\hat{\Phi}_d(\xi)$ will be considered here. The pressure disturbance, which may arise from combustion induced fluctuations when considering the model of a gas turbine, will accelerate the flow. As pointed out by van de Wal and Willems (1996), the flow disturbances may arise from processes upstream of the compressor, other compressors in series or an air cleaner in the compressor duct. In the case of an aircraft jet engine, large angle of attack or altitude variations may cause mass flow disturbances according to van de Wal and Willems (1996) and DeLaat *et al.* (1996). Also, DeLaat *et al.* (1996) reports of a number of aircraft maneuvers (full-rudder sideslips, wind-up turns, etc.) causing inlet airflow disturbances in the jet engine of a F-15 fighter.

In the analysis of Simon and Valavani (1991) $\hat{\Phi}_d(\xi)$ is set to zero. Disturbances in stall/surge control are also studied by Haddad *et al.* (1997), with disturbances assumed to converge to zero. Here, both types of disturbances, mass flow and pressure, will be considered. The disturbances are time varying, and the only assumption made at this point is boundedness, that is $\|\hat{\Phi}_d\|_\infty$ and $\|\hat{\Psi}_d\|_\infty$ exist. In addition to time varying disturbances, constant, or slow varying, offsets will be introduced into the model. This is of particu-

lar interest when e.g. a constant negative mass flow disturbance pushes the equilibrium over the surge line, initiating surge or rotating stall. The offsets in mass flow and pressure rise are termed d_ϕ and d_ψ, respectively. The constant bias d_ψ in pressure can also be thought of as reflecting some uncertainty in the compressor characteristic $\hat{\Psi}_c(\hat{\phi})$, and likewise and the mass flow bias d_ϕ can be thought of as reflecting a uncertainty in the throttle characteristic $\hat{\Phi}(\hat{\psi})$. A study of surge/stall control for compressors with uncertain compressor characteristic was also done by Leonessa *et al.* (1997*b*). With these disturbances the model becomes:

$$\dot{\hat{\psi}} = \frac{1}{4B^2 l_c} \left(\hat{\phi} - \hat{\Phi}_T(\hat{\psi}) - \hat{\Phi}_d(\xi) - d_\phi \right) \tag{2.39}$$

$$\dot{\hat{\phi}} = \frac{1}{l_c} \left(-\hat{\psi} + \hat{\Psi}_c(\hat{\phi}) - \hat{\Psi}_v(\hat{\phi}) + \hat{\Psi}_d(\xi) + d_\psi \right.$$
$$\left. - \frac{3HJ}{4} \left(\frac{\Phi}{W} - 1 \right) - \frac{W^2 J}{2\gamma^2} \right)$$

$$\dot{J} = \varrho J \left(1 - \left(\frac{\Phi}{W} - 1 \right)^2 - \frac{J}{4} \right) - \frac{4W\varrho}{3H\gamma^2} J\Phi,$$

and in the case of pure surge

$$\dot{\hat{\psi}} = \frac{1}{4B^2 l_c} \left(\hat{\phi} - \hat{\Phi}_T(\hat{\psi}) - \hat{\Phi}_d(\xi) - d_\phi \right) \tag{2.40}$$

$$\dot{\hat{\phi}} = \frac{1}{l_c} \left(-\hat{\psi} + \hat{\Psi}_c(\hat{\phi}) - \hat{\Psi}_v(\hat{\phi}) + \hat{\Psi}_d(\xi) + d_\psi \right). \tag{2.41}$$

2.3 Surge Control

In this section controllers will be designed for the pure surge case. First the undisturbed case is studied, then disturbances are added, and finally adaption will be used to stabilize the system in the presence of constant disturbances.

2.3.1 Undisturbed Case

Theorem 2.1 *The controller*

$$u = c_2(\Phi - \phi_0), \tag{2.42}$$

where $c_2 > a_m$ and a_m is the maximum positive slope of the compressor characteristic $\hat{\Psi}_c(\hat{\phi})$, renders the equilibrium (ϕ_0, ψ_0) of (2.16) GAS. □

Proof: The backstepping methodology of Krstić *et al.* (1995*a*) will be employed in deriving the control law.

Step 1. Two error variables are defined as $z_1 = \hat{\psi}$ and $z_2 = \hat{\phi} - \alpha$. The control Lyapunov function (clf) for this step is chosen as

$$V_1 = 2B^2 l_c z_1^2 \tag{2.43}$$

with time derivative along the solution trajectories of (2.38) given by

$$\dot{V}_1 = z_1 \left(-\hat{\Phi}_T(z_1) + z_2 + \alpha \right). \tag{2.44}$$

The throttle is assumed passive, that is $\hat{\psi} \hat{\Phi}_T(\hat{\psi}) \geq 0 \ \forall \hat{\psi}$. We have

$$\hat{\psi} \hat{\Phi}_T(\hat{\psi}) \geq 0 \ \Rightarrow \ -z_1 \hat{\Phi}_T(z_1) \leq 0 \tag{2.45}$$

As it is desirable to avoid cancelation of useful nonlinearities in (2.44), the stabilizing function α is not needed and accordingly $\alpha = 0$, which gives

$$\dot{V}_1 = -\hat{\Phi}_T(z_1) z_1 + z_1 z_2. \tag{2.46}$$

Although the virtual control α is not needed here, in the interest of consistency with the following sections, this notation is kept.

Step 2. The derivative of z_2 is

$$\dot{z}_2 = \frac{1}{l_c} \left(\hat{\Psi}_c(z_2) - z_1 - u \right). \tag{2.47}$$

The clf for this step is

$$V_2 = V_1 + \frac{l_c}{2} z_2^2 \tag{2.48}$$

with time derivative

$$\dot{V}_2 = -z_1 \hat{\Phi}_T(z_1) + z_2 \left(\hat{\Psi}_c(z_2) - u \right). \tag{2.49}$$

Notice that V_2 as defined by (2.48) is similar to the incremental energy of Simon and Valavani (1991).

Control law. The control variable u will be chosen so that (2.49) is made negative definite. To this end we define the *linear* control law

$$u = c_2 z_2, \tag{2.50}$$

where the controller gain $c_2 > 0$ is chosen so that

$$z_2 \Psi_c(z_2) - c_2 z_2^2 < 0. \tag{2.51}$$

Using (2.35) this implies that c_2 must satisfy

$$-k_3 z_2^2 \underbrace{\left(z_2^2 + \frac{k_2}{k_3} z_2 + \frac{k_1 + c_2}{k_3} \right)}_{f(z_2)} < 0. \qquad (2.52)$$

Analyzing (2.52), by finding the roots of $f(z_2)$ defined above, it is seen that (2.52) is satisfied if c_2 is chosen according to

$$c_2 > \frac{k_2^2}{4k_3} - k_1. \qquad (2.53)$$

Although (2.53) implies that the compressor characteristic must be known in order to determine c_2, it can be shown that the knowledge of a bound on the positive slope of the characteristic is sufficient. Differentiating (2.35) twice with respect to $\hat{\phi}$, reveals that the maximum positive slope occurs for

$$\hat{\phi} = \hat{\phi}_m = -\frac{k_2}{3k_3} \qquad (2.54)$$

and is given by

$$a = \left. \frac{d\hat{\Psi}_c(\hat{\phi})}{d\hat{\phi}} \right|_{\hat{\phi}=\hat{\phi}_m} = \frac{k_2^2}{3k_3} - k_1 = \frac{3H}{2W}. \qquad (2.55)$$

Assuming that only an upper bound a_m on the positive slope of $\hat{\Psi}_c(\hat{\phi})$ is known, a conservative condition for c_2 is

$$c_2 > a_m \geq a > \frac{k_2^2}{4k_3} - k_1. \qquad (2.56)$$

Thus the price paid for not knowing the exact coefficients of the compressor characteristic is a somewhat conservative condition for the controller gain c_2. Notice also that no knowledge of Greitzer's B-parameter or its upper bound is required in formulating the controller. The final expression for $\dot{V}_2$ is then

$$\dot{V}_2 = -z_1 \hat{\Phi}_T(z_1) + \hat{\Psi}_c(z_2) z_2 - c_2 z_2^2 = -W(z_1, z_2) \leq 0. \qquad (2.57)$$

The closed loop system can be written as

$$\dot{z}_1 = \frac{1}{4B^2 l_c}(-\hat{\Phi}_T(z_1) + z_2) \qquad (2.58)$$

$$\dot{z}_2 = \frac{1}{l_c}(-z_1 + \hat{\Psi}(z_2) - c_2 z_2). \qquad (2.59)$$

It follows that the equilibrium point $z_1 = z_2 = 0$ is GAS, and the same result holds for the equilibrium (ϕ_0, ψ_0). □

Remark 2.1 *By combining (2.84) and (2.50), the following control law for the CCV gain is found:*

$$c_2(\Phi - \phi_0) = \Psi_v(\Phi) - \Psi_v(\phi_0) \tag{2.60}$$

$$\Downarrow$$

$$\gamma = \sqrt{\frac{\Phi + \phi_0}{c_2}}. \tag{2.61}$$

Notice that this control law requires measurement of mass flow coefficient only.   □

Remark 2.2 *Although not showing stability, Bendixon's criterion can be used to show that the controller (2.50) guarantees that no limit cycles (surge oscillations) exist. Bendixon's criterion states (somewhat simplified) that no limit cycles exists in a dynamical system defined on a simply connected region $D \subset \mathbb{R}^2$ if the divergence of the system is not identically zero and does not change sign in D. For an exact statement of Bendixon's criterion and the proof, see any textbook on dynamical systems, e.g. Perko (1991). The divergence $\nabla \cdot \boldsymbol{f}$ of the system $\dot{x} = \boldsymbol{f}(x)$ defined by (2.16) is*

$$\nabla \cdot \boldsymbol{f} = -\frac{1}{4B^2 l_c} \frac{\partial \hat{\Phi}_T(\hat{\psi})}{\partial \hat{\psi}} + \frac{1}{l_c} \left(\frac{\partial \hat{\psi}_c(\hat{\phi})}{\partial \hat{\phi}} - \frac{\partial u}{\partial \hat{\phi}} \right). \tag{2.62}$$

The slope of the throttle is always positive, so the first term in (2.62) is always negative. To make the second term also negative, it is sufficient that $\frac{\partial u}{\partial \hat{\phi}}$ dominates $\frac{\partial \hat{\psi}_c(\hat{\phi})}{\partial \hat{\phi}}$, which is exactly what is ensured by the controller in Theorem 2.1. Thus, according to Bendixon's criterion, no surge oscillations can exist for the closed loop system.   □

2.3.2   Determination of ϕ_0

As a consequence of the controller (2.42) being designed after the system equations are transformed to the new coordinates, its implementation depends on knowledge of the equilibrium value ϕ_0. The equilibrium is located at the intersection of the equivalent compressor characteristic $\Psi_e(\Phi)$ and the throttle characteristic Φ_T^{-1}. By combining (2.84), (2.42) and (2.61), it is seen that

$$\begin{aligned}
\Psi_v(\phi_0) &= (u + \Psi_v(\phi_0))|_{\Phi = \phi_0} \\
&= \left(c_2(\Phi - \phi_0) + \frac{c_2}{\Phi + \phi_0} \phi_0^2 \right)\bigg|_{\Phi = \phi_0} \\
&= \frac{c_2 \phi_0}{2}. \tag{2.63}
\end{aligned}$$

At the equilibrium, we have

$$\Psi_c(\phi_0) - \Psi_v(\phi_0) = \frac{1}{\gamma^2}\phi_0^2, \tag{2.64}$$

or by using (2.63), ϕ_0 is found by solving the following 3rd order equation

$$\psi_{co} + H\left(1 + \frac{3}{2}\left(\frac{\phi_0}{W} - 1\right) - \frac{1}{2}\left(\frac{\phi_0}{W} - 1\right)^3\right) - \frac{c_2\phi_0}{2} = \frac{2}{\gamma^2}\phi_0^2, \tag{2.65}$$

with respect to ϕ_0, and its value is to be used in the control law (2.42). Solving (2.65) requires knowledge of the compressor characteristic. If this is not the case, alternatives to finding ϕ_0 explicitly are, using an adaption scheme like the one suggested by Bazanella *et al.* (1997) for a genreal nonlinear system with unknown equilibrium or it is possible to use throttle control in addition to the CCV control to control ϕ using ϕ_0 as the reference. If none of these alternatives are attractive, an approximation for ϕ_0 can be used. In this case, asymptotic stability cannot be shown, but convergence to a set and avoidance of surge is easily shown. Defining $\Delta\phi$ as

$$\Delta\phi = \phi_0 - \phi_{aprx}, \tag{2.66}$$

where ϕ_{aprx} is the approximation used for feedback, and ϕ_0 is the actual and unknown value of the equilibrium. By using the same Lyapunov function as is Theorem 2.1, and

$$u = c_2(\Phi - \phi_{aprx}) = c_2(\Phi - \phi_0 + \Delta\phi), \tag{2.67}$$

the time derivative of V_2 is found and upper bounded by

$$\dot{V}_2 \leq -z_1\hat{\Phi}(z_1) + z_2(\hat{\Psi}_c(z_2) - c_2z_2)z_2 - z_2c_2\Delta\phi. \tag{2.68}$$

Application of Young's inequality[4] to the last term in (2.68) gives

$$-z_2c_2\Delta\phi \leq \frac{c_2}{2}\left(\frac{z_2^2}{\eta_0} + (\Delta\phi)^2\eta_0\right), \tag{2.69}$$

where η_0 is a constant, and it follows that

$$\begin{aligned}\dot{V}_2 &\leq -z_1\hat{\Phi}_T(z_1) + z_2(\hat{\Psi}_c(z_2) - c_2(1 - \frac{1}{2\eta_0})z_2)z_2 + \eta_0(\Delta\phi)^2 \\ &= -W(z_1, z_2) + \eta_0(\Delta\phi)^2, \end{aligned} \tag{2.70}$$

---

[4]In its simplest form Young's inequality states that

$$\forall a, b : ab \leq \frac{1}{2}(\frac{a^2}{c} + cb^2) \ \forall c > 0.$$

where the definition of W is obvious. By choosing η_0 and c_2 such that

$$c_2\left(1 - \frac{1}{2\eta_0}\right) > a_m, \tag{2.71}$$

is satisfied, it can be shown that $W(z_1, z_2)$ is radially unbound and positive definite. Thus, $\dot{V}_2 < 0$ outside a set $\mathcal{R}_\Delta$. This set can be found in the following manner: According to Krstić et al. (1995a), the fact that $V_2(z_1, z_2)$ and $W(z_1, z_2)$ is positive definite and radially unbounded, and $V_2(z_1, z_2)$ is smooth, implies that there exists class-$\mathcal{K}_\infty$ functions β_1, β_2 and β_3 such that

$$\beta_1(|z|) \leq V_2(z) \leq \beta_2(|z|) \tag{2.72}$$
$$\beta_3(|z|) \leq W(z) \tag{2.73}$$

where $z = (z_1 \quad z_2)^{\mathrm{T}}$. Following the proof of Lemma 2.26 in Krstić et al. (1995a), we have that the states of the model are uniformly ultimately bounded, and that they converge to the residual set

$$\mathcal{R}_\Delta = \left\{ z \ : \ |z| \leq \beta_1^{-1} \circ \beta_2 \circ \beta_3^{-1}\left(\eta(\Delta\phi)^2\right) \right\}. \tag{2.74}$$

From (2.70) it follows that $\dot{V}_2$ is negative whenever $W(z) > \eta_0(\Delta\phi)^2$. Combining this with (2.73) it can be concluded that

$$|z(\xi)| > \beta_3^{-1}\left(\eta(\Delta\phi)^2\right) \ \Rightarrow \ \dot{V}_2 < 0. \tag{2.75}$$

This means that if $|z(0)| \leq \beta_3^{-1}\left(\eta(\Delta\phi)^2\right)$, then

$$V_2(z(\xi)) \leq \beta_2 \circ \beta_3^{-1}\left(\eta(\Delta\phi)^2\right), \tag{2.76}$$

which in turn implies that

$$|z(\xi)| \leq \beta_1^{-1} \circ \beta_2 \circ \beta_3^{-1}\left(\eta(\Delta\phi)^2\right). \tag{2.77}$$

If, on the other hand $|z(0)| > \beta_3^{-1}\left(\eta(\Delta\phi)^2\right)$, then $V_2(z(\xi)) \leq V_2(z(0))$, which implies

$$|z(\xi)| \leq \beta_1^{-1} \circ \beta_2(|z(0)|). \tag{2.78}$$

Combining (2.77) and (2.78) leads to the global uniform boundedness of $z(\xi)$:

$$\|z\|_\infty \leq \max\left\{ \beta_1^{-1} \circ \beta_2 \circ \beta_3^{-1}\left(\eta(\Delta\phi)^2\right), \ \beta_1^{-1} \circ \beta_2(|z(0)|) \right\}, \tag{2.79}$$

while (2.75) and (2.72) prove the convergence of $z(\xi)$ to the residual set defined in (2.74).

It is trivial to establish the fact that no limit cycles, and hence surge oscillations, can exist inside this set using Bendixon's criterion. It is seen from

(2.74), that the size of the set $\mathcal{R}_\Delta$ is dependent on the square of the equilibrium estimate error $\Delta\phi$ and the parameter η_0. A more accurate estimate ϕ_{aprx}, or a smaller value of η_0, both implies a smaller set. A smaller value of η_0 will, by equation (2.71), require a larger controller gain c_2, which is to be expected.

2.3.3 Time Varying Disturbances

First, time varying pressure disturbances will be considered. That is, $\hat{\Phi}_d(\xi)$, d_ϕ and d_ψ are set to zero as in Simon and Valavani (1991).

Theorem 2.2 (Time varying pressure disturbances)
The controller
$$u = (c_2 + d_2)(\Phi - \phi_0),\qquad(2.80)$$

where c_2 is chosen as in Theorem 2.1, and $d_2 > 0$ guarantees that the states of the model (2.40) are globally uniformly bounded, and that they converge to a set. $\qquad\square$

Proof: The controller will be derived using backstepping.

Step 1. Identical to Step 1 in the proof of Theorem 2.1.

Step 2. The time derivative of z_2 is

$$\dot{z}_2 = \frac{1}{l_c}\left(\hat{\Psi}_c(\hat{\phi}) - z_1 + \hat{\Psi}_d(\xi) - u\right).\qquad(2.81)$$

V_2 is chosen as
$$V_2 = V_1 + \frac{l_c}{2}z_2^2,\qquad(2.82)$$

where $\dot{V}_2$ can be bounded according to

$$\dot{V}_2 = -\hat{\Phi}_T(z_1)z_1 + z_2\left(\hat{\Psi}_c(\hat{\phi}) + \hat{\Psi}_d(\xi) - u\right).\qquad(2.83)$$

Control law. To counteract the effect of the disturbance, a damping factor $d_2 > 0$ is included and u is chosen as

$$u = c_2 z_2 + d_2 z_2.\qquad(2.84)$$

c_2 is chosen so that (2.56) is satisfied. Inserting (2.84) in (2.83) gives

$$\dot{V}_2 = -z_1\hat{\Phi}_T(z_1) + \hat{\Psi}_c(z_2)z_2 - c_2 z_2^2 + \hat{\Psi}_d(\xi)z_2 - d_2 z_2^2.\qquad(2.85)$$

Use of Young's inequality gives

$$z_2 \hat{\Psi}_d(\xi) \leq d_2 z_2^2 + \frac{\hat{\Psi}_d^2(\xi)}{4d_2} \leq d_2 z_2^2 + \frac{\|\hat{\Psi}_d\|_\infty^2}{4d_2}, \qquad (2.86)$$

and $\dot{V}_2$ can be bounded according to

$$\dot{V}_2 \leq -W(z_1, z_2) + \frac{\hat{\Psi}_d^2(\xi)}{4d_2} \leq -W(z_1, z_2) + \frac{1}{4d_2}\|\hat{\Psi}_d\|_\infty^2 \qquad (2.87)$$

where

$$W(z_1, z_2) = z_1 \hat{\Phi}(z_1) - (\hat{\Psi}_c(z_2)z_2 - c_2 z_2^2) \qquad (2.88)$$

is radially unbounded and positive definite. This implies that $\dot{V}_2 < 0$ outside a set $\mathcal{R}_1$ in the $z_1 z_2$ plane.

By using (2.72) and (2.73) again, it follows from similar calculations as in (2.75)-(2.79), that $z(\xi)$ is globally uniformly bounded and that $z(\xi)$ converges to the residual set

$$\mathcal{R}_1 = \left\{ z \; : \; |z| \leq \beta_1^{-1} \circ \beta_2 \circ \beta_3^{-1} \left(\frac{\|\hat{\Psi}_d\|_\infty^2}{4d_2} \right) \right\}. \qquad (2.89)$$

$\square$

Remark 2.3 *Notice that the controller (2.84) is essentially the same as (2.50), with the only difference being that (2.84) requires a larger gain in order to suppress the disturbance. Consequently, Remark 2.1 also applies here.* $\square$

It is now shown that an additional assumption on the disturbance ensures that the controller (2.84) not only makes the states globally uniformly bounded, but also guarantees convergence to the origin.

Corollary 2.1 (Convergence to the origin)
If the disturbance term $\hat{\Psi}_d(\xi)$ is upper bounded by a monotonically decreasing non-negative function $\overline{\Psi}_d(\xi)$ such that

$$|\hat{\Psi}_d(\xi)| \leq \overline{\Psi}_d(\xi) \; \forall \xi \geq 0 \qquad (2.90)$$

and

$$\lim_{\xi \to \infty} \overline{\Psi}_d(\xi) = 0, \qquad (2.91)$$

the controller (2.84) ensures that the states of the model (2.40), with pressure disturbances, converge to the origin. $\square$

Proof: Inspired by the calculations for a simple scalar system starting on page 75 in Krstić *et al.* (1995*a*) , we introduce the signal

$$s(z, \xi) = V_2(z)e^{c\xi}, \tag{2.92}$$

where $c > 0$ is a constant, for use in the proof:

$$
\begin{aligned}
\frac{d}{dt}s(z, \xi) &= \frac{d}{dt}\left\{V_2(z)e^{c\xi}\right\} \\
&= \left(\dot{V}_2(z) + cV_2(z)\right)e^{c\xi} \\
&\leq \left(-W(z) + \frac{\hat{\Psi}_d^2(\xi)}{4d_2} + cV_2(z)\right)e^{c\xi} \\
&\leq (-\beta_3(|z|) + c\beta_2(|z|))\,e^{c\xi} + \frac{\hat{\Psi}_d^2(\xi)}{4d_2}e^{c\xi}. \tag{2.93}
\end{aligned}
$$

By choosing c according to

$$c \leq \beta_2^{-1} \circ \beta_3(|z|) \leq \beta_2^{-1} \circ \beta_3(\|z\|_\infty), \tag{2.94}$$

where the existence of $\|z\|_\infty$ follows from (2.89), (2.93) gives

$$\frac{d}{dt}\left\{V_2(z)e^{c\xi}\right\} \leq \frac{\hat{\Psi}_d^2(\xi)}{4d_2}e^{c\xi}. \tag{2.95}$$

By integrating (2.95) and using an argument similar to the one in the proof of lemma 2.24 in Krstić *et al.* (1995*a*), it can be shown that

$$V_2(z(\xi)) \leq V_2(z(0))e^{-c\xi} + \frac{1}{4cd_2}\left(\overline{\Psi}_d^2(0)e^{-\frac{c\xi}{2}} + \overline{\Psi}_d^2(\xi/2)\right). \tag{2.96}$$

Since $\lim_{\xi\to\infty}\overline{\Psi}_d^2(\xi/2) = 0$ it follows that

$$\lim_{\xi\to\infty}V_2(z(\xi)) = 0. \tag{2.97}$$

As V_2 is positive definite it follows that

$$\lim_{\xi\to\infty}z(\xi) = 0. \tag{2.98}$$

Thus we have shown that under the additional assumptions (2.90) and (2.91) on the disturbance term, $z(\xi)$ converges to the origin. This also implies that $\hat{\phi}$ and $\hat{\psi}$ converge to the origin and that $\Phi(\xi)$ and $\Psi(\xi)$ converge to the point of intersection of the compressor and throttle characteristic. $\qquad\square$

Notice that the positive constant c introduced in (2.92) is used for analysis only, and is *not* included in the implementation of the control law.

At this point we include the flow disturbance $\hat{\Phi}_d(\xi)$ in the analysis.

Theorem 2.3 (Time varying pressure and flow disturbances)
The controller

$$u = c_2 z_2 - k_3 \left(\alpha^3 + 3\alpha z_2^2 \right) - k_2 \hat{\phi}^2 - k_1 \alpha$$
$$+ \frac{d_1}{4B^2} \left(-\hat{\Phi}_T(z_1) + \hat{\phi} \right) + d_2 z_2 \left(1 + \frac{d_1^2}{4B^2} \right), \qquad (2.99)$$

where $c_2 > |k_1|$, $\alpha = -d_1 z_1$ and $d_1, d_2 > 0$ guarantees that the states of the model (2.39) with both mass flow disturbances and pressure disturbances are globally uniformly bounded and that they converge to a set. □

Proof: The backstepping procedure is as follows:

Step 1. As before two error variables z_1 and z_2 are defined as $z_1 = \hat{\psi}$ and $z_2 = \hat{\phi} - \alpha$. Again, V_1 is chosen as

$$V_1 = 2B^2 l_c z_1^2, \qquad (2.100)$$

with time derivative

$$\dot{V}_1 = z_1 \left(-\hat{\Phi}_T(z_1) + z_2 - \hat{\Phi}_d(\xi) + \alpha \right), \qquad (2.101)$$

where (2.39) is used. The virtual control α is chosen as

$$\alpha = -d_1 z_1, \qquad (2.102)$$

where $-d_1 z_1$ is a damping term to be used to counteract the disturbance $\hat{\Phi}_d(\xi)$. $\dot{V}_1$ can now be written as

$$\dot{V}_1 = -d_1 z_1^2 + z_1 z_2 - \hat{\Phi}_d(\xi) z_1 - \hat{\Phi}_T(z_1) z_1, \qquad (2.103)$$

and upper bounded according to

$$\dot{V}_1 \leq -\hat{\Phi}_T(z_1) z_1 + z_1 z_2 + \frac{\|\hat{\Phi}_d\|_\infty^2}{4d_1}. \qquad (2.104)$$

To obtain the bound in (2.104), Young's inequality has been used to obtain

$$-\hat{\Phi}_d(\xi) z_1 \leq d_1 z_1^2 + \frac{\hat{\Phi}_d^2(\xi)}{4d_1} \leq d_1 z_1^2 + \frac{\|\hat{\Phi}_d\|_\infty^2}{4d_1}. \qquad (2.105)$$

Step 2. The derivative of z_2 is

$$\dot{z}_2 = \frac{1}{l_c} \left(\hat{\Psi}_c(\hat{\phi}) - z_1 + \hat{\Psi}_d(\xi) - \frac{\partial \alpha}{\partial z_1} \frac{1}{4B^2 l_c} \left(-\hat{\Phi}_T(z_1) + \hat{\phi} \right) \right.$$
$$\left. + \frac{1}{4B^2 l_c} \frac{\partial \alpha}{\partial z_1} \hat{\Phi}_d(\xi) - u \right). \qquad (2.106)$$

From (2.102) it is seen that

$$\frac{\partial \alpha}{\partial z_1} = -d_1. \tag{2.107}$$

V_2 is chosen as

$$V_2 = V_1 + \frac{l_c}{2} z_2^2. \tag{2.108}$$

Using (2.104) and (2.106), an upper bound on $\dot{V}_2$ is

$$\dot{V}_2 \leq -\hat{\Phi}_T(z_1)z_1 + \frac{\|\hat{\Phi}_d\|_\infty^2}{4d_1} + z_2\left(\hat{\Psi}_c(\hat{\phi}) + \hat{\Psi}_d(\xi)\right.$$

$$\left. + \frac{d_1}{4B^2}\left(-\hat{\Phi}_T(z_1) + \hat{\phi}\right) - \frac{d_1}{4B^2}\hat{\Phi}_d(\xi) - u\right). \tag{2.109}$$

<u>Control law</u>. To counteract the effect of the disturbances, a damping factor d_2 must be included and u is chosen as

$$u = c_2 z_2 - k_3\left(\alpha^3 + 3\alpha z_2^2\right) - k_2\hat{\phi}^2 - k_1\alpha$$

$$+ \frac{d_1}{4B^2}\left(-\hat{\Phi}_T(z_1) + \hat{\phi}\right) + d_2 z_2\left(1 + \frac{d_1^2}{4B^2}\right). \tag{2.110}$$

The parameter c_2 is now chosen according to

$$c_2 > |k_1|. \tag{2.111}$$

Inserting (2.99) in (2.109) gives

$$\dot{V}_2 \leq -(c_2 + k_1)z_2^2 - k_3(z_2^4 + 3\alpha^2 z_2^2) - \hat{\Phi}_T(z_1)z_1 + \frac{\|\hat{\Phi}_d\|_\infty^2}{4d_1}$$

$$-d_2 z_2^2 + |z_2|\|\hat{\Psi}_d\|_\infty + \frac{d_1}{4B^2}|z_2|\|\hat{\Phi}_d\|_\infty - \frac{d_1^2}{4B^2}d_2 z_2^2. \tag{2.112}$$

Using Young's inequality twice gives

$$|z_2|\|\hat{\Psi}_d\|_\infty \leq d_2 z_2^2 + \frac{\|\hat{\Psi}_d\|_\infty^2}{4d_2} \tag{2.113}$$

$$\frac{d_1}{4B^2}|z_2|\|\hat{\Phi}_d\|_\infty \leq \frac{1}{4B^2}\left(d_1^2 d_2 z_2^2 + \frac{\|\hat{\Phi}_d\|_\infty^2}{4d_2}\right). \tag{2.114}$$

The final upper bound for $\dot{V}_2$ can now be written as

$$\dot{V}_2 \leq -W(z_1, z_2) + \frac{1}{\nu_1}\|\hat{\Phi}_d\|_\infty^2 + \frac{1}{\nu_2}\|\hat{\Psi}_d\|_\infty^2 \tag{2.115}$$

where

$$\frac{1}{\nu_1} = \left(\frac{1}{4d_1} + \frac{1}{16B^2 d_2}\right), \quad \frac{1}{\nu_2} = \frac{1}{4d_2} \tag{2.116}$$

and

$$W(z_1, z_2) = (c_2 + k_1)z_2^2 + k_3(z_2^4 + 3\alpha^2 z_2^2) + \hat{\Phi}(z_1)z_1 \tag{2.117}$$

is radially unbounded and positive definite. This implies that $\dot{V}_2 < 0$ outside a set $\mathcal{R}_2$ in the $z_1 z_2$ plane. As in section 6.1, the functions $V_2(z)$ and $W(z)$ exhibit the properties in (2.72). Again, it can be shown that this implies that $z(\xi)$ is globally uniformly bounded and that $z(\xi)$ converges to the residual set

$$\mathcal{R}_2 = \left\{ z : |z| \leq \beta_1^{-1} \circ \beta_2 \circ \beta_3^{-1} \left(\frac{\|\hat{\Psi}_d\|_\infty^2}{\nu_1} + \frac{\|\hat{\Phi}_d\|_\infty^2}{\nu_2} \right) \right\}. \tag{2.118}$$

□

Remark 2.4 *Notice that the control law (2.99), as opposed to (2.84), requires knowledge of the coefficients in the compressor characteristic, the throttle characteristic and the B-parameter.* □

Remark 2.5 *Once the bounds on the disturbances $\|\hat{\Phi}_d\|_\infty$ and $\|\hat{\Psi}_d\|_\infty$ are known, the size of the set $\mathcal{R}_2$ in the $z_1 z_2$ plane can be made arbitrary small by choosing the damping factors d_1 and d_2 sufficiently large. The same comment applies to the set $\mathcal{R}_1$ defined in (2.89).* □

Corollary 2.2 (Convergence to the origin)
If the assumptions on $\hat{\Psi}_d(\xi)$ in equations (2.119) and (2.120) hold, and the following assumption on $\hat{\Phi}_d(\xi)$ is made:

$$|\hat{\Phi}_d(\xi)| \leq \overline{\Phi}_d(\xi) \ \forall \xi \geq 0 \tag{2.119}$$

and

$$\lim_{\xi \to \infty} \overline{\Phi}_d(\xi) = 0, \tag{2.120}$$

where $\overline{\Phi}_d(\xi)$ is a monotonically decreasing non-negative function. Then, the states of the model (2.40) converge to the origin. □

Proof: By using the same arguments as in the proof of Corollary 2.1, but with two disturbance terms, it can be shown that

$$V_2(z(\xi)) \leq V_2(z(0))e^{-c\xi} + \frac{1}{c\nu_1}\left(\overline{\Phi}_d^2(0)e^{-\frac{c\xi}{2}} + \overline{\Phi}_d^2(\xi/2)\right)$$
$$+ \frac{1}{c\nu_2}\left(\overline{\Psi}_d^2(0)e^{-\frac{c\xi}{2}} + \overline{\Psi}_d^2(\xi/2)\right). \tag{2.121}$$

Now $\lim_{\xi \to \infty} \overline{\Psi}_d^{\,2}(\xi/2) = 0$ and $\lim_{\xi \to \infty} \overline{\Phi}_d^{\,2}(\xi/2) = 0$ implies that $\lim_{\xi \to \infty} V_2(z(\xi)) = 0$ and by the positive definiteness of V_2 it follows that

$$\lim_{\xi \to \infty} z(\xi) = 0. \qquad (2.122)$$

Thus we have shown that under the assumptions (2.90), (2.91), (2.119) and (2.120) on the disturbance terms, $z(\xi)$ converge to the origin. This also implies that $\hat{\phi}(\xi)$ and $\hat{\psi}(\xi)$ converges to the origin and that $\Phi(\xi)$ and $\Psi(\xi)$ converge to the point of intersection of the compressor and throttle characteristic. $\square$

A simulation of the response of the control law (2.99) with both mass flow and pressure disturbances is presented in Chapter 3, where it is compared to a passivity based controller.

2.3.4   Adaption of Constant Disturbances

A constant or slow varying disturbance in mass flow can cause the equilibrium of the compression system to be moved into the unstable area of the compressor map. Therefore, the problem of being able to stabilize the system in this case is a very important one. In addition constant disturbances in pressure is considered simultaneously. Consider the following model

$$\dot{\hat{\psi}} = \frac{1}{4B^2 l_c} \left(\hat{\phi} - \hat{\Phi}_T(\hat{\psi}) - d_\phi \right)$$

$$\dot{\hat{\phi}} = \frac{1}{l_c} \left(\hat{\Psi}_c(\hat{\phi}) - \hat{\psi} - d_\psi - u \right), \qquad (2.123)$$

where d_ϕ and d_ψ are constant and unknown disturbances in mass flow and pressure, respectively. Godhavn (1997) used adaptive backstepping for adaption of constant or slow varying sea current disturbances in a surface ship model. The same approach will now be employed here to stabilize (2.123). Two adaption laws will be designed in order to estimate the unknown disturbances and allow them to be counteracted by the control. This approach will result in an control law with integral action. Further information on integral action in backstepping designs can be found in Fossen (1999).

Theorem 2.4 *The controller*

$$u = \frac{l_c}{\gamma_1} z_1 + c_2 z_2 - k_3 \left(\overline{d}_\phi^3 + 3\overline{d}_\phi z_2^2 \right) - k_2 \hat{\phi}^2 - k_1 \overline{d}_\phi + \overline{d}_\psi, \qquad (2.124)$$

where the estimates $\overline{d}_\phi$ and $\overline{d}_\psi$ are updated with

$$\dot{\overline{d}}_\phi = -\frac{1}{\gamma_1} z_1 \qquad (2.125)$$

$$\dot{\overline{d}}_\psi = -\frac{1}{\gamma_2} z_2, \qquad (2.126)$$

where $\frac{1}{\gamma_1}$ and $\frac{1}{\gamma_2}$ are adaption gains, makes the equilibrium of (2.123) globally asymptotically stable. The states of the model converge to their equilibrium values and the parameter error dynamics are GAS.   □

Proof: Adaptive backstepping is used

Step 1. The error variables z_1 and z_2 are defined as $z_1 = \hat{\psi}$ and $z_2 = \hat{\phi} - \alpha$. The first clf, V_1, is chosen as

$$V_1 = 2B^2 l_c z_1^2 + \frac{\gamma_1}{2} \tilde{d}_\phi^2, \tag{2.127}$$

where

$$\tilde{d}_\phi \overset{\triangle}{=} d_\phi - \overline{d}_\phi, \tag{2.128}$$

is the parameter error and $\overline{d}_\phi$ is an estimate of d_ϕ. The time derivative of V_1 now is

$$\dot{V}_1 = z_1 \left(-\hat{\Phi}_T(z_1) + z_2 - d_\phi + \alpha \right) - \gamma_1 \tilde{d}_\phi \dot{\overline{d}}_\phi, \tag{2.129}$$

where (2.123) is used. Let the virtual control α be chosen as

$$\alpha = \overline{d}_\phi, \tag{2.130}$$

and the estimate $\overline{d}_\phi$ be updated as

$$\dot{\overline{d}}_\phi = -\frac{1}{\gamma_1} z_1. \tag{2.131}$$

Thus, the terms including $\tilde{d}_\phi$ in (2.129) are cancelled out, and $\dot{V}_1$ can now be written as

$$\dot{V}_1 = z_1 z_2 - \hat{\Phi}_T(z_1) z_1. \tag{2.132}$$

Step 2. The second clf is chosen as

$$V_2 = V_1 + \frac{l_c}{2} z_2^2 + \frac{\gamma_2}{2} \tilde{d}_\psi^2 = \frac{1}{2} z^T P z + \frac{1}{2} \tilde{d}^T \Gamma^{-1} \tilde{d}, \tag{2.133}$$

where

$$\tilde{d}_\psi \overset{\triangle}{=} d_\psi - \overline{d}_\psi, \tag{2.134}$$

is the parameter error, $\overline{d}_\psi$ is an estimate of d_ψ,

$$\tilde{d} = (\tilde{d}_\phi \ \tilde{d}_\psi), \quad P = \begin{pmatrix} 4B^2 l_c & 0 \\ 0 & l_c \end{pmatrix}, \text{ and } \Gamma = \begin{pmatrix} \gamma_1 & 0 \\ 0 & \gamma_2 \end{pmatrix}. \tag{2.135}$$

Using (2.123), $\dot{V}_2$ is calculated as

$$\dot{V}_2 = -\hat{\Phi}_T(z_1) z_1 + z_2(\hat{\Psi}_c(\hat{\phi}) - u + \frac{l_c}{\gamma_1} z_1 + d_\psi) - \gamma_2 \tilde{d}_\psi \dot{\overline{d}}_\psi. \tag{2.136}$$

Let the estimate $\bar{d}_\psi$ be updated as

$$\dot{\bar{d}}_\psi = -\frac{1}{\gamma_2}z_2, \qquad (2.137)$$

and the control be chosen as

$$u = \frac{l_c}{\gamma_1}z_1 + c_2 z_2 - k_3\left(\alpha^3 + 3\alpha z_2^2\right) - k_2\hat{\phi}^2 - k_1\alpha + \bar{d}_\psi. \qquad (2.138)$$

Using the calculations from the case of time varying disturbances it can be shown that $\dot{V}_2$ can be upper bounded as

$$\dot{V}_2 \leq -(c_2 + k_1)z_2^2 - k_3(z_2^4 + 3\alpha^2 z_2^2) - \hat{\Phi}_T(z_1)z_1 \qquad (2.139)$$

By inserting the update laws (2.131) and (2.137) and the control (2.138) in equations (2.123), it can be shown that the error dynamics get the following form

$$\dot{z} = P^{-1}\left(A_z(z,\tilde{d}) + P_z z + \tilde{d}\right) \qquad (2.140)$$

$$\dot{\tilde{d}} = -\Gamma z, \qquad (2.141)$$

where

$$A_z(z,\tilde{d}) = \begin{pmatrix} -\hat{\Phi}_T(z_1) \\ -c_2 z_2 - k_3(z_2^3 + 3\alpha^2 z_2) \end{pmatrix} \quad \text{and} \quad P_z = \begin{pmatrix} 0 & 1 \\ -1 & 0 \end{pmatrix}. \qquad (2.142)$$

The stability result follows from application of LaSalle's theorem. From (2.139) it is seen that

$$\dot{V}_2 \equiv 0 \Rightarrow z \equiv 0 \Rightarrow \dot{z} \equiv 0. \qquad (2.143)$$

Inserting (2.143) into (2.140) we find that $\tilde{d} \equiv 0$. Thus the origin of (2.140) is GAS. $\qquad \square$

This result could also have been stated by using the more general Theorem 4.12 in Krstić *et al.* (1995*a*) or the results in Krstić (1996).

Remark 2.6 *The stability properties of the proposed scheme of two parameter update laws and control law, can also be established through passivity analysis of the error dynamics.*

The model (2.140)-(2.141) has some useful properties that will be taken advantage of in the stability proof: The vector $-A_z$ *consists of sector nonlinearities, the matrices* P *and* Γ *are both diagonal and positive definite, and the matrix* P_z *is skew symmetric. Consider the positive function*

$$S(z) = \frac{1}{2}z^T P z \qquad (2.144)$$

and calculate the time derivative of (2.144) along solution trajectories of (2.140):

$$
\begin{aligned}
\frac{d}{d\xi} S(z) &= z^{\mathrm{T}} P \dot{z} \\
&= z^{\mathrm{T}} \left(A_z(z, \tilde{d}) + P_z z + \tilde{d} \right) \\
&= z^{\mathrm{T}} A_z(z, \tilde{d}) + z^{\mathrm{T}} \tilde{d}.
\end{aligned} \tag{2.145}
$$

The last step follows from the fact that P_z is skew symmetric. As both elements in $A_z(z, \overline{d})$ are sector nonlinearities, the following inequality will always hold:

$$
-z^{\mathrm{T}} A_z(z, \tilde{d}) > 0. \tag{2.146}
$$

Integrating (2.145) from 0 to t and using (2.146) results in

$$
\int_0^\xi z^{\mathrm{T}}(\sigma) \tilde{d}(\sigma) d\sigma = S(z(\xi)) - S(z(0)) + \int_0^\xi -z^{\mathrm{T}} A_z(z, \overline{d}) d\sigma. \tag{2.147}
$$

From this dissipation inequality it is concluded that the mapping $\tilde{d} \mapsto z$ is strictly passive with $S(z) = z^{\mathrm{T}} P z$ as storage function and $-z^{\mathrm{T}} A_z(z, \tilde{d})$ as dissipation rate. Inspection of (2.141) reveals that the mapping $z \mapsto -\tilde{d}$ is a passive integrator, and thus the system (2.140)-(2.141) is a negative feedback interconnection of a strictly passive and a passive system. This implies that the equilibrium $(z, \tilde{d}) = (0, 0)$ is globally uniformly stable and that $z(\xi)$ converges to the origin as $\xi \to \infty$. The structure of the system is shown in Figure 2.6.   □
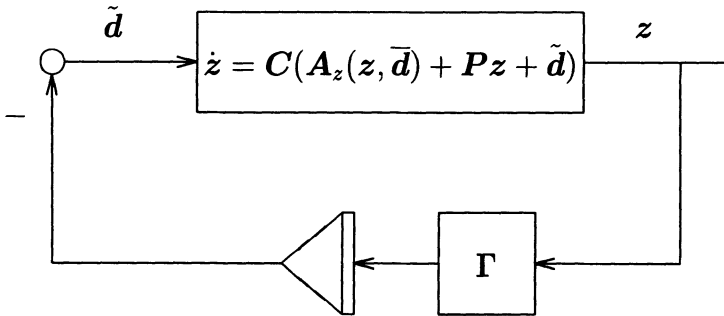
Figure 2.6: *Negative feedback interconnection of strictly passive system with passive system*

Remark 2.7 *The result of this section also holds if either of the two constant disturbances are set to zero. In the case of $d_\phi \equiv 0$ and $d_\psi \neq 0$, the controller*

(2.124) with parameter update law (2.126) is equivalent to an ordinary linear PI-control law in z_2:

$$u = c_2 z_2 - \int_0^\xi \frac{1}{\gamma_2} z_2(\sigma) d\sigma. \tag{2.148}$$

By the same arguments as in the above proof, $z = 0$ is GAS and $\bar{d}_\psi = \int_0^\xi \frac{1}{\gamma_2} z_2(\sigma) d\sigma$ converges to the true value of d_ψ. □

2.4 Control of Rotating Stall

In this section CCV controllers will be derived for the full Moore-Greitzer model (2.36). As in the section on surge control, two cases will be studied here as well. First, a stabilizing stall/surge controller is designed for the undisturbed model. Then, pressure disturbances are included in the model, and a second controller is derived. For use in the stability proofs of this section, the following lemma is needed:

Lemma 2.1 *The squared amplitude of rotating stall has an upper bound:*

$$\exists\, J_{\max} < \infty \quad \text{such that} \quad J(\xi) < J_{\max} \; \forall\, \xi > 0 \tag{2.149}$$

□

Proof:
The proof is similar to that of section 2.4 in Krstić *et al.* (1995*a*):

$$
\begin{aligned}
\dot{J} &= J\left(1 - \left(\frac{\Phi}{W} - 1\right)^2 - \frac{J}{4} - \frac{1}{\gamma^2}\frac{4W\Phi}{3H}\right)\varrho, \\
&= -\frac{J^2\varrho}{4} - \varrho J\left(\frac{\Phi^2}{W^2} - \frac{2\Phi}{W}\right) - \varrho J\frac{4W}{3H\gamma^2}\phi \\
&\leq -\frac{J^2\varrho}{4} + \frac{2\varrho}{W}J|\Phi| + \varrho J\frac{4W}{3H\gamma^2}|\Phi| \\
&\leq -\frac{J^2\varrho}{8} - \frac{\varrho J}{8}\left(J - \frac{16}{W}|\Phi| - \frac{32W}{3H\gamma^2}|\Phi|\right)
\end{aligned}
\tag{2.150}
$$

When $J(\xi) > 16|\Phi(\xi)|\left(\frac{1}{W} + \frac{2W}{3H\gamma^2}\right)$, $J(\xi)$ will decay faster than the solution $w(\xi)$ of the differential equation

$$\dot{w} = -\frac{w^2\varrho}{8}, \tag{2.151}$$

so that an upper bound of $J(\xi)$ is given by

$$J(\xi) < \frac{J(0)}{1 + J(0)\frac{\varrho\xi}{8}} + 16 \sup_{0 \leq \tau < \xi} |\Phi(\tau)| \left(\frac{1}{W} + \frac{2W}{3H\gamma_{\min}^2} \right) \triangleq J_{\max}, \quad (2.152)$$

where $\gamma_{\min} > 0$ is a lower bound on the throttle gain. Equation (2.152) states that J is bounded if ϕ is bounded. An upper bound on ϕ is given by the choking of the mass flow:

$$\Phi \leq \phi_{choke}, \quad (2.153)$$

so that a conservative value for $J_{\max}$ is

$$J_{\max} = \frac{J(0)}{1 + J(0)\frac{\varrho\xi}{8}} + 16\phi_{choke} \left(\frac{1}{W} + \frac{2W}{3H\gamma_{\min}^2} \right). \quad (2.154)$$

$\square$

The following assumption on the mass flow coefficient is also needed:

Assumption 2.1 *The lower bound on ϕ is given by the minimum value obtained during a deep surge cycle. This lower bound is negative, and is given by*

$$\exists\, \phi_m > 0 \ \text{ such that } \ \Phi(\xi) > -\phi_m \forall \xi > 0. \quad (2.155)$$

$\square$

The assumption is not a conservative one. Compressors in general are not intended or designed for operation with reversed mass flow, so it is reasonable to assume that the lowest value of mass flow is reached during the extreme condition of deep surge, more precisely at the negative peak of a deep surge cycle.

2.4.1   Undisturbed Case

Theorem 2.5 *Consider the system (2.36) evolving in the set*

$$\mathcal{A} = \left\{ \Psi, \Phi, J \mid \Psi \in I\!R, \ \Phi \in [-\phi_m, \phi_{choke}], \ J \in I\!R^+ \right\} \quad (2.156)$$

with the controller

$$u = (c_2 + c_3)(\Phi - \phi_0), \quad (2.157)$$

where $c_2 > a_m$ and a_m is the maximum positive slope of the compressor characteristic, and $c_3 > 0$ is chosen according to

$$c_3^{\min} < c_3 < c_3^{\max}, \quad (2.158)$$

where $c_3^{\min}$ and $c_3^{\max}$ are lower and upper bounds to be computed. The origin of the closed loop system is then asymptotically stable with a region of attraction equal to $\mathcal{A}$.

$\square$

Proof:

The backstepping methodology of Krstić *et al.* (1995*a*) is now employed to design a controller for (2.36)

Step 1. Let the error variables z_1 and z_2 be chosen as

$$z_1 = \hat{\psi} \text{ and } z_2 = \hat{\phi} - \alpha, \tag{2.159}$$

and the CLF for this step be

$$V_1 = 2B^2 l_c z_1^2. \tag{2.160}$$

The time derivative of V_1 along solution trajectories is

$$\dot{V}_1 = z_1 \left(-\hat{\Phi}_T(z_1) + z_2 + \alpha \right). \tag{2.161}$$

As before, the throttle is assumed passive, such that $\hat{\psi}\hat{\Phi}(\hat{\psi}) \geq 0 \ \forall \hat{\psi}$. It follows that

$$\hat{\psi}\hat{\Phi}_T(\hat{\psi}) \geq 0 \ \Rightarrow \ -z_1 \hat{\Phi}_T(z_1) \leq 0. \tag{2.162}$$

It is recognized that there is no need to cancel out terms in (2.161). Thus, the stabilizing function α is not needed and can be chosen as $\alpha = 0$, which in turn gives

$$\dot{V}_1 = -\hat{\Phi}_T(z_1)z_1 + z_1 z_2. \tag{2.163}$$

Although $\alpha = 0$ here, the notation of z_1 and z_2 is kept in the interest of consistency with section 2.4.2

Step 2. The derivative of z_2 is

$$\dot{z}_2 = \frac{1}{l_c}\left(-z_1 + \hat{\Psi}_c(z_2) - \frac{3H}{4}J\left(\frac{\Phi}{W} - 1 \right) - \frac{W^2 J}{2\gamma^2} - u \right). \tag{2.164}$$

The clf for this step is

$$V_2 = V_1 + \frac{l_c}{2}z_2^2 + \frac{1}{\varrho J_{\max}}J, \tag{2.165}$$

and $\dot{V}_2$ is calculated as

$$\begin{aligned} \dot{V}_2 &= -z_1\hat{\Phi}_T(z_1) + z_2(\hat{\Psi}_c(z_2) - u) + \frac{J}{J_{\max}}\left(1 - \left(\frac{\Phi}{W} - 1 \right)^2 \right. \\ &\left. -\frac{J}{4} - \frac{1}{\gamma^2}\frac{4W}{3H}\Phi \right) - \frac{3H}{4}\left(\frac{\Phi}{W} - 1 \right)z_2 J - \frac{W^2 J}{2\gamma^2}z_2. \end{aligned} \tag{2.166}$$

By choosing u according to

$$u = (c_2 + c_3)z_2, \tag{2.167}$$

where $c_2 > 0$ and $c_3 > 0$ are constants, $\dot{V}_2$ can be written

$$\dot{V}_2 = \sum_{i=1}^{4} \left(\dot{V}_2\right)_i. \tag{2.168}$$

The four terms in (2.168) are

$$\left(\dot{V}_2\right)_1 = -z_1 \hat{\Phi}_T(z_1), \tag{2.169}$$

$$\left(\dot{V}_2\right)_2 = z_2(\hat{\Psi}_c(z_2) - c_2 z_2), \tag{2.170}$$

$$\left(\dot{V}_2\right)_3 = \frac{J}{J_{max}} \left(1 - \left(\frac{\Phi}{W} - 1\right)^2 - \frac{1}{\gamma^2}\frac{4W}{3H}\Phi\right), \tag{2.171}$$

$$\left(\dot{V}_2\right)_4 = -\begin{bmatrix} J & z_2 \end{bmatrix} P(\Phi) \begin{bmatrix} J \\ z_2 \end{bmatrix}, \tag{2.172}$$

where

$$P(\Phi) = \begin{bmatrix} \frac{1}{4J_{max}} & \frac{3H}{8}\left(\frac{\Phi}{W} - 1\right) + \frac{W^2}{4\gamma^2} \\ \frac{3H}{8}\left(\frac{\Phi}{W} - 1\right) + \frac{W^2}{4\gamma^2} & c_3 \end{bmatrix}. \tag{2.173}$$

Due to the passivity of the throttle, $\left(\dot{V}_2\right)_1 < 0$. As shown in section 2.3, if c_2 is chosen as

$$c_2 > a_m \geq a > \frac{k_2^2}{4k_3} - k_1, \tag{2.174}$$

where a_m is the maximum positive slope of the compressor characteristic, then $\left(\dot{V}_2\right)_2 < 0$.

By choosing the controller gains sufficiently large, $\left(\dot{V}_2\right)_3$ can be made negative for $\phi > 0$. As the proposed controller (2.167) is of the same form as (2.42), the expression (2.61) for γ, with gain (c_2+c_3), can be used. For $\left(\dot{V}_2\right)_3$ to be negative the following must be satisfied

$$1 - \left(\frac{\Phi}{W} - 1\right)^2 - \frac{4W}{3H}\frac{\Phi(c_2 + c_3)}{\Phi + \phi_0} < 0 \tag{2.175}$$

$$\Downarrow \quad \Phi > 0$$

$$c_2 + c_3 > \frac{3H}{4W}\frac{\Phi + \phi_0}{\Phi}\left(-\left(\frac{\Phi}{W} - 1\right)^2 + 1\right) \tag{2.176}$$

$$c_2 + c_3 > \frac{3H}{4W}(\Phi + \phi_0)\left(\frac{2}{W} - \frac{\Phi}{W^2}\right) \triangleq G_1(\Phi) \tag{2.177}$$

Simple calculations shows that the maximum of $G_1(\Phi)$ is for $\Phi = W - \frac{\phi_0}{2}$, and that this maximum is given by

$$\max_{\Phi > 0} G_1(\Phi) = \frac{3H}{4W^2} \left(\frac{\phi_0^2}{4W} + W + \phi_0 \right). \tag{2.178}$$

By choosing

$$c_2 + c_3 > \frac{3H}{4W^2} \left(\frac{\phi_0^2}{4W} + W + \phi_0 \right), \tag{2.179}$$

which implies

$$c_3 > \frac{3H}{4W^2} \left(\frac{\phi_0^2}{4W} + W + \phi_0 \right) - c_2 \stackrel{\triangle}{=} \underline{C}_1(c_2), \tag{2.180}$$

it follows that $\left(\dot{V}_2 \right)_3$ is made negative for $\phi > 0$.

For $\phi < 0$ the sum $\left(\dot{V}_2 \right)_3 + \left(\dot{V}_2 \right)_2$ can be made negative for $\phi > -\phi_m$, that is

$$z_2(\hat{\Psi}_c(z_2) - c_2 z_2) < -\frac{J}{J_{\max}} \left(1 - \left(\frac{\Phi}{W} - 1 \right)^2 - \frac{1}{\gamma^2} \frac{4W}{3H} \Phi \right) \tag{2.181}$$

Using (2.61) and $\frac{J}{J_{\max}} < 1$, and rearranging (2.181) gives

$$\frac{c_3}{\Phi + \phi_0} \Phi > G_2(\Phi, c_2), \tag{2.182}$$

where

$$G_2(\Phi, c_2) \stackrel{\triangle}{=} \frac{4W}{3H} \left(z_2 \hat{\Psi}_c(z_2) - c_2 z_2^2 + 1 - \left(\frac{\Phi}{W} - 1 \right)^2 \right) - \frac{c_2}{\Phi + \phi_0} \Phi. \tag{2.183}$$

It can be shown that it is sufficient that (2.182) is satisfied at the end points of the interval:

$$G_2(-\phi_m, c_2) < \frac{\phi_m}{\phi_m - \phi_0} c_3 \tag{2.184}$$

$$G_2(0, c_2) < 0. \tag{2.185}$$

By inspection of (2.183) it is easily shown that (2.185) is always satisfied. It is assumed that $\phi_0 > \phi_m$, so that the condition in (2.184) can be rewritten as

$$c_3 < \frac{\phi_m - \phi_0}{\phi_m} G_2(-\phi_m, c_2) \stackrel{\triangle}{=} \overline{C}_2(c_2, \phi_m). \tag{2.186}$$

Plots of $\left(\dot{V}_2 \right)_2$, $\left(\dot{V}_2 \right)_3$ and their sum are shown in Figure 2.7.
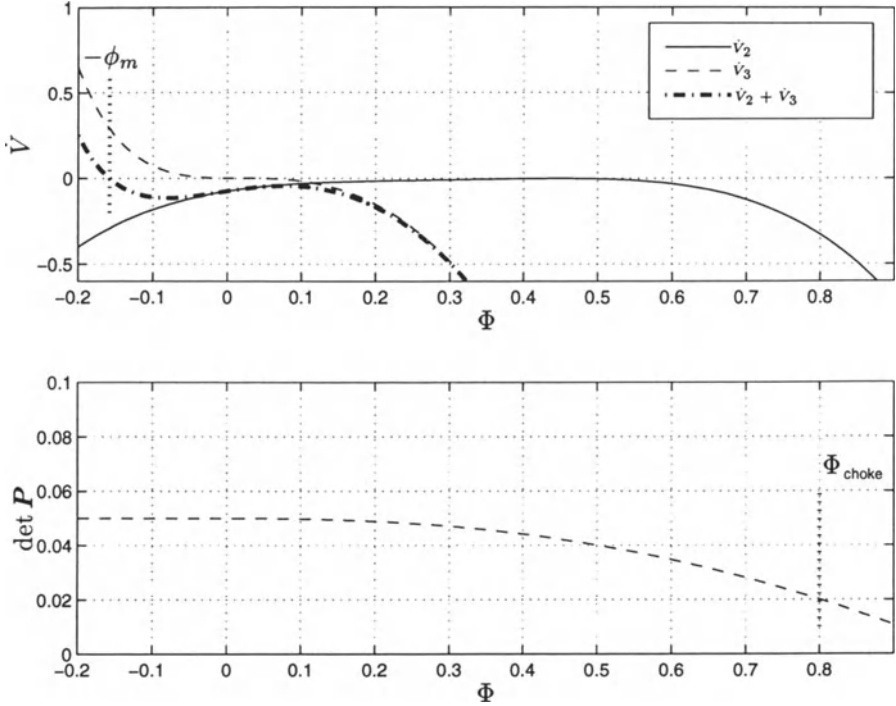
Figure 2.7: *Upper plot illustrates that $\dot{V}_2 + \dot{V}_3 < 0$ for $\Phi > -\phi_m$. Lower plot illustrates that $\det P > 0$ for $\Phi < \phi_{choke}$.*

Finally, c_3 must be chosen so that P is positive definite for $-\phi_m < \phi < \phi_{choke}$. The determinant of P is given by

$$\det P = \frac{c_3}{4J_{max}} - \left(\frac{3H}{8} \left(\frac{\Phi}{W} - 1 \right) + \frac{W^2}{4\gamma^2} \right)^2 > 0. \qquad (2.187)$$

A plot of $\det P$ is shown in the lower part of Figure 2.7. Again, a sufficient condition for $\det P > 0$ for $-\phi_m < \Phi < \phi_{choke}$ is that $\det P(\phi_{choke}) > 0$ and $\det P(-\phi_m) > 0$. As shown in Appendix F, this leads to the following conditions on c_3:

$$\max \left\{ \underline{C}_3(c_2, \phi_{choke}), \underline{C}_4(c_2, \phi_m) \right\} < c_3 < \min \left\{ \overline{C}_3(c_2, \phi_{choke}), \overline{C}_4(c_2, \phi_m) \right\} \qquad (2.188)$$

Choosing c_3 according to (2.188) ensures that

$$\left(\dot{V}_2 \right)_4 < 0, \quad -\phi_m < \Phi < \phi_{choke}. \qquad (2.189)$$

The requirements (2.174), (2.180), (2.186) and (2.188) are summarized as

$$c_2 > a_m \geq a > \frac{k_2^2}{4k_3} - k_1, \qquad (2.190)$$

and

$$c_3 > \max \left\{ \underline{C}_1(c_2), \underline{C}_3(c_2, \phi_{choke}), \underline{C}_4(c_2, \phi_m) \right\} \triangleq c_3^{\min} \qquad (2.191)$$

$$c_3 < \min \left\{ \overline{C}_2(c_2, \phi_m), \overline{C}_3(c_2, \phi_{choke}), \overline{C}_4(c_2, \phi_m) \right\} \triangleq c_3^{\max} \qquad (2.192)$$

Provided c_2 and c_3 are chosen according to (2.190) to (2.192), $\dot{V}_2$ is upper bounded as

$$\dot{V}_2 \leq -U(z_1, z_2, J). \qquad (2.193)$$

As $V_2 : \mathcal{A} \to \mathbb{R}$, $V_2(0) = 0$, V_2 is positive definite and continuously differentiable on $\mathcal{A}$, and $\dot{V}(z) < 0$ for $z \in \mathcal{A} - \{0\}$, the origin of the system is asymptotically stable with region of attraction equal to $\mathcal{A}$. $\qquad \square$

By doing the same calculations as in Remark 2.1, the control law for the CCV gain is found to be:

$$\gamma = \sqrt{\frac{\Phi + \phi_0}{(c_2 + c_3)}}. \qquad (2.194)$$

Notice that this control law requires sensing of mass flow ϕ only. The analysis leading to this control law was conservative, resulting in a large value of the parameter c_3, that is c_3 has to be chosen as $c_3 > c_3^{\min}$. As was the case in Krstić *et al.* (1995*b*), the controller should be implemented with a lower gain than dictated by the Lyapunov analysis. Consider the closed loop Jacobian of the model (2.36) with control law (2.157):

$$\boldsymbol{A}_{cl} = \begin{pmatrix} -\frac{1}{4B^2 l_c} a_\Phi & \frac{1}{4B^2 l_c} & 0 \\ -\frac{1}{l_c} - \frac{3H}{4l_c W} & \frac{1}{l_c} a_\Psi - \frac{c_2 + c_3}{l_c} & 0 \\ 0 & 0 & \varrho \left(-\frac{\phi_0^2}{W^2} + \frac{2\phi_0}{W} \right) - \frac{4W\varrho(c_2 + c_3)}{6H} \end{pmatrix}, \qquad (2.195)$$

where

$$a_\Psi = \left. \frac{\partial \hat{\Phi}_T(z_1)}{\partial z_1} \right|_{z_1 = 0} \quad \text{and} \quad a_\Phi = \left. \frac{\partial \hat{\Psi}_c(z_2)}{\partial z_2} \right|_{z_2 = 0}. \qquad (2.196)$$

It can be shown that if $\boldsymbol{A}_{cl}$ is Hurwitz for $c_3 > c_3^{\min}$, $\boldsymbol{A}_{cl}$ is also Hurwitz for $c_3 = 0$. The closed loop system is therefore locally stable with $c_3 = 0$.

2.4.2 Disturbed Case

The backstepping procedure is now used to design a controller that ensures boundedness of the states in the presence of pressure disturbances.

Theorem 2.6 *Consider the model (2.39) with time varying pressure disturbances only, that is $\hat{\Psi}_d(\xi) \neq 0$ and $\hat{\Phi}_d(\xi) \equiv 0$, evolving on the set $\mathcal{A}$. Let the controller u be defined as*

$$u = (c_2 + c_3)z_2 + d_2 z_2 \qquad (2.197)$$

where $d_2 > 0$, c_2 satisfies

$$c_2 > a_m, \qquad (2.198)$$

where a_m is an upper bound on the positive slope of the compressor characteristic, and c_3 satisfies

$$c_3^{\min} < c_3 < c_3^{\max} \qquad (2.199)$$

where $c_3^{\min}$ and $c_3^{\max}$ are defined in (2.191) and (2.192). Then (2.197) makes the states of the model (2.39) uniformly ultimately bounded and ensures convergence to a set. □

Proof:
This result follows by combining the proofs of Theorem 2.3 and Theorem 2.5. The Lyapunov function

$$V_2 = V_1 + \frac{l_c}{2} z_2^2 + \frac{1}{J_{\max}\varrho} J \qquad (2.200)$$

will have an upper bound on its time derivative given by

$$\dot{V}_2 \leq -U(z_1, z_2, J) + \frac{\hat{\Psi}_d^2(\xi)}{4d_2} \qquad (2.201)$$

where

$$U(z_1, z_2, J) = \sum_{i=1}^{4} \left(\dot{V}_2\right)_i. \qquad (2.202)$$

and the four terms $\left(\dot{V}_2\right)_i$ are given by (2.169)-(2.172) provided the control is chosen as (2.197).

Provided c_2 is chosen according to (2.190) and c_3 satisfies (2.191) and (2.192), then $\dot{V}_2 < 0$ outside a set $\mathcal{R}_3$. According to Krstić *et al.* (1995a), the fact that $V_2(z_1, z_2, J)$ is positive definite, radially unbounded and smooth, and

$U(z_1, z_2, J)$ is positive definite for $-\phi_m < \Phi < \phi_{choke}$ implies that there exists class-$\mathcal{K}_\infty$ functions β_1, β_2 and a class-$\mathcal{K}$ function β_3 such that

$$\left.\begin{array}{c} \beta_1(|z|) \leq V_2(z) \leq \beta_2(|z|) \\ \beta_3(|z|) \leq U(z) \end{array}\right\} \qquad (2.203)$$

where $z = (z_1, \; z_2, \; J)^{\mathrm{T}}$. This implies that $z(\xi)$ is uniformly ultimately bounded and that $z(\xi)$ converges to the set

$$\mathcal{R}_3 = \left\{ z : |z| \leq \beta_1^{-1} \circ \beta_2 \circ \beta_3^{-1} \left(\frac{\|\hat{\Psi}_d\|_\infty^2}{4d_2} \right) \right\}. \qquad (2.204)$$

$\square$

Remark 2.5 is also applicable to this case.

Remark 2.8 *The case of stabilizing rotating stall in the case of disturbances in mass flow as well as pressure rise, can be studied by combining Theorem 2.3 and Theorem 2.5. It is straightforward to extend the results on convergence to the origin and adaption of constant mass flow disturbances and pressure disturbances from Section 2.3 to the control design in this section.* $\square$

2.5 Simulations

In this section, the proposed controllers of this chapter are simulated. Results form both surge and stall control, with and without disturbances, will be shown. The compressor characteristic

$$\Psi_c(\phi) = \psi_{c0} + H \left(1 + \frac{3}{2} \left(\frac{\Phi}{W} - 1 \right) - \frac{1}{2} \left(\frac{\Phi}{W} - 1 \right)^3 \right), \qquad (2.205)$$

of Moore and Greitzer (1986) is used in all simulations. The throttle will be set so that the intersection of the throttle line and the compressor characteristic is located on the part of the characteristic that has positive slope, resulting in an unstable equilibrium. After some time, the controllers will be switched on, demonstrating that the system is stabilized.

2.5.1 Surge Control

Surge control will now be demonstrated. A Greitzer parameter of $B = 1.8$ is used in the simulations. The throttle gain is set to $\gamma = 0.61$ and thus the equilibrium is unstable. The initial conditions of the systems were chosen as

$$(\Phi_0, \; \Psi_0) = (0.6, \; 0.6). \qquad (2.206)$$

In Figure 2.8, it is shown how the controller (2.42) with $c_2 = 1$ stabilizes the system.
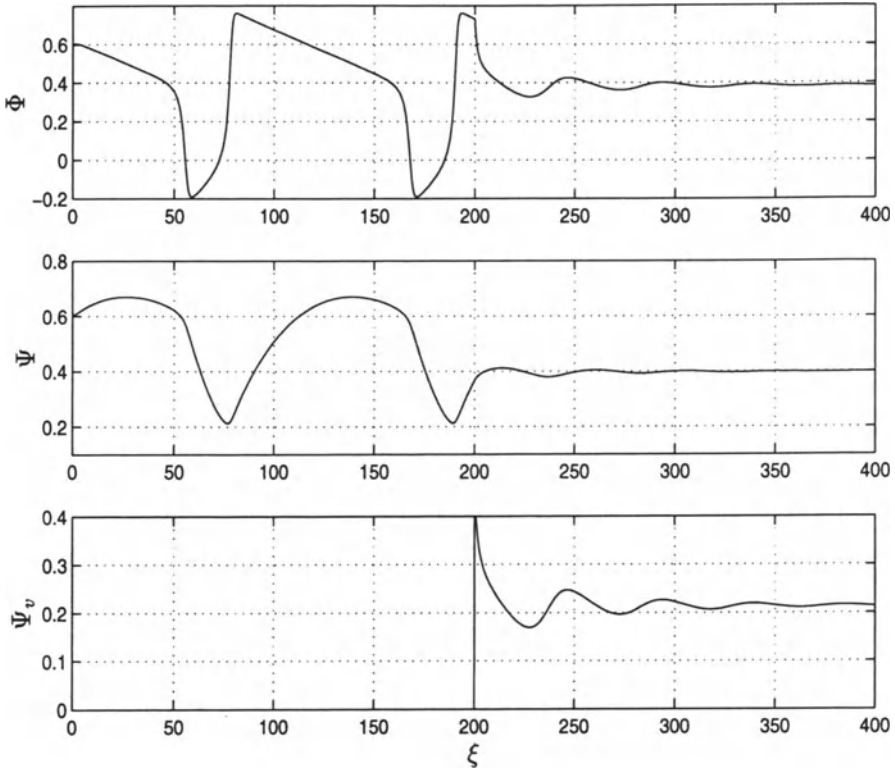
Figure 2.8: *The throttle gain is set to $\gamma = 0.61$, and the compressor is surging. The controllers are switched on at $\xi = 200$.*

In Figure 2.9 noise has been added, and the system is stabilized by the controller (2.99) with $c_2 = 1$, $d_1 = 0.3$ and $d_2 = 3$.

A simulation of surge induced by a constant disturbance is showed in Figure 2.10. The compression system is initially operating stably with a throttle setting of $\gamma = 0.65$ yielding a stable equilibrium. At $\xi = 200$ the constant disturbances $d_\phi = -0.1$ and $d_\psi = 0.05$ are introduced into the system, resulting in the state of the system being pushed over the surge line. Consequently, surge oscillations emerge. At $\xi = 420$ the adaptive controller (2.124) with update laws (2.125), and as can be seen, the surge oscillations are brought to rest. The parameters of the controller were $c_2 = 1.1$, $\vartheta_1 = 9$ and $\vartheta_2 = 20$. The disturbances are unknown to the controller, but as guaranteed by Theorem 2.4 their estimates converges to the true values.
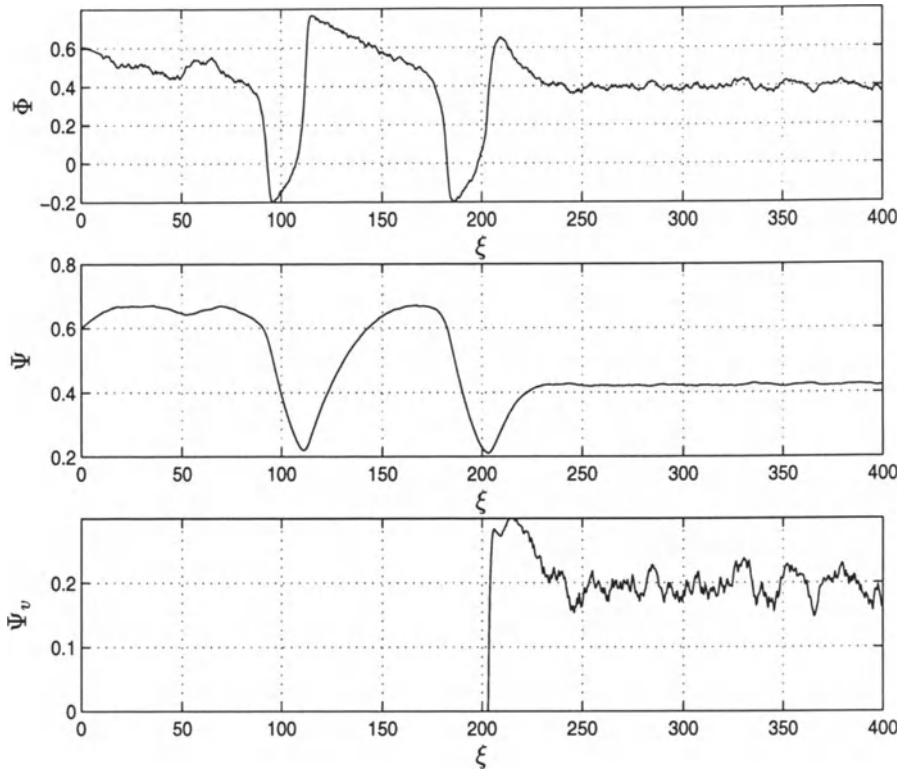
Figure 2.9: *Same situation as in Figure 2.8. However, here disturbances are taken into account. The pressure and the mass flow disturbances are both white noise varying between ±0.05.*

2.5.2 Rotating Stall Control

In this section some simulation results of the proposed controllers for rotating stall are presented. In Figure 2.11 the response of system (2.36) with controller (2.167) is shown. The throttle gain is set at $\gamma_T = 0.61$, resulting in an unstable equilibrium for the unactuated system. The initial conditions of the systems were chosen as

$$(\Phi_0 \, ; \Psi_0, \; J_0) = (0.6, \; 0.6, \; 0.05). \qquad (2.207)$$

The B-parameter is set to $B = 0.5$ for all the rotating stall simulations. Thus, the compressor enter rotating stall, and J increases until J_e is reached. At $\xi = 250$ the controller is switched on, and J decreases until $J = 0$ is reached. As discussed at the end of Section 2.4.1, the controller gains are chosen as $c_3 = 0$ and $c_2 = 1$. The simulation results are also plotted together with the compressor characteristic and the in-stall characteristic in Figure 2.12. As
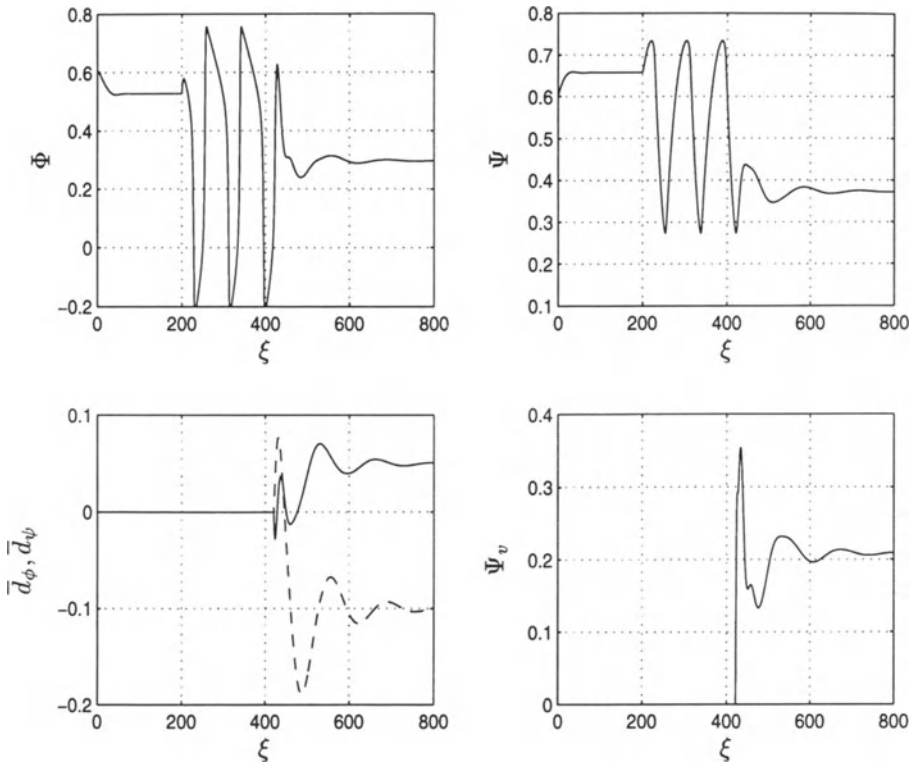
Figure 2.10: *Disturbance induced surge stabilized by the adaptive controller (2.124).*

the compressor is stabilized it is seen that the pressure loss associated with the CCV is slightly less than that associated with operating in rotating stall, which would have been the case if e.g. the throttle control scheme of Krstić *et al.* (1995*b*) had been used.

The effect of pressure disturbances is shown in Figure 2.13. The B-parameter is $B = 0.5$ and the compressor stalls. The pressure disturbance is white noise of amplitude 0.1. Throttle setting and initial conditions were left unchanged. The control law (2.197) with parameters $c_2 = 1$ and $d_2 = 0.1$ is switched on at $\xi = 250$, bringing the compressor out of rotating stall, and damping the disturbances.
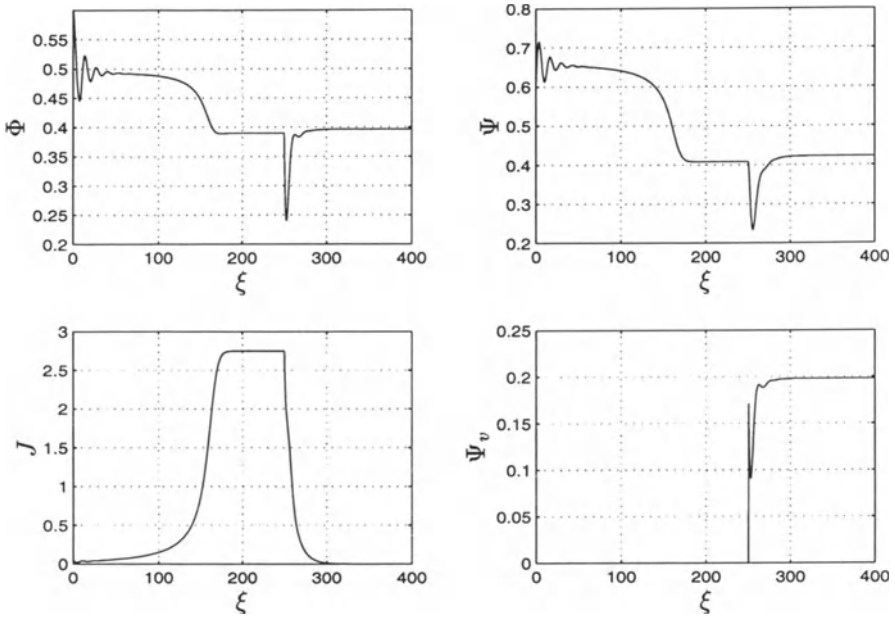
Figure 2.11: *Stabilization of rotating stall*
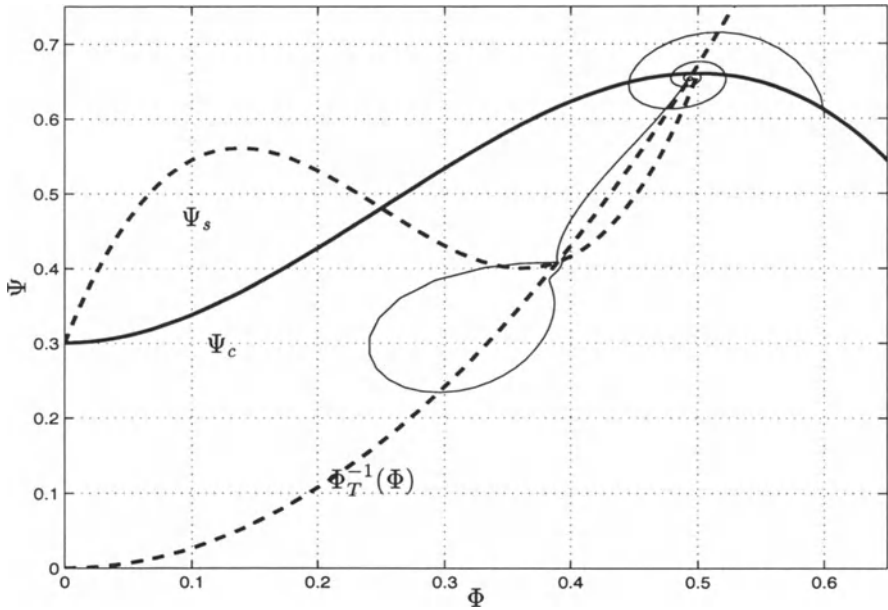
Figure 2.12: *Same simulation as in Figure 2.11*
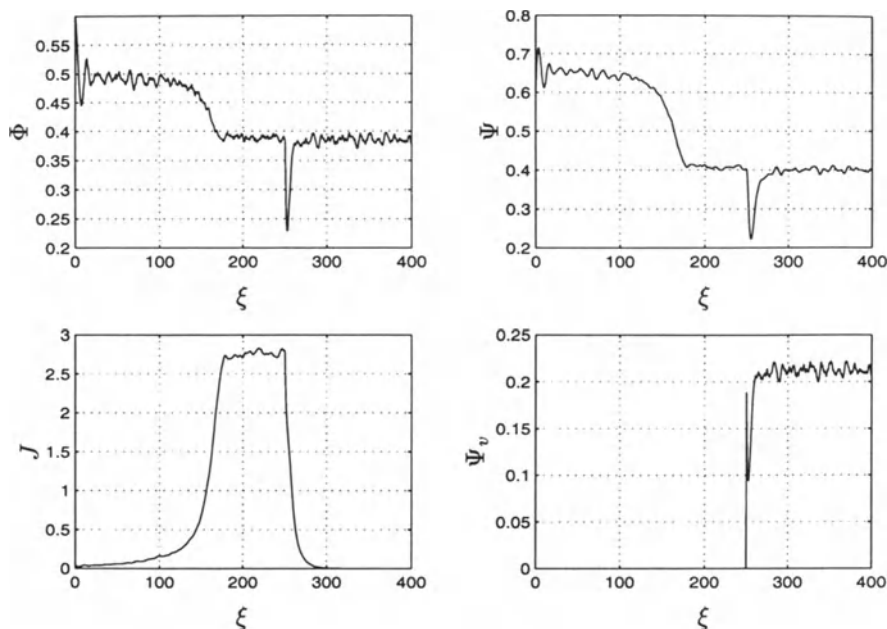
Figure 2.13: *Stabilization of rotating stall with pressure disturbances*

2.6 Conclusion

In this chapter, anti surge and stall controllers for a close-coupled valve in series with a compressor have been developed. First, surge was studied, and by the application of the backstepping methodology, a control law which uses feedback from mass flow only was derived. Global asymptotic stability was proven. Only an upper bound on the slope of the compressor characteristic was required to implement this controller. The controller was used both in the case of no disturbances and in the presence of pressure disturbances.

A more complicated surge control law was derived for the case of both pressure disturbances and mass flow disturbances. In order to implement this controller, the compressor characteristic and the B-parameter must be known. Global uniform boundedness and convergence to a set was proven. By assuming the disturbances upper bounded by a monotonically decreasing nonnegative function, convergence to the origin was proven. In order to stabilize the compression system in the presence of constant disturbances, or biases, in mass flow and pressure, an adaptive version of the surge controller was derived. This controller ensures global asymptotic stability.

Then, controllers for rotating stall were considered. The close coupled valve

was incooperated into the Moore-Greitzer model, and controllers were derived that enables stabilization of rotating stall beyond the surge line. Without disturbances, an asymptotically stable equilibrium is ensured, and in the presence of pressure disturbances uniform boundedness was proven.

PASSIVITY BASED SURGE CONTROL

3.1 Introduction

In this chapter passivity will be used to derive a surge controller for a compression system when time varying disturbances are considered in both pressure as well as mass flow.

The stabilizability of a system is related to the possibility of rendering it *passive* via feedback. The relevance of using passivity as a building block for control systems design stems, not just from the important role this concept plays in stability analysis, but also from the invariance of this property vis a vis feedback interconnection (Desoer and Vidyasagar 1975), (Nicklasson 1996). An advantage of of the approach is enhanced robustness properties due to the fact that cancellation of nonlinearities is avoided. Passivity and input/output methods have been used in many control applications such as mechanical systems in general, electrical machines in Nicklasson (1996), marine vehicles in Johannessen (1996), vibration damping in Kanestrøm and Egeland (1994) and so on. To the authors best knowledge this is the first attempt to apply this method to the compressor surge control problem.

3.1.1 Motivation

In the previous chapter, backstepping was employed to derive a stabilizing control law when time varying disturbances were taken into account. The control law (2.99) resulting from this approach is repeated here for con-

veinience:

$$u = c_2 z_2 - k_3 \left(\alpha^3 + 3\alpha z_2^2 \right) - k_2 \hat{\phi}^2 - k_1 \alpha \qquad (3.1)$$
$$+ \frac{d_1}{4B^2} \left(-\hat{\Phi}_T(z_1) + \hat{\phi} \right) + d_2 z_2 \left(1 + \frac{d_1^2}{4B^2} \right),$$

where $c_2 > |k_1|$, $\alpha = -d_1 z_1$ and $d_1, d_2 > 0$. Of particular interest here, will be the use of input/output methods to design controllers with disturbance rejection capabilities. This is motivated by the fact that the surge controller (3.1) is of high order, requires detailed knowledge of the nonlinearities of the model and the fact that simulations indcate that a simple proprtional controller will stabilize the system.

3.1.2   Notation

A brief introduction to passivity and $\mathcal{L}_2$ is given here. For a comprehensive treatment of these concepts, consult Desoer and Vidyasagar (1975) and van der Schaft (1996), from which the notation is taken. The signal space $\mathcal{L}_2$ consists, somewhat simplified, of all functions $f : \mathbb{R}_+ \to \mathbb{R}$ that satisfy

$$\int_0^\infty |f(\xi)|^2 d\xi < \infty. \qquad (3.2)$$

The truncation of f to $[0, T]$ is defined as

$$f_T(\xi) = \begin{cases} f(\xi) &, \quad 0 \leq \xi < T \\ 0 &, \quad \xi \geq T \end{cases}, \qquad (3.3)$$

and the set $\mathcal{L}_{2e}$, the extension of $\mathcal{L}_2$, consists of all functions f such that $f_T \in \mathcal{L}_2$. A mapping $\mathcal{G} : u \mapsto y$ with input $u \in \mathcal{L}_{2e}$ and output $y \in \mathcal{L}_{2e}$ is said to be passive if there exists a constant β so that

$$\int_0^T u(\xi) y(\xi) d\xi \geq \beta \qquad (3.4)$$

for all $u \in L_{2e}$ and all $T \geq 0$. The inner product on $\mathcal{L}_{2e}$ is

$$\langle u, y \rangle_T = \int_0^T u(\xi) y(\xi) d\xi, \qquad (3.5)$$

and the truncated norm is

$$\|u\|_T^2 = \langle u, u \rangle_T. \qquad (3.6)$$

A concept that will be used in this chapter is that of strict output passivity. The mapping $\mathcal{G} : u \mapsto y$ is strict output passive if $\exists\, \kappa > 0$ and $\exists\, \beta$ such that

$$\langle y, u \rangle = \langle \mathcal{G}u, u \rangle \geq \kappa \|\mathcal{G}u\|_T^2 + \beta \quad \forall u \in \mathcal{L}_{2e}, \quad \forall T \geq 0. \qquad (3.7)$$

For use in the stability analysis of this Chapter we need the the following theorem from van der Schaft (1996)

Theorem 3.1 (The passivity theorem)
Consider the closed loop system $\Sigma_{\mathcal{G}_1,\mathcal{G}_2}$ *with*

$$u_1 = e_1 - \mathcal{G}_1(u_2) \tag{3.8}$$

$$u_2 = e_2 + \mathcal{G}_1(u_1), \tag{3.9}$$

where $\mathcal{G}_1, \mathcal{G}_2 : \mathcal{L}_{2e} \mapsto \mathcal{L}_{2e}$. *If* $\mathcal{G}_1$ *and* $\mathcal{G}_2$ *are strictly output passive then the closed loop system* $\Sigma_{\mathcal{G}_1,\mathcal{G}_2}$ *is* $\mathcal{L}_2$-*stable.* $\qquad\Box$

The proof is given in van der Schaft (1996).

3.2 Model

A compression system consisting of a compressor, axial or centrifugal, in series with a close-coupled valve, a plenum volume and a throttle is studied, consult Figure 2.3. The system is presented in section 2.2.4, and repeated here for convenience:

$$\dot{\hat{\psi}} = \frac{1}{4B^2 l_c}(\hat{\phi} - \hat{\Phi}_T(\hat{\psi})) \tag{3.10}$$

$$\dot{\hat{\phi}} = \frac{1}{l_c}(\hat{\Psi}_c(\hat{\phi}) - u - \hat{\psi}),$$

where $u = \hat{\Psi}_v$, and the equivalent compressor characteristic is $\hat{\Psi}_e = \hat{\Psi}_c - \hat{\Psi}_v$. The notation $\dot{x}$ is to be understood as differentiation with respect to nondimensional time $\xi = \frac{Ut}{R}$ as in the previous chapter.

Assumption 3.1 *The throttle is assumed to be a passive component, moreover the constant* $\kappa_2 > 0$ *can always be chosen sufficiently small so that the characteristic satisfies the sector condition:*

$$\forall \hat{\psi} \; \exists \; \kappa_2 \; \text{such that} \; \hat{\Phi}_T(\hat{\psi})\hat{\psi} \geq \kappa_2\hat{\psi}^2, \tag{3.11}$$

Our aim will be to design a control law $u = \hat{\Psi}_v(\hat{\phi})$ for the valve such that the compressor also can be operated stably on the left side of the original surge line without going into surge.

3.3 Passivity

The passivity properties of the model (3.10) will now be analyzed. Our goal is to represent the system as a feedback interconnection of two blocks. Then, the idea is to use the control u to ensure that the blocks are strictly output passive and thus rendering the closed loop system $\mathcal{L}_2$-stable.

3.3.1   Passivity of Flow Dynamics

Consider the non-negative function

$$V_1(\hat{\phi}) = \frac{l_c}{2}\hat{\phi}^2 \tag{3.12}$$

The time derivative of (3.12) along solution trajectories of (3.10) is

$$\dot{V}_1 = -\hat{\psi}\hat{\phi} + \Psi_e(\hat{\phi})\hat{\phi}. \tag{3.13}$$

Then, it is evident that

$$\begin{aligned}
\left\langle -\hat{\psi}, \hat{\phi} \right\rangle_T &= \left\langle -\hat{\Psi}_e(\hat{\phi}), \hat{\phi} \right\rangle_T + V_1(\xi) - V_1(0) \\
&\geq \left\langle -\hat{\Psi}_e(\hat{\phi}), \hat{\phi} \right\rangle_T - V_1(0)
\end{aligned} \tag{3.14}$$

Hence, the flow dynamics

$$\mathcal{G}_1 : -\hat{\psi} \mapsto \hat{\phi}, \tag{3.15}$$

where $\mathcal{G}_1 : \mathcal{L}_{2e} \to \mathcal{L}_{2e}$ is an input-output mapping, can be given certain passivity properties if the equivalent compressor characteristic $\hat{\Psi}_e(\hat{\phi})$ can be shaped appropriately by selecting the valve control law $\hat{\Psi}_v(\hat{\phi})$.

3.3.2   Passivity of Pressure Dynamics

Proposition 3.1 *The pressure dynamics*

$$\mathcal{G}_2 : \hat{\phi} \mapsto \hat{\psi}, \tag{3.16}$$

where $\mathcal{G}_2 : \mathcal{L}_{2e} \to \mathcal{L}_{2e}$ is an input-output mapping, are strictly output passive.   □

Proof : Consider the nonnegative function

$$V_2(\hat{\psi}) = 2B^2 l_c \hat{\psi}^2. \tag{3.17}$$

Differentiating V_2 along the solution trajectories of (3.10) gives

$$\dot{V}_2 = \hat{\psi}\hat{\phi} - \hat{\phi}(\hat{\psi})\hat{\psi}. \tag{3.18}$$

In view of Assumption 3.1 and (3.18) it follows that

$$\left\langle \hat{\psi}, \hat{\phi} \right\rangle_T = \left\langle \hat{\phi}(\hat{\psi}), \hat{\psi} \right\rangle_T + \int_0^T \dot{V}_2 d\xi$$

$$
\begin{aligned}
&= \int_0^T \hat{\Phi}_T(\hat{\psi})\hat{\psi}d\xi + \int_0^T \dot{V}_2 d\xi \\
&\geq \kappa_2 \int_0^T \psi^2(\xi)d\xi + V_2(\xi) - V_2(0) \\
&\geq \kappa_2 \|\hat{\psi}\|_T^2 - V_2(0).
\end{aligned}
\tag{3.19}
$$

Hence,

$$
\left\langle \mathcal{G}_2\hat{\phi}, \hat{\phi} \right\rangle_T \geq \kappa_2 \|\mathcal{G}_2\hat{\phi}\|_T^2 - V_2(0),
\tag{3.20}
$$

and $\mathcal{G}_2$ is strictly output passive according to Definition 2.2.1 in van der Schaft (1996). $\square$

Remark 3.1 *In Simon and Valavani (1991), the incremental energy*

$$
V = \frac{l_c}{2}\hat{\psi}^2 + 2B^2 l_c \hat{\phi}^2,
\tag{3.21}
$$

with different coefficients due to the choice of nondimensional time, was used as a Lyapunov function candidate. The selection of the functions V_1 and V_2 used here is obviously inspired by this function. $\square$

3.3.3   Control Law

The following simple control law is proposed:

Proposition 3.2 *Let the control law be given by*

$$
u = \hat{\Psi}_v = c\hat{\phi}
\tag{3.22}
$$

where $c > \frac{k_2^2}{4k_3} - k_1 + \kappa_1$ and $\kappa_1 > 0$ is a design parameter. Then the equivalent compressor characteristic $-\hat{\Psi}_e(\hat{\phi})$ will satisfy the sector condition

$$
\left\langle -\hat{\Psi}_e(\hat{\phi}), \hat{\phi} \right\rangle_T \geq \int_0^T \kappa_1 \hat{\phi}^2(\xi)d\xi = \kappa_1 \|\hat{\phi}\|_T^2
\tag{3.23}
$$

$\square$

Proof :
The compressor characteristic is defined in equation (2.26). The equivalent compressor characteristic $\hat{\Psi}_e(\hat{\phi})$ is then given by

$$
\hat{\Psi}_e(\hat{\phi}) = -k_3\hat{\phi}^3(\xi) - k_2\hat{\phi}^2(\xi) - (k_1 + c)\hat{\phi}(\xi)
\tag{3.24}
$$

Consider the inner product

$$\left\langle -\hat{\Psi}_e(\hat{\phi}), \hat{\phi} \right\rangle_T = \int_0^T \hat{\phi}(\xi) \left(k_3 \hat{\phi}^3(\xi) + k_2 \hat{\phi}^2(\xi) + (k_1 + c)\hat{\phi}(\xi) \right) d\xi$$

$$= \int_0^T \hat{\phi}^2(\xi) \left(k_3 \hat{\phi}^2(\xi) + k_2 \hat{\phi}(\xi) + (k_1 + c) \right) d\xi. \quad (3.25)$$

It is noted that $K(\hat{\phi}) \triangleq k_3 \hat{\phi}^2 + k_2 \hat{\phi} + (k_1 + c)$ has a minimum value for $\hat{\phi} = -\frac{k_2}{2k_3}$. This minimum is calculated to be

$$K(\hat{\phi}) = k_3 \hat{\phi}^2 + k_2 \hat{\phi} + (k_1 + c) \geq -\frac{k_2^2}{4k_3} + k_1. \quad (3.26)$$

With the choice

$$c \geq \frac{k_2^2}{4k_3} - k_1 + \kappa_1 \quad (3.27)$$

it it follows from (3.24) that

$$k_3 \hat{\phi}^2(\xi) + k_2 \hat{\phi}(\xi) + (k_1 + c) \geq \kappa_1. \quad (3.28)$$

By inserting (3.28) into (3.25) we get

$$\left\langle -\hat{\Psi}_e(\hat{\phi}), \hat{\phi} \right\rangle_T \geq \int_0^T \kappa_1 \hat{\phi}^2(\xi) d\xi = \kappa_1 \|\hat{\phi}\|_T^2, \quad (3.29)$$

$\square$

Provided $u = \hat{\Psi}_v$ is chosen as in (3.22), it follows from (3.14) and (3.29) that also the flow dynamics are made strictly output passive, that is

$$\left\langle \mathcal{G}_1(-\hat{\psi}), -\hat{\psi} \right\rangle_T \geq \kappa_1 \|\mathcal{G}_1(-\hat{\psi})\|_T^2 - V_1(0), \quad (3.30)$$

We now state a stability reslult for the closed loop system $\Sigma_{\mathcal{G}_1, \mathcal{G}_2}$, shown in Figure 3.1.

Theorem 3.2 *The closed loop system $\Sigma_{\mathcal{G}_1, \mathcal{G}_2}$ consisting of the model (2.38) and control law (3.1) is $\mathcal{L}_2$-stable.*
$\square$
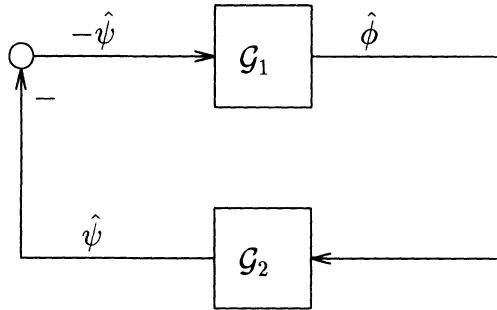
Figure 3.1: *The closed loop system* $\Sigma_{\mathcal{G}_1,\mathcal{G}_2}$

Proof :
The closed loop system $\Sigma_{\mathcal{G}_1,\mathcal{G}_2}$, shown in Figure 3.1, is a feedback interconnection of the two systems $\mathcal{G}_1 : -\hat{\psi} \mapsto \hat{\phi}$ and $\mathcal{G}_2 : \hat{\phi} \mapsto \hat{\psi}$. As stated in (3.20) and (3.30), the two mappings satisfy

$$\left\langle -\hat{\psi}, \mathcal{G}_1(-\hat{\psi}) \right\rangle \geq \kappa_1 \|\mathcal{G}_1(-\hat{\psi})\|_T^2 - V_1(0) \tag{3.31}$$

$$\left\langle \hat{\phi}, \mathcal{G}_2\hat{\phi} \right\rangle \geq \kappa_2 \|\mathcal{G}_2\hat{\phi}\|_T^2 - V_2(0) \tag{3.32}$$

for all $T \geq 0$ and all $\hat{\phi}, \hat{\psi} \in \mathcal{L}_{2e}$. According to the *passivity theorem*, Theorem 3.1, $\Sigma_{\mathcal{G}_1,\mathcal{G}_2}$ is $\mathcal{L}_2$-stable. $\square$

3.4   Disturbances
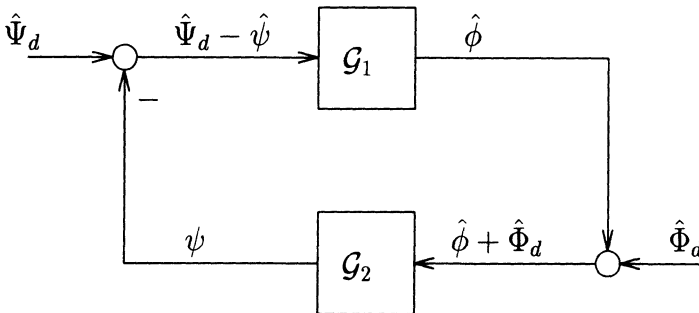
Figure 3.2: *The closed loop system* $\Sigma_{\mathcal{G}_1,\mathcal{G}_2}$ *with disturbances*

Consider the case when the compression system is subject to disturbances $\hat{\Phi}_d(\xi)$ in mass flow and $\hat{\Psi}_d(\xi)$ in pressure rise as in Section 2.2.5. The model is repeated here for convenience:

$$\dot{\hat{\psi}} = \frac{1}{4B^2 l_c}(\hat{\phi} + \hat{\Phi}_d(\xi) - \hat{\Phi}_T(\hat{\psi})) \qquad (3.33)$$

$$\dot{\hat{\phi}} = \frac{1}{l_c}(\hat{\Psi}_c(\hat{\phi}) - u - \hat{\psi} - \hat{\Psi}_d(\xi))$$

It is assumed that $\hat{\Psi}_d(\xi), \hat{\Phi}_d(\xi) \in \mathcal{L}_{2e}$. A stability result for the closed loop system shown in Figure 3.2 is now stated:

Theorem 3.3 *The system (3.33) under control (3.22) is $\mathcal{L}_2$-stable if the disturbances $\hat{\Phi}_d(\xi)$ in mass flow and $\hat{\Psi}_d(\xi)$ in pressure rise are taken into account.* □

Proof :
Redefine $\mathcal{G}_1$ as $\mathcal{G}_1 : -(\hat{\psi} - \hat{\Psi}_d) \mapsto \hat{\phi}$ and $\mathcal{G}_2$ as $\mathcal{G}_2 : \hat{\phi} + \hat{\Phi}_d \mapsto \hat{\psi}$. The result follows by repeating the analysis in the preceding sections and replacing $-\hat{\psi}$ with $-\hat{\psi} + \hat{\Psi}_d$ when establishing the strict output passivity of $\mathcal{G}_1$, and replacing $\hat{\phi}$ with $\hat{\phi} + \hat{\Phi}_d$ when establishing the strict output passivity of $\mathcal{G}_2$. □

The structure of the closed loop system is shown in Figure 3.2. Disturbance rejection of $\mathcal{L}_2$-disturbances in the Moore Greitzer model is also studied by Haddad *et al.* (1997), where throttle control of both surge and rotating stall is considered. While achieving global results and disturbance rejection for disturbances in both mass flow and rotating stall amplitude, the controller found by Haddad *et al.* (1997) is of high order, requires detailed knowledge of the compression system parameters and also needs full state feedback.

3.5 Simulations

Now the system (3.33) with control law (3.22) is simulated. The result is given in Figure 3.3. The controller gain was set to $c = 1.1$, and the controller was switched on at $\xi = 300$. The disturbances were

$$\hat{\Phi}_d(\xi) = 0.25 e^{-0.0015\xi} \cos(0.4\xi)$$

$$\hat{\Psi}_d(\xi) = 0.2 e^{-0.0025\xi} \sin(0.6\xi), \qquad (3.34)$$

which has the same structure as the $\mathcal{L}_2$-disturbances considered in Haddad *et al.* (1997).
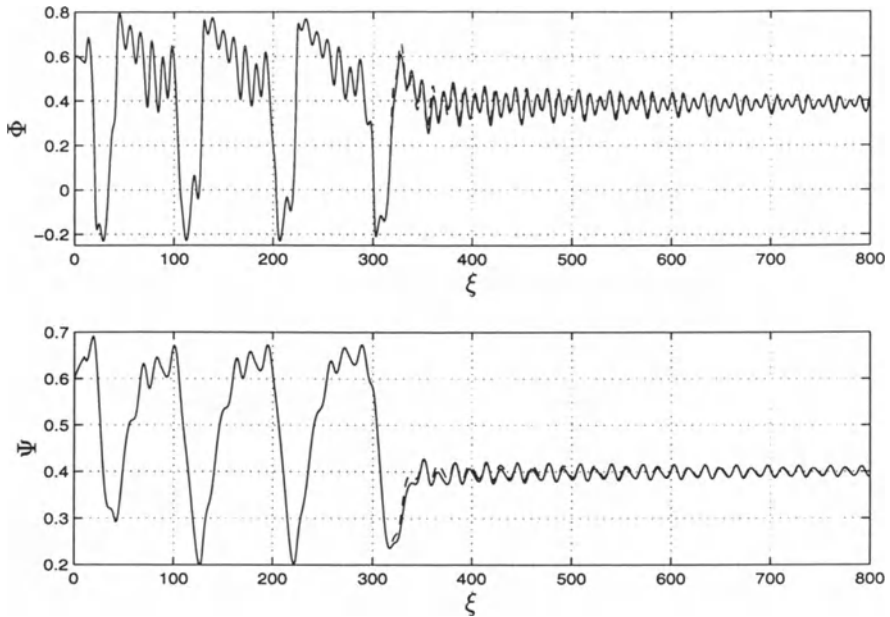
Figure 3.3: *Comparison of closed loop response with passivity based (solid lines) and backstepping based (dashed lines) controllers.*

Also plotted in Figure 3.3 is the response of the controller (3.1), simulated with the same disturbances. The parameters for (3.1) were chosen as $c_2 = 1$, $d_1 = 0.3$, $d_2 = 0.1$. As can be seen, the two set of responses are almost indistinguishable. Figure 3.3 also illustrates the result of Corollary 2.2, where the controller (3.1) guarantees convergence to the equilibrium in the presence of disturbances upper bounded by a monotonically decreasing non-negative function.

In Figure 3.4, the time varying disturbance terms are shown. The control action is plotted in Figure 3.5. The control action of the passivity based controller is plotted with a solid line, and the action of the backstepping based controller is plotted with a dashed line. The lower plot is a blown up version of the upper, and as previously mentioned, the differences are small. The most noteworthy one being that the passive controller creates a higher pressure drop initially. The small difference in control action can be explained with the low damping d_1 and d_2 chosen for (3.1), but with the current disturbances that is all that was needed.

One advantage of the backstepping controller (3.1) compared to the passivity based (3.22) is that (3.1) ensures convergence to a set when the disturbances are *not* in $\mathcal{L}_2$, whereas the approach in this chapter demands that they are in $\mathcal{L}_2$.
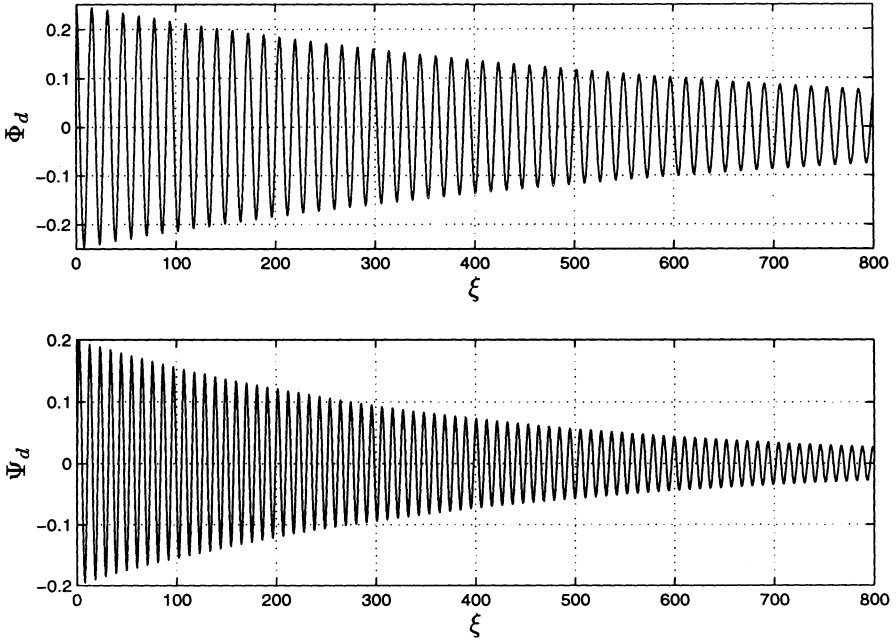
Figure 3.4: *The disturbances.*
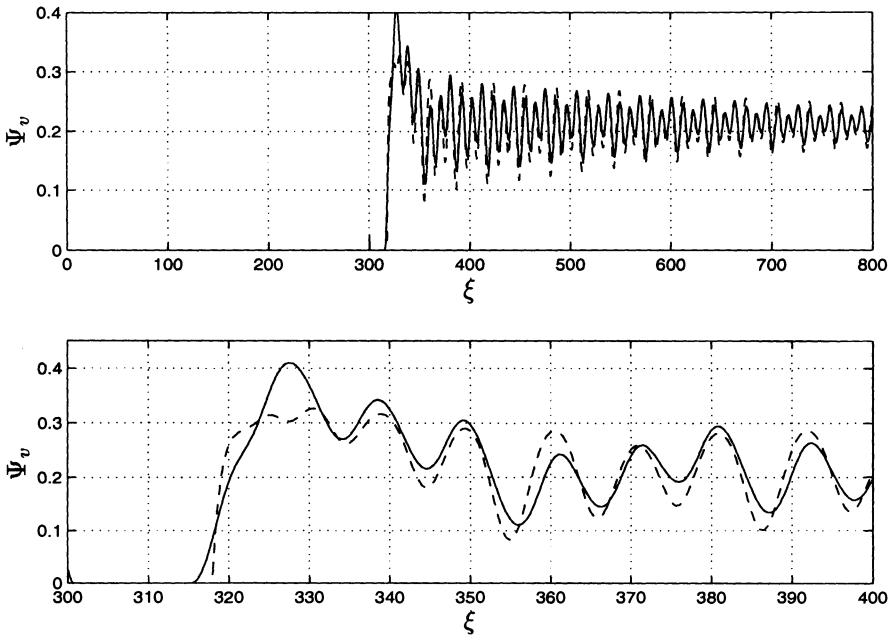
Figure 3.5: *Comparison of the CCV pressure drop for the two controllers.*

3.6 Concluding Remarks

In this chapter the passivity properties of the Greitzer model was used to derive a surge control law for a close coupled valve. The results in this chapter, when not taking disturbances into account, are similar to the results in section 2.3.1. However, using input/output theory and passivity it was possible to show that the proportional controller $u = c\hat{\phi}$ yielded an $\mathcal{L}_2$-stable system in the presence of both mass flow disturbances as well as pressure disturbances. Compared to the more complicated controller (3.1) the advantages of the input/output approach over the Lyapunov based approach of backstepping, in this particular case, should be evident.

However, it is believed that the simple controller $u = c\hat{\phi}$ also could have been derived using backstepping, but with considerable more involved algebraic manipulations, and possibly a new choice of Lyapunov function candidate.

It is straightforward to show that the stability result is still valid if the control law (3.22) is changed as long as the sector condition (3.23) hold. Thus, a more sophisticated controller could be used in order to e.g. minimize the steady state pressure drop over the CCV or improve transient performance, and still stability could be shown.

When comparing with the results on rotating stall control in Haddad *et al.* (1997), the passivity based method used here shows promise for developing a simple, low order, partial state feedback controller when rotating stall is also taken into account, and still achieving disturbance rejection. This is an interesting open problem.

CHAPTER 4

A MOORE-GREITZER TYPE MODEL FOR AXIAL COMPRESSORS WITH NON-CONSTANT SPEED

4.1 Introduction

In this Chapter we propose an extension to the Moore-Greitzer model, where non-constant rotational speed of the compressor is taken into account. The consequence of this is that the new model includes the B-parameter as a state. Higher harmonics of rotating stall will also be included in the model.

In the original work of Moore and Greitzer, the compressor speed is assumed to be constant. Greitzer and Moore (1986) concluded that low values of Greitzer's B-parameter B lead to rotating stall, while high values of B lead to surge. Whether to term the B-parameter "high" or "low", is in this context dependent on the design parameters of the compressor at hand, as Day (1994) points out. There exists a $B_{critical}$ for which $B > B_{critical}$ will lead to surge and $B < B_{critical}$ will lead to rotating stall. However, this $B_{critical}$ is different for each compressor. As B is proportional to the angular speed of the machine, it is of major concern for stall/surge controller design to include the spool dynamics in a stall/surge-model, in order to investigate the influence of time varying speed on the stall/surge transients.

It is known from the gas turbine literature, see e.g. Mattingly (1996) or Cohen *et al.* (1996), that acceleration of a single-shaft engine possibly can drive the
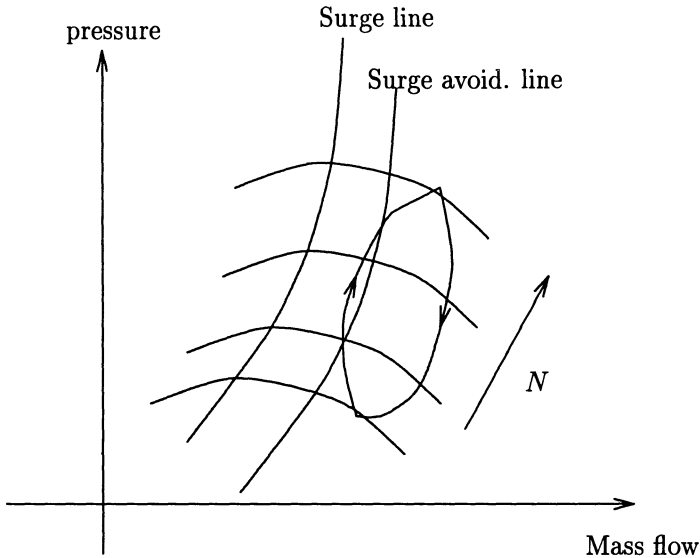
Figure 4.1: *Compressor transient trajectories in gas turbine.*

compressor into rotating stall. The Moore-Greitzer model can be viewed as a simplified model of a single shaft gas turbine. Acceleration of such engines is achieved by increasing the fuel flow to the combustor which in turn increases the turbine temperature and torque. The exit pressure of the compressor may then increase before the increase in compressor flow and speed has taken off. For engine deceleration, the effect is exact the opposite. This behavior is illustrated in Figure 4.1. The use of a large surge margin will restrict the magnitude of allowable transients. In modern jet engines several measures have been taken to prevent stall during acceleration. These measures include bleed valves, the use of multiple spools or variable stator blades. Gas turbines with multiple spools, i.e. twin-spools, will have different transient trajectories than the single spool case. In such machines the trajectory may approach the surge line during deceleration instead of acceleration. This topic will not be treated further in this book, a discussion is given in Cohen *et al.* (1996).

A model for centrifugal compressors with non-constant speed was presented by Fink *et al.* (1992). In Gravdahl and Egeland (1997*f*) a similar model was derived, and surge and speed control was investigated. However, both the models of Fink *et al.* (1992) and Gravdahl and Egeland (1997*f*) were developed for centrifugal machines, and do not include rotating stall as a state.

The model of Moore and Greitzer (1986) is based on a first harmonics approximation of rotating stall, using a Galerkin procedure. A fundamental

shortcoming of the low order, three state More Greitzer model is the one
mode approximation. Mansoux *et al.* (1994) found that higher order modes
interact with the first harmonic during stall inception. Relaxation of the
one mode approximation has been presented by Adomatis and Abed (1993),
Mansoux *et al.* (1994), Gu *et al.* (1996) and Leonessa *et al.* (1997a), and
control designs for such models have been reported by several authors, see
Table 4.1 below. Also, Banaszuk *et al.* (1997a) report of design of stall/surge
controllers without using a Galerkin approximation, that is for the full PDE
model. Leonessa *et al.* (1997a) highlight the importance of including higher
order modes of rotating stall in the model, and demonstrate that the control
law proposed by Krstić *et al.* (1995a), which was based on a one mode model,
fails when applied to a higher order model.

In Table 4.1, the development in stall/surge modeling and control is outlined.
Hansen *et al.* (1981) demonstrated that the model of Greitzer (1976a) also
applies to centrifugal compressors. It seems that the modeling and control
of an axial compression system including both rotating stall and spool speed
is an open problem. The problem of non-constant speed is also listed among
topics for further research in Greitzer and Moore (1986).

Reference(s)	states	A/C	M/C/S
Greitzer (1976a)	Φ, Ψ	A	M
Hansen *et al.* (1981)	Φ, Ψ	C	M
Several, see de Jager (1995). Also Gravdahl and Egeland (1997b)	Φ, Ψ	A/C	C
Fink *et al.* (1992)	Φ, Ψ, B	C	M
Gravdahl and Egeland (1998a)	Φ, Ψ, B	C	MCS
Moore and Greitzer (1986)	Φ, Ψ, J	A	M
Eveker and Nett (1991)	Φ, Ψ, B	A	MC
Several, see de Jager (1995). Also Gravdahl and Egeland (1997c)	Φ, Ψ, J	A	C
Mansoux *et al.* (1994)	Φ, Ψ, J_i	A	M
Leonessa *et al.* (1997a)	Φ, Ψ, J_i	A	MC
Adomatis and Abed (1993) Hendrickson and Sparks (1997) Humbert and Krener (1997)	Φ, Ψ, J_i	A	C
Gravdahl and Egeland (1997a)	Φ, Ψ, J, B	A	MS
Gravdahl and Egeland (1997d)	Φ, Ψ, J_i, B	A	MS

Table 4.1: *Outline of the development in compressor stall/surge modeling
and control. A=Axial, C=Centrifugal, M=Modeling, C=stall/surge control,
S=Speed control. The model of Eveker and Nett (1991) uses states with
dimensions.*
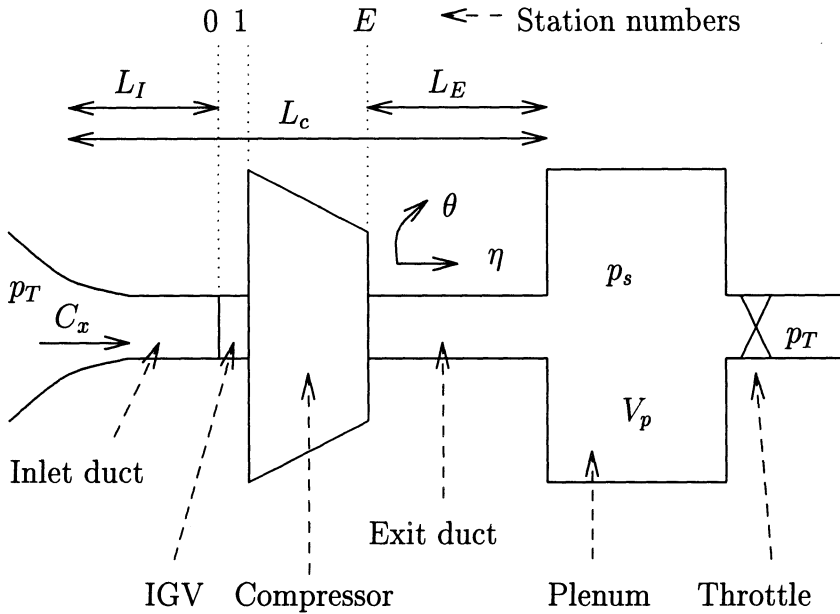
Figure 4.2: *Principal drawing of the compression system of (Moore and Greitzer 1986). The station numbers are used as subscripts in the following.*

4.2   Preliminaries

The compression system is essentially the same as in Chapter 2, and consists of an inlet duct, inlet guide vanes (IGV), axial compressor, exit duct, plenum volume and a throttle. The differences, compared to Chapter 2, are that the compressor speed is non-constant, and a CCV is not included. The system is shown in Figure 4.2. Our aim is to develop a model for this system in the form

$$\dot{z} = f(z), \tag{4.1}$$

where $z = (\Phi,\ \Psi,\ J_i,\ B)^{\mathrm{T}} \in \mathbb{R}^q$ and

- Φ is the circumferentially averaged flow coefficient

- Ψ is the total-to-static pressure rise coefficient

- J_i is the squared amplitude mode i of angular variation (rotating stall)

- B is Greitzer's B-parameter which is proportional to the speed of the compressor.

- $i = 1 \ldots N$ is the rotating stall mode number. N is the maximum number of stall modes determined by the gas viscosity.

- The dimension of the state space is $q = N + 3$.

The modeling of the compression system relies heavily on the modeling in Moore and Greitzer (1986). However, the assumption of constant speed U, and thus constant B, is relaxed and a momentum balance for the spool is included. The gas viscosity as introduced by Adomatis and Abed (1993) is also taken into account, and N modes are included in the model as opposed to the work of Moore and Greitzer (1986) where a first harmonic approximation was used.

Moore and Greitzer (1986) define nondimensional time as

$$\xi_{MG} = \frac{Ut}{R}, \tag{4.2}$$

where U is the rotor tangential velocity at mean radius, R is the mean compressor radius and t is actual time in seconds. As we here consider time varying U, this normalization will not be used. Instead we propose to use

$$\xi = \frac{U_d t}{R}, \tag{4.3}$$

where U_d is the *desired* constant velocity of the wheel. Note that if

$$U_d = U = const \Rightarrow \xi = \xi_{MG}. \tag{4.4}$$

All distances are nondimensionalized with respect to R, that is the nondimensional duct lengths, see Figure 4.2, are defined as

$$l_I = \frac{L_I}{R} \text{ and } l_E = \frac{L_E}{R}. \tag{4.5}$$

The axial coordinate is denoted η and the circumferential coordinate is the wheel angle θ. Greitzer's B-parameter is defined as

$$B \triangleq \frac{U}{2a_s} \sqrt{\frac{V_p}{A_c L_c}}, \tag{4.6}$$

where a_s is the speed of sound, V_p is the plenum volume, A_c is the compressor duct flow area and L_c is the total length of compressor and ducts. B and U are related as

$$U = bB, \tag{4.7}$$

where

$$b \triangleq 2a_s \sqrt{\frac{A_c L_c}{V_p}} \tag{4.8}$$

is a constant.

4.3   Modeling

4.3.1   Spool Dynamics

The momentum balance of the spool can be written

$$I\frac{d\omega}{dt} = \tau_t - \tau_c, \tag{4.9}$$

where ω is the angular speed, I is the spool moment of inertia, and τ_t and τ_c are the drive (turbine) torque and compressor torque respectively. Cohen *et al.* (1996) note that the net torque $\tau_t - \tau_c$ is the difference between two quantities of similar magnitude, so a small change in either may result in a much larger change in the torque available for acceleration. For a jet engine, the turbine torque will depend on, and be determined by, the fuel flow to the combustion chamber. Then, the turbine torque will be given by

$$\tau_t = \frac{\eta_{mech} m_t c_p \Delta T_{turbine}}{2\pi N}. \tag{4.10}$$

Here, the turbine torque τ_t will be treated as an input to the model, and the underlying details in producing this torque will not be studied further. Using

$$\omega = U/R, \tag{4.11}$$

and equations (4.3) and (4.6), the spool dynamics (4.9) can be written

$$\frac{2a_s I U_d}{R^2}\sqrt{\frac{A_c L_c}{V_p}}\frac{dB}{d\xi} = \tau_t - \tau_c. \tag{4.12}$$

As in Fink *et al.* (1992), torques are nondimensionalized according to

$$\Gamma = \Gamma_t - \Gamma_c = \frac{\tau_t - \tau_c}{\rho A_c R U^2}, \tag{4.13}$$

where ρ is the constant inlet density. Now, (4.12) can be written

$$\frac{dB}{d\xi} = \Lambda_1 B^2(\Gamma_t - \Gamma_c), \tag{4.14}$$

where the constant Λ_1 is defined as

$$\Lambda_1 \triangleq \frac{\rho R^3 A_c}{I U_d}b. \tag{4.15}$$

As the compressor torque equals the change of angular momentum of the fluid, see for instance Mattingly (1996), the compressor torque can be written

$$\tau_c = m_c R(C_{\theta 2} - C_{\theta 1}) \tag{4.16}$$

where $C_{\theta 1}$ and $C_{\theta 2}$ are the tangential fluid velocity at the rotor entrance and exit respectively. Assuming that C_x, the flow velocity in the axial direction, is the same at entrance and exit,

$$\tau_c = m_c R C_x (\tan \beta_1 - \tan \beta_2) \tag{4.17}$$

where β_1 and β_2 fluid angles at the rotor entrance and exit respectively. The fluid angles are time varying. However, Cohen *et al.* (1996) show that

$$\tan \beta_{1b} - \tan \beta_{2b} = \tan \beta_1 - \tan \beta_2, \tag{4.18}$$

where β_{1b} and β_{b2} constant blade angles at the rotor entrance and exit respectively. The compressor mass flow is given by

$$m_c = \rho A_c U \Phi. \tag{4.19}$$

The combination of (4.17), (4.18) and (4.19) result in

$$\tau_c = R \rho A_c \Phi^2 U^2 (\tan \beta_{1b} - \tan \beta_{2b}), \tag{4.20}$$

and by (4.13) the nondimensional compressor torque is

$$\Gamma_c = \Phi^2 (\tan \beta_{1b} - \tan \beta_{2b}). \tag{4.21}$$

In terms of the compressor speed U, the dynamics of the spool can be written

$$\frac{dU}{d\xi} = \frac{\Lambda_1}{b} \Gamma U^2. \tag{4.22}$$

4.3.2   Compressor

Moore (1984*a*) give the pressure rise over a single blade row as

$$\frac{p_E - p_1}{\frac{1}{2}\rho U^2} = F(\phi) - \tau \frac{d\phi}{dt}, \tag{4.23}$$

where

$$\phi = \frac{C_x}{U} \tag{4.24}$$

is the local axial flow coefficient, $F(\phi)$ is the pressure rise coefficient in the blade passage, C_x is the velocity component along the x-axis, and τ is a coefficient of pressure rise lag. According to Moore and Greitzer (1986), $\frac{d\phi}{dt}$ can be calculated as

$$\frac{d\phi}{dt} = \left(\frac{\partial \phi}{\partial t}\right)_{rotor} + \left(\frac{\partial \phi}{\partial t}\right)_{stator}. \tag{4.25}$$

Using (4.3) it is seen that

$$\left(\frac{\partial \phi}{\partial t}\right)_{rotor} = \frac{\partial \phi}{\partial \xi}\frac{\partial \xi}{\partial t} + \frac{\partial \phi}{\partial \theta}\frac{\partial \theta}{\partial t}$$

$$= \frac{U_d}{R}\frac{\partial \phi}{\partial \xi} + \frac{\partial \phi}{\partial \theta}\frac{U(t)}{R} \tag{4.26}$$

$$\left(\frac{\partial \phi}{\partial t}\right)_{stator} = \frac{U_d}{R}\frac{\partial \phi}{\partial \xi}, \tag{4.27}$$

where the unsteadiness of the flow through the stator passage reflects the accelerations associated with transients effects. For the rotor there is also unsteadiness due to the rotor blades moving with velocity $U(t)$ through a circumferentially nonuniform flow. Considering a compressor of N_s stages, we get

$$\frac{p_E - p_1}{\frac{1}{2}\rho U^2} = N_s F(\phi) - \frac{1}{2a}\left(2\frac{\partial \phi}{\partial \xi} + \frac{U}{U_d}\frac{\partial \phi}{\partial \theta}\right), \tag{4.28}$$

where

$$a \triangleq \frac{R}{N_s \tau U_d} \tag{4.29}$$

is a constant. Note that if $U(\xi) = $ const and $U_d \equiv U$ such that $\xi = \xi_{MG}$, equation (4.28) is reduced to equation (5) in Moore and Greitzer (1986). It is noted that the flow coefficient ϕ can depend on both ξ and θ, even though the atmospheric stagnation pressure p_T is constant. The average of ϕ around the wheel is defined as

$$\frac{1}{2\pi}\int_0^{2\pi} \phi(\xi,\theta)d\theta \triangleq \Phi(\xi). \tag{4.30}$$

Further

$$\phi = \Phi(\xi) + g(\xi,\theta) \text{ and } h = h(\xi,\theta), \tag{4.31}$$

where h is a circumferential coefficient. As no circulation occurs in the entrance duct it is clear that the averages of g and h vanish:

$$\int_0^{2\pi} g(\xi,\theta)d\theta = \int_0^{2\pi} h(\xi,\theta)d\theta = 0. \tag{4.32}$$

4.3.3   Entrance Duct and Guide Vanes

The fact that the rotational speed of the wheel now is assumed time varying does not change the conditions upstream of the compressor. Therefore, the equations stated in Moore and Greitzer (1986) are still valid, and will be presented here. The pressure difference over the IGVs, where the flow is axial, can be written

$$\frac{p_1 - p_0}{\rho U^2} = \frac{1}{2}K_G h^2, \tag{4.33}$$

where $0 < K_G \leq 1$ is the entrance recovery coefficient. If the IGVs are lossless $K_G = 1$. Upstream of the IGV irrotational flow is assumed so that a (unsteady) velocity potential $\tilde{\phi}$ exists. The gradient of $\tilde{\phi}$ gives axial and circumferential velocity coefficients everywhere in the entrance duct. At the IGV entrance point (denoted by subscript '0') we have

$$(\tilde{\phi}_\eta)_0 = \Phi(\xi) + g(\xi, \theta) \text{ and } (\tilde{\phi}_\theta)_0 = h(\xi, \theta), \tag{4.34}$$

where partial differentiation with respect to η and θ is denoted by subscripts. Bernoulli's equation for unsteady, frictionless and incompressible flow will be used to calculate the pressure drop in the entrance duct. As in Moore and Greitzer (1986) and White (1986), this can be written

$$\frac{p_T - p_0}{\rho U^2} = \frac{1}{2}(\phi^2 + h^2) + (\tilde{\phi}_\xi)_0, \tag{4.35}$$

where the term $(\tilde{\phi}_\xi)_0$ is due to unsteadiness in Φ and g. A straight inlet duct of nondimensional length l_I is considered, and the velocity potential can be written

$$\tilde{\phi} = (\eta + l_I)\Phi(\xi) + \tilde{\phi}'(\xi, \eta), \tag{4.36}$$

where $\tilde{\phi}'$ is a disturbance velocity potential such that

$$\tilde{\phi}'\Big|_{\eta=-l_I} = 0 \ , \ (\tilde{\phi}'_\eta)_0 = g(\xi, \theta) \text{ and } (\tilde{\phi}'_\theta)_0 = h(\xi, \theta). \tag{4.37}$$

Equation (4.35) can now be written

$$\frac{p_T - p_0}{\rho U^2} = \frac{1}{2}(\phi^2 + h^2) + l_I \frac{d\Phi}{d\xi} + (\tilde{\phi}'_\xi)_0. \tag{4.38}$$

4.3.4 Exit Duct and Guide Vanes

Downstream of the compressor, the flow is complicated and rotational. As in Moore and Greitzer (1986), the pressure p in the exit duct is assumed to differ only slightly from the static plenum pressure $p_s(\xi)$, such that the pressure coefficient P satisfies Laplace's equation.

$$P \triangleq \frac{p_s(\xi) - p}{\rho U^2} \ , \ \nabla^2 P = 0. \tag{4.39}$$

The axial Euler equation, see for instance White (1986), is used to find the pressure drop across the exit duct. The Euler equation is the inviscid form of the differential equation of linear momentum. If integrated along a streamline of the flow, the Euler equation will yield the frictionless Bernoulli equation. The Euler equation in the x-coordinate, neglecting gravity, can be written as

$$-\frac{dp}{dx} = \rho \frac{dC_x}{dt}. \tag{4.40}$$

Employing the chosen nondimensionalization of time and distance,

$$\frac{d}{dt} = \frac{U_d}{R}\frac{d}{d\xi} \text{ and } \frac{d}{dx} = \frac{1}{R}\frac{d}{d\eta}, \tag{4.41}$$

we get

$$\frac{dp_E}{dx} = -\rho U^2 \frac{1}{R}(P_\eta)_E \tag{4.42}$$

$$\frac{dC_x}{dt} = \frac{U_d}{R}\frac{d}{d\xi}\left\{(\tilde{\phi}_\eta)_0 U\right\}. \tag{4.43}$$

Inserting (4.42) and (4.43) in (4.40) we get the following expression for the axial Euler equation, evaluated at E, where time varying U has been taken into account

$$(P_\eta)_E = \frac{U_d}{U^2}\frac{d}{d\xi}\left\{(\tilde{\phi}_\eta)_0 U\right\}$$

$$= \frac{U_d}{U^2}\left((\tilde{\phi}_{\eta\xi})_0 U + (\tilde{\phi}_\eta)_0 \frac{dU}{d\xi}\right). \tag{4.44}$$

From (4.34) we have

$$(\tilde{\phi}_{\eta\xi})_0 = \Phi_\xi(\xi) + (\tilde{\phi}'_{\eta\xi})_0. \tag{4.45}$$

Inserting (4.34) and (4.45) into (4.44) we get

$$(P_\eta)_E = \frac{U_d}{U}\left(\frac{d\Phi}{d\xi} + (\tilde{\phi}'_{\eta\xi})_0\right) + \frac{U_d}{U^2}\frac{dU}{d\xi}\left(\Phi(\xi) + (\tilde{\phi}'_\eta)_0\right). \tag{4.46}$$

At the duct exit, $\eta = l_E$, we want that $p = p_s$, that is $P = 0$. Thus, when integrating (4.46), the constant of integration is chosen such that

$$P = \frac{U_d}{U(\xi)}\left((\eta - l_E)\frac{d\Phi}{d\xi} - \tilde{\phi}'_\xi\right) + \frac{U_d}{U^2}\frac{dU}{d\xi}\left((\eta - l_E)\Phi(\xi) - \tilde{\phi}'\right). \tag{4.47}$$

Finally, we get

$$\frac{p_s - p_E}{\rho U^2} = (P)_E = \frac{U_d}{U(\xi)}\left(-l_E\frac{d\Phi}{d\xi} - (m-1)(\tilde{\phi}'_\xi)_0\right)$$

$$+ \frac{U_d}{U^2}\frac{dU}{d\xi}\left(-l_E\Phi(\xi) - (m-1)(\tilde{\phi}')_0\right), \tag{4.48}$$

where, as in Moore (1984c) and Moore and Greitzer (1986), the compressor duct flow parameter[1] m has been included. It is noted that if $U(\xi) =$const and $U_d \equiv U$ such that $\xi = \xi_{MG}$, equation (4.48) is reduced to equation (20) in Moore and Greitzer (1986).

---

[1]$m = 1$ for a very short exit duct, and $m = 2$ otherwise.

4.3.5 Overall Pressure Balance

Using the preceding calculations, we now want to calculate the net pressure rise from the upstream reservoir total pressure p_T to the plenum static pressure p_s at the discharge of the exit duct. This is done by combining equations (4.28), (4.33), (4.38) and (4.48) according to

$$
\begin{aligned}
\frac{p_s - p_T}{\rho U^2} \;=\; & (NF(\phi) - \frac{1}{2}\phi^2) - (l_I + l_E\frac{U_d}{U} + \frac{1}{a})\frac{d\Phi}{d\xi} \\
& + \left((1-m)\frac{U_d}{U} - 1\right)(\tilde{\phi}'_\xi)_0 - \frac{1}{2}(1 - K_G)h^2 \\
& + \frac{U_d}{U^2}\frac{dU}{d\xi}\left(-l_E\Phi(\xi) - (m-1)(\tilde{\phi}')_0\right) \\
& - \frac{1}{2a}\left(2(\tilde{\phi}'_{\xi\eta})_0 + \frac{U}{U_d}(\tilde{\phi}'_{\eta\theta})_0\right),
\end{aligned}
\tag{4.49}
$$

where

$$
\begin{aligned}
2\frac{\partial\phi}{\partial\xi} + \frac{\partial\phi}{\partial\theta} \;=\; & 2\frac{\partial\Phi}{\partial\xi} + 2\frac{\partial g}{\partial\xi} + \frac{\partial g}{\partial\theta} \\
\;=\; & 2\frac{\partial\Phi}{\partial\xi} + 2(\tilde{\phi}'_{\xi\eta})_0 + (\tilde{\phi}'_{\eta\theta})_0
\end{aligned}
\tag{4.50}
$$

has been used. By defining [2]

$$
\begin{aligned}
\Psi(\xi) \;&=\; \frac{p_s - p_T}{\rho U^2} \\
\Psi_c(\phi) \;&=\; NF(\phi) - \frac{1}{2}\phi^2 \\
l_c(U) \;&=\; l_I + l_E\frac{U_d}{U} + \frac{1}{a} \\
m_U(U) \;&=\; (1-m)\frac{U_d}{U} - 1,
\end{aligned}
\tag{4.51}
$$

and assuming $K_G \equiv 1$, (4.49) can be written

$$
\begin{aligned}
\Psi(\xi) \;=\; & \Psi_c(\phi) - l_c(U)\frac{d\Phi}{d\xi} + m_U(U)(\tilde{\phi}'_\xi)_0 \tag{4.52} \\
& + \frac{U_d}{U^2}\frac{dU}{d\xi}\left(-l_E\Phi(\xi) - (m-1)(\tilde{\phi}')_0\right) \\
& - \frac{1}{2a}\left(2(\tilde{\phi}'_{\xi\eta}) + \frac{U}{U_d}(\tilde{\phi}'_{\eta\theta}) - \mu(\tilde{\phi}'_{\eta\theta\theta})\right)_0,
\end{aligned}
$$

which, when assuming $U = U_d$ and $\mu = 0$, reduces to equation (26) in Moore and Greitzer (1986). In (4.52) the μ-term is included in order to

---

[2]Notice that $l_c \neq L_c R$. As in Fink *et al.* (1992) L_c, used in the definition of B, is a constant. See equation (4.6).

account for viscous transportation of momentum in the compressor. Viscosity was first introduced into the Moore-Greitzer model by Adomatis and Abed (1993), and included in the analysis of Gu *et al.* (1996) and Hendrickson and Sparks (1997). Adomatis and Abed (1993) conclude that the effect of viscous damping *must* be included in a multi mode Moore-Greitzer model. This to ensure that the large velocity gradients associated with higher modes will be damped out. Without viscosity, all the modes would have the same amplitude in fully developed rotating stall.

Equation (4.52) requires knowledge of the disturbance velocity potential $\tilde{\phi}'$ and its derivatives. As $\tilde{\phi}'$ satisfies Laplace's equation $\nabla^2 \tilde{\phi}' = 0$ it has a Fourier series. This Fourier series has N terms, where the number N is dependent on μ. According to Adomatis and Abed (1993) and Gu *et al.* (1996),

$$N = \begin{cases} \infty & \text{for} \quad \mu = 0 \\ \text{finite} & \text{for} \quad \mu > 0 \end{cases}. \tag{4.53}$$

By using (4.7), equation (4.52) can be written in terms of B, and by integration of (4.52) over one cycle with respect to θ, we get

$$\Psi(\xi) + l_c(B)\frac{d\Phi}{d\xi} + l_E \frac{U_d \Gamma \Lambda_1}{b} \Phi(\xi) = \frac{1}{2\pi} \int_0^{2\pi} \psi_c(\phi) d\theta, \tag{4.54}$$

which is the annulus averaged momentum balance.

4.3.6   Plenum Mass Balance

The mass balance in the plenum can be written

$$\frac{d}{d\xi}(\rho_p V_p) = m_c - m_t, \tag{4.55}$$

where ρ_p is the plenum density, m_c is the mass flow entering the plenum from the compressor, and m_t is the mass flow leaving through the throttle. Assuming the pressure variations in the plenum isentropic, we have

$$\frac{dp_p}{d\xi} = \frac{a_s^2}{V_p}(m_c - m_t), \tag{4.56}$$

which is shown in detail in Appendix C. By nondimensionalizing pressure with ρU^2, mass flow with $\rho U A_c$, transforming to nondimensional time ξ, and taking account for (4.6), (4.56) can be written

$$\frac{d\Psi}{d\xi} = \frac{\Lambda_2}{B}(\Phi - \Phi_T) - \frac{2}{B}\frac{dB}{d\xi}\Psi, \tag{4.57}$$

where the constant Λ_2 is defined as

$$\Lambda_2 \triangleq \frac{R}{L_c U_d}b. \tag{4.58}$$

Using (4.14) we get

$$\frac{d\Psi}{d\xi} = \frac{\Lambda_2}{B}(\Phi - \Phi_T) - 2\Lambda_1 \Gamma B \Psi. \tag{4.59}$$

The model of the compression system now consists of the torque balance for the spool (4.14), the local momentum balance (4.52), the annulus averaged momentum balance (4.54) and the mass balance of the plenum (4.59).

The compression system characteristics are taken from Moore and Greitzer (1986). The usual third order polynomial steady state compressor characteristic presented in Chapter 2 is used, and repeated here for convenience:

$$\Psi_c(\Phi) = \psi_{c0} + H \left(1 + \frac{3}{2}(\frac{\Phi}{W} - 1) - \frac{1}{2}(\frac{\Phi}{W} - 1)^3\right), \tag{4.60}$$

where the parameters ψ_{c0}, H and W are defined in Chapter 2.

The throttle characteristics is again taken to be

$$\Phi_T(\Psi) = \gamma_T \sqrt{\Psi}. \tag{4.61}$$

4.3.7 Galerkin Procedure

In order to transform the PDE (4.52) into a set of ODEs, a Galerkin approximation is employed. The disturbance velocity potential $\tilde{\phi}'$ is represented by the function $(\tilde{\phi}')^*$:

$$(\tilde{\phi}')^* = \sum_{n=1}^{N(\mu)} \frac{W}{n} e^{n\eta} A_n(\xi) \sin(n\theta - r_n(\xi)), \tag{4.62}$$

where $A_n(\xi)$ is the amplitude of mode number n of rotating stall and $r_n(\xi)$, $n = 1 \ldots N(\mu)$ are unknown phase angles. The residue R_n, for use in the Galerkin approximation, is defined as

$$R_n \triangleq (\tilde{\phi}'_\xi)^*_0 - (\tilde{\phi}'_\xi)_0, \tag{4.63}$$

and using (4.52) and (4.62), R_n can be calculated as

$$
\begin{aligned}
R_n = {}& \frac{W}{n} \left(\frac{dA_n}{d\xi} \sin \zeta_n - A_n \frac{dr_n}{d\xi} \cos \zeta_n\right) \\
& - \frac{1}{m_B(B)} \left\{ \Psi(\xi) + l_c(B)\frac{d\Phi}{d\xi} + l_E\frac{U_d\Gamma\Lambda_1}{b}\Phi - \Psi_c\left(\Phi + W A_n(\xi) \sin \zeta_n\right) \right. \\
& + \frac{U_d\Gamma\Lambda_1(m-1)W}{bn}A_n(\xi) \sin \zeta_n + \frac{W}{2a}\left(2\left(\frac{dA_n}{d\xi} \sin \zeta_n - A_n \frac{dr_n}{d\xi} \cos \zeta_n\right)\right. \\
& \left.\left. + \frac{Un}{U_d}A_n(\xi) \cos \zeta_n + \mu n^2 A_n(\xi) \sin \zeta_n\right)\right\},
\end{aligned}
\tag{4.64}
$$

where

$$\zeta_n \triangleq n\theta - r_n(\xi). \tag{4.65}$$

The Galerkin approximation is calculated using the weight functions

$$h_1 = 1, \ h_2 = \sin\zeta_n, \ h_3 = \cos\zeta_n \tag{4.66}$$

and the inner product

$$\langle R_n, h_i \rangle = \frac{1}{2\pi} \int_0^{2\pi} R_n(\zeta) h_i(\zeta) d\zeta. \tag{4.67}$$

Calculating the moments

$$M_i = \langle R_n, h_i \rangle \ \text{for} \ i = 1, 2, 3 \tag{4.68}$$

results in

$$
\begin{aligned}
M_1 &= \frac{1}{2\pi} \left(\Psi(\xi) + l_c(B)\frac{d\Phi}{d\xi} + l_E \frac{U_d \Gamma \Lambda_1}{b} \Phi(\xi) \right. \\
&\quad \left. + \int_0^{2\pi} \Psi_c \left(\Phi + W A_n(\xi) \sin\zeta_n \right) d\zeta_n \right) \\
M_2 &= \frac{1}{2\pi} \left(\frac{U_d \Gamma \Lambda_1 (m-1)}{bn} A_n(\xi) + \frac{\mu n^2}{2Wa} A_n(\xi) \right. \\
&\quad + \frac{dA_n}{d\xi} \left(\frac{1}{a} - \frac{m_B(B)}{n} \right) \\
&\quad \left. + \int_0^{2\pi} \Psi_c \left(\Phi + W A_n(\xi) \sin\zeta_n \right) \sin\zeta_n d\zeta_n \right) \\
M_3 &= \frac{1}{2\pi} \left(-\left(\frac{dr_n}{d\xi} \left(\frac{1}{a} - \frac{m_B(B)}{n} \right) - \frac{bBn}{2aU_d} \right) A(\xi) \right. \\
&\quad \left. + \int_0^{2\pi} \Psi_c \left(\Phi + W A_n(\xi) \sin\zeta_n \right) \cos\zeta_n d\zeta_n \right)
\end{aligned}
\tag{4.69}
$$

It is recognized that, due to $\Psi_c(\phi)$ being even in ϕ, the last term in M_3 vanishes. Demanding $M_3 = 0$ and assuming $A_n \neq 0$ the phase angles r_n must satisfy

$$\frac{dr_n}{d\xi} = \frac{\frac{n}{2}\frac{b}{U_d}}{1 - \frac{m_B(B)a}{n}} B = \frac{n^2 b}{2U_d(n - m_B(B)a)} B. \tag{4.70}$$

Notice that time varying B implies that the phase angles r_n are not constant, which was the case in the constant speed, first harmonic model of Moore and Greitzer (1986) and the constant speed, higher order models of Adomatis and Abed (1993) and Gu et al. (1996).

4.3.8 Final Model

By evaluating the integrals in (4.69) using (4.60), demanding $M_1 = M_2 = 0$, and using (4.14) and (4.59), the following model for the compression system is found:

$$\frac{d\Phi}{d\xi} = \frac{H}{l_c(B)}\left(-\frac{\Psi - \psi_{c0}}{H} + 1 + \frac{3}{2}(\frac{\Phi}{W} - 1)(1 - \frac{J}{2})\right.$$
$$\left. -\frac{1}{2}(\frac{\Phi}{W} - 1)^3 - \frac{l_E U_d \Gamma \Lambda_1}{bH}\Phi\right) \tag{4.71}$$

$$\frac{d\Psi}{d\xi} = \frac{\Lambda_2}{B}(\Phi - \Phi_T) - 2\Lambda_1 \Gamma B \Psi \tag{4.72}$$

$$\frac{dJ_n}{d\xi} = J_n\left(1 - (\frac{\Phi}{W} - 1)^2 - \frac{J_n}{4} - \frac{\mu n^2 W}{3aH}\right.$$
$$\left. -\frac{2U_d \Gamma \Lambda_1(m-1)W}{3bHn}\right)\frac{3aHn}{(n - m_B(B)a)W} \tag{4.73}$$

$$\frac{dB}{d\xi} = \Lambda_1 \Gamma B^2 \tag{4.74}$$

where $n = 1 \ldots N(\mu)$, J_n is defined as the square of the stall amplitude A_n

$$J_n(\xi) \overset{\triangle}{=} A_n^2(\xi). \tag{4.75}$$

and

$$J(\xi) \overset{\triangle}{=} \frac{1}{N(\mu)}\sum_{n=1}^{N(\mu)} J_n(\xi). \tag{4.76}$$

The model (4.71)-(4.74) is in the desired form of (4.1).

In the case of pure rotating stall, $\frac{dJ_n}{d\xi} = 0$ and $\Gamma = 0$, the equilibrium values of J_n is found from (4.73) to be

$$J_{ne} = 4\left(1 - \left(\frac{\Phi}{W} - 1\right)^2 - \mu\frac{n^2 W}{3aH}\right), \tag{4.77}$$

which corresponds to the result by Gu *et al.* (1996).

If the Galerkin approximation is carried out with only one term in the Fourier expansion of $\tilde{\phi}'$ and assuming $\mu = 0$, as was done in Gravdahl and Egeland (1997a), equation (4.73) is changed to

$$\frac{dJ_1}{d\xi} = J_1\left(1 - (\frac{\Phi}{W} - 1)^2 - \frac{J_1}{4} - \frac{2U_d \Gamma \Lambda_1(m-1)W}{3bH}\right)\frac{3aH}{(1 - m_B(B)a)W}. \tag{4.78}$$

The rest of the model is left unchanged, and the model is similar to that of Moore and Greitzer except for time varying B.

It should be noted that the model developed in this chapter also can be reduced to other well known compression system models. This is summed up in table 4.2.

Changes made to (4.71)-(4.74)	Redefine nondim. time acc. to	Gives the model of
$U = U_d,\ \Gamma = 0$ $J \equiv 0,\ \frac{dB}{d\xi} = 0$ $N = 1,\ \mu = 0$	$\xi := \frac{Ut}{R}$	Greitzer (1976a)
$\Gamma = 0$ $\frac{dB}{d\xi} = 0,\ U = U_d$ $N = 1,\ \mu = 0$	$\xi := \frac{Ut}{R}$	Moore and Greitzer (1986)
$J \equiv 0$ $N = 1,\ \mu = 0$	$\xi := t\omega_H$	Fink et $al.$ (1992) (Centrifugal)
$N = 1,\ \mu = 0$	–	Gravdahl and Egeland (1997a)
$U = U_d,\ \Gamma = 0$ $\frac{dB}{d\xi} = 0$ $m = \lambda tanh(nl_I)$	$\xi := \frac{Ut}{R}$	Gu et $al.$ (1996)
$U = U_d,\ \Gamma = 0$ $\frac{dB}{d\xi} = 0$	$\xi := \frac{Ut}{R}$	Adomatis and Abed (1993)

Table 4.2: *In this table it is shown how the model derived in this chapter can be reduced to other known models form the literature. ω_H is the Helmholtz frequency defined as $\omega_H = a_s \left(\frac{A_c}{L_c V_p} \right)^{\frac{1}{2}}$.*

4.4   Simulations

Here some simulations of the model developed in this chapter will be presented. For speed control, a simple P-type controller of the form

$$\Gamma_t = c_{speed}(U_d - U), \tag{4.79}$$

will be used. The nondimensional drive torque Γ_t is used as the control, and feedback from compressor speed U is assumed. In Gravdahl and Egeland (1997f) compressor speed was controlled in a similar manner, and stability was proven using Lyapunov's theorem. The desired speed was set to $U_d = 215m/s$ in both the following simulations. Numerical values for the parameters in the model are given in Appendix E.

4.4.1 Unstable Equilibrium, $\gamma = 0.5$

In Figure 4.3, the response of the model (4.71)-(4.74) with speed control (4.79) and $c_{speed} = 1$ is shown. Only the first harmonic J_1 of rotating stall is included in this simulation. Initial values were chosen as

$$(\Phi, \ \Psi, \ J_1, \ B)_0 = (0.55, \ 0.65, \ 0.1, \ 0.1), \tag{4.80}$$

such that the (Φ, Ψ)-trajectory starts on the stable part of the compressor characteristic as can be seen in Figure 4.4.
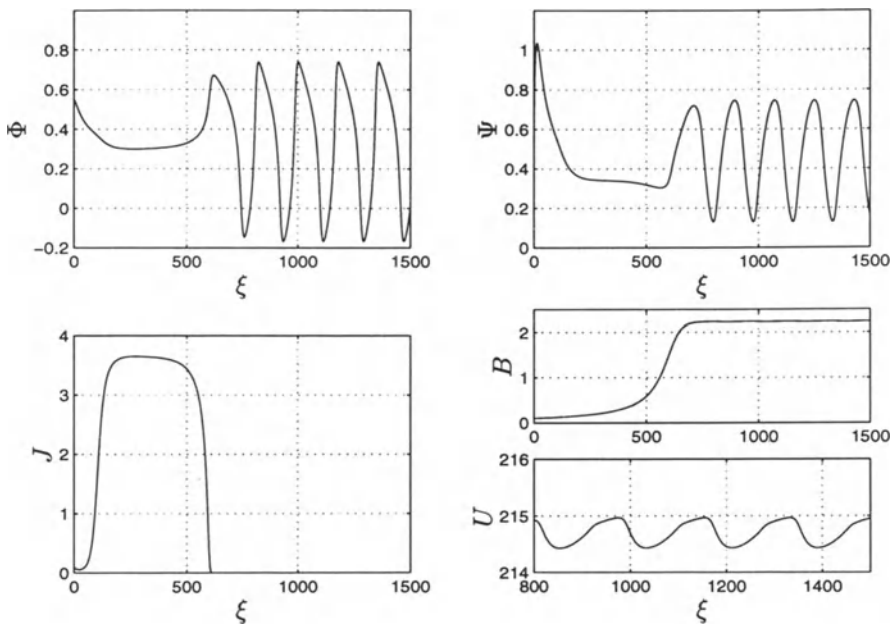
Figure 4.3: *Simulation of the system (4.71)-(4.74). Low B leads to rotating stall, and high B leads to surge.*

The throttle gain was set at $\gamma = 0.5$ so that the equilibrium is to the left of the local maximum of the characteristic. As can be seen from Figure 4.3, the compressor goes into rotating stall as B (and thus compressor speed U) is low. Moreover, when the applied torque from the speed controller cause B to increase, the stall amplitude J falls off and the compressor goes into surge. This is what could be expected according to Greitzer and Moore (1986). The surge oscillations have a period of $\xi \approx 180$, which correspond to a surge frequency of about 10Hz. A desired speed of $U_d = 215m/s$ corresponds to a desired B-parameter of $B_d = U_d/b = 2.23$. After $\xi \approx 1500$ this value is reached. As the compressor torque Γ_c varies with ϕ, see equation (4.21), we

would expect oscillations in speed U as the compressor is in surge. This is confirmed by the lower right plot in Figure 4.3. In the upper plot of Figure 4.4, the trajectory starts on the stable part of the characteristic, then rotating stall occurs and the trajectory approaches the intersection of the throttle and in-stall characteristics. As B increases, the resulting surge oscillations are clearly visible.
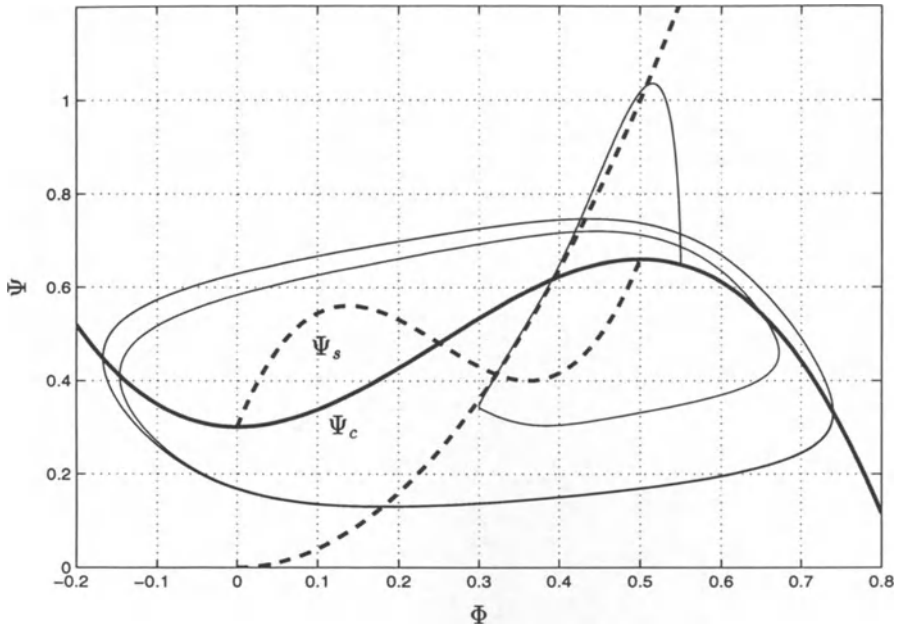
Figure 4.4: *Simulation result superimposed on the compression system characteristics. The compressor characteristic, the in-stall characteristic and the throttle characteristic are drawn with solid, dashed and dash-dot lines respectively.*

Now, the model is simulated using $N = 3$, that is three harmonics. Initial values were chosen as

$$(\Phi, \Psi, B, J_1, J_2, J_3)_0 = (0.55, 0.65, 0.1, 0.1, 0.05, 0.01). \qquad (4.81)$$

The upper plot in Figure 4.5 shows the response of the three first harmonics of the squared amplitude of rotating stall J_1, J_2 and J_3. The response is otherwise similar to that of Figure 4.3. The lower plot is a magnified version of the 200 first time units of the upper plot, and shows that during stall inception, the second harmonic J_2 dominates the first harmonic J_1. This emphasizes the importance of using higher order approximations of the Moore-Greitzer model. This phenomenon was also observed by Mansoux *et al.* (1994) for constant speed compressors.

The previous simulations have both used a desired speed of $U_d = 215m/s$ resulting in a high B-parameter and driving the compressor into surge. Now, the desired speed is changed to $U_d = 75m/s$ which corresponds to a B-parameter of 0.78. This is sufficiently low for the compressor studied here to become stuck in rotating stall. The simulation is shown in Figure 4.6 using three harmonics of the squared amplitude of rotating stall. The first harmonic J_1 has the highest equilibrium value. This equilibrium value decreases with mode number n due to the effect of viscosity, as stated in equation (4.77).
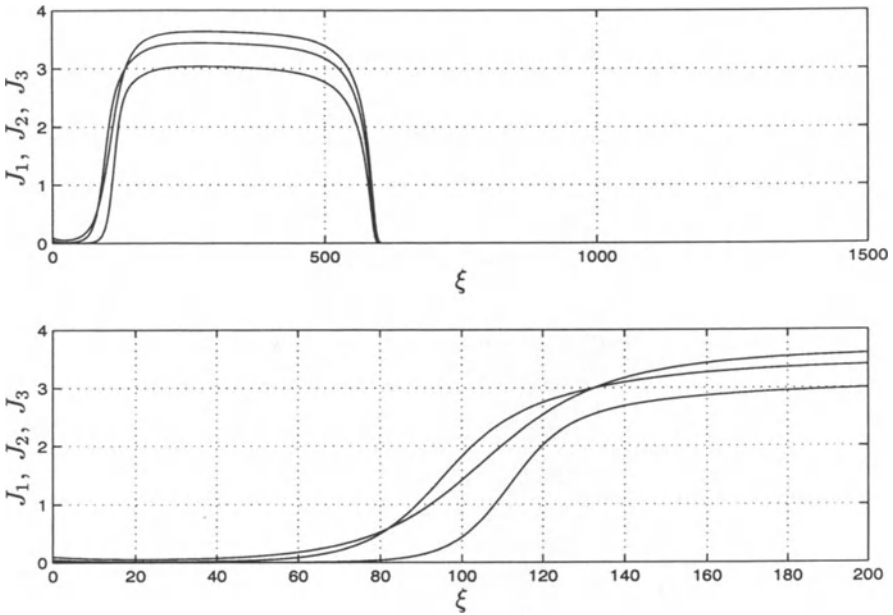
Figure 4.5: *The three first harmonics of rotating stall. The first harmonic J_1 has the highest maximum value. This maximum value decreases with mode number du to the effect of viscosity. The lower plot shows that J_2 dominates J_1 during stall inception.*

4.4.2 Stable Equilibrium $\gamma = 0.65$

In Figure 4.7, the impact of the spool dynamics on a stable equilibrium of the compression system is illustrated. Only J_1 is used in this simulation, and the initial values in (4.80) were used. Similar plots can be produced also if higher harmonics are included. The throttle gain was set at $\gamma = 0.65$, giving a stable equilibrium, and the speed controller gain was again chosen as $c_{speed} = 1$. The solid trajectories show the system response to a speed change
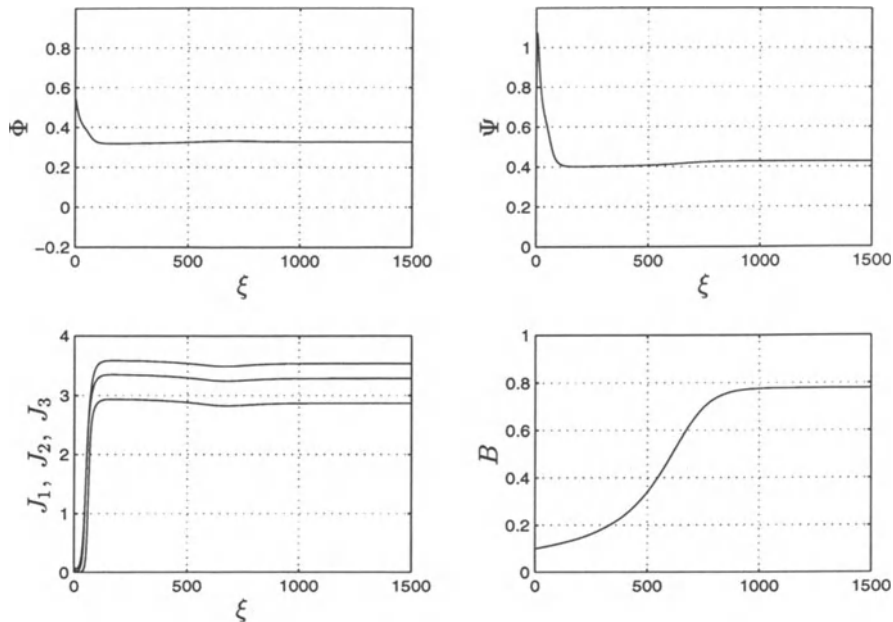
Figure 4.6: *System response with low U_d, resulting in the compressor being stuck in rotating stall.*

from $U = 0.05m/s$ to $U = 215m/s$. It can be seen that the acceleration of U affects the other states of the model. This is due to the couplings with speed U and torque Γ in the model. Of special interest here, is the stall amplitude. The initial value of $J(0) = 0.05$ grows to nearly fully developed rotating stall as the machine is accelerating, but is quickly damped out as desired speed is reached. In Figure 4.8, the response is plotted together with the compressor and throttle characteristics, and the transient caused by the acceleration can easily be seen.

Simulations show that this stalling can be avoided by accelerating the compressor at a lower rate, that is by using a smaller c_{speed}. Tøndel (1996) used a low pass filtered velocity reference in order to achieve slow enough acceleration to avoid stall. This could possibly also be achieved with other, more advanced speed controllers, and is a topic for further research.

In contrast, the dashed trajectories in Figure 4.7 show the response without the spool dynamics. Now, the initial value $J(0) = 0.05$ is damped out very quickly, and Φ and Ψ converge to their equilibrium values. The transient effects observed are due to the initial conditions.
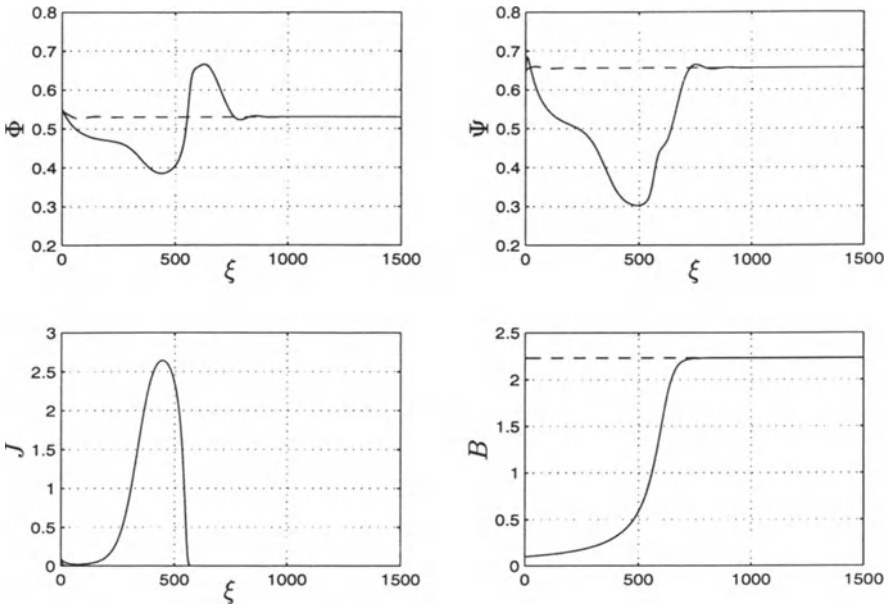
Figure 4.7: *Stable equilibrium with and without B-dynamics*
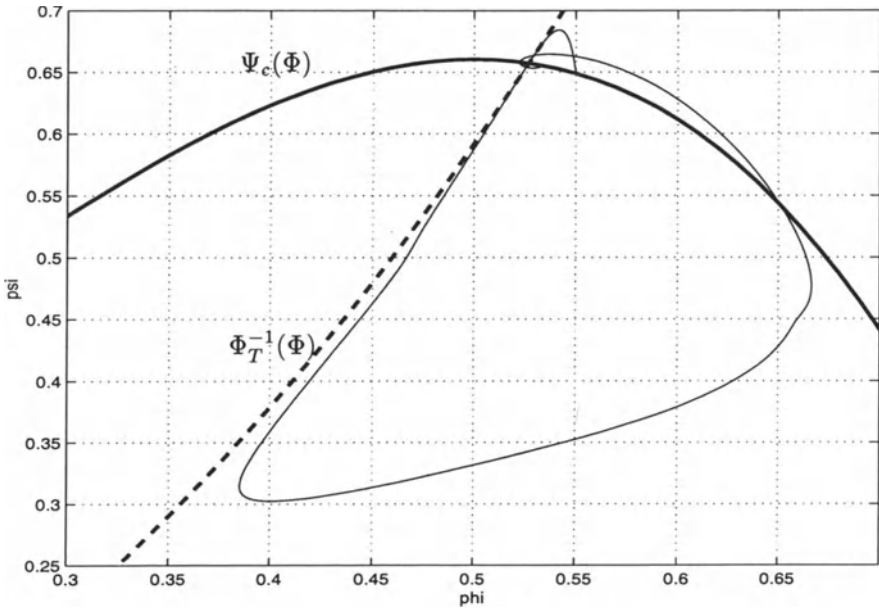
Figure 4.8: *Effect of acceleration plotted on the compressor characteristic*

4.5   Concluding Remarks

In this Chapter, a multi mode Moore-Greitzer axial compressor model with spool dynamics was derived. This resulted in a model with time varying B-parameter. Through simulations it was demonstrated that the model was capable of demonstrating both rotating stall and surge, and that the type of instability depended on the compressor speed. Compressor speed was controlled with a simple proportional control law. In the original Moore Greitzer model, only the first mode of rotating stall was included. The simulations in this chapter show that during stall inception, higher order modes can dominate the first mode. This is in accordance with known results, and is shown here to be valid also for variable speed compressors.

Further work on this topic includes:

1. Stability analysis and stall/surge control design for variable speed axial compressors and

2. The use of simultaneous speed control and stall/surge control to achieve rapid acceleration without stalling the compressor.

CHAPTER 5

MODELLING AND CONTROL OF SURGE FOR A CENTRIFUGAL COMPRESSOR WITH NON-CONSTANT SPEED

5.1   Introduction

In this Chapter the compressor characteristic for a variable speed centrifugal compressor is investigated. This characteristic is incooperated in a model similar to that of Fink *et al.* (1992), and surge phenomena is studied in connection with varying compressor speed. Energy losses in the compressor components are used to derive the characteristic, making a departure from the usual cubic characteristic most commonly encountered in the surge control literature. Inspired by Ferguson (1963) and Watson and Janota (1982), fluid friction and incidence losses, as well as other losses, in the compressor components are modeled, and a variable speed compressor characteristic is developed based on this. Both annular and vaned diffusers are studied. Surge and speed controllers for variable speed centrifugal compressors are presented and analyzed. The speed is controlled with a PI-control law.

Axial and centrifugal compressors mostly show similar flow instabilities, but in centrifugal compressors, the matching between components, such as impeller and diffuser, influences the stability properties. According to Emmons *et al.* (1955), de Jager (1995) and others, rotating stall is believed to have little effect on centrifugal compressor performance. The modeling and analysis
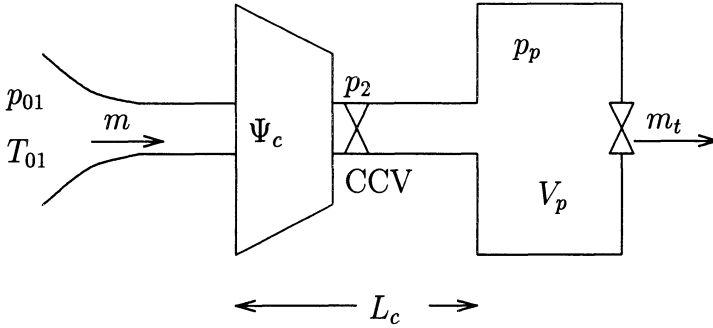
Figure 5.1: *Compression system with CCV.*

in this Chapter is thus restricted to surge. Hansen *et al.* (1981) showed that the model of Greitzer (1976*a*) is also applicable to centrifugal compressors, and this model will also be used here.

Since compressors are variable speed machines, it is of interest to investigate the influence of speed transients on the surge dynamics. Models describing this interaction were developed in Eveker and Nett (1991) for axial compressors and in Fink *et al.* (1992) for centrifugal compressors. As surge can occur during acceleration of the compressor speed, it is of major concern to develop controllers that simultaneously can control both surge and compressor speed.

For surge control, the CCV is again employed. Semi-global exponential stability results for the proposed controllers are given using Lyapunovs method. The results are confirmed through simulations.

5.2   Model

We are considering a compression system consisting of a centrifugal compressor, close coupled valve, compressor duct, plenum volume and a throttle. The throttle can be regarded as a simplified model of a turbine. The system is shown in Figure 5.1. The model, which will be developed in this Chapter, and is to be used for controller design has the following structure:

$$
\begin{aligned}
\dot{p}_p &= \frac{a_{01}^2}{V_p}\left(m - m_t\right)\\
\dot{m} &= \frac{A_1}{L_c}\left(p_2 - p_p\right)\\
\dot{\omega} &= \frac{1}{I}\left(\tau_t - \tau_c\right),
\end{aligned}
\tag{5.1}
$$

where m is the compressor mass flow, p_p is the plenum pressure, p_2 is the pressure downstream of the compressor, a_{01} is the inlet stagnation sonic velocity, L_c is the length of compressor and duct, A_1 is the area of the impeller eye (used as reference area), I is the spool moment of inertia, τ_t is the drive torque and τ_c is the compressor torque. The two first equations of (5.1) are equivalent to the model of Greitzer (1976a) which was also used in Chapter 2 and 3, whereas the whole model (5.1) is similar to the model of Fink *et al.* (1992). It should also be noted that models similar to (5.1) are used in modeling the compressor in internal combustion engine turbochargers, see Foss *et al.* (1989). In the turbocharger case, p_p would be the intake manifold or intercooler pressure. In addition to the assumptions used in the derivation of model of Greitzer (1976a), it is now assumed that the gas angular momentum in the compressor passages is negligible compared to rotor angular momentum.

Note that in the model used throughout this chapter, the states are *with* dimension, as opposed to the previous chapters, where nondimensional states were used. This is due to the fact that the normalization usually employed in the turbomachinery literature involves division with the compressor speed U, see Appendix C. As U is taken to be time varying in this Chapter, this normalization will produce additional nonlinear terms in the model. By inspecting the model (4.71)-(4.74) in the preceding Chapter, one can see that the normalization was responsible for introducing the nonlinear term in the differential equation for the pressure rise coefficient Ψ, and also for the quadratic term in B in the differential equation for B. This was also done in the model developed by Fink *et al.* (1992), and would happen to the model in this Chapter if normalization was to be used. As the model we are developing in this Chapter is to be used for controller design and stability analysis, it is desirable to keep the model as simple as possible in order to reduce the complexity of the analysis. Therefore, a model with dimensions is used.

The angular speed of the compressor ω is included as a state in addition to mass flow and pressure rise which are the states in Greitzer's surge model. The equation for $\dot{p}_p$ follows from the mass balance in the plenum, assuming the plenum process isentropic, the derivation is shown in Appendix C. The equation for $\dot{m}$ follows from the impulse balance in the duct. In the following, the model (5.1) will be developed in detail. In particular, expressions must be found for the terms p_2 and τ_c. It will also be shown that an expression for the compressor characteristic results from this derivation.

The calculation of the compressor pressure rise will be based on energy transfer and energy losses in the various parts of the compressor. In the following Sections, the different components of the centrifugal compressor will be studied. The centrifugal compressor consists essentially of a rotating impeller which imparts a high velocity to the gas, and a number of fixed diverging passages in which the gas is decelerated with a consequent rise in static pres-

sure. A schematic drawing of a compressor is shown in Figure 1.3. The innermost part of the impeller is known as the inducer, or the impeller eye, where the gas is sucked into the compressor. The part of the compressor containing the diverging passages is known as the diffuser. The diffuser can be vaned, as in Figure 1.3, or vaneless. A vaneless diffuser (also known as an annular diffuser) is a simple annular channel with increasing cross-sectional area. The choice of diffuser type depends on the application of the compressor. After leaving the diffuser, the gas may be collected in a volute (also known as a scroll), as shown in Figure 1.4.

The energy transfer *to* the gas takes place in the impeller. In the ideal case, this energy is converted into a pressure rise. However, a number of losses occur in the compressor, the main ones being friction losses and incidence losses in the impeller and the diffuser. These losses shape the compressor characteristic, and the incidence losses are the cause of the positive slope of the characteristic, which in turn determines the area of the compressor characteristic where surge occurs. Therefore, these components will be studied in detail in the following. A number of other losses, e.g. losses in the volute, are taken into account as drops in efficiency.

The modeling using friction and incidence losses assumes that the mass flow m is positive, that is deep surge with flow reversal is not taken into account during the development of the model. However, some modifications are made in Section 5.4 so that the final model also covers the case of deep surge.

5.2.1 Impeller

Incoming gas (air) enters the impeller eye (the inducer) of the compressor with absolute velocity C_1, see Figure 5.2. The mass flow m and C_1 is given by

$$C_1 = \frac{1}{\rho_{01} A_1} m, \qquad (5.2)$$

where ρ_{01} is the constant stagnation inlet density. The tangential velocity U_1, at diameter D_1, of the inducer is calculated as

$$U_1 = \frac{D_1}{2}\omega = D_1 \pi N, \qquad (5.3)$$

where ω is the angular velocity of the impeller and N is the number of revolutions per second. The average diameter D_1 is defined according to

$$D_1^2 = \frac{1}{2}(D_{t1}^2 + D_{h_1}^2), \qquad (5.4)$$

where D_{t1} and D_{h_1} are the diameters at inducer tip and hub casing respectively. The circle with diameter D_1 and area A_1 divides the inducer in two
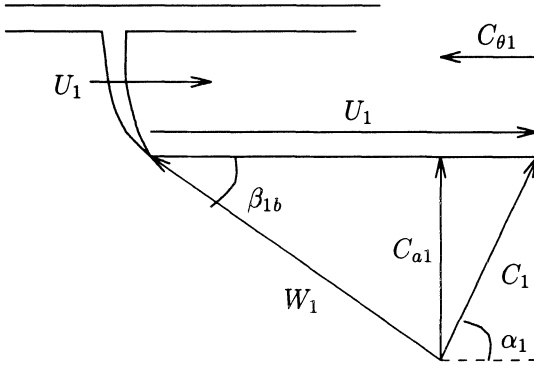
Figure 5.2: *Velocity triangle at inducer. Section through inducer at radius* $r_1 = D_1/2$.

annuli of equal area. The axial component of C_1 is C_{1a} and the velocity relative to the blades is W_1. From Figure 5.2 it is seen that the gas velocity W_1 relative to the impeller is

$$W_1^2 = C_1^2 + U_1^2 - 2U_1 C_{\theta 1}. \tag{5.5}$$

At the impeller tip, the gas leaves the impeller with velocity C_2 and flow angle α_2 as shown in Figure 5.3. The diameter at the impeller tip is D_2, the tangential tip velocity is U_2, the axial component of C_2 is C_{2a} and the gas velocity relative to the rotor blades is W_2. The constant angle β_{2b} is known as the backsweep angle. However, the flow angle β_2 usually deviates from β_{2b} due to slip, a phenomenon described in Section 5.3.2.
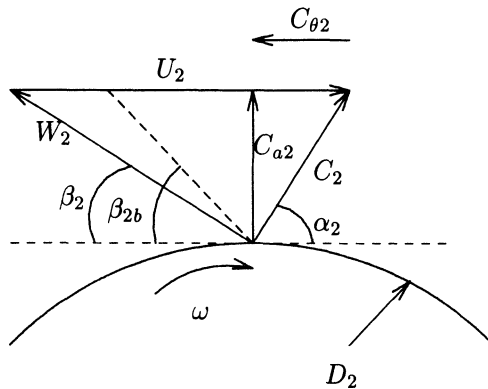
Figure 5.3: *Velocity triangle at impeller tip.*

5.2.2 Diffuser

Centrifugal compressors are usually fitted with either a vaneless (annular) or a vaned diffuser. The influence of the diffuser upon compressor performance cannot be over emphasized, as a considerable proportion of the fluid energy at the impeller tip is kinetic energy and its efficient transformation into static pressure is important (Ferguson 1963).

Annular Diffuser

The annular diffuser is a simple annular channel in which the fluid loses velocity and gains static pressure. One disadvantage of the annular diffuser is its size, as its outlet radius must be twice its inlet radius if the velocity is to be halved in it (Ferguson 1963). Its advantages are its price and wide range of operation.

Vaned Diffuser

In a vaned diffuser, vanes are used to guide the flow so that he overall rate of diffusion is higher than in an annular diffuser. This leads to a smaller size, but higher production costs. The vaned diffuser has a higher efficiency but less mass flow range than the annular diffuser. This is due to stalling of the diffuser vanes for low mass flows.

5.3 Energy Transfer

5.3.1 Ideal Energy Transfer

For turbomachines, applied torque equals the change in angular momentum of the fluid:

$$\tau_c = m(r_2 C_{\theta 2} - r_1 C_{\theta 1}), \qquad (5.6)$$

where τ_c is the compressor torque, $r_1 = \frac{D_1}{2}$, $r_2 = \frac{D_2}{2}$ and $C_{\theta 2}$ is the tangential component of the gas velocity C_2. Power delivered to the fluid is

$$
\begin{aligned}
\dot{W}_c &= \omega \tau_c = \omega m(r_2 C_{\theta 2} - r_1 C_{\theta 1}) \\
&= m(U_2 C_{\theta 2} - U_1 C_{\theta 1}) = m \Delta h_{0c,ideal}
\end{aligned}
\qquad (5.7)
$$

where $\Delta h_{0c,ideal}$ is the specific enthalpy delivered to the fluid without taking account for losses. Equation (5.7) is known as Euler's pump equation. An alternative form of the Euler equation can be found by combining

$$W_j^2 = C_j^2 + U_j^2 - 2U_j C_j, \quad j = 1, 2, \qquad (5.8)$$

which is found from Figure 5.2 and Figure 5.3, with (5.7), which results in

$$\dot{W}_c = \underbrace{\frac{1}{2}m(C_2^2 - C_1^2)}_{E_1} + \underbrace{\frac{1}{2}m(U_2^2 - U_1^2)}_{E_2} + \underbrace{\frac{1}{2}m(W_1^2 - W_2^2)}_{E_3}. \qquad (5.9)$$

According to Watson and Janota (1982) this formulation throws light on the nature of the energy transfer and the mechanism of pressure rise in the compressor. The term E_1 represents the change in absolute kinetic energy occuring in the impeller. The term E_2 represents the change of energy due to the movement of the rotating gas from one radius of rotation to another. This is the centrifugal energy which raises the static pressure in the impeller. The term E_3 represents the change in kinetic energy due to the change of relative velocity, resulting in a further change of static pressure within the rotor.

Following Watson and Janota (1982), the effect of the backsweep angle β_{2b} on the energy transfer can be shown as follows. From Figure 5.3 it can be seen that

$$C_{\theta 2} = U_2 - C_{a2} \cot \beta_{2b}. \qquad (5.10)$$

It now follows from (5.7) that

$$\Delta h_{0c,ideal} = \left(1 - \frac{C_{a2}}{U_2} \cot \beta_{2b}\right) U_2^2 \triangleq \mu_e U_2^2, \qquad (5.11)$$

where μ_e is known as the energy transfer coefficient.
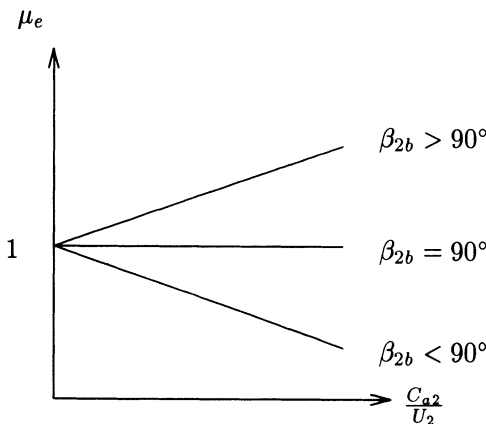
Figure 5.4: *Effect of β_{2b} and $\frac{C_{a2}}{U_2}$ on energy transfer.*

The energy transfer coefficient relates energy transfer to the energy achievable with a radial vaned impeller of the same diameter. For the *ideal* radial vaned

impeller, $\mu_e = 1$. For a given value of β_{2b} there is a linear relationship between μ_e and $\frac{C_{a2}}{U_2}$. This is shown in Figure 5.4. As can be seen, if backswept impeller blades, $\beta_{2b} < 90°$, were considered, $\Delta h_{0c,ideal}$ would decrease with increasing m. This has the effect of enlarging the range of mass flows over which the compressor can operate without going into surge. This will be discussed in more depth in Section 5.4.

For simplicity the following two assumptions are made:

1. A radially vaned (no backsweep) impeller is considered with $\beta_{2b} = 90°$, and

2. There is no pre-whirl, that is $\alpha_1 = 90° \Rightarrow C_{\theta 1} = 0$.

The assumption of no backsweep will be used in order to simplify the analysis, and $\beta_{2b} \neq 90°$ can easily be taken into account.

5.3.2 Slip

For an ideal radially vaned impeller, the whirl or tangential component of the gas velocity leaving the impeller tip should equal U_2. However, due to the inertia of the gas between the impeller blades, the tangential gas velocity tends to be less than U_2. This effect is known as *slip*. The flow is deflected away from the direction of rotation of the impeller, which it leaves at an angle smaller than the vane angle as shown in Figure 5.5.
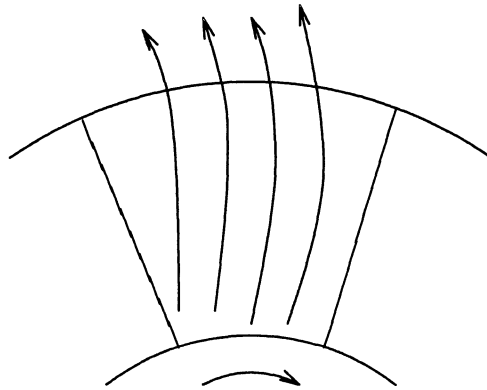
Figure 5.5: *Slip: Relative flow through impeller.*

The slip factor is defined as

$$\sigma \triangleq \frac{C_{\theta 2}}{U_2},\qquad(5.12)$$

and is a positive number less than unity. The slip factor depends largely on the number of impeller blades, but also on the passage geometry, the impeller eye tip to exit diameter ratio and mass flow rate. There exist many approximations for the slip factor, the one appropriate to radial vaned impeller which seems to agree best with experiment is that due to Stanitz:

$$\sigma \approx 1 - \frac{0.63\pi}{i} \approx 1 - \frac{2}{i},\qquad(5.13)$$

where i is the number of impeller blades. Other expressions for the slip factor are

$$\frac{1}{\sigma} \approx 1 + \frac{6.2e^{\frac{2}{3}}}{i}\qquad(5.14)$$

of Baljé (1952), and the Stodola slip factor

$$\sigma \approx 1 - \frac{\pi}{i}\frac{\sin\beta_{2b}}{1 - \frac{C_{2a}}{U_2}\cot\beta_{2b}},\qquad(5.15)$$

which also covers non radially vaned impellers. Ferguson (1963) concludes that the Stanitz slip factor agrees remarkably well with experiments for radially vaned impellers.

From (5.7), and using (5.12), we have that the ideal specific enthalpy delivered to the fluid is

$$\Delta h_{0c,ideal} = \frac{\dot{W}_{c,ideal}}{m} = \sigma U_2^2.\qquad(5.16)$$

Notice that as a consequence of the choice $\alpha_1 = \beta_{2b} = 90°$, we have that $\Delta h_{0c,ideal}$ is independent of mass flow m, and ideally we would have the same energy transfer for all mass flows. However, due to various losses, the energy transfer will not be constant, and this will now be included in the analysis.

According to Watson and Janota (1982), Ferguson (1963), Nisenfeld (1982) and other authors, the two major losses in centrifugal compressors, expressed as specific enthalpies, are:

1. Incidence losses in impeller and diffuser, Δh_{ii} and Δh_{id}

2. Fluid friction losses in impeller and diffuser, Δh_{fi} and Δh_{fd}

The incidence losses and fluid friction losses play an important role in determining the region of stable operation for the compressor. Other losses, such as back flow losses, clearance losses and losses in the volute will be taken into

account when computing the efficiency of the compressor. There also exist other losses such as inlet casing losses, mixing losses and leakage losses, but these will be ignored in the following. For a further treatment on this topic, some references are Baljé (1952), Johnston and Dean (1966), Whitfield and Wallace (1975) and Cumpsty (1989).

5.3.3   Compressor Torque

Using the assumption of no pre whirl and equation (5.6), the compressor torque is

$$\tau_c^+ = mr_2 C_{\theta 2} = mr_2 \sigma U_2, \; m > 0. \tag{5.17}$$

The torque calculated in (5.17) is for forward flow. However, the compressor may enter deep surge, that is reversal of flow, and there is need for an expression for the compressor torque at negative mass flow. According to Koff and Greitzer (1986), an axial compressor in reversed flow can be viewed as a throttling device. Here it is assumed that a centrifugal compressor in reversed flow can be approximated with a turbine. This allows for the use of Euler's turbine equation:

$$\tau_c^- = m(r_1 C_{\theta 1} - r_2 C_{\theta 2}) = -mr_2 \sigma U_2, \; m < 0. \tag{5.18}$$

Combination of (5.17) and (5.18) gives

$$\tau_c = |m| r_2 \sigma U_2, \; \forall m \tag{5.19}$$

which is in accordance with the compressor torque used by Fink *et al.* (1992).

Disc Friction Torque

The torque set up by the rotation of the impeller in a fluid is modeled as rotation of a disc. When a disc is rotated in a fluid, a resistive torque is set up given by

$$\tau_{df} = 2 \int_{r_1}^{r_2} \tau_{tan} 2\pi r^2 dr, \tag{5.20}$$

where r_1 is the radius of the shaft, r_2 is the radius of the disc and τ_{tan} is the tangential component of the shear stress between the disc and fluid. According to Ferguson (1963) the torque can be approximated by

$$\tau_{df} = \frac{C_m \rho r_2^5 \omega^2}{2} = \frac{2 C_m \rho r_2^5}{D_1^2} U_1^2 \tag{5.21}$$

where C_m is a torque coefficient depending on the disc Reynolds number and the space between the disc and the casing, ρ is the density of the fluid and ω is the angular velocity of the disc. In (5.21) it has been assumed that $r_1 \ll r_2$.

5.3.4 Incidence Losses

The losses due to incidence onto the rotor and vaned diffuser play an important role in shaping the compressor characteristic. There exist several methods of modeling this loss, and a comparative study is given by Whitfield and Wallace (1973). The two most widely used approaches are:

(1) The so called "NASA shock loss theory"[1] reported in Futral and Wasserbauer (1965), Whitfield and Wallace (1973) and Watson and Janota (1982), which is based upon the tangential component of kinetic energy being destroyed.

(2) A constant pressure incidence model reported by Whitfield and Wallace (1973) where it is assumed that the flow just inside the blades has adapted to the blades via a constant pressure process.

Watson and Janota (1982) conclude that for centrifugal compressors, the differences between the two models are small. According to Whitfield and Wallace (1973), the main difference lies in the prediction of the incidence angle at which zero loss occurs. For model (1) zero loss is predicted when the flow angle at the inlet equals the blade angle. This is not the case for model (2). Based on this, and the simplicity of (1), the NASA shock loss theory is used here. As Ferguson (1963) points out, the term shock loss is misleading as nothing akin to shock occurs in practice, but the simple notion of shock is used to explain the shape of the compressor characteristic.

Depending on whether the mass flow is lower or higher than the design flow, positive or negative stall is said to occur. The use of model (2) leads to a loss varying with the square of the mass flow, symmetrical about the design flow. Ferguson (1963) states that the incidence loss in practice increase more rapidly with reduction of flow below design flow, than with increase of flow above the design flow. This leads to a steeper compressor characteristic below the design point than above. According to Sepulchre and Kokotović (1996) and Wang and Krstić (1997b), such a characteristic is said to be right skew.

Impeller

The velocity of the incoming gas relative to the inducer is denoted W_1. In off-design operation there will be a mismatch between the *fixed* blade angle β_{1b} and the direction of the gas stream $\beta_1 = \beta_1(U_1, C_1)$, as shown in Figure 5.6. The angle of incidence is defined by

$$\beta_i \stackrel{\triangle}{=} \beta_{1b} - \beta_1. \tag{5.22}$$

---

[1] The name stems from the report Futral and Wasserbauer (1965), where the method was used for predicting the off-design performance of radial turbines.
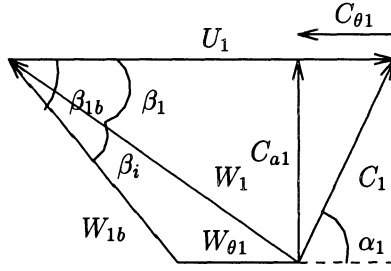
Figure 5.6: *Incidence angles at inducer.*

As the gas hits the inducer, its velocity instantaneously changes its direction to comply with the blade inlet angle β_{1b}. The direction is changed from β_1 to β_{1b}, and the kinetic energy associated with the tangential component $W_{\theta 1}$ of the velocity is lost. That is, the incidence loss can be expressed as

$$\Delta h_{ii} = \frac{W_{\theta 1}^2}{2}. \tag{5.23}$$

The incidence loss model in equation (5.23) is a simple one-dimensional model. According to Ferguson (1963), it approximates the loss owing to boundary-layer build-up for low angles of incidence and the increased losses resulting from flow separation at higher angles of incidence. Beyond a critical incidence angle the flow can no longer adhere to the suction side of the blade. Flow separation from the surface creates a stall condition subsequently encouraging reversal of flow (Watson and Janota 1982). From Figure 5.6 it is easily seen that

$$\cos \beta_1 = \frac{U_1 - C_{\theta 1}}{W_1} \quad \text{and} \quad \sin \beta_1 = \frac{C_{a1}}{W_1}. \tag{5.24}$$

Furthermore,

$$W_{\theta 1} = \frac{\sin(\beta_{1b} - \beta_1)}{\sin \beta_{1b}} W_1 = (\cos \beta_1 - \cot \beta_{1b} \sin \beta_1) W_1. \tag{5.25}$$

Inserting (5.24) in (5.25) gives

$$W_{\theta 1} = U_1 - C_{\theta 1} - \cot \beta_{1b} C_{a1}. \tag{5.26}$$

and the incidence loss (5.23) can be written

$$\Delta h_{ii} = \frac{1}{2} \left(U_1 - C_{\theta 1} - \cot \beta_{1b} C_{a1} \right)^2 = \frac{1}{2} \left(U_1 - \frac{\cot \beta_{1b} m}{\rho_{01} A_1} \right)^2 \tag{5.27}$$

where the second equality if found using (5.2) and the assumption of no pre-whirl, $\alpha_1 = 90°$. Similar results are presented in Chapter 5 in Ferguson (1963).
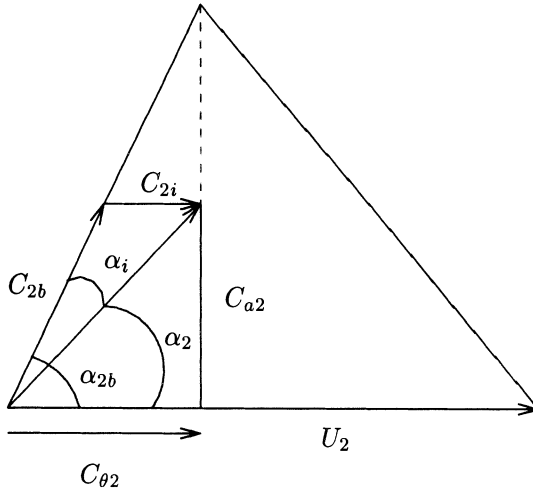
Figure 5.7: *Incidence angles at diffuser.*

Diffuser

According to Watson and Janota (1982), the losses in the vaned diffuser can be modeled with friction/incidence losses in a similar manner as in the impeller. Similar to the inducer incidence loss, it is assumed that the velocity of the fluid entering the diffuser is instantaneously changed to comply with the fixed diffuser inlet angle α_{2b}. The direction is changed from α_2 to α_{2b}, and the kinetic energy associated with the tangential component C_{2i} of the velocity is lost, see Figure 5.7. That is, the incidence loss can be expressed as

$$\Delta h_{id} = \frac{C_{2i}^2}{2}. \tag{5.28}$$

Using Figure 5.7 it is seen that

$$
\begin{aligned}
\Delta h_{id} &= \frac{1}{2} \left(C_{\theta 2} - \cot \alpha_{2b} C_{a2} \right)^2 \\
&= \frac{1}{2} \left(\sigma U_2 - \cot \alpha_{2b} C_{a2} \right)^2. \tag{5.29}
\end{aligned}
$$

For simplicity the choice[2] $C_{a1} = C_{a2}$ is made. The diffuser inlet angle α_{2b}, is now designed such that there is minimum incidence loss in both impeller and diffuser for the same mass flow m. For $\beta_i = 0$, we have that

$$U_1 = C_{a1} \cot \beta_{1b} \quad \Rightarrow \quad C_{a2} = U_1 \tan \beta_{1b}. \tag{5.30}$$

---

[2]This is a design choice, and other choices will lead to different expression for the diffuser angle α_{2b}

From Figure 5.7 and (5.30), it follows that

$$\tan \alpha_{2b} = \frac{C_{a2}}{C_{\theta 2}} = \frac{U_1 \tan \beta_{1b}}{\sigma U_2} \tag{5.31}$$

and

$$\alpha_{2b} = \text{atan}\left(\frac{D_1 \tan \beta_{1b}}{\sigma D_2}\right), \tag{5.32}$$

and consequently the diffuser incidence loss (5.29) can be written

$$\Delta h_{id} = \frac{1}{2}\left(\frac{\sigma D_2 U_1}{D_1} - \frac{m \cot \alpha_{2b}}{\rho_{01} A_1}\right)^2. \tag{5.33}$$

5.3.5 Frictional Losses

Impeller

According to Ferguson (1963) loss due to friction can be calculated as

$$\Delta h_{fi} = C_h \frac{l}{D} \frac{W_{1b}^2}{2}, \tag{5.34}$$

where C_h is the surface friction loss coefficient,[3] l is the mean channel length and D is the mean hydraulic channel diameter. This friction loss is actually calculated for constant area pipes of circular cross-section. The friction loss coefficient C_h is defined as in Watson and Janota (1982):

$$C_h = 4f, \tag{5.35}$$

where the friction factor f depends on the Reynolds number. Many different formulas for the friction factor have been published, see e.g. Ferguson (1963) or White (1986). Here we will use Blasius' formula:

$$f = 0.3164(Re)^{-0.25}. \tag{5.36}$$

According to White (1986), (5.36) was found empirically for turbulent flow in smooth pipes with Reynolds number Re below 100.000. The mean hydraulic channel diameter D is defined as

$$D = \frac{4A}{a}, \tag{5.37}$$

where the cross-section area A and perimeter a are mean values for the passage. The mean hydraulic diameter D corresponds to a circle with area A

---

[3]The friction loss considered here is due to friction in the impeller. According to Watson and Janota (1982) diffusion losses in the impeller are small compared to impeller friction losses, but they may be included in the analysis by choosing C_h to suit.

and perimeter a. Although the passages between the blades in the compressor are neither circular nor of constant area, Baljé (1952) reports of good agreement between theory and measurement using (5.36).

Using Figure 5.6, it is seen that

$$\frac{W_{1b}}{\sin \beta_1} = \frac{W_1}{\sin \beta_{1b}}, \tag{5.38}$$

and using $\sin \beta_1 = \frac{C_{a1}}{W_1}$ we get

$$W_{1b} = \frac{C_1}{\sin \beta_{1b}}. \tag{5.39}$$

Inserting (5.2) and (5.39) in (5.34) gives

$$\Delta h_{fi} = \frac{C_h l}{2D\rho_1^2 A_1^2 \sin^2 \beta_{1b}} m^2 = k_{fi} m^2. \tag{5.40}$$

As can be seen the friction losses are quadratic in mass flow and independent of wheel speed U. Equation (5.40) represents the loss due to friction of a mass flow m through a pipe of hydraulic diameter D.

Diffuser

The loss due to fluid friction in the diffuser can be modeled in a similar manner as in the impeller:

$$\Delta h_{fd} = k_{fd} m^2. \tag{5.41}$$

In the vaned diffuser a pipe friction loss is calculated for each diffuser passage.

5.3.6 Efficiency

The isentropic efficiency of the compressor is defined as, see e.g. Cumpsty (1989) or any other text on turbomachinery,

$$\eta_i(m, U_1) = \frac{\Delta h_{0c,ideal}}{\Delta h_{0c,ideal} + \Delta h_{loss}}. \tag{5.42}$$

where the Δh_{loss}-term is the sum of the friction and incidence losses from the previous sections. Furthermore, the efficiency will be corrected with losses in the volute and the additional losses arising from clearance and back-flow. The efficiency is also dependent on the ability of the diffuser to convert the

kinetic energy of the flow into pressure. Collection the various losses, the isentropic efficiency from equation (5.43) is adjusted to

$$\eta_i(m, U_1) = \frac{\Delta h_{0c,ideal}}{\Delta h_{0c,ideal} + \Delta h_{loss}} - \Delta \eta_{bf} - \Delta \eta_c - \Delta \eta_v - \Delta \eta_d, \qquad (5.43)$$

where

$$\Delta h_{loss} = \Delta h_{if} + \Delta h_{ii} + \Delta h_{df} + \Delta h_{di}. \qquad (5.44)$$

The additional losses are discussed below. In Figure 5.8, the efficiency is plotted. In the upper plot, the compressor is equipped with a vaned diffuser and in the lower plot with an annular diffuser. As can be seen, the vaned diffuser offer a higher efficiency, but a narrower range of flow compared with the annular diffuser.
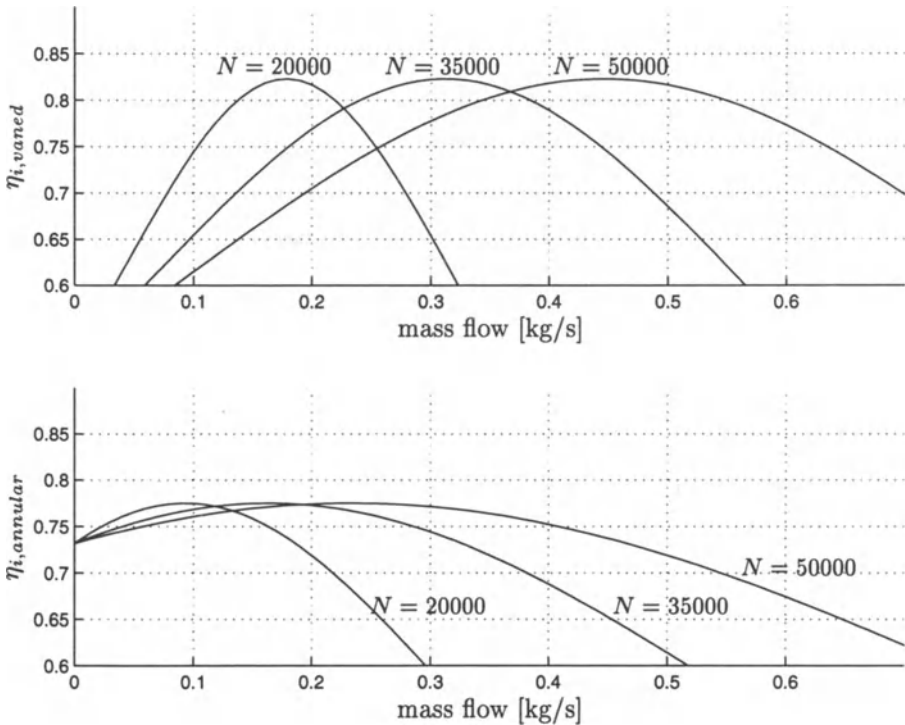
Figure 5.8: *Efficiencies for compressor with vaned (upper plot) and annular (lower plot) diffuser. The compressor speed N is given in [rpm].*

Clearance

Cohen *et al.* (1996) state that owing to the action of the vanes in carrying the gas around with the impeller, there will be a slightly higher pressure on

the forward face of a vane than on the trailing face. The gas will tend to flow round the edges of the vanes in the clearance space between the impeller and the casing. Pampreen (1973) found that the clearance loss of a centrifugal compressor can be approximated by

$$\Delta\eta_c = 0.3\frac{l_{cl}}{b},\qquad(5.45)$$

where l_{cl} is the axial clearance and b is the impeller tip width. As can be seen the clearance loss increases with with clearance. Other approximate expressions for this loss are reported by Cumpsty (1989). A shroud attached to the vanes would reduce the clearance loss, but at the same time it would introduce higher friction losses. Due to this, and increased manufacturing difficulties, shrouds are not used on impellers for gas turbines, but they have been used on turbo chargers, according to Cohen *et al.* (1996).

Back-flow

The back-flow loss occurs because the compressor has to reprocess the gas that has been reinjected into the impeller due to pressure gradients existing in the impeller tip region. Watson and Janota (1982) states that unfortunately, no theory or mathematical model exists to describe the backflow loss, which ideally should be treated as another aerodynamic design parameter. Due to the lack of accurate modeling of this loss, Watson and Janota (1982) suggest a loss of 3 points of efficiency as typical:

$$\Delta\eta_{bf} = 0.03.\qquad(5.46)$$

Watson and Janota (1982) also reports of a result by Coppage et.al. (1956) who recommended the following expression for the back flow loss:

$$\Delta\eta_{bf} = 0.02\sqrt{\frac{C_{\theta 2}}{C_{r2}}}D_f^2 U_2^2,\qquad(5.47)$$

where D_f is a diffusion factor.

Volute

In the volute, a loss will take place mainly due to the inability of the volute to use the radial kinetic energy out of the diffuser. Cumpsty (1989) assumes this loss to lie within 2-5 point of efficiency:

$$0.02 \leq \Delta\eta_v \leq 0.05.\qquad(5.48)$$

This loss is likely to be higher for compressor with a vaned diffuser than with an annular diffuser, as a larger part of the total kinetic energy at the outlet of the vaned diffuser is in the radial direction. A more comprehensive treatment of loss in volutes can be found in Lorett and Gopalakrishnan (1986).

Diffusion

The purpose of the diffuser is to decelerate the flow with high kinetic energy, and thus convert this into pressure. This can be achieved more or less efficient depending on the construction of the diffuser. Due to inadequate diffusion in the diffuser, there will be a degradation $\Delta\eta_d$ in the efficiency η_i. The efficiency drop $\Delta\eta_d$ is dependent on the pressure recovery coefficient, see e.g. Cumpsty (1989) or Watson and Janota (1982), but for simplicity $\Delta\eta_d$ will be considered constant here. According to Watson and Janota (1982), vaned diffusers offer a 2 to 7 points increase in efficiency compared to annular diffusers.

5.4   Energy Transfer and Pressure Rise

Including the losses, the total specific energy transfer can be calculated by subtracting (5.40), (5.27), (5.33) and (5.41) from (5.16):

$$\Delta h_{0c}(U_1, m) = \Delta h_{0c,ideal} - \Delta h_{if} - \Delta h_{ii} - \Delta h_{df} - \Delta h_{di}. \qquad (5.49)$$

Δh_{0c} is a second degree polynomial in m, and as opposed to the ideal case, we see that energy transfer to the fluid is varying with mass flow m. This is shown in Figure 5.9.

To find an expression for the pressure rise we now need a relation between pressure rise and energy transfer. For *forward flow*, the pressure rise is modeled as

$$p_2 = \left(1 + \frac{\eta_i(m, U_1)\Delta h_{0c,ideal}}{T_{01}c_p}\right)^{\frac{\kappa}{\kappa-1}} p_{01} = \Psi_c(U_1, m)p_{01} \; \forall \; m > 0, \quad (5.50)$$

where the losses have been taken into account, and $\Psi_c(U_1, m)$ is the compressor characteristic. It is shown in Appendix C how to arrive at (5.50).

Remark 5.1 *A somewhat different approach is taken by Cohen et al. (1996) in order to include the losses in the compressor stage into the equation for the pressure rise. By introducing the power input factor ψ_p, the pressure ratio can be written*

$$p_2 = \left(1 + \frac{\psi_p \eta_c \Delta h_{0c,ideal}}{T_{01}c_p}\right)^{\frac{\kappa}{\kappa-1}} p_{01}, \qquad (5.51)$$

where, as in (5.50), $\Delta h_{0c,ideal} = \sigma U_2^2$. The power input factor is a number greater than unity, and represents an increase in work input needed to overcome the losses. Cohen et al. (1996) emphasize that the power input factor ψ_p and the slip factor σ are neither independent of one another nor of the overall isentropic efficiency η_c. The power input factor will not be used further in this text.

In order to model the compressor pressure rise for negative mass flow (deep surge), it is assumed that the pressure rise is proportional to the square of the mass flow for $m < 0$, that is,

$$\Psi_c(U_1, m) = \begin{cases} c_n m^2 + \psi_{c0}(U_1) & , \quad m \leq 0, \\ \left(1 + \frac{\eta_i(m, U_1)\Delta h_{0c,ideal}}{T_{01}c_p}\right)^{\frac{\kappa}{\kappa-1}} & , \quad m > 0 \end{cases}, \qquad (5.52)$$

where the choice

$$\psi_{c0}(U_1) = \left(1 + \frac{\eta_i(m, U_1)\Delta h_{0c,ideal}}{T_{01}c_p}\right)^{\frac{\kappa}{\kappa-1}}\Bigg|_{m=0}, \qquad (5.53)$$

of the shut off value ψ_{c0} ensures that $\Psi_c(U_1, m)$ is continuous in m. According to Willems (1996) and Day (1994), the back-flow characteristic defines the resistance which the rotating blades offer to flow in reversed direction. Day (1994) states that, in reversed flow the compressor can be regarded as a throttling device with a positive pressure bias. Compressor characteristics for negative flow are shown in Figure 5.12 and Figure 5.14.

A quadratic characteristic for reversed flow is also proposed by Hansen *et al.* (1981) for centrifugal compressors, and by Mansoux *et al.* (1994), Willems (1996) and Day (1994) for axial compressors. It is widely accepted in the literature (see e.g. Greitzer (1981)) that the compressor characteristic has a negative slope for negative mass flow. This slope depends on the choice of the constant c_n.

We now have an expression for the pressure p_2 needed in the model (5.1). Notice that for each speed N, both the pressure rise (5.50) and the efficiency (5.43) reach maximum for the same value of mass flow m. Thus, the maximum efficiency is reached on the surge line, stressing the need for active control in order to be able to operate safely in the neighborhood of the surge line. The inlet stagnation temperature T_{01}, specific heat capacity c_p and κ are assumed constant. The ideal energy transfer and the losses are shown for a compressor with annular diffuser in Figure 5.9. In the case of vaned diffuser, the curves look similar, but with a steeper slope due to the incidence losses at the diffuser. The curves are calculated for a compressor speed of $N = 35,000$rpm.

As mentioned in Section 5.3.1, backswept impeller blades will have an effect on the stability of the compressor. This can be seen from Figure 5.4 and Figure 5.9. Backsweep will imply that $\Delta h_{0c,ideal}$ would decrease for increasing values of mass flow, and thus shifting the maximum of Δh_{0c} as shown in Figure 5.9 to the right, effectively shifting the surge line towards lower mass flows. Consequently, the compressor can process a lower mass flow without going into surge.
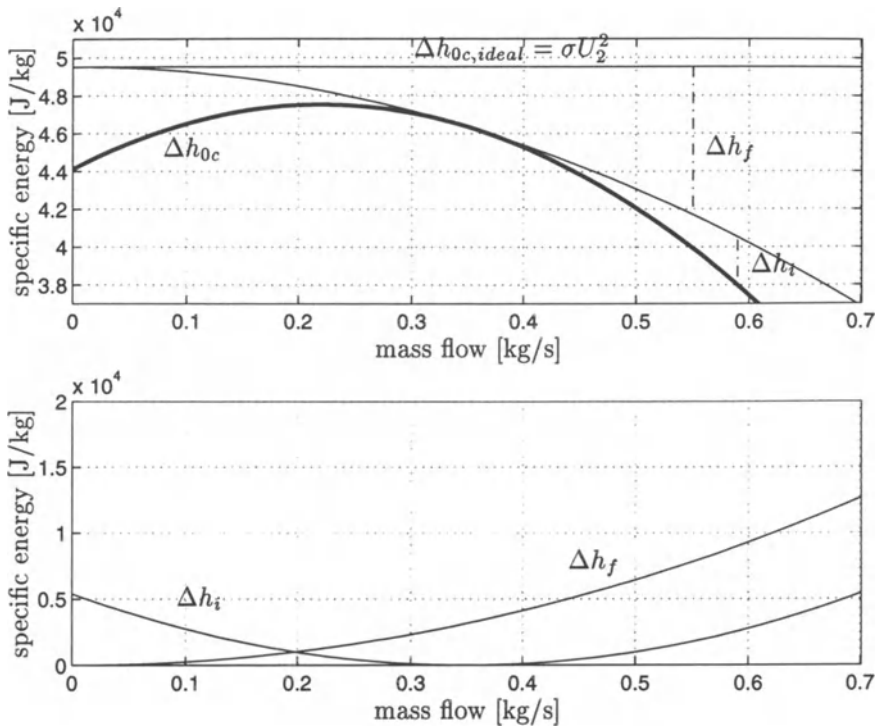
Figure 5.9: *Energy transfer for $N = 35,000$ rpm.*

The compressor pressure characteristic as calculated from equation (5.50) is showed in Figure 5.10.

In Figures 5.9 and 5.10 the numerical values for the compressor parameters is taken from Fink *et al.* (1992). Comparing the compressor map in Figure 5.10 with Figure 3 in Fink *et al.* (1992), which is based on physical measurements, we see that they are almost similar.

The surge line is the line in the compressor map that divides the map into an area of stable compressor operation and unstable (surge) operation. The line passes through the local maxima of the constant speed lines in the map, and is drawn with a solid line in figure 5.12.

5.5   Choking

When the flow reaches sonic velocity at some cross-section of the compression system, the flow chokes. Assuming isentropic flow, Dixon (1978) calculated
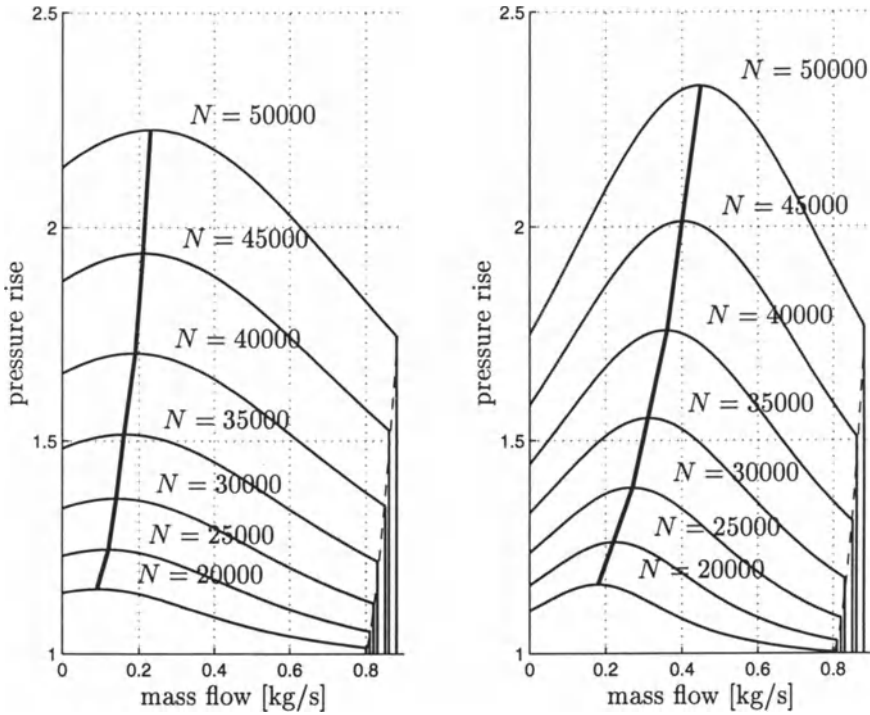
Figure 5.10: *Centrifugal compressor characteristic. The left plot is for an annular diffuser, and the right for a vaned diffuser. The dashed lines to the right are choke lines, also known as stone walls.*

the choking flow for the components most likely to choke in centrifugal compressors, the impeller eye (the inducer) and at the entry of the diffuser.

The effect of choking can be seen in Figure 5.10, where a choke line, also known as a stone wall, has been drawn. In this text, the effect of choking is treated in a approximate manner. Due to sonic effects, the pressure rise would fall off more gradually when approaching the stone wall than shown in Figure 5.10. Dixon (1978) showed that the mass flows for which choking occurs are:

- **Choking in impeller**

$$m_{choke}(U_1) = A_1 \rho_{01} a_{01} \left[\frac{2 + (\kappa - 1)\left(\frac{U_1}{a_{01}}\right)^2}{\kappa + 1} \right]^{\frac{(\kappa+1)}{2(\kappa-1)}}, \qquad (5.54)$$

where

$$\rho_{01} = \frac{p_{01}}{RT_{01}} \quad \text{and} \quad a_{01} = \sqrt{\kappa R T_{01}} \qquad (5.55)$$

is the inlet stagnation density and inlet stagnation sonic velocity, respectively. It is seen than the choking mass flow is dependent on blade speed U_1. Thus the impeller can accept a greater limiting mass flow rate at higher rotational speeds. By inserting $U_1 = 0$ in (5.54) the expression for choked flow through a nozzle is found. This is shown in Appendix C.

- **Choking in the diffuser entry**

$$
m_{choke}(U_2) = A_4 \rho_{01} a_{01} \frac{1 + (\kappa - 1)\eta_{imp}\sigma \left(\frac{U_2}{a_{01}}\right)^2}{\sqrt{1 + (\kappa - 1)\sigma \left(\frac{U_2}{a_{01}}\right)^2}} \left(\frac{2}{\kappa + 1}\right)^{\frac{(\kappa+1)}{2(\kappa-1)}},
$$

(5.56)

where A_4 is the flow area of the diffuser entry, and η_{imp} is the impeller efficiency.

5.6   Dynamic Model

To complete the dynamic model (5.1), an expression for the throttle mass flow is needed. The mass flow m_t through the throttle is modeled as

$$
m_t = k_t \sqrt{p_p - p_{01}},
$$

(5.57)

where k_t is the throttle gain proportional to throttle opening and p_p is the plenum pressure. The momentum balance of the spool is

$$
I\dot{\omega} = \tau_t - \tau_c.
$$

(5.58)

Using (5.3) it is seen that

$$
\omega = \frac{2U_1}{D_1} \Rightarrow \dot{\omega} = \frac{2\dot{U}_1}{D_1},
$$

(5.59)

and thus we get a differential equation for U_1,

$$
\dot{U}_1 = \frac{D_1}{2I} (\tau_t - \tau_c).
$$

(5.60)

The drive torque τ_t may be delivered by a turbine, and will be used as a control variable for speed control. The compressor and spool can only rotate in one direction, and the speed is assumed upper bounded:

$$
0 \le U_1(t) < U_m.
$$

(5.61)

Assumption (5.61) is a technicality needed in the stability proof, and is not crucial to the derivation of the model. Using (5.19) and (5.60), and inserting

equations (5.50) and (5.57) in (5.1), we get the following dynamic model for the compression system:

$$\dot{p}_p = \frac{a_{01}^2}{V_p}(m - k_t\sqrt{p_p - p_{01}})$$

$$\dot{m} = \frac{A}{L}\left(\left(1 + \frac{\eta_i(m, U_1)\Delta h_{0c,ideal}}{T_{01}c_p}\right)^{\frac{\kappa}{\kappa-1}} p_{01} - p_p\right) \quad (5.62)$$

$$\dot{U}_1 = \frac{D_1}{2I}(\tau_t - \tau_c).$$

It is worth noticing that a time varying U is equivalent with a time varying B-parameter (Fink et $al.$ 1992). Greitzer's B-parameter, as defined in Greitzer (1976a), is given by $B = \frac{U_1}{2a_{01}}\sqrt{\frac{V_p}{A_1 L_c}}$, where V_p is the plenum volume and L_c is the length of the compressor and duct. Using (5.60), a nonlinear differential equation for B can be found.

5.7   Surge Control Idea

The reason for equilibria to the left of the surge line being unstable, and causing the compressor to go into surge, is the positive slope of the characteristic in this area. From Figure 5.9 it is seen that the positive slope is due to the incidence losses at low mass flows. From the expression for the incidence loss, equation (5.27), it is clear that a variable blade angle β_{1b} would make it possible to minimize the incidence losses over a range of mass flows. Thus variable inducer blades might be used as a means of surge stabilization.

On the other hand, the maximum energy transfer and minimum incidence loss do not occur for the same mass flow. This is due to the friction losses. The friction shifts the point of maximum energy transfer, and consequently pressure rise, to the left of the point of minimum incidence loss. From this, we conclude that the friction losses in fact have a stabilizing effect, and introducing additional fluid friction would move the point of maximum energy transfer to the left. The result of this is that the surge line will be shifted to the left, and the area of stable compressor operation is expanded.

This motivates us to introduce a valve in series with compressor. The valve will introduce a pressure drop into the system, and the characteristic of the valve will have the same qualitative impact on the equivalent compressor characteristic as introducing more fluid friction. The pressure drop over this valve will serve as the control variable, and it will be used to introduce additional friction at low mass flows in order to avoid surge. The use of a close coupled valve for constant speed centrifugal compressor surge control was studied by Dussourd et $al.$ (1977), Jungowski et $al.$ (1996) and Pinsley et $al.$ (1991).

5.8   Controller Design and Stability Analysis

The equivalent compressor characteristic for compressor and close coupled valve is defined as

$$\Psi_e(m, U_1) = \Psi_c(m, U_1) - \Psi_v(m), \qquad (5.63)$$

where $\Psi_v(m)p_{01}$ is the pressure drop across the CCV and

$$\Psi_c(m, U_1) = \left(1 + \frac{\eta_i(m, U_1)\Delta h_{0c,ideal}}{T_{01}c_p}\right)^{\frac{\kappa}{\kappa-1}}. \qquad (5.64)$$

Assume p_0, m_0 to be the equilibrium values of pressure and mass flow as dictated by the intersection of the throttle and compressor characteristics, and U_d to be the desired spool speed. Define the following error variables

$$\hat{p} = p_p - p_0, \quad \hat{m} = m - m_0, \quad \hat{U} = U_1 - U_d. \qquad (5.65)$$

The equations of motion (5.62) are now transformed so that the origin becomes the equilibrium under study. Notice that no assumptions are made about the numeric values of m_0 and p_0, so that the equilibrium can be on either side of the surge line. The equilibrium values are calculated using the same method as described in Section 2.3.2. Define

$$\begin{align}
\hat{m}_t(\hat{p}) &= m_t(\hat{p} + p_0) - m_0 & (5.66)\\
\hat{\Psi}_c(\hat{m}, \hat{U}) &= \Psi_c(\hat{m} + m_0, \hat{U} + U_d) - p_0 & (5.67)\\
\hat{\Psi}_v(\hat{m}, \hat{U}) &= \Psi_v(\hat{m} + m_0, \hat{U} + U_d) - p_0 & (5.68)
\end{align}$$

By including the CCV (5.63), and using (5.66)-(5.68), the model (5.62) can be written in the form

$$\begin{align}
\dot{\hat{p}} &= \frac{a^2}{V_p}(\hat{m} - \hat{m}_t(\hat{p}))\\
\dot{\hat{m}} &= \frac{A}{L}\left(\left(\hat{\Psi}_c(\hat{m}, \hat{U}) - \hat{\Psi}_v(\hat{m})\right)p_{01} - \hat{p}\right) & (5.69)\\
\dot{\hat{U}}_1 &= \frac{D_1}{2I}(\hat{\tau}_t - \hat{\tau}_c)
\end{align}$$

where a hat denotes transformation to the new coordinates (5.65), and

$$(\hat{p}\ \hat{m}\ \hat{U})^{\mathrm{T}} = (0\ 0\ 0)^{\mathrm{T}} \qquad (5.70)$$

is the equilibrium. The expressions for the characteristics $\hat{m}_t(\hat{p})$, $\hat{\Psi}_c(\hat{m}, \hat{U})$ and $\hat{\Psi}_v(\hat{m})$ are found in a similar manner as in Chapter 2. From (5.19) it is known that

$$\tau_c = \frac{D_2^2\sigma}{2D_1}|m|U_1 = \frac{D_2^2\sigma}{2D_1}\mathrm{sgn}(m)mU_1. \qquad (5.71)$$

As in Nicklasson (1996), a scaled hyperbolic tangent function will be used to mimic the signum function in the analysis in order to avoid additional difficulties regarding continuity:

$$\tau_c = \frac{D_2^2 \sigma}{2D_1} \tanh(\frac{m}{\varsigma}) m U_1, \tag{5.72}$$

where $\varsigma > 0$ is a sufficiently large constant. The torque $\hat{\tau}_c$ is defined as

$$\hat{\tau}_c = \tau_c - \tau_{co} \tag{5.73}$$

and calculated as

$$\begin{aligned}
\tau_c &= \frac{D_2^2 \sigma}{2D_1} \tanh(\frac{m}{\varsigma})(\hat{m} + m_0)(\hat{U} + U_d) \\
&= \underbrace{\frac{D_2^2 \sigma}{2D_1} \tanh(\frac{m}{\varsigma})(\hat{m} + m_0)(\hat{m}\hat{U} + \hat{m}U_d + m_0\hat{U})}_{\hat{\tau}_c} \\
&\quad + \underbrace{\frac{D_2^2 \sigma}{2D_1} \tanh(\frac{m}{\varsigma}) m_0 U_d}_{\tau_{c0}} .
\end{aligned} \tag{5.74}$$

By choosing

$$\hat{\tau}_t = \tau_t - \tau_{co}, \tag{5.75}$$

the last equation in (5.69) follows from the last equation in (5.62).

Theorem 5.1 *The surge control law*

$$\hat{\Psi}_v = k_v \hat{m}, \tag{5.76}$$

and the speed PI control law

$$\begin{aligned}
\hat{\tau}_t &= -k_p \hat{U} - k_i \hat{I}, \\
\dot{\hat{I}} &= \hat{U},
\end{aligned} \tag{5.77}$$

where

$$k_p > 0, \quad k_i > 0 \text{ and } k_v > \sup_{\hat{U}, \hat{m}} \left\{ \frac{\partial \hat{\Psi}_c(\hat{m}, \hat{U})}{\partial \hat{m}} \right\} + \delta_1, \tag{5.78}$$

and $\delta_1 > 0$, makes the origin of (5.69) semi-global exponentially stable. □

Proof:
Define

$$z \triangleq \begin{pmatrix} \hat{U} \\ \hat{I} \end{pmatrix} \text{ and } P \triangleq \begin{pmatrix} \frac{2I}{D_1} & \lambda \\ \lambda & k_i \end{pmatrix}, \tag{5.79}$$

where $\lambda > 0$ and $k_i > 0$ are design parameters. Consider the following Lyapunov function candidate

$$V(\hat{p}, \hat{m}, \hat{U}, \hat{I}) = \frac{1}{2} \left(V_{\hat{p}} + V_{\hat{m}} + V_{spool} \right), \qquad (5.80)$$

where

$$V_{\hat{p}} = \frac{V_p}{a_{01}^2 \rho_{01}} \hat{p}^2 \;, \quad V_{\hat{m}} = \frac{L}{A_1 \rho_{01}} \hat{m}^2 \text{ and } V_{spool} = \boldsymbol{z}^{\mathrm{T}} \boldsymbol{P} \boldsymbol{z}. \qquad (5.81)$$

As all coefficients in (5.80) are constant it follows that V is positive definite and radially unbounded, provided that λ is chosen such that $\boldsymbol{P} > 0$, that is

$$\lambda < \sqrt{\frac{2 I k_i}{D_1}}. \qquad (5.82)$$

Calculating the time derivative of (5.80) along the solutions of (5.69) and accounting for (5.77) gives

$$\begin{aligned}
\dot{V} &= \hat{m} \left(\hat{\Psi}_c(\hat{m}, \hat{U}) - \hat{\Psi}_v(\hat{m}) \right) \frac{p_{01}}{\rho_{01}} - \frac{1}{\rho_{01}} \hat{p} \hat{m}_t(\hat{p}) - k_p \hat{U}^2 \\
&\quad + \lambda \hat{U}^2 - \frac{\lambda k_i D_1}{2I} \hat{I}^2 - \frac{\lambda k_p D_1}{2I} \hat{U} \hat{I} - \hat{U} \hat{\tau}_c - \frac{\lambda D_1}{2I} \hat{I} \hat{\tau}_c. \qquad (5.83)
\end{aligned}$$

The last term in (5.83) can be upper bounded as

$$\begin{aligned}
-\frac{\lambda D_1}{2I} \hat{I} \hat{\tau}_c &= -\frac{\lambda D_2^2 \sigma}{4I} \left(\tanh(\frac{m}{\varsigma}) \hat{m} U + m_0 \hat{U} \right) \hat{I} \\
&\leq \frac{\lambda D_2^2 \sigma}{4I} \left(\frac{U_m}{2} \left(\frac{\hat{m}^2}{\eta_1} + \eta_1 \hat{I}^2 \right) + m_0 \hat{U} \hat{I} \right) \qquad (5.84)
\end{aligned}$$

using (5.19), (5.61) and Young's inequality. The parameter $\eta_1 > 0$ can be chosen freely. The $\hat{U} \hat{\tau}_c$-term can be upper bounded as

$$\begin{aligned}
-\hat{U} \hat{\tau}_c &= -\frac{D_2^2 \sigma}{2D_1} \tanh(\frac{m}{\varsigma}) \left((\hat{m} + m_0) \hat{U} + \hat{m} U_d \right) \hat{U} \\
&\leq -\frac{D_2^2 \sigma}{2D_1} \tanh(\frac{m}{\varsigma}) m \hat{U}^2 + \frac{D_2^2 \sigma}{4D_1} \left(\frac{\hat{m}^2}{\eta_2} + \eta_2 (U_d \hat{U})^2 \right). \qquad (5.85)
\end{aligned}$$

Now, (5.83) can be upper bounded as

$$\begin{aligned}
\dot{V} &\leq \hat{m} \left(\hat{\Psi}_c(\hat{m}, \hat{U}) - \hat{\Psi}_v(\hat{m}) \right) \frac{p_{01}}{\rho_{01}} - \frac{D_2^2 \sigma}{2D_1} \tanh(\frac{m}{\varsigma}) m \hat{U}^2 \\
&\quad + \left(\frac{\sigma \lambda D_2^2 U_m}{8 I \eta_1} + \frac{D_2^2 \sigma}{4 D_1 \eta_2} \right) \hat{m}^2 - \frac{1}{\rho_{01}} \hat{p} \hat{m}_t(\hat{p}) - \boldsymbol{z}^{\mathrm{T}} \boldsymbol{R} \boldsymbol{z}, \qquad (5.86)
\end{aligned}$$

where

$$R = \begin{pmatrix} k_p - \lambda - \frac{D_2^2 \sigma U_d^2 \eta_2}{4D_1} & \frac{\lambda}{4I}\left(D_1 k_p - \frac{\sigma D_2^2 m_0}{2}\right) \\ \frac{\lambda}{4I}\left(D_1 k_p - \frac{\sigma D_2^2 m_0}{2}\right) & \frac{\lambda}{2I}\left(k_i D_1 - \frac{\sigma D_2^2 U_m \eta_1}{4}\right) \end{pmatrix}. \tag{5.87}$$

Demanding $R > 0$ gives the following conditions on k_p, η_1 and λ

$$k_p > \frac{D_2^2 \sigma U_d^2 \eta_2}{4D_1}, \tag{5.88}$$

$$\eta_1 < \frac{4k_i D_1}{\sigma D_2 U_m} \tag{5.89}$$

and

$$\lambda < \min\{\lambda_1, \lambda_2\}, \tag{5.90}$$

where

$$\lambda_1 = k_p - \frac{D_2^2 \sigma U_d^2 \eta_2}{4D_1} \tag{5.91}$$

and

$$\lambda_2 = \frac{\left(k_p - \frac{D_2^2 \sigma U_d^2 \eta_2}{4D_1}\right)\left(k_i D_1 - \frac{\sigma D_2 U_m \eta_1}{4}\right)}{k_i D_1 - \frac{\sigma D_2 U_m \eta_1}{4} + \frac{1}{8I}\left(D_1 k_p - \frac{\sigma D_2 m_0}{2}\right)^2}. \tag{5.92}$$

It is assumed that $\hat{m}_t$ satisfies the sector condition

$$\hat{p}\hat{m}_t(\hat{p}) > \delta_2 \hat{p}^2, \tag{5.93}$$

that is, the throttle is assumed passive as in Simon and Valavani (1991). As $\hat{p}\hat{m}_t(\hat{p})$ is of order $\frac{3}{2}$ in $\hat{p}$, (5.93) does not hold globally. However, for a given $\hat{p}_{max}$ such that

$$|\hat{p}(t)| \leq \hat{p}_{max} \; \forall \, t > 0 \tag{5.94}$$

it will always be possible to chose δ_2 small enough for (5.93) to hold for $|\hat{p}(t)| \leq \hat{p}_{max}$. This is the same assumption as made in Assumption 3.1. Now, the CCV pressure drop $\Psi_v(\hat{m})$ is to be chosen such that for the first term in (5.86), the condition

$$-\hat{m}\left(\hat{\Psi}_c(\hat{m}, \hat{U}) - \hat{\Psi}_v(\hat{m})\right)\frac{p_{01}}{\rho_{01}} > 0 \; \forall \hat{U} \tag{5.95}$$

is satisfied. Since $\frac{p_{01}}{\rho_{01}} > 0$, sufficient conditions for (5.95) to hold is

$$-\left(\hat{\Psi}_c(\hat{m}, \hat{U}) - \hat{\Psi}_v(\hat{m})\right)\bigg|_{\hat{m}=0} = 0 \tag{5.96}$$

and

$$\frac{\partial}{\partial \hat{m}}\left(-\hat{\Psi}_c(\hat{m}, \hat{U}) + \hat{\Psi}_v(\hat{m})\right) > 0. \tag{5.97}$$

It can be recognized that

$$\hat{\Psi}_c(0,\hat{U}) \;=\; \Psi_c(m_0,U_d) - \Psi_c(m_0,U_d) = 0, \qquad (5.98)$$

$$\hat{\Psi}_v(\hat{m}) \;=\; k_v\hat{m} \Rightarrow \hat{\Psi}_v(0) = 0, \qquad (5.99)$$

and thus (5.96) is satisfied. From (5.97), we get

$$-\frac{\partial}{\partial\hat{m}}\hat{\Psi}_c(\hat{m},\hat{U}) + k_v > 0, \qquad (5.100)$$

and it follows that choosing k_v according to

$$k_v > \sup_{\hat{U},\hat{m}}\left\{\frac{\partial\hat{\Psi}_c(\hat{m},\hat{U})}{\partial\hat{m}}\right\}, \qquad (5.101)$$

guarantees that (5.97), and thereby (5.95) being satisfied. Moreover, if k_v is chosen as

$$k_v > \sup_{\hat{U},\hat{m}}\left\{\frac{\partial\hat{\Psi}_c(\hat{m},\hat{U})}{\partial\hat{m}}\right\} + \delta_1, \qquad (5.102)$$

where $\delta_1 > 0$, we get $\hat{m}\Psi_v(\hat{m}) > \delta_1\hat{m}^2$, and (5.95) is modified to

$$-\hat{m}\left(\hat{\Psi}_c(\hat{m},\hat{U}) - \hat{\Psi}_v(\hat{m})\right)\frac{p_{01}}{\rho_{01}} > \frac{p_{01}}{\rho_{01}}\delta_1\hat{m}^2 \;\forall\hat{U}. \qquad (5.103)$$

Consequently, $\dot{V}$ can now be upper bounded as

$$\dot{V} \leq -\left(\frac{p_{01}}{\rho_{01}}\delta_1 - \frac{\sigma\lambda D_2^2 U_m}{8I\eta_1} - \frac{D_2^2\sigma}{4D_1\eta_2}\right)\hat{m}^2 - \delta_2\hat{p}^2 - \frac{1}{2}z^\mathrm{T}Rz \quad \forall \; \hat{m},\hat{p},z$$

$$(5.104)$$

We now set out to compare the coefficients of V and $\dot{V}$. The cross terms in $\hat{U}$ and $\hat{I}$ are upper bounded using Young's inequality,

$$\lambda\hat{U}\hat{I} \;\leq\; \frac{\lambda}{2}\left(\frac{\hat{U}^2}{\eta_3} + \eta_3\hat{I}^2\right) \qquad (5.105)$$

$$-\frac{\lambda(4D_1k_p - \sigma D_2^2 m_0)}{2I}\hat{U}\hat{I} \;\leq\; \frac{\lambda(4D_1k_p - \sigma D_2^2 m_0)}{4I} \times$$
$$\left(\hat{U}^2/\eta_4 + \eta_4\hat{I}^2\right), \qquad (5.106)$$

where $\eta_3 > 0$ and $\eta_4 > 0$ are constants that can be chosen freely. Using (5.105) and (5.106) and comparing the coefficients in (5.80) and (5.104), it can be recognized that if the following inequalities are satisfied for some constant $\varpi > 0$:

$$\delta_1 - \frac{\sigma\lambda D_2^2 U_m\rho_{01}}{8I\eta_1 p_{01}} - \frac{D_2^2\sigma\rho_{01}}{4D_1\eta_2 p_{01}} \;>\; \varpi\frac{L}{A\rho_{01}} \qquad (5.107)$$

$$\delta_2 \; > \; \varpi \frac{V_p}{a_{01}^2 \rho_{01}}, \tag{5.108}$$

$$k_p - \lambda - \frac{\lambda(4D_1 k_p - \sigma D_2^2 m_0)}{4I\eta_4} \; > \; \varpi\left(\frac{I}{D_1} + \frac{\lambda}{2\eta_3}\right), \tag{5.109}$$

$$\lambda k_i - \frac{\lambda(4D_1 k_p - \sigma D_2^2 m_0)}{4I}\eta_4 \; > \; \varpi\left(\frac{k_i}{D_1} + \frac{\varpi\eta_3}{2}\right), \tag{5.110}$$

the following holds

$$\dot{V} \leq -\varpi V \;\; \Rightarrow \;\; V(t) \leq V(0)e^{-\varpi t}. \tag{5.111}$$

If η_1 is chosen according to (5.89), and δ_1 is chosen according to

$$\delta_1 > \frac{\sigma \lambda D_2^2 U_m \rho_{01}}{8I\eta_1 p_{01}} + \frac{D_2^2 \sigma \rho_{01}}{4D_1 \eta_2 p_{01}}, \tag{5.112}$$

and k_v is chosen so that $k_v > \sup_{\hat{U},\hat{m}} \left\{ \frac{\partial \hat{\Psi}_c(\hat{m},\hat{U})}{\partial \hat{m}} \right\} + \delta_1$, and λ is chosen according to (5.82) and (5.90), then the inequalities (5.107)-(5.110) are satisfied for some $\varpi > 0$. By (5.111) the origin of (5.69) is exponentially stable. Due to assumption (5.94), the stability result holds whenever $|\hat{p}(0)| \leq \hat{p}_{max}$, and thus the origin is semi globally exponentially stable. $\qquad \square$

Notice that the parameter ϖ can be used to calculate a lower bound on the convergence rate of the system.

Providing the parameters k_i and λ with appropriate units, V is a energy-like function of unit $[J]$. The term

$$V_{\hat{U}} = \frac{1}{2}z_1 P_{11} z_1 = \frac{I}{2D_1^2}\hat{U}^2 \tag{5.113}$$

is recognized as the kinetic energy, expressed in the new coordinates, of the rotating spool.

Desired compressor speed U_d can now be achieved regardless of the equilibrium is located to the right or to the left of the original surge line. The integral term in (5.77) is added in order to robustify the controller with respect to unmodeled disturbance torques.

5.9 Simulations

The two cases of unstable centrifugal compressors with annular and vaned diffuser are now simulated with and without surge control.

Annular Diffuser

First, we consider a compressor fitted with an annular diffuser. In Figure 5.11 the response (solid lines) of the compression system during surge is shown. The set point for compressor speed was $U_d = 150\text{m/s} \Rightarrow N \approx 50.000\text{rpm}$ and the speed control law (5.77) parameters were set to $k_p = 0.1$ and $k_i = 0.07$. The throttle gain was set to $k_t = 0.0003$ which gives an unstable equilibrium to the left of the surge line. Notice the oscillation in speed U_1. These variations in spool speed during surge was first described by Eveker and Nett (1991) for an axial compressor. This simulation is also shown in Figure 5.12, where the pressure rise has been plotted versus the mass flow in the compressor characteristic. As can be seen, the compressor undergoes severe (deep) surge oscillations, and the compressor speed oscillates around the desired value.
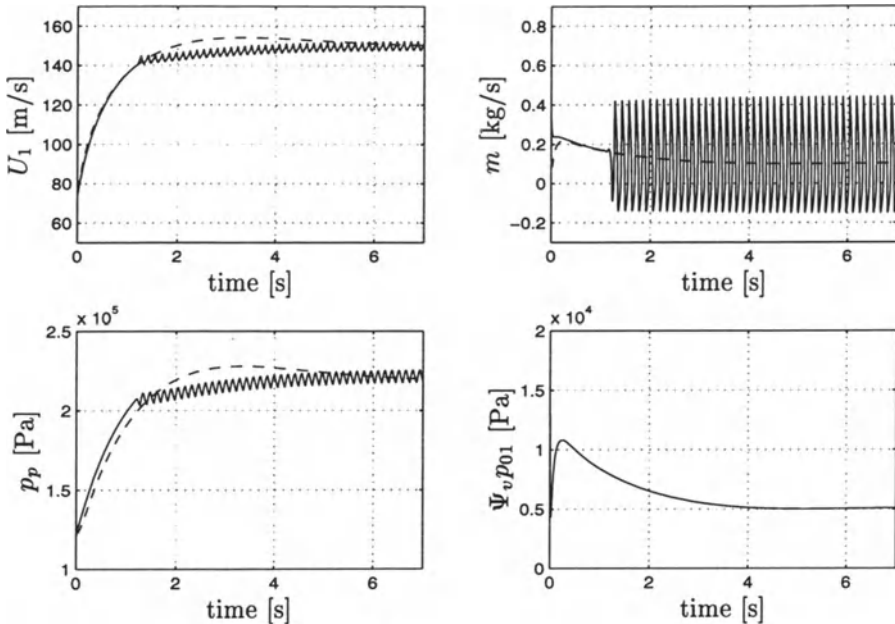
Figure 5.11: *Transient response of centrifugal compression system with annular diffuser. Without surge control, the compressor goes into surge, shown with solid lines. The system response with the surge controller is shown with dashed lines.*

Now, the surge controller (5.76) is used with $k_v = 0.5$. The speed set point, speed controller parameters and throttle gain are left unchanged. The results are shown in Figure 5.11 using dashed lines. The desired speed is reached and
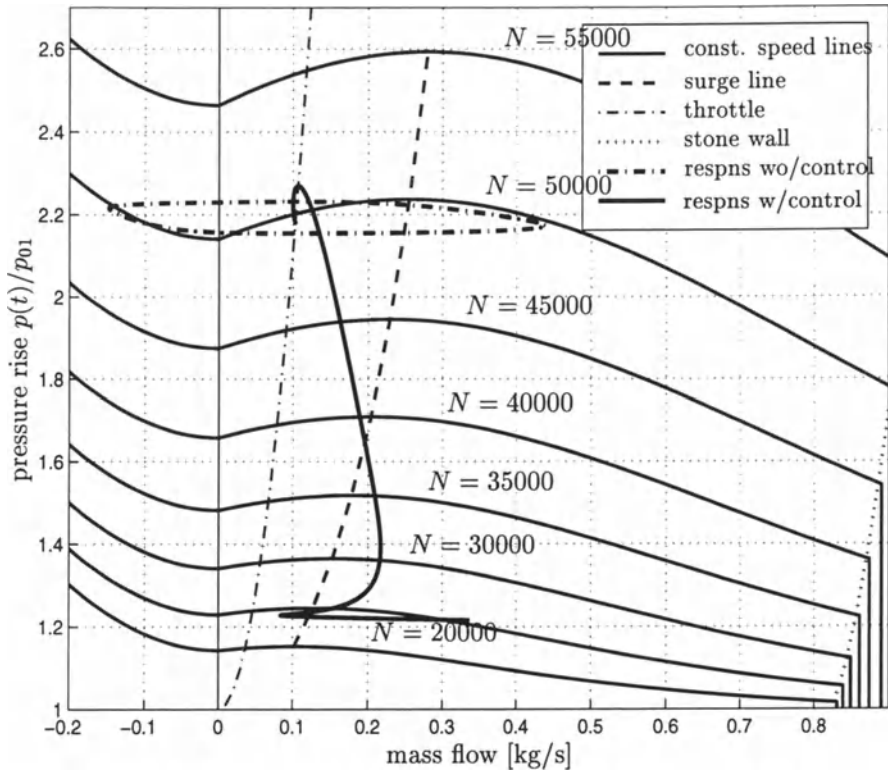
Figure 5.12: $(m(t), p(t)/p_{01})$-trajectories plotted together with the compressor characteristic. N is the compressor speed in rpm. In the case of no surge control, the surge cycle is clearly visible, but with surge control the state converges to the intersection of the throttle and the compressor characteristic.

the surge oscillations are eliminated. As previously mentioned there is a loss associated with the CCV control approach. The pressure drop over the valve is shown in the lower right corner of Figure 5.11. At equilibrium the pressure drop for this particular case is approximately 5kPa. Compared to the pressure rise over the compressor at this equilibrium, well over 200kPa, this seems little when taken into account that the compressor now is operating in an area of the compressor map previously not possible. The CCV loss is dependent on the controller gain k_v. In this simulation the gain was set to $k_v = 0.5$ to dominate the maximum positive slope of the compressor characteristic. The resulting trajectory of this simulation in also plotted in Figure 5.12. As can be seen the equilibrium is located somewhat below the intersection of the throttle line and the $N = 50,000$ line of the compressor characteristic. This is due to the pressure drop over the CCV.

Vaned Diffuser

Now, the case of a compressor with vaned diffuser is simulated. The response of the compression system with speed control only is shown in Figure 5.13 (solid lines). The speed control parameters were set to $k_p = 0.1$ and $k_i = 0.07$, and the throttle gain was set at $k_T = 0.00075$. As the vaned diffuser gives a steeper and more narrow characteristic, the amplitude of the pressure oscillations is larger than for the annular diffuser. This is also the case for the speed and mass flow oscillations.

When the surge control is in use, we get the response plotted with dashed lines in Figure 5.13, and as can be seen the oscillations are avoided at the cost of a pressure loss over the CCV. Since the positive slope of the compressor characteristic is larger in this case compared to the annular diffuser, this pressure drop is also larger. However, a pressure drop of 35kPa over the valve is still less than the pressure rise of 180kPa over the compressor.
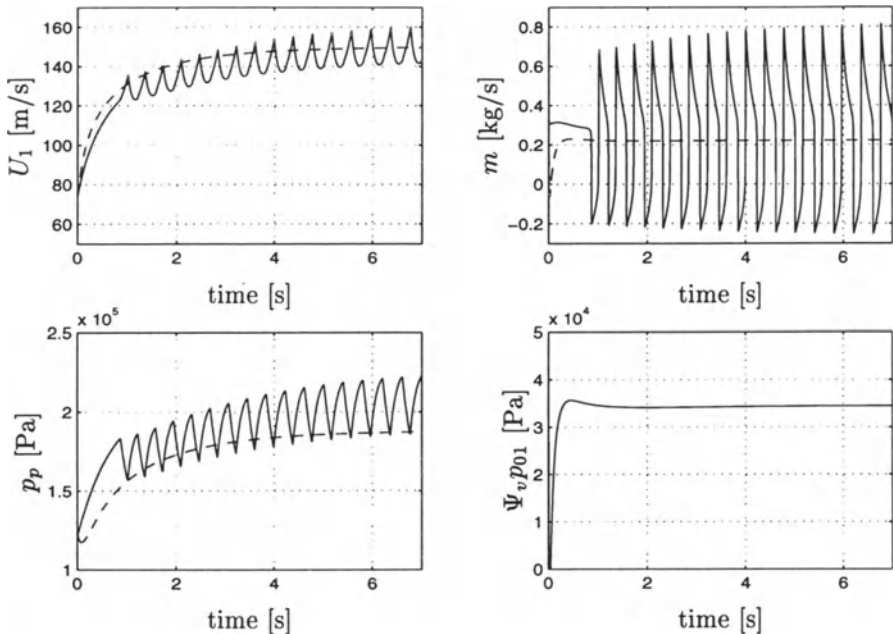
Figure 5.13: *Transient response of centrifugal compression system with vaned diffuser. Without surge control, the compressor goes into surge. This is plotted with a solid line. The dashed lines is the system response when the CCV surge controller is in use.*

The result of this simulation is also shown in Figure 5.14, where mass flow versus pressure rise is plotted together with the compressor characteristic.

The response of the system with CCV control is also shown. This is plotted with a thick solid line. The stabilization is clearly illustrated. The equivalent characteristic is not plotted, but the stabilized trajectory approaches the intersection of the throttle line and the $N = 50.000$ line of the *equivalent* characteristic. Due to the higher CCV gain k_v in the case of vaned diffuser than in the case of annular diffuser, the difference between Ψ_e and Ψ_e is greater in this case.

By comparing the in-surge response of the two cases, it is seen that the frequency of the surge oscillations is lower for the vaned diffuser (3Hz), than for the annular diffuser (7Hz). This is in accordance with Greitzer (1981) and Willems (1996) where it is shown that the surge frequency depends on the slope of the compressor characteristic in such a way that a steeper slope leads to lower frequency, and a less steep slope leads to higher frequency.
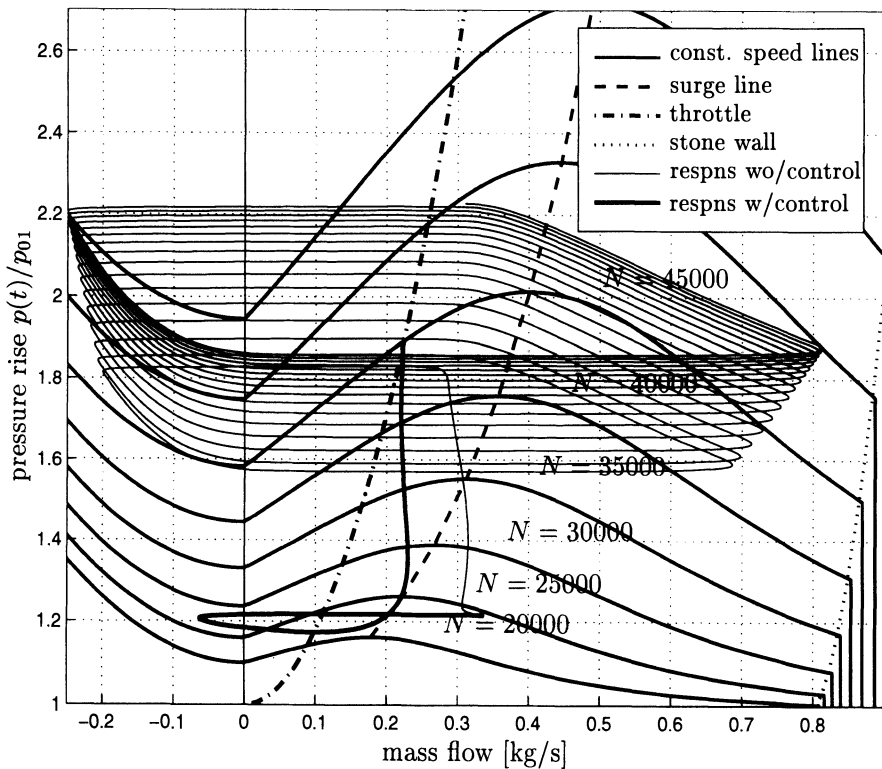
Figure 5.14: $(m(t), p(t)/p_{01})$-*trajectories plotted together with the compressor characteristic. N is the compressor speed in rpm. In the case of no surge control, the surge cycle is clearly visible, but with surge control the state converges to the intersection of the throttle and the compressor characteristic.*

5.10   Conclusion

In this Chapter, a dynamic model of a centrifugal compression system with non-constant compressor speed was presented. The compressor characteristic was derived by calculating the energy transfer and losses in the components of the compressor. Incidence and friction losses in the impeller and the diffuser were considered in addition to other losses. Both vaned and annular diffusers were considered.

Control laws for surge and speed of the centrifugal compression system were developed. A close coupled valve was chosen as an actuator for the control of surge. Using Lyapunov's method, the systems equilibrium was showed to be semi-global exponentially stable. Through simulations it was confirmed that the compressor can operate stably and reach desired speed in the previous unstable area to the right of the surge line in the compressor map.

From a surge control point of view, the main difference between the annular and vaned diffusers are the steeper slope of the compressor characteristic when a vaned diffuser is used. A consequence of this is that if a close coupled valve is used to control surge, a greater pressure drop must be accepted over the valve in the case of a vaned diffuser than in the case of an annular diffuser.

CHAPTER 6

CONCLUDING REMARKS AND
FURTHER RESEARCH

6.1   Conclusions

In this text, modeling and control of surge and rotating stall in axial and centrifugal compressors have been studied.

First, surge and stall controllers for a close coupled valve in series with a compressor were developed. Using backstepping, a surge control law for the close coupled valve was derived. Global asymptotic stability was proven. A more complicated surge control law was derived for the case of both pressure disturbances and mass flow disturbances. Global uniform boundedness and convergence was proven. In order to stabilize the compression system in the presence of constant disturbances, or biases, in mass flow and pressure, an adaptive version of the surge controller was derived. This controller ensures global asymptotic stability. Then, controllers for rotating stall were considered. The close coupled valve was incooperated into the Moore-Greitzer model, and controllers were derived that enables stabilization of rotating stall beyond the surge line. Without disturbances, an asymptotically stable equilibrium is ensured, and in the presence of pressure disturbances uniform boundedness was proven.

Then, the passivity properties of the Greitzer model was used to derive a surge control law for a close coupled valve. This resulted in a simple proportional control law, that was capable of stabilizing the compression system in the presence of both mass flow disturbances as well as pressure disturbances.

A multi mode Moore-Greitzer axial compressor model with spool dynam-

ics was derived. This resulted in a model with time varying B-parameter. Through simulations it was shown that the model was capable of representing both rotating stall and surge, and that the type of instability depended on the compressor speed. In the original Moore Greitzer model only the first mode of rotating stall is included. The simulations in this chapter show that during stall inception, higher order modes can dominate the first mode. This is in accordance with known results, and is shown here to be valid also for variable speed compressors.

A dynamic model of a centrifugal compression system with non-constant compressor speed was presented. The compressor characteristic was derived by calculating the energy transfer and losses in the components of the compressor. Incidence and friction losses in the impeller and the diffuser were considered in addition to other losses. Both vaned and annular diffusers were studied. Control laws for surge and speed of the centrifugal compression system were developed. A close coupled valve was chosen as an actuator for the control of surge. Using Lyapunov's method, the systems equilibrium was showed to be semi-global exponentially stable. Through simulations it was confirmed that the compressor can operate stable and reach desired speed in the previous unstable area to the right of the surge line in the compressor map.

6.2   Further research

6.2.1   Mass flow measurements

The surge and stall controllers presented in this text all depend on sensing of mass flow. This sensing requirement has been regarded troublesome by several authors. According to Krstić and Wang (1998) measurement of the mass flow, in connection to stall control of jet engines, represents a challenge, but it is not expected to be insurmountable.

According to Hendricks and Gysling (1994) axial velocity is readily measured in low-speed flows using hot wire anemometers, but these sensors are not practical in high speed turbomachinery. Here, velocity could be synthesized from total and static pressure measurements.

This method is actually used by Badmus *et al.* (1996), where a surge controller is based on the measurement the nondimensionalized dynamic inlet pressure:

$$\tilde{p}_d = \frac{p_d}{\rho U^2}. \tag{6.1}$$

As the dynamic pressure is given by

$$p_d = \frac{\rho C_x^2}{2}, \tag{6.2}$$

it follows that

$$\tilde{p}_d = \frac{1}{2}\phi^2, \tag{6.3}$$

and finally

$$\frac{1}{2}\phi^2 = \frac{1}{\rho U^2}\left(p_{total} - p_{static}\right). \tag{6.4}$$

Following Botros and Henderson (1994), flow measurements in centrifugal compression systems often pose serious problems for anti-surge control. The signals are generally noisy, inaccurate, and in some cases, nonlinear and non-repeatable. Furthermore, generally the flow measurement elements constitute a pressure loss element and hence a waste of energy.

Due to the difficulties connected to mass flow measurement, a topic for further research is design of stall and surge controllers based on feedback from pressure.

CCV control

There are several topics for further research in connection with CCV control. Some of these include

- As formulated in this text, the control laws influence the equilibrium point. This is a consequence of the controller being designed and analyzed in a shifted coordinate system. Current work is aimed at avoiding this.

- There is a pressure drop penalty connected to the CCV approach. It is desirable to minimize this pressure drop, and a preliminary investigation shows that much less pressure drop that dictated by the stability analysis can be used. The drawback of this, it seems, is that the stability results become local as opposed to global.

- It is of interest to study disturbances also in the $\dot{J}$-equation, not only in mass flow and pressure.

- As the CCV only can introduce a pressure drop, and is not able to increase pressure, it would be of interest to investigate CCV-control along the lines of one-sided control as discussed by Willems and de Jager (1998a).

BIBLIOGRAPHY

Abed, E.H. and J.-H. Fu (1986). Local feedback stabilization and bifurcation control, I. Hopf bifurcation. *Systems & Control Letters* **7**, 11–17.

Abed, E.H. and J.-H. Fu (1987). Local feedback stabilization and bifurcation control, II. Stationary bifurcation. *Systems & Control Letters* **8**, 467–473.

Abed, E.H., P.K. Houpt and W.M. Hosny (1990). Bifurcation analysis of surge and rotating stall in axial flow compressors. In: *Proceedings of the 1990 American Control Conference.* San Diego. pp. 2239–2246.

Abed, E.H., P.K. Houpt and W.M. Hosny (1993). Bifurcation analysis of surge and rotating stall in axial flow compressors. *Journal of Turbomachinery* **115**, 817–824.

Adomatis, R.A. and E.H. Abed (1993). Local nonlinear control of stall inception in axial flow compressors. In: *Proceedings of the AIAA/SAE/ASME/ASEE Joint Propulsion Conference.* Monterey, CA.

Badmus, O.O., C.N. Nett and F.J. Schork (1991). An integrated full-range surge control / rotating stall avoidance compressor control system. In: *Proceedings of the 1991 American Control Conference.* pp. 3173–3180.

Badmus, O.O., S. Chowdhury and C.N. Nett (1996). Nonlinear control of surge in axial compression systems. *Automatica* **32**(1), 59–70.

Badmus, O.O., S. Chowdhury, K.M. Eveker and C.N. Nett (1995a). Control-oriented high-frequency turbomachinery modelling: Single-stage compression system one-dimensional modell. *Journal of Turbomachinery* **117**, 47–61.

Badmus, O.O., S. Chowdhury, K.M. Eveker, C.N. Nett and C.J. Rivera (1995b). Simplified approach for control of rotating stall, Part 1: Theoretiacal development. *Journal of Propulsion and Power* **11**(6), 1195–1209.

Badmus, O.O., S. Chowdhury, K.M. Eveker, C.N. Nett and C.J. Rivera (1995c). Simplified approach for control of rotating stall, Part 2: Experimental results. *Journal of Propulsion and Power* **11**(6), 1210–1223.

Baghdadi, S. and J.E. Lueke (1982). Compressor stability analysis. *Journal of Fluids Engineering* **104**, 242–249.

Baillieul, J., S. Dahlgren and B. Lehman (1995). Nonliear control designs for systems with bifurcations with applications to stabilization and control of compressors. In: *Proceedings of the 35th Conference on Decision and Control.* New Orleans, LA. pp. 3062–3067.

Balchen, J.G and K.I. Mummé (1988). *Process control : Structures and applications.* Van Nostrand Reinhold Company. New York.

Baljé, O.E. (1952). A contribution to the problem of designing radial turbomachines. *Transactions of the ASME* **74**, 451–472.

Banaszuk, A. and A.J. Krener (1997). Design of controllers for MG3 compressor models with general characteristics using graph backstepping. In: *Proceedings of the 1997 American Control Conference.* Albuquerque, NM.

Banaszuk, A. and A.J. Krener (1998). Design of controllers for MG3 compressor models with general characteristics using graph backstepping. *Automatica.* To appear.

Banaszuk, A., H.A. Hauksson and I. Mezić (1997*a*). A backstepping controller for a partial differential equation model of compression system instabilities. In: *Proceedings of the 36th Conference on Decision and Control.* San Diego, CA. pp. 1050–1055.

Banaszuk, A., H.A. Hauksson and I. Mezić (1997*b*). Control of stall and surge in compressors based on Moore-Greitzer PDE model. In: *Proceedings of the 1997 International Conference on Control Applications.* Hartford, CT. pp. 677–682.

Banaszuk, A., H.A. Hauksson and I. Mezić (1998). A backstepping controller for a nonlinear partial differential equation model of compression system instablities. *SIAM Journal of Control and Optimization.* To appear.

Bazanella, A.S., P.V. Kokotović and A.S. e Silva (1997). On the control of dynamic systems with unknown operating point. In: *Proceedings of the 1997 European Control Conference.* Brussels, Belgium.

Behnken, R.L. (1997). Nonlinear control and modeling of rotating stall in an axial flow compressor. PhD thesis. California Institute of Technology. Technical report CDS 96-014.

Behnken, R.L. and R.M. Murray (1997). Combined air injection control of rotating stall and bleed valve control of surge. In: *Proceedings of the 1997 American Control Conference.* Albuquerque, NM.

Behnken, R.L., R. D'Andrea and R.M. Murray (1995). Control of rotating stall in a low-speed axial flow compressor using pulsed air injection: Modelling, simulations, and experimental validation. In: *Proceedings of the 35th Conference on Decision and Control.* New Orleans, LA. pp. 3056–3061.

Biss, D. and M.J. Grimble (1994). Robust control of a 1.5MW free turbine with complex load: Linear controller designs. In: *Proceedings of the ASME Engineering systems design and analysis 94 conference.* Vol. 6. London, UK. pp. 139–147.

Biss, D., M. Schautt and M.F. Walz (1994). Robust control of a 1.5MW free turbine with complex load: Nonliear closed loop simulations. In: *Proceedings of IEE Control'94.* pp. 1176–1181. Conference Publication No. 389.

Botros, K.K. (1994). Transient phenomena in compressor stations during surge. *Journal of Engineering for Gas Turbines and Power* **116**, 133–142.

Botros, K.K. and J.F. Henderson (1994). Developments in centrifugal compressor surge control–a technology assessment. *Journal of turbomachinery* **116**, 240–249.

Botros, K.K., P.J. Campbell and D.B. Mah (1991). Dynamic simulation of compressor station operation including centrifugal compressor and gas turbine. *Journal of Engineering for Gas Turbines and Power* **113**, 300–311.

Brown, D., L. Rachul and K. Williams (1997). NASA Researching Engine Airflow Controls to Improve Performance, Fuel Efficiency. NASA press release, downloaded from Usenet newsgroup sci.space.news. Release: 97-183.

Cargill, A.M. and C. Freeman (1991). High-speed compressor surge with application to active control. *Journal of Turbomachinery* **113**, 303–311.

Cherkassky, V.M. (1980). *Pumps, fans, compressors.* Mir Publishers. Moscow.

Cheshire, L.J. (1945). The design and development of centrifugal compressors for aircraft gas turbines. *Proceedings of the Institution of Mechanical Engineers* **153**, 426–443.

Cohen, H., G.F.C. Rogers and H.I.H Saravanamuttoo (1996). *Gas turbine theory.* 4th ed.. Longman. Essex.

Covert, E.E. (1995). Evolution of the commercial airliner. *Scientific American* **273**(3), 82–85.

Cumpsty, N.A. (1989). *Compressor Aerodynamics*. Longman.

Cumpsty, N.A. and E.M. Greitzer (1982). A simple model for compressor stall cell propagation. *Journal of Engineering for Power* **104**, 170–176.

D'Andrea, R., R.L. Behnken and R.M. Murray (1995). Active control of rotating stall using pulsed air injection: experimantal results on a low-speed, axial flow compressor. In: *Proceeding of the 1995 SPIE international symposium on aerospace/defence sensing & control and dual-use photonics*. Orlando ,FL.

D'Andrea, R., R.L. Behnken and R.M. Murray (1996). Active control of an axial flow compressor via pulsed air injection. Technical Report CIT/CDS 95-029. Caltech. Submitted, ASME J. Turbomachinery.

Davis, M.W. and W.F. O'Brien (1987). A Stage-by-stage post-stall compression system modelling technique. In: *Proceedings of AIAA/SAE/ASME/ASEE 23rd Joint Propulsion Conference*. San Diego, CA. pp. 1–14.

Day, I.J. (1993a). Active suppression of rotating stall and surge in axial compressors. *Journal of Turbomachinery* **115**, 40–47.

Day, I.J. (1993b). Stall inception in axial flow compressors. *Journal of Turbomachinery* **115**, 1–9.

Day, I.J. (1994). Axial compressor performance during surge. *Journal of propulsion and power* **10**(3), 329–336.

de Jager, B. (1995). Rotating stall and surge control : A survey. In: *Proceedings of the 35th Conference on Decision and Control*. New Orleans, LA. pp. 1857–1862.

Dean, R.C. (1974). The fluid dynamic design of advanced compressors. *Von Karman lectures*. I bestilling fra NTUB.

Dean, R.C. and L.R. Young (1977). The time domain of centrifugal compressor and pump stability and surge. *Journal of fluids engineering* **99**, 53–63.

DeLaat, J.C., R.D. Southwick and G.W. Gallops (1996). High stability engine control (HISTEC). In: *Proceedings of AIAA/SAE/ASME/ASEE 32nd Joint Propulsion Conference*. Lake Buena Vista, FL. NASA TM 107272, AIAA-96-2586.

Desoer, C.A. and M. Vidyasagar (1975). *Feedback systems: Input-Output Properties*. Academic Press.

Dixon, S.L. (1978). *Thermodynamics of turbomachinery*. 3rd ed.. Pergamon Press.

Dussourd, J.L., G.W. Pfannebecker and S.K. Singhania (1976). Considerations for the control of surge in dynamic compressors using close coupled resistances. In: *Centrifugal compressor and pump stability, stall and surge* (P.C. Tramm and R.C. Dean, Eds.). pp. 1–28. ASME. New Orleans, Louisiana. Presented at the 1976 Joint gas turbine and fluids engineering divisions' Conference.

Dussourd, J.L., G.W. Pfannebecker and S.K. Singhania (1977). An experimental investigation of the control of surge in radial compressors using close coupled resistances. *Journal of Fluids Engineering* **99**, 64–76.

Eastop, T.D. and A.McConkey (1986). *Applied thermodynamics for engineering technologists*. 4th ed.. Longman. New York.

Elder, R.L. and M.E. Gill (1985). A discussion of the factors affecting surge in centrifugal compressors. *Journal of Engineering for Gas Turbines and Power* **107**, 499–506.

Emmons, H.W., C.E. Pearson and H.P. Grant (1955). Compressor surge and stall propagation. *Transactions of the ASME* **77**, 455–469.

Epstein, A.H. (1986). 'Smart' engine components: A micro in every blade. *Aerospace America* pp. 60–64.

Epstein, A.H., J.E. Ffowcs Williams and E.M. Greitzer (1989). Active suppression of aerodynamic instabilities in turbomachines. *Journal of Propulsion and Power* **5**(2), 204–211.

Erskine, J.B. and N. Hensman (1975). Vibration induced by pump instability and surging. In: *Vibrations and noise in pump, fan, and compressor installations*. The Institution of Mechanical Engineers. Mechanical Engineering Publications limited. Southamton, UK. pp. 87–98.

Escuret, J.F. and V. Garnier (1996). Stall inception measurments in a high-speed multistage compressor. *Journal of Turbomachinery* **118**(4), 690–697.

Eveker, K.M. and C.N. Nett (1991). Model development for active surge control rotating stall avoidance in aircraft gas turbine engines. In: *Proceedings of the 1991 American Control Conference*. pp. 3166–3172.

Eveker, K.M., D.L. Gysling, C.N. Nett and O.P. Sharma (1995). Integrated control of stall and surge in aeroengines. In: *Proceedings of the 1995 SPIE Conference on sensing, acutation and control in aeropropulsion*. Orlando, FL. pp. 21–35.

Ferguson, T.B. (1963). *The centrifugal compressor stage*. Butterworths. London.

Feulner, M.R., G.J. Hendricks and J.D. Paduano (1996). Modeling for control of rotating stall in high-speed multistage axial compressors. *Journal of Turbomachinery* **118**, 1–10.

Ffowcs Williams, J.E. and W.R. Graham (1990). An engine demonstration of active surge control. In: *Proceedings of the gas turbine and aeroengine congress and exposition.* Brussels, Belgium. ASME paper no. 90-GT-224.

Ffowcs Williams, J.E. and X.Y. Huang (1989). Active stabilization of compressor surge. *Journal of Fluid Mech.* **204**, 245–262.

Ffowcs Williams, J.E., M.F.L. Harper and D.J. Allwright (1993). Active stabilization of compressor instability and surge in a working engine. *Journal of Turbomachinery* **115**, 68–75.

Fink, D.A., N.A. Cumpsty and E.M. Greitzer (1992). Surge dynamics in a free-spool centrifugal compressor system. *Journal of Turbomachinery* **114**, 321–332.

Foss, A.M, R.P.G. Heath, P. Heyworth, J.A. Cook and J.Mc Lean (1989). Thermodynamic simulation of a turbo-charged spark ignition engine for electric control development. In: *Proceedings of the Seventh IMechE International Conference on Automotive Electronics.* London. pp. 195–202. Paper no C391/044.

Fossen, T.I. (1999). Nonlinear backstepping designs: Applications to mechanical systems and ship control. In press.

Futral, S.M. and C.A. Wasserbauer (1965). Off design performance prediction with experimental verification for a radial-inflow turbine. Technical Report TN D-2621. NASA.

Garnier, V.H., A.H. Epstein and E.M. Greitzer (1991). Rotating waves as a stall inception indication in axial compressors. *Journal of Turbomachinery* **113**, 290–302.

Giannissis, G.L., A.B. McKenzie and R.L. Elder (1989). Experimental investigation of rotating stall in a mismatched trhee-stage axial flow compressor. *Journal of Turbomachinery* **111**, 418–425.

Godhavn, J.-M. (1997). Topics in nonlinear motion control: nonholonomic, underactuated and hybrid systems. PhD thesis. Norwegian University of Science and Technology. Dept of Engineering Cybernetics.

Gravdahl, J.T. (1998). Modeling and control of surge and rotating stall in compressors. PhD thesis. Norwegian University of Science and Technology.

Gravdahl, J.T. and O. Egeland (1997*a*). A Moore-Greitzer axial compressor model with spool dynamics. In: *Proceedings of the 36th IEEE Conference on Decision and Control.* San Diego, CA. pp. 4714–4719.

Gravdahl, J.T. and O. Egeland (1997*b*). Compressor surge control using a close-coupled valve and backstepping. In: *Proceedings of the 1997 American Control Conference.* Albuquerque, NM.

Gravdahl, J.T. and O. Egeland (1997*c*). Control of the three-state Moore-Greitzer compressor model using a close-coupled valve. In: *Proceedings of the 1997 European Control Conference.* Brussels, Belgium.

Gravdahl, J.T. and O. Egeland (1997*d*). Modeling of rotating stall and surge in a free spool axial compression system. *Submitted to Journal of Turbomachinery.*

Gravdahl, J.T. and O. Egeland (1997*e*). Passivity based compressor surge control using a close-coupled valve. In: *Proceedings of the 1997 COSY Workshop on Control of Nonlinear and Uncertain Systems* (A. Isidori and F. Allgöwer, Eds.). Zurich, Switzerland. pp. 139–143.

Gravdahl, J.T. and O. Egeland (1997*f*). Speed and surge control for a low order centrifugal compressor model. In: *Proceedings of the 1997 International Conference on Control Applications.* Hartford, CT. pp. 344–349.

Gravdahl, J.T. and O. Egeland (1998*a*). Centrifugal compressor surge and speed control. *IEEE Transactions on Control Systems Technology.* Accepted, to appear.

Gravdahl, J.T. and O. Egeland (1998*b*). Close Coupled Valve control of surge and rotating stall in compressors. *Submitted to Automatica.*

Gravdahl, J.T. and O. Egeland (1998*c*). Speed and surge control for a low order centrifugal compressor model. *Modeling, Identification and Control* **19**(1), 13–29.

Gravdahl, J.T. and O. Egeland (1998*d*). Two results on compressor surge control with disturbance rejection. In: *Proceedings of the 37th IEEE Conference on Decision and Control.* To appear.

Greitzer, E.M. (1976*a*). Surge and Rotating stall in axial flow compressors, Part I: Theoretical compression system model. *Journal of Engineering for Power* **98**, 190–198.

Greitzer, E.M. (1976*b*). Surge and rotating stall in axial flow compressors, Part II: Experimental results and comparison with theory. *Journal of Engineering for Power* **98**, 199–217.

Greitzer, E.M. (1977). Coupled compressor-diffuser flow instability. *Journal of aircraft* **14**(3), 233–238.

Greitzer, E.M. (1980). REVIEW–Axial compressor stall phenomena. *Journal of Fluids Engineering* **102**, 134–151.

Greitzer, E.M. (1981). The stability of pumping systems – The 1980 Freeman scholar lecture. *Journal of Fluids Engineering* **103**, 193–242.

Greitzer, E.M. (1985*a*). An introduction to unsteady flow in turbomachines. In: *Thermodynamics and Fluid Mechanics of turbomachinery* (A.Ş. Üçer, P. Stow and Ch. Hirsch, Eds.). Vol. II of *NATO ASI Series, Series E: Applied Sciences - No. 97B*. pp. 967–1024. Martin Nijhoff Publishers.

Greitzer, E.M. (1985*b*). Flow instabilities in turbomachines. In: *Thermodynamics and Fluid Mechanics of turbomachinery* (A.Ş. Üçer, P. Stow and Ch. Hirsch, Eds.). Vol. II of *NATO ASI Series, Series E: Applied Sciences - No. 97B*. pp. 1025–1079. Martin Nijhoff Publishers.

Greitzer, E.M. (1998). Smart jet engines: Case history of a multidiciplinary research program. *JSME International journal, Series B: Fluids and thermal engineering* **41**(1), 90–101.

Greitzer, E.M. and F.K. Moore (1986). A theory of post-stall transients in a axial compressor systems: Part II–Application. *Journal of Engineering for Gas Turbines and Power* **108**, 231–239.

Greitzer, E.M. and H.R. Griswold (1976). Compressor-diffuser interaction with circumferential flow distortion. *The journal of mechanical engineering science* **18**(1), 25–43.

Gu, G., A. Sparks and S. Banda (1997*a*). Bifurcation based nonlinear feedback control for rotating stall in axial compressors. *Int.J. of control* **68**(6), 1241–1257.

Gu, G., S. Banda and A. Sparks (1996). An overview of rotating stall and surge control for axial flow compressors. In: *Proceedings of the 35th Conference on Decision and Control*. Kobe, Japan.

Gu, G., X. Chen, A. Sparks and S. Banda (1997*b*). Bifurcation stabilization with local output feedback. In: *Proceedings of the 1997 American Control Conference*. Albuquerque, NM.

Gysling, D.L., J. Dugundji, E.M. Greitzer and A.H. Epstein (1991). Dynamic control of centrifugal compressors surge using tailored structures. *Journal of Turbomachinery* **113**, 710–722.

Haddad, W.M., J.L. Fausz, V.-S. Chellaboina and A. Leonessa (1997). Non-linear robust disturbance rejection controllers for rotating stall and surge in axial flow compressors. In: *Proceedings of the 1997 International Conference on Control Applications*. Hartford, CT. pp. 767–772.

Hansen, K.E., P. Jørgensen and P.S. Larsen (1981). Experimental and theoretical study of surge in a small centrifugal compressor. *Journal of Fluids Engineering* **103**, 391–394.

Harris, L.P. and H.A. Spang (1991). Compressor modelling and active control of stall/surge. In: *Proceedings of the 1991 American Control Conference*. pp. 2392–2397.

Haynes, J.M., G.J. Hendricks and A.H. Epstein (1994). Active stabilization of rotating stall in a three-stage axial compressor. *Journal of Turbomachinery* **116**, 226–239.

Hendricks, G.J. and D.L. Gysling (1994). Theoretical study of sensor-actuator schemes for rotating stall control. *Journal of Propulsion and Power* **10**(1), 101–109.

Hendrickson, E.S. and A.G. Sparks (1997). On the suitability of bifurcation stabilization control laws for high order Moore-Greitzer compressor models. In: *Proceedings of the 1997 American Control Conference*. Albuquerque, NM.

Heywood, J.B. (1988). *Internal combustion engine fundamentals*. McGraw-Hill.

Horlock, J.H. (1958). *Axial flow compressors: Fluid mechanics and Thermodynamics*. Butterworths scientific publications. London.

Humbert, J.S. and A.J. Krener (1997). Analysis of higher order Moore-Greitzer compressor models. In: *Proceedings of the 1997 International Conference on Control Applications*. Hartford, CT. pp. 651–656.

Hunziker, R. and G. Gyarmathy (1994). The operational stability of a centrifugal compressor and its dependence on the characterisitics of the subcomponents. *Journal of Turbomachinery* **116**(2), 250–259.

Hynes, T.P. and E.M. Greitzer (1987). A method for assessing effects of circumferential flow distortion on compressor stability. *Journal of Turbomachinery* **109**, 371–379.

Ishii, H. and Y. Kashiwabara (1996). Study on surge and rotating stall in axial compressors (a numerical model and parametric study for multiblade-row compressors). *JSME International Journal, Series B, Fluids and thermal engineering* **39**(3), 621–632.

Johannessen, E. (1996). Sythesis of dissipative output feedback controllers. PhD thesis. Norwegian University of Science and Technology.

Johnson, D. (1985). The Norwegian gas turbine pioneer: Aegidius Elling. *Energy world* pp. 10–12.

Johnson, D. and R.J. Mowill (1968). Ægedius Elling – A Norwegian gas turbine pioneer. Norsk Teknisk Museum.

Johnston, J.P. and R.C. Dean (1966). Losses in vaneless diffusers of centrifugal compressors and pumps. Analysis, experiment and design. *Journal of Engineering for Power* pp. 49–62.

Jungowski, W.M., M.H. Weiss and G.R. Price (1996). Pressure oscillations occurring in a centrifugal compressor system with and without passive and active surge control. *Journal of Turbomachinery* **118**, 29–40.

Kanestrøm, R. and O. Egeland (1994). Nonlinear active vibration damping. *IEEE Transactions on Automatic Control* **39**(9), 1925–1928.

Khalak, A. and R.M. Murray (1994). Experimental evaluation of air injection for actuation of rotating stall in a low speed axial fan. In: *Proceedings of ASME Turbo Expo '95*.

Koff, S.G. and E.M. Greitzer (1986). Axisymmetrically stalled flow performance for multistage axial compressors. *Journal of Turbomachinery* **108**, 216–249.

Krstić, M. (1996). Invariant manifolds and asymptotic properties of adaptive nonlinear stabilizers. *IEEE Transactions on automatic control* **41**(6), 817–829.

Krstić, M. and H.-H. Wang (1997). Control of Deep-Hysteresis aeroengine compressors–Part II : Design of control laws. In: *Proceedings of the 1997 American Control Conference*. Albuquerque, NM.

Krstić, M. and H.-H. Wang (1998). Exremum seeking feedback: Stability proof and application to an aeroengine compressor model. *Submitted to Automatica*. Revised on January 26, 1998.

Krstić, M. and P.V. Kokotović (1995). Lean backstepping designs for jet engine compressor model. In: *Proceedings of the 4th IEEE Conference on Control Applications*. pp. 1047–1052.

Krstić, M., D. Fontaine, P.V. Kokotović and J.D. Paduano (1998). Useful nonlinearities and global stabilization of bifurcations in a model of jet engine surge and stall. *IEEE Trancactions on Automatic Control*. to appear.

Krstić, M., I. Kanellakopoulos and P.V. Kokotović (1995a). *Nonlinear and Adaptive Control Design*. John Wiley & Sons Inc.

Krstić, M., J.M. Protz, J.D. Paduano and P.V. Kokotović (1995b). Backstepping designs for jet engine stall and surge control. In: *Proceedings of the 35th Conference on Decision and Control*. New Orleans, LA. pp. 3049–3055.

Larsen, M., B. Coller, R. Sepulchre and P.V. Kokotovič (1997). Dynamic control of axial compressors. In: *Proceedings of the 1997 International Conference on Control Applications*. Hartford, CT. pp. 663–670.

Lawless, P.B., K.H. Kim and S. Fleeter (1994). Characteriszation of abrupt rotating stall initiation in an axial flow compressor. *Journal of Propulsion and Power* **10**(5), 709–715.

Leonessa, A., V.-S. Chellaboina and W.M. Haddad (1997a). Globally stabilizing controllers for multi-mode axial flow compressor models via equilibria-dependent lyapunov functions. In: *Proceedings of the 1997 International Conference on Control Applications*. Hartford, CT. pp. 63–68.

Leonessa, A., V.-S. Chellaboina and W.M. Haddad (1997b). Robust stabilization of axial flow compressors with uncertain pressure-flow maps. In: *Proceedings of the 1997 International Conference on Control Applications*. Hartford, CT. pp. 671–676.

Liaw, D.-C. and E.H. Abed (1992). Stability analysis and control of rotating stall. In: *Proceedings of NOLCOS'92: Nonlinear Control System Design Symposium* (M. Fliess, Ed.). Bourdaux, France. pp. 88–93.

Liaw, D.-C. and E.H. Abed (1996). Active control of compressor stall inception: a bifurcation-theoretic approach. *Automatica* **32**(1), 109–115.

Longley, J.P. (1994). A review of nonsteady flow models for compressor stability. *Journal of turbomachinery* **116**, 202–215.

Lorenzo, C.F., F.P. chiaramonte and C.M. Mehalic (1986). Determination of compressor in-stall characteristics from engine surge transients. *Journal of Propulsion and Power* **4**(2), 133–142.

Lorett, J.A. and S. Gopalakrishnan (1986). Interaction between impeller and volute of pumps at off-design conditions. *Journal of fluids engineering* **108**, 12–18.

Macdougal, I. and R.L. Elder (1983). Simulation of centrifugal compressor transient performance for process plant applications. *Journal of Engineering for Power* **105**, 885–890.

Mansoux, C.A., D.L. Gysling, J.D. Setiawan and J.D. Paduano (1994). Distributed nonlinear modeling and stability analysis of axial compressor stall and surge. In: *Proceedings of the 1994 American Control Conference*. Baltimore, Maryland. pp. 2305–2316.

Mattingly, J.D. (1996). *Elements of gas turbine propulsion*. McGraw-Hill series in aeronautical and aerospace engineering. McGraw-Hill.

Mazzawy, R.S. (1980). Surge induced structural loads in gas turbines. *Journal of engineering for power* **102**, 162–168.

McCaughan, F.E. (1989). Application of Bifurcation theory to axial flow compressor instability. *Journal of Turbomachinery* **111**, 426–433.

McCaughan, F.E. (1990). Bifurcation analysis of axial flow compressor stability. *SIAM Journal of Applied Mathematics* **50**(5), 1232–1253.

Mees, A.I. (1983). A plain man's guide to bifurcations. *IEEE Transactions on Circuits and Systems* **30**(8), 512–517.

Meuleman, C., F. Willems, R. de Lange and B. de Jager (1998). Surge in a low-speed radial compressor. In: *Proceedings of the 1998 ASME International Gas Turbine & Aeroengine Congress & Exhibition*. Stckholm, Sweden. ASME paper no 98-GT-426.

Moore, F.K. (1984a). A theory of rotating stall of multistage axial compressors: Part I–Small disturbances. *Journal of Engineering for Gas Turbines and Power* **106**, 313–320.

Moore, F.K. (1984b). A theory of rotating stall of multistage axial compressors: Part II–Finite disturbances. *Journal of Engineering for Gas Turbines and Power* **106**, 321–326.

Moore, F.K. (1984c). A theory of rotating stall of multistage axial compressors: Parts I,II,III. *J. of Engineering for Gas Turbines and Power* **106**, 313–336.

Moore, F.K. (1986). Stall transients of axial compression systems with inlet distortion. *Journal of Propulsion and Power* **2**(6), 552–561.

Moore, F.K. and E.M. Greitzer (1986). A theory of post-stall transients in a axial compressor systems: Part I–Development of equations. *Journal of Engineering for Gas Turbines and Power* **108**, 68–76.

Nakagawa, K., M. Fujiwara, T. Nishioka, S. Tanaka and Y. Kashiwabara (1994). Experimental and numerical analysis of active suppression of centrifugal compressor surge by suction-side valve control. *JSME International Journal, Series B, Fluids and thermal engineering* **37**(4), 878–885.

Nicklasson, P.J. (1996). Passivity-based control of electric machines. PhD thesis. Norwegian Institute of Technology. Dept of Engineering Cybernetics.

Nisenfeld, A.E. (1982). *Centrifugal compressors: principles of operation and control*. Instrument society of America.

Nishihara, Y. (1993). Surging behaviour of gas turbines. *JSME International Journal, Series B, Fuids and thermal engineering* **36**(4), 567–576.

Oliva, S.M. and C.N. Nett (1991). A general nonlinear dynamical analysis of a second-order, one-dimensional, theoretical compression system model. In: *Proceedings of the 1991 American Control Conference*. pp. 3158–3165.

Onions, R.A. and A.M. Foss (1982). Improvements in the dynamic simulation of gas turbines. In: *AGARD conference proceedings no 324, Engine handling*. Marathon, Greece.

Ordys, A.W., A.W. Pike, M.A. Johnson, R.M Katebi and M.J. Grimble (1994). *Modelling and simulation of power generation plants*. Advances in Industrial Control. Springer-verlag. London.

Osborn, W.M. and J.M. Wagner (1970). Effect of simulated downstream flow blockage doors on the performance of an axial-flow fan rotor. Technical Report TN D-6071. NASA.

Paduano, J.D., A.H. Epstein, L. Valavani, J.P. Longley, E.M. Greitzer and G.R. Guenette (1993). Active control of rotating stall in a low-speed axial compressor. *Journal of Turbomachinery* **115**, 48–56.

Paduano, J.D., A.H. Epstein, L. Valavani, J.P. Longley, E.M. Greitzer and G.R. Guenette (1994). Modelling for control of rotating stall. *Automatica* **30**(9), 1357–1373.

Pampreen, R.C. (1973). Small turbomachinery compressor and fan aerodynamics. *Journal of engineering for power* **95**, 251–256.

Perko, L. (1991). *Differential equations and dynamical systems*. Vol. 7 of *Texts in Applied Mathematics*. Springer-Verlag.

Pichot, P. (1986). *Compressor application engineering: Compressor equipment*. Vol. 1. Gulf Publishing Company.

Pinsley, J.E., G.R. Guenette, A.H. Epstein and E.M. Greitzer (1991). Active stabilization of centrifugal compressor surge. *Journal of Turbomachinery* **113**, 723–732.

Protz, J.M. and J.D. Paduano (1997). Rotating stall and surge: Alternate modeling and control concepts. In: *Proceedings of the 1997 International Conference on Control Applications*. Hartford, CT. pp. 866–873.

Qi, O.F., N.R.L Maccallum and P.J. Gawthrop (1992*a*). Improving dynamic response of a single-spool gas turbine engine using a nonlinear controller. In: *Proceedings if the 1992 IEEE CCA*. Dayton, Ohio.

Qi, O.F., P.J. Gawthrop and N.R.L Maccallum (1992*b*). Model-based observer: A gas turbine engine case study. In: *Proceedings of the 1992 IEEE CDC*.

Rowen, W.I. (1983). Simplified mathematical representations of heavy-duty gas turbines. *Journal of engineering for power* **105**, 865–869.

Ruffles, P.C (1996). Innovation in aero engines. *The Aeronautical Journal* **100**(1000), 473–484.

Saravanamutto, H.I.H. (1982). An overview of engine dynamic response and mathematical modeling concepts. In: *AGARD conference proceedings no 324, Engine handling*. Marathon, Greece.

Saravanamuttoo, H.I.H. and A.J. Fawke (1970). Simulation of gas turbine dynamic performance. In: *Proceedings of the ASME Gas turbine conference*. Brussels, Belgium. ASME paper No 70-GT-23.

Sepulchre, R. and P. Kokotović (1996). Shape signifiers for throttle control of a low-order compressor model.

Simon, J.S. and L. Valavani (1991). A Lyapunov based nonlinear control scheme for stabilizing a basic compression system using a close-coupled control valve. In: *Proceedings of the 1991 American Control Conference*. pp. 2398–2406.

Simon, J.S., L. Valavani, A.H. Epstein and E.M. Greitzer (1993). Evaluation of approaches to active compressor surge stabilization. *Journal of Turbomachinery* **115**, 57–67.

Simon, S. (1993). Feedback stabilization of compression systems. PhD thesis. MIT.

Sparks, A. and G. Gu (1997). Control of compressor rotating stall without distributed sensing using bifurcation stabilization. In: *Proceedings of the 1997 American Control Conference*. Albuquerque, NM.

Staroselsky, N. and L. Ladin (1979). Improved surge control for centrifugal compressors. *Chemical engineering* pp. 175–184.

Stenning, A.H. (1980). Rotating stall and surge. *Journal of fluids engineering* **102**, 14–21.

Stetson, H.D. (1982). Designing for stability in advanced turbine engines. In: *AGARD conference proceedings no 324, Engine handling*. Marathon, Greece.

Sugiyama, Y., W. Tabakoff and A. Hamed (1989). J85 Surge transient simulation. *Journal of Propulsion and Power* 5(3), 375–381.

Takata, H. and S. Nagano (1972). Nonlinear analysis of rotating stall. *Journal of engineering for power* 94, 279–293.

Takata, H. and Y. Tsukuda (1977). Stall margin improvement by casing treatment – its mechanism and effectiveness. *Journal of engineering for power* pp. 121–133.

Thorley, A.R.D. and C.H. Tiley (1987). Unsteady and transient flow of compressible fulids in pipelines – a review of theoretical and some experimental studies. *The International journal of heat and fluid flow* 8(1), 3–15.

Tøndel, J.P. (1996). Control of gas turbine under transients. Master's thesis. Norwegian University of Science and Technology. Dept. of Engineering Cybernetics. (In Norwegian).

Toyama, K., P.W. Runstadtler and R.C. Dean (1977). An experimental study of surge in centrifugal compressors. *Journal of fluids engineering* 99, 115–131.

van de Wal, M (1998). Selection of inputs and outputs for control. PhD thesis. Technische Universitet Eindhoven.

van de Wal, M. and F. Willems (1996). Selection of actuators and sensors for compressor control. Technical Report WFW 96.155. Eindhoven University of Technology.

van de Wal, M., F. Willems and B. de Jager (1997). Selection of actuators and sensors for active surge control. In: *Proceedings of the 1997 International Conference on Control Applications*. Hartford, CT. pp. 121–127.

van der Schaft, A.J. (1996). L_2-*gain and passivity techniques in nonlinear control*. Vol. 218 of *Lecture notes in Control and Information Sciences*. Springer-Verlag. Heidelberg.

van Schalkwyk, C.M., R.K. Mehra and J.D. Paduano (1997). Semi-active stabilization of axial compressors with circumferential inlet distortion using low bandwidth actuators. In: *Proceedings of the 1997 International Conference on Control Applications*. Hartford, CT. pp. 874–879.

Wang, H.-H. (1998). Bifurcation control and extremum seeking for aeroengine compressors and bioreactors. PhD thesis. University of Maryland.

Wang, H.-H. and M. Krstić (1997*a*). Control of Deep-Hysteresis aeroengine compressors–Part I : A Moore-Greitzer type model. In: *Proceedings of the 1997 American Control Conference*. Albuquerque, NM.

Wang, H.-H. and M. Krstić (1997*b*). Control of deep hysteresis compressors under limited actuator bandwidth. In: *Proceedings of the 1997 International Conference on Control Applications*. Hartford, CT. pp. 657–662.

Wang, H.-H., S. Yeung and M. Krstić (1998). Experimental application of extremum seeking on an axial-flow compressor. In: *Proceedings of th 1998 American Control Conference*. Philadelphia, PA.

Wang, H.O., R.A Adomaitis and E.H. Abed (1994). Nonlinear analysis and control of rotating stall in axial flow compressors. In: *Proceedings of the 1994 American Control Conference*. Baltimore, ML. pp. 2317–2321.

Wang, Y. and R.M. Murray (1997). Effects of noise, magnitude saturation and rate limits on rotating stall control. In: *Proceedings of the 36th IEEE Conference on Decision and Control*.

Wang, Y. and R.M. Murray (1998). Effects of the shape of compressor characteristics on actuator requirements for rotating stall control. In: *Proceedings of the 1998 American Control Conference*.

Watson, N. and M.S. Janota (1982). *Turbocharging the internal combustion engine*. MacMillan.

Weigl, H.J. and J.D. Paduano (1997). Application of $\mathcal{H}_\infty$ control with eigenvalue perturbations to stabilize a transonic compressor. In: *Proceedings of the 1997 International Conference on Control Applications*. Hartford, CT. pp. 691–698.

White, F.M. (1986). *Fluid mechanics*. 2nd ed.. McGraw-Hill. New York.

Whitfield, A. and F.J. Wallace (1973). Study of incidence loss models in radial and mixed-flow turbomachinery. In: *Proceedings of the conference on heat and fluid flow in steam and gas turbine plant*. The instn. of Mech. Engnrs.. U. of Warwick, Coventry. pp. 122–128.

Whitfield, A. and F.J. Wallace (1975). Performance prediction for automotive turbocharger compressors. *Proceedings of the institution of mechanical engineers* **189**(12), 59–67.

Whittle, Sir Frank (1953). *JET. The story of a Pioneer*. Frederick Muller Ltd. London.

Whittle, Sir Frank (1981). *Gas turbine aerodynamics*. Pergamon Press.

Willems, F. (1996). Modeling and control of compressor flow instabilities. Technical Report WFW 96.151. Eindhoven University of Technology.

Willems, F. and B. de Jager (1998*a*). Active compressor surge control using a one-sided controlled bleed/recycle valve. In: *Procceedings of the 1998 IEEE Conference on Decision and Control*. Tampa, Fl.

Willems, F. and B. de Jager (1998*b*). Modeling and control of rotating stall and surge: An overview. In: *Proceedings of the 1998 IEEE Conference on Control Applications*. Trieste, Italy.

Wo, A.M. and J.P. Bons (1994). Flow physics leading to system instability in a centrifugal pump. *Journal of Turbomachinery* **116**, 612–620.

Yeung, S. and R.M. Murray (1997*a*). Nonlinear control of rotating stall using axisymmetric bleed with continuous air injection on a low-speed, single stage, axial compressor. In: *Proceedings of the 33rd AIAA/ASME/SAE/ASEE Joint propulsion conference*. Seattle, WA.

Yeung, S. and R.M. Murray (1997*b*). Reduction of bleed valve rate requirements for control of rotating stall using continuous air injection. In: *Proceedings of the 1997 International Conference on Control Applications*. Hartford, CT. pp. 683–690.

Yeung, S. and R.M. Murray (1998). Simultaneous stabilization of stall and surge via axisymmetric air injection. Submitted to the 7th IEEE International Conference on Control Applications.

Yeung, S., Y. Wang and R.M. Murray (1998). Evaluation of bleed valve requirements in nonlinear control of rotating stall on axial flow compressors. Submitted to AIAA Journal of propulsion and power.

APPENDIX A
STABILITY OF THE GREITZER MODEL

When linearizing (1.9) around the equilibrium defined by the intersection of the throttle characteristic Ψ_T and the compressor characteristic Ψ_c, the following model is found

$$
\left(\begin{array}{c} \dot{\Phi} \\ \dot{\Psi} \end{array} \right) = \underbrace{\left(\begin{array}{cc} Ba_C & -B \\ \frac{1}{B} & -\frac{1}{Ba_T} \end{array} \right)}_{A} \left(\begin{array}{c} \Phi \\ \Psi \end{array} \right),
\tag{A.1}
$$

where $a_c = \frac{\partial \Psi_c}{\partial \Phi}\big|_{eq.}$ and $a_T = \frac{\partial \Psi_T}{\partial \Phi}\big|_{eq.}$ The eigenvalues of A are found to be

$$
\lambda = \frac{-\left(\frac{1}{Ba_T} - Ba_c \right) \pm \sqrt{\left(\frac{1}{Ba_T} - Ba_c \right)^2 - 4\left(1 - \frac{a_c}{a_T} \right)}}{2}.
\tag{A.2}
$$

The stability properties of the equilibrium will depend on the relative magnitude of the terms B, a_T and a_c. In Figure A.1 it is illustrated how the stability properties of the system vary with the terms

$$
T_a \triangleq \left(\frac{1}{Ba_T} - Ba_c \right)
$$

and

$$
T_b \triangleq \left(1 - \frac{a_c}{a_T} \right).
$$

Greitzer (1980) use T_a to determine dynamic stability, and T_b to determine static stability. As can be seen, T_b will be negative if the slope of the compressor characteristic is greater than the slope of the throttle characteristic.

$$\left(\frac{1}{Ba_T} - Ba_c\right)$$

Stable focus

$Im\lambda$

$Re\lambda$

$Im\lambda$ $Im\lambda$

$Re\lambda$ $Re\lambda$

Saddle   Stable node

$Im\lambda$ $Im\lambda$

Saddle   Unstable node

$Re\lambda$ $Re\lambda$

$\left(1 - \frac{a_c}{a_T}\right)$

$Im\lambda$

$Re\lambda$

Unstable focus
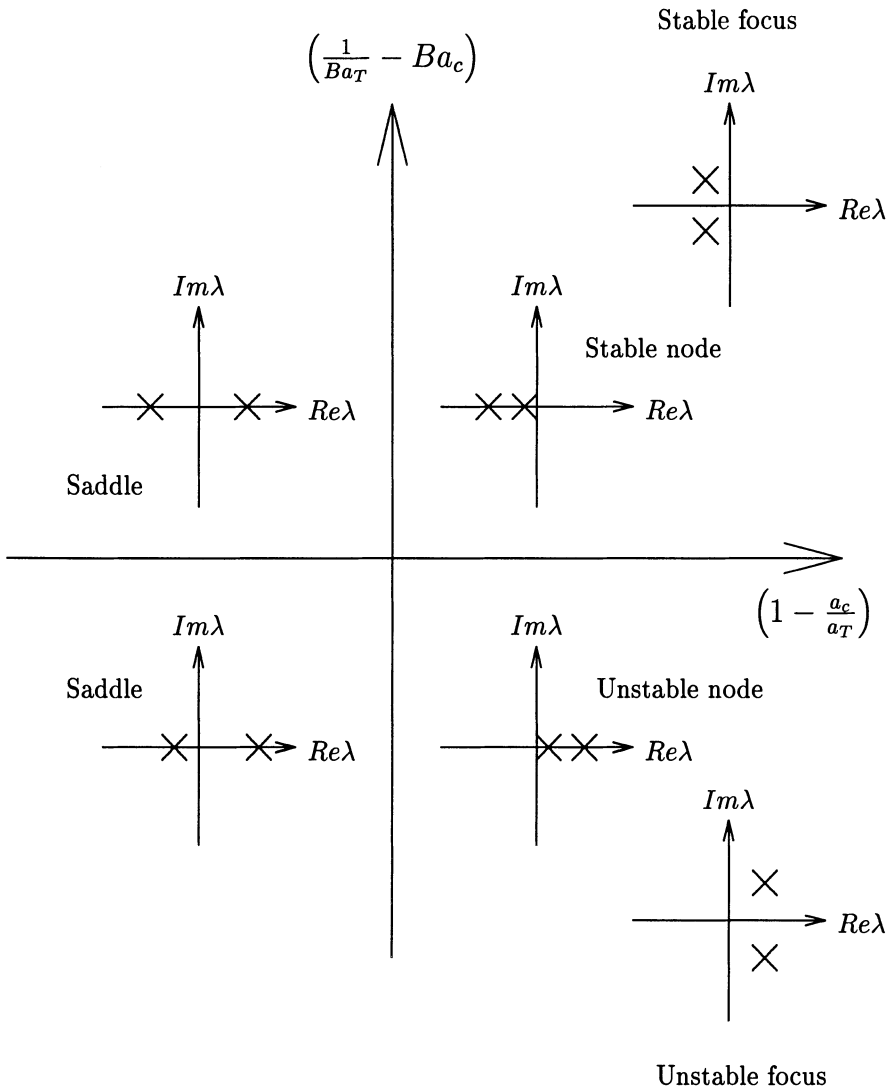
Figure A.1: *Stability of the linearized Greitzer model*

In Figure A.1, it is seen that if $T_b < 0$, the system have one eigenvalue in the left half-plane and one eigenvalue in the right half plane, and the equilibrium is thus a saddle-point, which is unstable. This kind of instability is named *static* by Greitzer (1980). On the other hand, if $T_b > 0$ and $T_a < 0$, the equilibrium can be one of two types, dependent on the numerical value of B. In this case, if $T_b^2 < 4T_a$ the equilibrium will be an unstable focus, and

if $T_b^2 > 4T_a$, the equilibrium will be an unstable node. The unstable focus is termed a dynamic instability and the unstable node a static instability by Greitzer (1980). According to Greitzer (1980), the instability will be dynamic (focus) provided that $T_a < 0$ and $T_b > 0$. As shown above, this is not entirely correct. Also seen in Figure A.1 is that if both $T_a > 0$ and $T_b > 0$, the equilibrium will be stable. Dependent on B, the equilibrium will be either a stable focus or a stable node.

It is to be emphasized that whether or not the instability is dynamic or static, the *nonlinear* system (1.9) will go into surge oscillations.

APPENDIX B

NOMENCLATURE

The nomenclature presented here mainly covers the symbols used in Chapter 2,3,4 and 5. In Chapter 1, the notation and many of the symbols used are taken from the reviewed literature.

Table B.1: Acronyms

CCV	Close Coupled Valve
CLF	Control Lyapunov Function
IGV	Inlet Guide vanes
ODE	Ordinary Differential Equation
PDE	Partial Differential Equation
PDF	Positive Definite Function
GAS	Globally Asymptotically Stable
GES	Globally Exponentially Stable
MG	Moore-Greitzer

Table B.2: Subscripts

0	Equilibrium value
c	Compressor
d	Disturbance or desired value
x, a	Axial
p	Plenum
η, θ, ξ	Partial derivative with respect to η, θ or ξ

Table B.3: Mathematical symbols

$(\dot{\cdot})$	Total time derivative, $\frac{d}{dt}$ or $\frac{d}{d\xi}$
$\frac{\partial}{\partial x}$	Partial derivative with respect to variable x
$(\cdot)^{-1}$	Inverse operator
$(\tilde{\cdot})$	Deviation from equilibrium, transformed coordinates
$\|\cdot\|_{\infty}$	The $\mathcal{L}_{\infty}$-norm of the function
	$f : \mathbb{R}^{+} \to \mathbb{R}$ is defined as $\|f\|_{\infty} = \sup_{t \geq 0} |f(t)|$
$|\cdot|$	Magnitude of vector
$(\cdot)^{T}$	Transpose operator
$\forall$	For all
$\exists$	Exists
$\mathbb{R}$	Real numbers
$\mathbb{R}^{+}$	Nonnegative real numbers $\{x \in \mathbb{R} : x \geq 0\}$
$\mathbb{R}^{n}$	Linear space of n-tuples in $\mathbb{R}$
∇	Divergence operator. $\nabla \cdot \boldsymbol{f}(x_1, x_2, \ldots) = \frac{\partial f_1}{\partial x_1} + \frac{\partial f_2}{\partial x_2} + \ldots$
$\mathcal{K}$	Class of functions. A function $f : [0, a) \to \mathbb{R}^{+}$ is said to
	belong to class $\mathcal{K}$ if it is strictly increasing and $f(0) = 0$.
$\mathcal{K}_{\infty}$	Class of functions. A function $f : [0, a) \to \mathbb{R}^{+}$ is said
	to belong to class $\mathcal{K}_{\infty}$ if it belongs to class $\mathcal{K}$,
	$a = \infty$ and $f(r) \to \infty$ as $r \to \infty$.
$\circ$	The function $f \circ g$ is the composition of
	the functions f and g
$\mapsto$	Mapping
$\mathcal{L}_2$	Space of square integrable functions. $f : \mathbb{R}_{+} \to \mathbb{R}$
	belongs to $\mathcal{L}_2$ iff $\int_0^{\infty} |f(t)|^2 dt < \infty$
$f_T(t)$	The truncation of f to $[0, T]$.
	$f_T(t) = \begin{cases} f(t) & , \quad 0 \leq t < T \\ 0 & , \quad\quad t \geq T \end{cases}$
$\mathcal{L}_{2e}$	The extension of $\mathcal{L}_2$. $f \in \mathcal{L}_{2e}$ iff $f_T \in \mathcal{L}_2$
$\mathcal{G}$	Input-output mapping
$\langle u, y \rangle_T$	Inner product on $\mathcal{L}_{2e}$. $\langle u, y \rangle_T = \int_0^T u(t)y(t)dt$
$\|u\|_T^2$	Truncated norm. $\|u\|_T^2 = \langle u, u \rangle_T$
$\text{sgn}(\cdot)$	Signum function
$\tanh(\cdot)$	Hyperbolic tangent
$\sup(\cdot)$	Supremum, lower upper bound

Table B.4: Latin Uppercase symbols

A_c	Flow area
$\boldsymbol{A_{cl}}$	Closed loop Jacobian
A_1	Reference flow area. Area of impeller eye.
A_n	Amplitude of mode number n of rotating stall
$\boldsymbol{A_z(z, \overline{d})}$	Nonlinear part of error dynamics
$\mathcal{A}$	Area of attraction
B	Greitzer B-parameter
$C_{\theta 1}, C_{\theta 2}$	Tangential fluid velocity at the rotor entrance and exit
C_x, C_{a1}, C_{a2}	Axial fluid velocity
C_1	Fluid velocity at inducer
C_2	Fluid velocity at diffuser entry
C_h	Surface friction loss coefficient
$\overline{C}_2, \overline{C}_3, \overline{C}_4$	Functions used to calculate upper bound on c_3 in the proof of Theorem 2.5
$\underline{C}_1, \underline{C}_3, \underline{C}_4$	Functions used to calculate lower bound on c_3 in the proof of Theorem 2.5
D	Hydraulic diameter
D_1, r_1	Average inducer diameter and radius
D_2, r_2	Diameter and radius at impeller tip
D_{t1}	Diameter at inducer tip
D_{h1}	Diameter at impeller hub casing
$F(\phi)$	Pressure rise coefficient in blade passage
$G_1(\phi), G_2(\phi)$	Functions used in the proof of Theorem 2.5
$\mathcal{G}_1, \mathcal{G}_2$	Input-output mappings
H	Compressor characteristic semi height
I	Spool and rotor moment of inertia
$\hat{I}$	Integral of $\hat{U}$
J	Squared amplitude of rotating stall
J_i	Mode i of squared amplitude of rotating stall
J_{ne}	Equilibrium value of J_n
$J_{\max}$	Maximum value of squared rotating stall amplitude
$K(\hat{\phi})$	Function, used in passivity analysis
K_G	Entrance recovery coefficient
L_c	Length of ducts and compressor
L_I	Length of inlet duct
L_E	Length of exit duct
M_1, M_2, M_3	Moments calculated in Galerkin approximation

continued from previous page	
N_s	Number of compressor stages
N	Number of revolutions per second
$N(\mu)$	Number of rotating stall modes
$\boldsymbol{P}$	Positive definite constant matrix
$\boldsymbol{P}_z$	Constant skew symmetric matrix
$P(\phi)$	Matrix used in proof of Theorem 2.5
Q	Supplied heat
R_n	Residue nr. n used in Galerkin approximation
R	Mean compressor radius
$\boldsymbol{R}$	Positive definite constant matrix
Re	Reynolds number
$\mathcal{R}_\Delta, \mathcal{R}_1, \mathcal{R}_2, \mathcal{R}_3$	Residual sets
$S(z)$	Storage function
T_{01}	Inlet stagnation temperature
$U(z_1, z_2, J)$	PDF
U	Tangential speed of rotor
U_1	Tangential speed of rotor, at diameter D_1
U_2	Tangential impeller tip speed
U_d	Desired tangential speed of rotor
U_m	Upper bound on U_1
V_p	Plenum volume
V_1, V_2	LFCs
$\left(\dot{V}_2\right)_i$	Term number i in $\dot{V}_2$
W	Compressor characteristic semi width
$W(z_1, z_2)$	PDF
W_1	Fluid velocity relative to moving impeller blades
W_{1b}	Component of W_1 in blade direction
$W_{\theta 1}$	Tangential component of W_1
$\dot{W}_c$	Compressor power

Table B.5: Latin lowercase symbols

a	Reciprocal time lag of the compressor passage
a	Compressor characteristic slope
a_s	Sonic velocity
a_m	Max positive slope of compressor characteristic
b	Constant. $U = bB$
c_2, c_3	Surge/stall controller gains
c	Constant. Used in convergence proof
c_{speed}	Speed controller gain
c_n	Slope of backflow characteristic

	continued from previous page
$c_3^{\min}, c_3^{\max}$	Lower and upper bound on c_3
c_p	Specific heat capacity at constant pressure
c_v	Specific heat capacity at constant volume
d_ϕ, d_ψ	Mass flow and pressure biases
d_1, d_2	Surge/stall controller damping coefficients
$\bar{d}_\psi, \bar{d}_\phi$	Estimates of biases
$\tilde{d}_\psi, \tilde{d}_\phi$	Estimation errors
$\tilde{d}$	$(\tilde{d}_\psi\ \tilde{d}_\phi)^{\mathrm{T}}$
f	Friction factor
$g(\xi, \theta)$	Disturbance of axial flow coefficient
$h(\xi, \theta)$	Circumferential velocity coefficient
h_1, h_2, h_3	Weight functions used in Galerkin approximation
h	Specific enthalpy
k_1, k_2, k_3	Compressor characteristic coefficients
k_v	Surge control law parameter
k_p, k_i	Proportional and integral gain of speed controller
l_c	Nondimensional compressor length
l_i	Nondimensional length of inlet duct
l_e	Nondimensional length of exit duct
l	Mean flow length
m, m_c	Compressor mass flow
m	Compressor duct flow parameter
m_{choke}	Choking mass flow
p	Pressure
p_p	Plenum pressure
$\hat{p}_{max}$	Upper bound on $\hat{p}$ used to calculate δ_2 (5.82)
p_0, m_0	Equilibrium value of p_p and m
r_n	Phase angle of mode number n of rotating stall
q	Dimension of state space in Chapter 4
$s(\xi, z)$	Signal. Used in convergence proof
s	Specific entropy
u	Control variable
v	Specific volume
z_1, z_2	Error variables
z	State vector. $z = (z_1\ z_2)^{\mathrm{T}}$

Table B.6: Greek uppercase symbols

$\Delta\eta_{bf}$	Loss in efficiency due to backflow
$\Delta\eta_c$	Loss in efficiency due to clearance
$\Delta\eta_v$	Loss in efficiency in the volute
$\Delta\eta_d$	Loss in efficiency due to incomplete diffusion

continued from previous page	
$\Delta\phi$	Approximation error $\Delta\phi = \phi_0 - \phi_{apprx}$ (2.64)
Δh_{0c}	Ideal specific enthalpy delivered to fluid
$\Delta h_{0c,ideal}$	Total specific enthalpy delivered to fluid
$\Delta h_{ii}, \Delta h_{id}$	Incidence losses in impeller and diffuser
$\Delta h_{fi}, \Delta h_{fd}$	Friction losses in impeller and diffuser
Γ_t	Nondimensional turbine (drive) torque
Γ_c	Nondimensional compressor torque
Γ	Positive definite constant matrix
Λ_1, Λ_2	Constants in MG model
$\Sigma_{\mathcal{G}_1,\mathcal{G}_2}$	Feedback interconnection of $\mathcal{G}_1$ and $\mathcal{G}_2$, Theorem 3.1
Φ	Axial mass flow coefficient, annulus averaged
$\Phi_T(\psi)$	Throttle mass flow coefficient
$\hat{\Phi}_d$	Time varying mass flow disturbance
$\overline{\Psi}_d(\xi)$	Monotonically decreasing non negative function
$\overline{\Phi}_d(\xi)$	Monotonically decreasing non negative functions
Ψ	Pressure coefficient
$\Psi_T(\phi)$	Throttle characteristic
$\Psi_v(\phi]$	CCV characteristic
$\Psi_c(\phi)$	Compressor characteristic
$\Psi_e(\phi)$	Equivalent compressor characteristic
$\Psi_s(\phi)$	In-stall characteristic
$\Psi_{es}(\phi)$	Equivalent in-stall characteristic
$\hat{\Psi}_d$	Time varying pressure disturbance

Table B.7: Greek lowercase symbols

α	Virtual control used in backstepping
$\alpha_1, \alpha_2, \beta_1, \beta_2$	Fluid angles
$\beta_{1b}, \beta_{2b}, \alpha_{1b}, \alpha_{2b}$	Constant blade angles
β_i	Angle of incidence
$\beta_1, \beta_2, \beta_3$	Class $\mathcal{K}_\infty$ functions
γ_T	Throttle gain, parameter proportional
	to throttle opening
γ	CCV gain, parameter prop. to valve opening
γ_1, γ_2	Adaption gains
δ_1, δ_2	Constants
$\lambda, \lambda_1, \lambda_2$	Constants
ζ_n	$\zeta_n \overset{\Delta}{=} n\theta - r_n(\xi)$
η	Nondimensional x-coordinate
$\eta_0, \eta_1, \eta_2, \eta_3, \eta_4$	Constants. Used in Young's inequality
η_i	Isentropic efficiency
	continued on next page

continued from previous page	
θ	Angular coordinate
κ_1, κ_2	Constants used in passivity proofs
κ	Ratio of specific heats, $\kappa = \frac{c_p}{c_v}$
μ	Viscosity
ν_1, ν_2	Constants
ϖ	Convergence rate
ξ	Nondimensional time
ϱ	Constant in the MG model
ρ	Density
ρ_{01}	Inlet stagnation density
σ	Slip factor
ς	Constant
τ_t	Turbine (drive) torque
τ_c	Compressor torque
τ_c^-, τ_c^+	Compressor torque for neg. and pos. flow
τ_{df}	Disc friction torque
ϕ	Local axial mass flow coefficient
ϕ_0	Equilibrium value of ϕ
ϕ_{apprx}	Approximation of ϕ_0
ϕ_{choke}	Upper bound on ϕ
ϕ_m	Lower bound on ϕ
$\tilde{\phi}$	Velocity potential
$\tilde{\phi}'$	Disturbance velocity potential
ψ_0	Equilibrium value of ψ
ψ_{c0}	Shut off value of compressor characteristic
ω_H	Helmholtz frequency
ω	Rotational velocity of spool

APPENDIX C

SOME THERMODYNAMIC AND
FLUID MECHANICAL RELATIONS

C.1 Flow and Pressure Coefficients

In this section various nondimensional quantities related to compressors are presented.

Flow Coefficient

The flow coefficient is defined as

$$\phi = \frac{C_x}{U}, \tag{C.1}$$

where C_x is the axial velocity and U is the blade speed. Using the ideal gas law it is found that

$$\phi = \frac{\rho_{01} R T_{01}}{p_{01}} \frac{C_x}{U} = \frac{\sqrt{R T_{01}}}{U} \frac{m \sqrt{R T_{01}}}{A p_{01}} = \frac{\sqrt{R T_{01}}}{U} F, \tag{C.2}$$

where F is known as the (nondimensional) flow function. Mention must be made to another form of nondimensional flow, *the corrected mass flow* defined as

$$m_{corr} = \frac{m \sqrt{T_{01}/T_{ref}}}{p_{01}/p_{ref}}. \tag{C.3}$$

The reference state is usually taken as sea level static. It can be shown that the corrected mass flow is related to the flow coefficient as

$$\phi = \frac{\sqrt{T_{01}/T_{ref}}}{p_{ref}\sqrt{R} U A} m_{corr}, \tag{C.4}$$

that is, for constant U, ϕ is proportional to m_{corr}.

Pressure Coefficient

The total to static pressure rise coefficient is defined as

$$\Psi = \frac{p_1 - p_{01}}{\rho U^2}.$$ (C.5)

In Cohen *et al.* (1996) it is shown that

$$\Psi = \eta_i \frac{c_p \Delta T_{0s}}{U^2} = \eta_i \frac{\Delta h_{0s}}{U^2},$$ (C.6)

where η_i is the isentropic efficiency, ΔT_{0s} is the temperature rise in the stage and h_{0s} is the enthalpy rise. The fraction $c_p \Delta T_{0s}/U^2$ is known as the temperature coefficient.

Speed Coefficient

Blade speed U can be nondimensionalized by dividing with inlet stagnation sonic velocity a_{01},

$$\frac{U}{a_{01}} = \frac{U}{\kappa R T_{01}} = \frac{D \pi N}{\kappa R T_{01}} = \frac{D \pi}{\kappa R T_{ref}} N_{corr},$$ (C.7)

where $N_{corr} = N/\sqrt{T_0/T_{ref}}$ is known as the *corrected speed*. Note that by introducing the Greitzer B-parameter it is found that

$$\frac{U}{a_{01}} = \frac{D \pi}{\kappa R T_{ref}} N_{corr} = 2B \sqrt{\frac{A_c L_c}{V_p}}.$$ (C.8)

Thus, B can be used as nondimensional compressor speed, and it is connected to N_{corr} as

$$N_{corr} = 2B \sqrt{\frac{A_c L_c}{V_p}} \frac{\kappa R T_{ref}}{D \pi}.$$ (C.9)

C.2   Isentropic Processes

Let s denote specific entropy, u denote specific internal energy, $v = V/m = \rho^{-1}$ denote specific volume and $h = u + pv$ denote specific enthalpy. Eastop and A.McConkey (1986) show that

$$ds = \frac{dQ}{T},$$ (C.10)

where

$$dQ = du + pdv$$ (C.11)

is known as the differential form of the non-flow energy equation. It follows that

$$T\,ds = du + p\,dv$$
$$T\,ds = dh - v\,dp. \tag{C.12}$$

With constant specific heat capacities c_p and c_v,

$$T\,ds = c_v\,dT + p\,dv$$
$$T\,ds = c_p\,dT - v\,dp. \tag{C.13}$$

For isentropic processes, that is reversible and adiabatic, $ds = 0$, and accordingly

$$dT = -\frac{p}{c_v}dv$$
$$dT = \frac{v}{c_p}dp, \tag{C.14}$$

which in turn implies

$$\frac{dp}{p} = -\kappa\frac{dv}{v}, \tag{C.15}$$

where $\kappa = \frac{c_p}{c_v}$ is the ratio of specific heats.

C.3 Mass Balance of the Plenum

The plenum process is assumed to be isentropic, which means that the differential form (C.15) of the isentropic relation is valid, so that

$$\frac{dp_p}{p_p} = -\kappa\frac{dv_p}{v_p} = \kappa\frac{d\rho_p}{\rho_p}, \tag{C.16}$$

where it has been used that

$$\rho = \frac{1}{v} \Rightarrow \frac{d\rho}{\rho} = -\frac{dv}{v}. \tag{C.17}$$

It follows that

$$\dot{p}_p = \frac{\kappa p_p}{\rho_p}\dot{\rho}_p = \kappa R T_p \dot{\rho}_p. \tag{C.18}$$

The mass balance of the plenum is

$$\dot{\rho}_p = \frac{1}{V_p}(m - m_t), \tag{C.19}$$

and it follows that

$$\dot{p}_p = \frac{\kappa R T_p}{V_p}(m - m_t) = \frac{a_s^2}{V_p}(m - m_t), \tag{C.20}$$

where $a_s = \sqrt{\kappa R T_p}$ is the plenum sonic velocity. As velocities in the plenum are assumed negligible, a_0 can be used in (C.20). The speed of sound in the plenum will wary as both temperature and pressure in the plenum varies with time. In Simon *et al.* (1993), a time mean speed of sound in the plenum, $\bar{a}_s$ was used. Another approach to avoid using the plenum sonic velocity was taken by Greitzer (1976*a*). It was recognized that by assuming that the temperature ratios of the compression system are near unity, the quantity $\rho_p / p_p = R T_p$ is not appreciably different from ρ_{01} / p_{01}. Thus, the speed of sound at ambient conditions can be used in (C.20). This approach is also taken in this thesis.

C.4   Flow through a Nozzle

The stagnation temperature is

$$T_0 = T + \frac{1}{2c_p} C_x^2, \qquad (C.21)$$

where T is the static temperature and C_x is the velocity of the flow. The Mach number is

$$M = \frac{C_x}{a_s}, \qquad (C.22)$$

where

$$a_s = \sqrt{\kappa R T}, \qquad (C.23)$$

is the sonic velocity. Then $C_x^2 = M^2 \kappa R T$ and it follows that

$$\frac{T_0}{T} = 1 + \frac{M^2 \kappa R}{2c_p} = 1 + \frac{\kappa - 1}{2} M^2. \qquad (C.24)$$

Using the isentropic relation

$$\frac{T_0}{T} = \left(\frac{p}{p_0} \right)^{\frac{(\kappa - 1)}{\kappa}}, \qquad (C.25)$$

it is found that

$$\frac{p_0}{p} = \left(1 + \frac{\kappa - 1}{2} M^2 \right)^{\frac{\kappa}{\kappa - 1}}. \qquad (C.26)$$

The mass flow is

$$m = \rho A C_x, \qquad (C.27)$$

where A is the flow cross-sectional area. Alternative forms are

$$
\begin{aligned}
m &= \rho A M a_s = A \rho \sqrt{\kappa R T} M = A \frac{p}{\sqrt{RT}} \sqrt{\kappa} M \\
&= A \frac{p_0}{\sqrt{R T_0}} \frac{p}{p_0} \sqrt{\frac{T_0}{T}} \sqrt{\kappa} M,
\end{aligned} \qquad (C.28)
$$

where it is used that $\rho = p/RT$. Then, by the use of (C.25) and (C.26), it is found that

$$m = A \frac{p_0}{\sqrt{RT_0}} \sqrt{\kappa} M \left(1 + \frac{\kappa - 1}{2} M^2\right)^{-\frac{\kappa+1}{2(\kappa-1)}}. \tag{C.29}$$

The critical mass flow, or choked flow, is found by inserting $M = 1$ and using the ideal gas law in the form $RT_0 = \rho_0/p_0$. This gives

$$m_{choke} = A\sqrt{\kappa \rho_0 p_0} \left(\frac{2}{\kappa + 1}\right)^{\frac{\kappa+1}{2(\kappa-1)}} \tag{C.30}$$

$$= A\rho_0 a_0 \left(\frac{2}{\kappa + 1}\right)^{\frac{\kappa+1}{2(\kappa-1)}}. \tag{C.31}$$

C.5 Compressor Pressure Rise

Here equation (5.50) for the compressor pressure rise is derived. The compressor total to static isentropic efficiency can be written

$$\eta_i(m, U_1) = \frac{h_{2s} - h_{01}}{h_{02} - h_{01}}, \tag{C.32}$$

where h_{2s} is the outlet static enthalpy obtained with isentropic compression, h_{01} is the inlet stagnation, or total, enthalpy and h_{02} is the outlet stagnation, or total, enthalpy.

Considering a perfect gas, we have that $h = Tc_p$, where c_p is the specific heat capacity at constant pressure. For a perfect gas, c_p is constant. The efficiency now is

$$\eta_i(m, U_1) = \frac{T_{2s} - T_{01}}{T_{02} - T_{01}} = \frac{\frac{T_{2s}}{T_{01}} - 1}{\frac{T_{02}}{T_{01}} - 1}. \tag{C.33}$$

Using the relation for isentropic compression (C.25),

$$\eta_i(m, U_1) = \frac{\left(\frac{p_2}{p_{01}}\right)^{\frac{\kappa-1}{\kappa}} - 1}{\frac{T_{02}}{T_{01}} - 1} = \frac{T_{01} c_p \left(\left(\frac{p_2}{p_{01}}\right)^{\frac{\kappa-1}{\kappa}} - 1\right)}{c_p(T_{02} - T_{01})}. \tag{C.34}$$

For a radially vaned impeller (Watson and Janota 1982):

$$\eta_i(m, U_1) = \frac{T_{01} c_p \left(\left(\frac{p_2}{p_{01}}\right)^{\frac{\kappa-1}{\kappa}} - 1\right)}{\Delta h_{0c,ideal}}, \tag{C.35}$$

which can be rearranged to

$$\frac{p_2}{p_{01}} = \left(1 + \frac{\eta_i(m, U_1) \Delta h_{0c,ideal}}{T_{01} c_p}\right)^{\frac{\kappa}{\kappa-1}}. \tag{C.36}$$

APPENDIX D

INCLUDING A CCV IN THE
MOORE-GREITZER MODEL

Equation numbers starting with MG are references to the paper Moore and Greitzer (1986).

Equation (MG5), which gives the pressure rise over the compressor is modified to

$$\underbrace{\frac{p_E - p_1}{\rho U^2} = N_s F(\phi) - \frac{1}{2a}\left(2\frac{\partial \phi}{\partial \xi} + \frac{\partial \phi}{\partial \theta}\right)}_{\text{Equation (5) in Moore and Greitzer (1986)}} - \Psi_v(\phi), \qquad (D.1)$$

where $\Psi_v(\phi)$ is the pressure drop across the CCV, and p_E now is the pressure at the exit of the CCV. Using equation (MG23), the pressure rise over the equivalent compressor is written

$$\Psi_e(\phi) = \underbrace{N_s F(\phi) - \frac{1}{2}\phi^2}_{\Psi_c(\phi)} - \Psi_v(\phi). \qquad (D.2)$$

Using this, the local (in θ) and annulus averaged momentum balances (equations (MG42) and (MG43)), are modified to

$$\Psi(\xi) + l_c\frac{d\Phi}{d\xi} = \psi_c(\Phi - Y_{\theta\theta}) - \psi_v(\Phi - Y_{\theta\theta}) - mY_\xi + \frac{1}{2a}\left(2Y_{\xi\theta\theta} + Y_{\theta\theta\theta}\right) \quad (D.3)$$

and

$$\Psi(\xi) + l_c\frac{d\Phi}{d\xi} = \frac{1}{2\pi}\int_0^{2\pi}\left\{\psi_c(\Phi - Y_{\theta\theta}) - \psi_v(\Phi - Y_{\theta\theta})\right\} d\theta. \qquad (D.4)$$

In the case of pure surge, that is $Y \equiv 0$, the two momentum balances are the same and is reduced to

$$\dot{\Phi} = \frac{1}{l_c}\left(\Psi_c(\Phi) - \Psi_v(\Phi) - \Psi\right), \qquad (D.5)$$

which is the same expression as used in Simon (1993). The CCV has a characteristic given by

$$\Psi_v(\phi) = \frac{1}{\gamma^2}\phi^2, \tag{D.6}$$

where $\gamma > 0$ is proportional to the valve opening. Y is now represented by a single harmonic approximation

$$Y^* = WA(\xi)sin(\theta - r(\xi)) = WA(\xi)sin(\zeta), \tag{D.7}$$

where $A(\xi)$ is the time varying stall amplitude. A residue R, is defined as

$$R \triangleq Y_\xi^* - Y_\xi. \tag{D.8}$$

The Galerkin approximation is calculated using the weight functions

$$h_1 = 1, \ h_1 = \sin\zeta, \ h_2 = \cos\zeta \tag{D.9}$$

and the inner product

$$\langle R, h_i \rangle = \frac{1}{2\pi}\int_0^{2\pi} R(\zeta)h_i(\zeta)d\zeta. \tag{D.10}$$

Calculating $\langle R, h_i \rangle = 0$ for $i = 1, 2, 3$, we get

$$M_1 = \frac{1}{2\pi}\int_0^{2\pi}\psi_e(\Phi + WA\sin\zeta)d\zeta = \Psi + l_c\frac{d\Phi}{d\xi} \tag{D.11}$$

$$M_2 = \frac{1}{2\pi}\int_0^{2\pi}\psi_e(\Phi + WA\sin\zeta)\sin\zeta d\zeta = (m + \frac{1}{a})\frac{dA}{d\xi} \tag{D.12}$$

$$M_3 = \frac{1}{2\pi}\int_0^{2\pi}\psi_e(\Phi + WA\sin\zeta)\cos\zeta d\zeta$$

$$= -(\frac{dr}{d\xi}(m + \frac{1}{a}) - \frac{1}{2a})A. \tag{D.13}$$

By using (D.2) and (2.9) the moments M_i are calculated to be

$$M_1 = \frac{\pi}{2}\left(4\psi_0 - \frac{2H\Phi^3}{W^3} - \frac{2W^2A^2}{\gamma^2} - \frac{3H\Phi A^2}{W} - \frac{4\Phi^2}{\gamma^2}\right.$$

$$\left. +\frac{6H\Phi^2}{W^2} + 3HA^2\right) \tag{D.14}$$

$$M_2 = \frac{\pi}{2}\left(-\frac{3H\Phi^2A}{W^2} - \frac{3HA^3}{4} - \frac{2AW\Phi}{\gamma^2} + \frac{6AH\Phi}{W}\right) \tag{D.15}$$

$$M_3 = 0. \tag{D.16}$$

By combining (D.11) to (D.13) with (D.14) to (D.16) and rearranging, the following differential equations, which correspond to (MG60) and (MG61),

for Φ and $J = A^2$ are found:

$$\dot{\Phi} = \frac{H}{l_c} \left(-\frac{\Psi - \psi_0}{H} - \frac{1}{2} \left(\frac{\Phi}{W} - 1 \right)^3 + 1 \right. \tag{D.17}$$

$$\left. +\frac{3}{2} \left(\frac{\Phi}{W} - 1 \right) \left(1 - \frac{J}{2} \right) - \frac{1}{\gamma^2} \left(\frac{W^2 J}{2H} + \frac{\Phi^2}{H} \right) \right) \tag{D.18}$$

$$\dot{J} = J \left(1 - \left(\frac{\Phi}{W} - 1 \right)^2 - \frac{J}{4} - \frac{1}{\gamma^2} \frac{4W\Phi}{3H} \right) \sigma. \tag{D.19}$$

The differential equations for ψ and r are left unchanged by the introduction of the CCV.

APPENDIX E

NUMERICAL VALUES USED IN SIMULATIONS

Symbol	value	Symbol	value	Symbol	value
R	0.1m	ρ	$1.15\frac{\text{kg}}{\text{m}^3}$	a_s	$340\frac{\text{m}}{\text{s}}$
l_E	8	l_I	2	L_c	3m
V_p	1.5m^3	A_c	0.01m^2	a	0.3
H	0.18	W	0.25	ψ_{c0}	0.3
I	0.03kgm^2	m	1.75		

Table E.1: Numerical values used in the simulations of Chapters 2, 3 and 4.

Symbol	value	Symbol	value	Symbol	value
D_2	0.128m	D_{t1}	0.074m	D_{h1}	0.032m
σ	0.9	p_{01}	10^5Pa	ρ_1	$1.15\frac{\text{kg}}{\text{m}^3}$
T_{01}	303K	α_1	$\pi/2$	β_{1b}	0.61
Re	100000	D	0.02m	κ	1.4
c_p	$1005\frac{\text{J}}{\text{kgK}}$	C_m	0.01	a_{01}	$340\frac{\text{m}}{\text{s}}$
V_p	0.21m^3	L_c	1.253m	J	$.001\text{kgm}^2$

Table E.2: Numerical values used in the simulations of Chapter 5.

APPENDIX F

BOUNDS ON THE CONTROLLER PARAMETERS OF THEOREM 2.5

In this appendix the upper and lower bounds on the controller gain c_3 defined in Theorem 2.5 are calculated. The numerical values used are

Sym.	value	Sym.	value	Sym.	value	Sym.	value
$J_{\max}$	4	W	0.25	H	0.18	ψ_{co}	0.3006
ϕ_{choke}	0.8	ϕ_m	0.2				

Table F.1: Numerical values

The equilibrium value of the mass flow coefficient ϕ_0 is found by solving equation (2.65) with respect to ϕ_0. The lower bound $\underline{C}_1$ defined in (2.180) is

$$\underline{C}_1 = \frac{3H}{4W^2}\left(\frac{\phi_0^2}{4W} + W + \phi_0\right) - c_2. \tag{F.1}$$

Using (2.186), the upper bound $\overline{C}_2$ is calculated as

$$\overline{C}_2 = \frac{\phi_m - \phi_0}{\phi_m}\frac{4W}{3H}\left((\phi_0 - \phi_m)\hat{\Psi}_c(\phi_0 - \phi_m) - c_2(\phi_0 - \phi_m)^2 - \frac{\phi_m^2}{W^2} - \frac{2\phi_m}{W}\right) + c_2 \tag{F.2}$$

With the help of symbolic toolbox in MATLAB, the following expressions are found for $\overline{C}_3$, $\overline{C}_4$, $\underline{C}_3$ and $\underline{C}_4$:

$$\underline{C}_3(c_2, \phi_{choke}) = -\frac{T_0 + T_1}{2V^4 J_{\max}} \tag{F.3}$$

$$\overline{C}_3(c_2, \phi_{choke}) = -\frac{T_0 - T_1}{2V^4 J_{\max}}, \tag{F.4}$$

where

$$
\begin{aligned}
T_0 &= -4\,\phi_{choke}^2 - 8\,\phi_{choke}\,\phi_0 - 4\,\phi_0^2 + 3\,HW\,J_{\max}\,\phi_{choke}\,\phi_0 \\
&\quad -3\,W^2 H J_{\max}\,\phi_{choke} - 3\,W^2 H J_{\max}\,\phi_0 + 3\,HW\,J_{\max}\,\phi_{choke}^2 \\
&\quad +2\,W^4 J_{\max}\,c_2 \\
T_1 &= -2\sqrt{2}\sqrt{T_2} \\
T_2 &= -\left(3\,HW\,J_{\max}\,\phi_{choke}^2 - 2\,\phi_{choke}^2 - 4\,\phi_{choke}\,\phi_0 \right. \\
&\quad -3\,W^2 H J_{\max}\,\phi_{choke} + 3\,HW\,J_{\max}\,\phi_{choke}\,\phi_0 \\
&\quad \left. +2\,W^4 J_{\max}\,c_2 - 2\,\phi_0^2 - 3\,W^2 H J_{\max}\,\phi_0\right)\left(\phi_{choke} + \phi_0\right)^2
\end{aligned}
$$

and

$$
\underline{C}_4(c_2, \phi_m) = -\frac{T_0 + T_1}{2V^4 J_{\max}} \tag{F.5}
$$

$$
\overline{C}_4(c_2, \phi_m) = -\frac{T_0 - T_1}{2V^4 J_{\max}}, \tag{F.6}
$$

where

$$
\begin{aligned}
T_0 &= -4\,(-\phi_m)^2 - 8\,(-\phi_m)\,\phi_0 - 4\,\phi_0^2 + 3\,HW\,J_{\max}\,(-\phi_m)\,\phi_0 \\
&\quad -3\,W^2 H J_{\max}\,(-\phi_m) - 3\,W^2 H J_{\max}\,\phi_0 + 3\,HW\,J_{\max}\,(-\phi_m)^2 \\
&\quad +2\,W^4 J_{\max}\,c_2 \\
T_1 &= -2\sqrt{2}\sqrt{T_2} \\
T_2 &= -\left(3\,HW\,J_{\max}\,(-\phi_m)^2 - 2\,(-\phi_m)^2 - 4\,(-\phi_m)\,\phi_0 \right. \\
&\quad -3\,W^2 H J_{\max}\,(-\phi_m) + 3\,HW\,J_{\max}\,(-\phi_m)\,\phi_0 \\
&\quad \left. +2\,W^4 J_{\max}\,c_2 - 2\,\phi_0^2 - 3\,W^2 H J_{\max}\,\phi_0\right)\left((-\phi_m) + \phi_0\right)^2
\end{aligned}
$$

As the value of ϕ_0 depends on the choice of c_2 and c_3, the gains have to be chosen first, then ϕ_0 is calculated, and finally the bounds $c_3^{\min}$ and $c_3^{\max}$ have to be calculated and checked against c_3. After some iterations of this procedure the following gains are used: $c_2 = 1$ and $c_3 = 0.55$, ϕ_0 is calculated to $\phi_0 = 0.34$ and the bounds are calculated to be

$$
\begin{aligned}
\underline{C}_1(c_2, \phi_0) &= 0.52 \\
\overline{C}_2(c_2, \phi_0, \phi_m) &= 2.24 \\
\underline{C}_3(c_2, \phi_0, \phi_{choke}) &= 0.33 \\
\overline{C}_3(c_2, \phi_0, \phi_{choke}) &= 419.34 \\
\underline{C}_4(c_2, \phi_0, \phi_m) &= 0.0011 \\
\overline{C}_4(c_2, \phi_0, \phi_m) &= 6.83.
\end{aligned}
$$

Now,

$$
\begin{aligned}
c_3^{\min} &= \max\{\underline{C}_1, \underline{C}_3, \underline{C}_4\} \\
&= \max\{0.52, 0.33, 0.0011\} \\
&= 0.52, \tag{F.7}
\end{aligned}
$$

and

$$
\begin{aligned}
c_3^{\max} &= \min\left\{\overline{C}_2(c_2, \phi_m),\ \overline{C}_3(c_2, \phi_{choke}),\ \overline{C}_4(c_2, \phi_m)\right\} \\
&= \min\{2.24,\ 419.34,\ 6.83\} \\
&= 2.24.
\end{aligned}
\tag{F.8}
$$

As can be seen the choice $c_3 = 0.55$ now satisfies

$$
c_3^{\min} = 0.52 < c_3 = 0.55 < c_3^{\max} = 2.24.
\tag{F.9}
$$